PhD Thesis

Laura Ann Rechner

Advanced techniques to minimize side effects for patients treated with mediastinal radiotherapy

Advanced techniques to minimize side effects for patients treated with mediastinal radiotherapy

PhD Thesis
Laura Ann Rechner, MSc

Departments
Niels Bohr Institute
University of Copenhagen
Copenhagen, Denmark

Department of Oncology
Section of Radiotherapy
Rigshospitalet
Copenhagen, Denmark

Primary Supervisor
Associate Professor Marianne C. Aznar, PhD
The University of Manchester, Manchester, United Kingdom
Niels Bohr Institute, University of Copenhagen, Denmark

Co-supervisors
Professor Ivan R. Vogelius, PhD, DMSc
Maja V. Maraldo, MD, PhD
Professor Lena Specht, MD, DMSc
Rigshospitalet and The University of Copenhagen, Denmark

Assessment Committee
Professor Jens Jørgen Gaardhøje, PhD
Internal Assessor
Niels Bohr Institute
University of Copenhagen, Copenhagen, Denmark

Professor Stine S. Korreman, PhD
Danish Centre for Particle Therapy
Aarhus University Hospital, Denmark

Professor N. George Mikhaeel, MD
Guy's & St Thomas' Hospital
King's College London, United Kingdom

Defense
December 6th, 2019
Auditorium 1, Rigshospitalet, Copenhagen

Acknowledgements

I would like to first and foremost thank the radiotherapy patients who agreed to be part of research studies, which is an invaluable contribution to medicine and science, and allows the continued efforts to improve treatments.

Thank you to my primary supervisor, **Marianne Aznar**. It means so much to me that you continued to be my supervisor from afar. You always made yourself available when I needed help, and you created exciting opportunities for me to visit your departments. I am grateful for your guidance, encouragement, hospitality, and friendship.

I would also like to thank my co-supervisors **Ivan Vogelius**, **Lena Specht**, and **Maja Maraldo**, who often took on various extra roles and responsibilities, being my local 'team.' Thank you for your guidance with both practical matters and research, and for providing different perspectives that challenged me and improved our projects.

Thank you to all of my coauthors who contributed to the manuscripts contained in this thesis. I am proud of the work that we have accomplished together and grateful for your ideas, efforts, edits, criticisms, questions, and guidance. Working with a diverse team for each study has been very rewarding. I would like to especially thank **Per Munck af Rosenschöld** and **Peter Meidahl Petersen**, who provided mentorship for the thymoma paper. Thanks to **Deborah Anne Schut** and **Tanja Stagaard Johansen** for their effort and expertise in doseplanning. Special thanks to **Arezoo Modiri** and **Line Bjerregaard Stick** for their hard work with the optimization paper, which was definitely a team effort. I would also like to specially thank **Edward Smith** and **Adam Aitkenhead** in Manchester for their collaboration on the LET and vRBE project. Thanks to **Patrik Brodin** and **Michael Junker Lundemann** for always quickly answering technical questions about scripting.

I would like to express my gratitude to the Department of Oncology, Section of Radiotherapy at Rigshospitalet for the support to pursue a PhD. I have learned so much from my colleagues in the department, and it is an exciting and vibrant place to work and study. Thank you to **Jens Peter Bangsgaard** for the encouragement and support to step away from the clinic and focus on research for a few years. Thank you to the 'basement' research group for the comradery throughout our studies, interesting discussions about projects and articles, and all the cake. Thanks for being fantastic office-mates **Michael Junker Lundemann**, **Anni Young Lundgaard**, **Karin Nielsen**, and **Anne Marie Lindegaard**. Thanks to Anni for the help with the Danish Summary. I will miss sitting together, but I hope I still see you often. Thanks to former students **Mirjana Josipovic**, **Katrin Håkansson**, **Jonas Scherman**, **Josefine Ståhl Kornerup**, **Henrik Hansen**, **Tobias Pommer**, **Marianne Falk**, and **Jenny Gorgisyan**, from whom I have learned so much about the field and the process of pursuing a PhD. I would like to thank **Anneli Edvardsson** and **Malin Kügele** from Lund for sharing thoughts and expertise about DIBH and mediastinal radiotherapy. Thanks to **Daniel Gasic** for surviving survival with me and the interesting discussions about LET. Thanks to **Mirjana Josipovic** and **Mikkel Skaarup** for being great TA partners at NBI.

Last, but certainly not least, I would like to thank my family, who have all been supportive of me throughout the years. I'd like to give a huge to thank you to my husband **Drew Rechner** for being my rock. Thank you for holding down the fort, especially recently as I finish up the PhD. Thank you for listening to me talk at length about details about my projects, proof-reading for me, and taking a real interest in what I do. I think of you when I'm feeling a little tired and having trouble with my work. I think "Drew would have the grit to just get this done, be more like Drew." And finally, thank you to my newest family member, **Henry Rechner**, who arrived mid-PhD and gives me so much joy when I get home from work.

Table of Contents

Summary

While radiotherapy damages tumor cells, it can also harm the surrounding healthy tissue. This damage can lead to acute and/or late toxicities. For patients with mediastinal tumors like Hodgkin lymphoma and thymic cancer, this could include pneumonitis, esophagitis, secondary cancers, or cardiac toxicity. The purpose of this thesis was to investigate how to best apply modern techniques in radiotherapy to reduce the dose to normal tissue and therefore the risk of toxicity for patients treated for cancer in the mediastinum.

The aims of this thesis ranged from applied to more exploratory. The first aim was to calculate the treatment margins for patients with mediastinal lymphoma treated at our institution with the modern techniques of deep inspiration breath hold (DIBH) and daily image guidance. The second aim was to investigate the impact of the two modern techniques of DIBH and proton therapy, relative to treatment in free breathing and photon therapy, for patients with Hodgkin lymphoma and thymic cancer. The third aim was to investigate biological uncertainties in proton therapy due to the linear energy transfer (LET) of the protons at the end of their range for pediatric patients with Hodgkin lymphoma. And finally, the fourth aim was to create photon therapy treatment plans that minimized the risk of both tumor recurrence and mortality from late toxicity from radiotherapy for patients with Hodgkin lymphoma. The methods for these aims included a retrospective analysis of set-up uncertainties, treatment planning comparisons for different combinations of techniques, Monte Carlo simulations for proton therapy plans, and using an in-house optimizer.

For aim 1, we found that a margin of approximately 1 cm was needed to include uncertainties from contouring, setup, and intra-fractional motion for the lymphoma patients treated at our institution with DIBH and daily image guidance. For aim 2, we found that both proton therapy and DIBH reduced the dose to normal tissues, but the technique that had a larger impact depended on the patient group. For aim 3, we did not find a clinically concerning distribution of LET or impact on biologically-weighted dose for pediatric patients with Hodgkin lymphoma. And for aim 4, we created "outcome-optimized" plans, but the optimizer was sensitive to model parameters and not ready for clinical use. The results of this thesis can be used to inform clinical practice and future research for patients with Hodgkin lymphoma and thymic cancer to reduce the radiation dose to normal tissue, and therefore the risk of acute and late toxicity.

Dansk Resumé

Mens stråleterapi er en effektiv behandling mod kræft, kan den også skade det omkringliggende normalvæv. Skaderne kan hos patienten manifestere sig som akutte og sene bivirkninger. For patienter med kræft i mediastinum (brystskillevæggen), såsom Hodgkin lymfom og thymuskræft, kan det være bivirkninger som stråleinduceret betændelse i lungerne eller spiserøret, sekundære kræftsygdomme og hjertekarsygdomme. Formålet med denne afhandling var at undersøge, om moderne strålebehandlingsteknikker gør det muligt at reducere stråledosis til det omkringliggende normalvæv og dermed reducere risikoen for behandlingsrelaterede bivirkninger hos patienter med kræft i mediastinum. For at opnå dette brugte vi metoder, der allerede i dag er anvendt inden for stråleterapien, men mere eksperimentelle metoder blev også afsøgt.

Formålet med studie 1 var at fastsætte behandlingsmarginer for patienter behandlet i vores klinik med lymfom i mediastinum, når moderne strålebehandlingsteknikker som strålebehandling i dybt holdt åndedræt (deep inspiration breath-hold, DIBH) og daglig billedvejledning blev brugt. I studie 2 sammenlignede vi de moderne strålebehandlingsteknikker, DIBH og protonterapi, med konventionel stråleterapi med fotoner i fri vejrtrækning. Formålet var at undersøge hvilken modalitet, der gav den største dosisreduktion til normalvævet hos patienter med Hodgkin lymfom og thymuskræft. Formålet med studie 3 var at undersøge den biologiske usikkerhed forbundet med den lineære energioverførsel (linear energi transfer, LET) i slutningen af protonernes rækkevidde i protonbehandling af børn med Hodgkin lymfom. Det sidste og 4. studie havde til formål at optimere strålebehandlingsplaner baseret på minimering af risikoen for både sygdomstilbagefald og risikoen for død af behandlingsrelaterede bivirkninger hos patienter med Hodgkin lymfom. Metoderne til at opnå ovenstående formål inkluderede en retrospektiv analyse af opsætningsusikkerhederne i forbindelse med strålebehandling, sammenligninger af behandlingsplaner for forskellige kombinationer af strålebehandlingsteknikker, Monte Carlo-simuleringer til protonterapiplaner og brugen af et internt optimeringsprogram.

I studie 1 fandt vi, at en margin på cirka 1 cm var nødvendig for at omfatte planlægnings-, opsætnings- og behandlingsusikkerheder, når patienter med Hodgkin lymfom modtager strålebehandling i DIBH med daglig billedvejledning. I studie 2 fandt vi, at både protonterapi og DIBH reducerede dosis til normalvævet, men hvilken teknik, der havde den største effekt, afhang af patientgruppen. I studie 3 fandt vi ikke noget klinisk bekymrende ved distribution af LET eller nogen påvirkning af den biologisk vægtede dosis i protonbehandling af børn med Hodgkin lymfom. I studie 4 udviklede vi risiko-optimerede planer, men optimeringsprogrammet var følsomt over for modelparametre og er ikke klar til klinisk brug. Resultaterne fra denne afhandling kan bruges i klinisk praksis og i fremtidig forskning til at reducere stråledosis til det omkringliggende normalvæv og dermed minimere risikoen for behandlingsrelaterede bivirkninger hos patienter med kræft i mediastinum.

Manuscripts included in this thesis

PAPER I   **Rechner LA**, Specht L, Josipovic M, Maraldo MV, Petersen PM, Aznar MC, Residual errors and PTV margins for modern radiotherapy for mediastinal lymphoma. *Submitted to the Journal of Applied Clinical Medical Physics.*

PAPER II   **Rechner LA**, Maraldo MV, Vogelius IR, Zhu XR, Dabaja BS, Brodin NP, Petersen PM, Specht L, Aznar MC. Life years lost attributable to late effects after radiotherapy for early stage Hodgkin lymphoma: The impact of proton therapy and/or deep inspiration breath hold. *Radiotherapy and Oncology* 125(1) 2017.

PAPER III   **Rechner LA**, Munck af Rosenschöld P, Bäck A, Johansen TS, Schut DA, Aznar MC, Nyman J, and Petersen PM. Proton therapy and deep inspiration breath hold for patients with thymic cancer. *Manuscript.*

PAPER IV   **Rechner LA** & Maraldo MV, Smith EAK, Lundgaard AY, Hjalgrim LL, Safwat A, MacKay RI, Aitkenhead AH, Aznar MC. Proton LET and variable RBE for pediatric patients with Hodgkin lymphoma. *Manuscript.*

PAPER V   **Rechner LA** & Modiri A, Stick LB, Maraldo, MV, Aznar MC, Rice SR, Sawant A, Bentzen SM, Vogelius IR, Specht LS. Biological optimization for mediastinal lymphoma radiotherapy – a preliminary study. *Submitted to Acta Oncologica.*

Proceedings not included in this thesis

Rechner L, Maraldo M V, Specht L, Petersen PM, Vogelius I, Bangsgaard JP, et al. Proton Therapy Versus IMRT for Mediastinal Lymphoma With and Without Breath Hold. Int J Radiat Oncol • Biol • Phys 2015;93:E458–9. doi:10.1016/j.ijrobp.2015.07.1717. Poster, ASTRO Annual Meeting, San Antonio, USA, October, 2015.

Rechner LA, Maraldo M V, Vogelius IR, Petersen PM, Zhu RX, Dabaja BS, et al. PO-0813: Cardiac Toxicity after Radiotherapy for Hodgkin Lymphoma: Impact of Breath Hold and Proton Therapy. Radiother Oncol 2017;123:S435. doi:10.1016/S0167-8140(17)31250-1. Poster, ESTRO Annual Meeting, Vienna, Austria, May 2017.

Maraldo M, **Rechner L,** Josipovic M, Petersen P, Specht L, Aznar M. PTV margins for mediastinal lymphoma in deep inspiration breath-hold using daily image guidance. Radiother Oncol 2018;127:S375–S375. Poster, ESTRO Annual Meeting, Barcelona, Spain, April 2018.

Lundgaard AY, **Rechner LA**, Lundemann M, Brodin NP, Joergensen M, Specht L, et al. EP-1251: Teens who fall in-between – Pediatric or adult radiotherapy regimens in Hodgkin lymphoma. Radiother Oncol 2018;127:S691–2. doi:https://doi.org/10.1016/S0167-8140(18)31561-5. Poster, ESTRO Annual Meeting, Barcelona, Spain, April 2018.

Maraldo M V, Lundgaard AY, Josipovic M, Bidstrup PE, **Rechner L**, Hansen R, et al. The Feasibility of Deep Inspiration Breath-Hold in Children: Results of the TEDDI Pilot Study. Int J Radiat Oncol • Biol • Phys 2018;102:e278. doi:10.1016/j.ijrobp.2018.07.893. Poster, ASTRO Annual Meeting, San Antonio, USA, October 2018.

Rechner L, Modiri A, Stick LB, Maraldo M V, Rice SR, Sawant A, et al. EP-1812 Outcome-optimized radiotherapy planning using risk modeling for lymphoma – a preliminary study. Radiother Oncol 2019;133:S982. doi:10.1016/S0167-8140(19)32232-7. Poster, ESTRO Annual Meeting, Milan, Italy, April 2019.

Rechner LA, Munck af Rosenschöld P, Bäck A, Johansen TS, Schut DA, Aznar MC, Nyman J, and Petersen PM. Proton therapy and deep inspiration breath hold for optimal radiotherapy for patients with thymoma. Poster, PTCOG Annual Meeting, Manchester, UK, June 2019.

Modiri A, **Rechner L**, Stick LB, Maraldo M V, Rice SR, Sawant A, et al. Is Underdosing the Target a Risk Worth Taking? Outcome Risk Modeling in Lymphoma Radiotherapy. Int J Radiat Oncol • Biol • Phys 2019;105:S173. doi:10.1016/j.ijrobp.2019.06.205. Oral Presentation, ASTRO Annual Meeting, Chicago, USA, September 2019.

Manuscripts not included in this thesis

Lundgaard AY, Hjalgrim LL, **Rechner LA**, Josipovic M, Joergensen M, Aznar MC, et al. TEDDI: Radiotherapy delivery in deep inspiration for pediatric patients - A NOPHO feasibility study. Radiat Oncol 2018;13. doi:10.1186/s13014-018-1003-4

Modiri A, Stick LB, Rice SR, **Rechner LA**, Vogelius IR, Bentzen SM, et al. Individualized estimates of overall survival in radiation therapy plan optimization - A concept study. Med Phys 2018;45:5332. doi:10.1002/mp.13211.

Abbreviations

GTV	Gross tumor volume
CTV	Clinical target volume
PTV	Planning target volume
CT	Computed Tomography
MRI	Magnetic resonance imaging
MV	Megavoltage
kV	Kilovoltage
CBCT	Cone-beam computed tomography
IGRT	Image guided radiotherapy
RBE	Relative biological effectiveness
LET	Linear energy transfer
DIBH	Deep inspiration breath hold
ILROG	International Lymphoma Radiation Oncology Group
OAR	Organ at risk
AP	Anterior-posterior
PA	Posterior-anterior
IMRT	Intensity modulated radiotherapy
SFO	Single-field optimization
MFO	Multi-field optimization
HR	Hazard ratio
LYL	Life years lost
VMAT	Volumetric modulated arc therapy
HU	Hounsfield unit

vRBE   Variable relative biological effectiveness

3DCRT   3-dimensional conformal radiotherapy

TPS   Treatment planning system

gEUD   Generalized equivalent uniform dose

PFS   Progression free survival

O-OPT   Outcome-optimized

IMPT   Intensity modulated proton therapy

4DCT   4-dimensional computed tomography

ITV   Internal target volume

MR-linac   Linear accelerator with on-board MRI

1. Introduction

Radiotherapy damages tumor cells, but it can also damage the surrounding healthy organs. Radiation damage to healthy organs can cause acute and/or late toxicities, which can sometimes result in serious side effects such as pain, loss of organ function, reduced quality of life, or premature death. Cancer patients are at a higher risk of side effects if their healthy organs are very close to the tumor and therefore receive a larger dose of radiation [1,2]. In addition, young patients are at a higher risk of side effects due to increased radiosensitivity [3], and their long life expectancy after treatment which gives time for late effects like secondary cancer and heart disease to develop [4–9]. Minimizing side effects while maintaining cure or control of the tumor is one of the central goals of radiotherapy and the main motivation of this work.

In mediastinal radiotherapy, acute toxicities from radiotherapy can result from unwanted radiation damage to the organs in the mediastinal region. One infrequent, but important, acute side effect of mediastinal radiotherapy is pneumonitis, which is an acute inflammation in the alveolar spaces (possibly a hypersensitivity pneumonitis) generally limited to the irradiated regions of the lung [10–12]. It may develop within 6 to 12 weeks after completion of radiotherapy. The symptoms are cough, shortness of breath, fever, and pleuritic chest pain. When the diagnosis is made, patients are treated with steroids for some weeks followed by slow tapering. Though rare, serious cases of pneumonitis can be fatal. Another acute side effect of mediastinal radiotherapy is esophagitis [13]. Esophagitis can cause pain and difficulty swallowing. In the most serious cases, esophagitis can cause necrosis or fistulas, and is life-threatening. Esophagitis may lead to fibrosis and stenosis with stricture formation, which may necessitate dilatation [14].

However, acute side effects are generally temporary, and the symptoms subside with time. Late effects do not subside and are an even greater concern after mediastinal radiotherapy since they are generally irreversible. Due to the proximity to the heart, patients who received mediastinal radiotherapy are at risk for late cardiac toxicity [5,15–17]. Life-threatening cardiac complications can include coronary artery disease, myocardial infarction, heart failure, valvular disease, and arrhythmias [5,11,15,17,18]. In addition to cardiac toxicity, patients treated with mediastinal radiotherapy are at risk for radiation-induced cancers in the irradiated tissues [6,19–24], such as breast cancer [21] and lung cancer [20]. Other factors also modify the risk of late effects after radiotherapy such as age at treatment and smoking status [20,25–27].

2. Background

2.1 Hodgkin Lymphoma

Hodgkin lymphoma occurs in 2.3 per 100,000 persons/year [28], with a bimodal incidence distribution, peaking at approximately 20-24 years and around 65-75 years of age [29,30]. Among adolescents and young adults, Hodgkin lymphoma is one of the most common types of cancer [31]. It is a cancer of the lymphoid tissue, often presenting in the neck and mediastinum (Figure 1). Patients with early-stage classical Hodgkin lymphoma have an excellent 5-year overall survival of approximately 90%. Treatment with combined modality therapy (chemotherapy followed by consolidary radiotherapy) has been shown to be superior to either modality alone [32–37]. Radiotherapy for Hodgkin lymphoma has historically utilized very large radiation fields (extended field radiation therapy or later involved field radiation therapy), developed at a time when radiotherapy was the only curative treatment modality. These treatments exposed organs such as the breasts, heart, and lungs to high doses of radiation [38–40]. Follow-up studies from this patient group have shown increased risks of late effects such as of secondary cancers and heart disease [15–17,20,21,41,42], where both chemotherapy and radiotherapy contribute to the risks [17,42]. When effective chemotherapy became available, it was gradually realized that prophylactic irradiation of apparently uninvolved lymph node regions was no longer necessary. Modern, very limited radiotherapy (involved node radiotherapy (INRT) or involved site radiation therapy (ISRT))[43,44]) to lower doses was introduced, leading to sparing of large volumes of normal tissues [44–47]. Even in the modern context, protecting the healthy organs surrounding the tumor as much as possible remains a major priority [48–50].
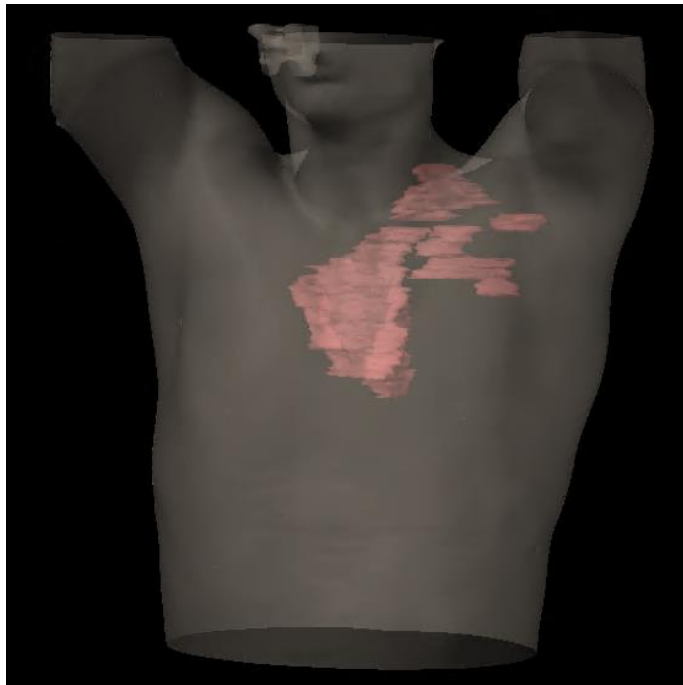
Figure 1. Patient with Hodgkin lymphoma (stage IIA) presenting in the mediastinum, left axilla, and lower neck region (pink).
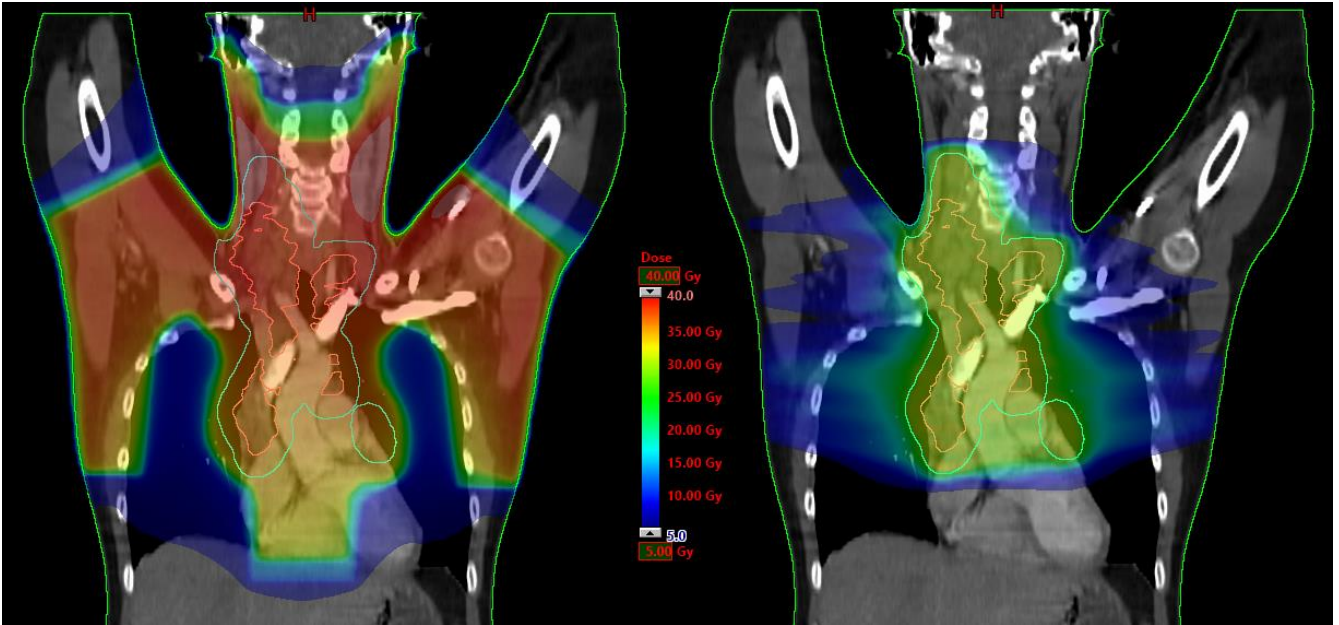
Figure 2. Example of historical radiotherapy for Hodgkin lymphoma (mantle field, left, prescription dose 36 Gy) compared to modern radiotherapy (involved node radiotherapy, right, prescription dose 30.6 Gy) showing the decrease in the amount of tissue treated and decrease in radiation dose [45]. The clinical target volume and planning target volume used for involved node radiotherapy are shown in pink and cyan, respectively.

2.2 Thymic Cancer

Thymic epithelial tumors include thymoma and thymic carcinoma, and are rare malignancies of the thymus gland in the anterior mediastinum, occurring in approximately 0.15 per 100,000 persons/year [51,52]. Approximately 50% of patients are younger than 57 years old at diagnosis, and the disease-specific survival is 85% at 10 years [53]. The treatment is individualized depending on the extent of disease and may include some combination of surgery, chemotherapy, and radiotherapy [54], where radiotherapy has been shown to improve overall survival for patients with regional disease [55]. Many patients who are referred for radiotherapy have had a sternotomy and therefore have stainless steel wires in their sternum from the surgery (Figure 3). Prospective randomized clinical trials are unlikely to take place in rare disease sites like thymic cancer, and therefore simulated trials are a means to investigate the potential impact of new techniques.

Figure 3. Patient with thymoma (stage III) in the mediastinum (pink) and surgical stainless steel wire loops in the sternum (white).

2.3 Summary of Modern Techniques for Mediastinal Radiotherapy

2.3.1 Image Guided Radiotherapy

Imaging has always been an integral part of radiotherapy planning, initially with X-ray films, and since the 1970s with computed tomography (CT) [56]. Since that time, in-room imaging for patient setup has been developed, beginning with two-dimensional portal megavoltage (MV) imaging [57], then kilovoltage (kV) imaging for better image contrast [58], and then three-dimensional imaging such as kV cone-beam computed tomography (CBCT) [59]. Daily image guided radiotherapy (IGRT) has been shown to reduce the setup uncertainty and improve patient positioning [60]. The current standard-of-care for IGRT at Rigshospitalet for patients with mediastinal Hodgkin lymphoma and thymic cancer is daily CBCT (Figure 4).
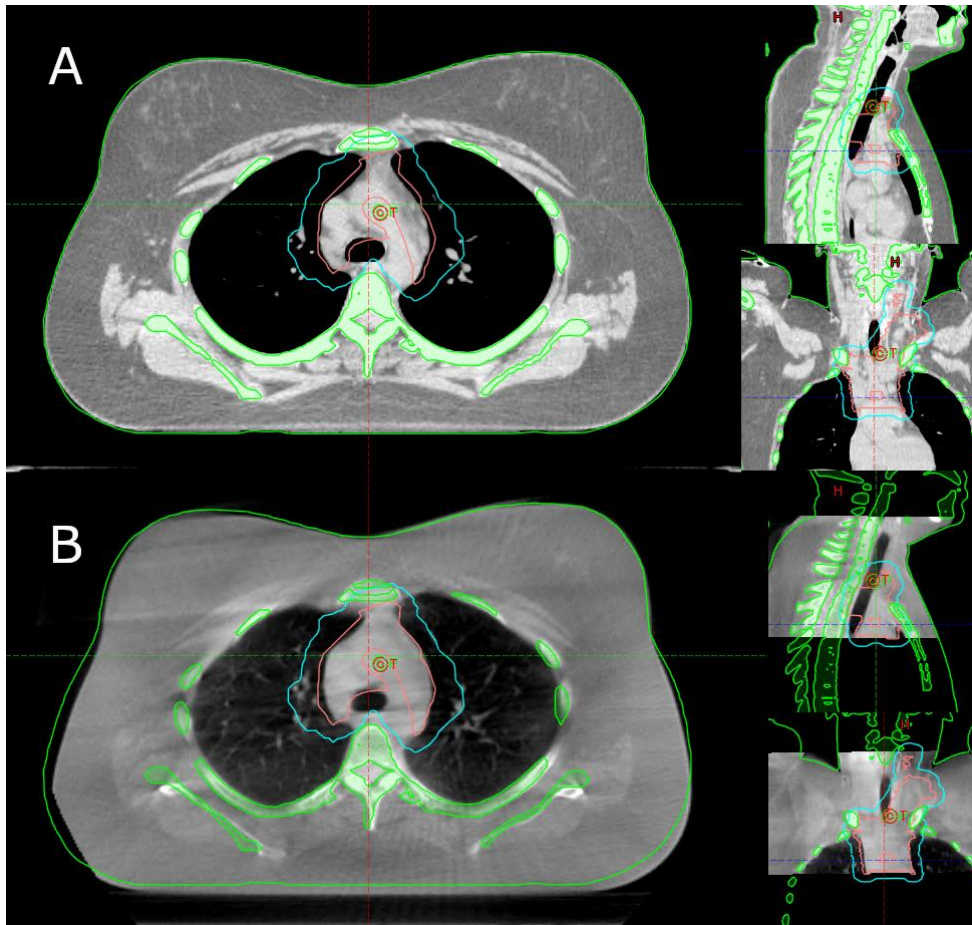
Figure 4. Planning CT (A) compared to daily CBCT (B) used for daily setup for radiotherapy for a patient with Hodgkin lymphoma. Patient contours from the planning CT (A) (body: green, bone: green, clinical target volume (CTV): pink, planning target volume (PTV): light blue) are overlayed on the daily anatomy from the CBCT (B) to show the accuracy of the daily position relative to what was assumed when the radiotherapy was planned.

When planning how to give radiotherapy, the physician delineates the region that contains the visible or palpable tumor (the gross tumor volume (GTV)), and, for solid tumors, adds an expansion to include possible microscopic disease (the clinical target volume (CTV)). For Hodgkin lymphoma, the GTV is delineated both before and after chemotherapy. Based on the pre- and post-chemotherapy GTVs, the CTV is delineated as the tissue volume which contained macroscopic lymphoma before chemotherapy, and which is likely to contain microscopic disease after chemotherapy. If no chemotherapy is given, margins are included in the CTV to cover areas with high risk of microscopic disease. To ensure radiotherapy coverage of the CTV, an additional safety margin for uncertainties in the delivery of the radiotherapy is added (the planning target volume (PTV)) [61]. One consideration for the size of the CTV-to-PTV margin is the setup uncertainty [62], which is dependent on the IGRT technique and other factors such as patient immobilization. To minimize the dose to the surrounding normal tissue and therefore the risk of side effects, margins should be as small as achievable [63].

16

2.3.2 Proton Therapy

Proton therapy has been used to treat cancer since 1958 [64], but commercially available systems have only been available since 2001 [65,66]. Since that time, proton therapy has steadily become more widely accessible and is currently (as of 2019) available at 81 facilities distributed over 20 countries [67]. Denmark has recently opened the Danish Centre for Particle Therapy in Aarhus and has been treating patients since January 2019.

The rationale for proton therapy is that it has the potential to reduce the radiation dose to normal tissues. This stems from the physics of how protons interact with tissue – they deposit some dose on the way to the tumor, the largest amount of dose at the end of their range (e.g. in the tumor) (at the Bragg peak; Figure 5), then little to no dose beyond [65,66,68]. Therefore, depending on the patient anatomy and the location of the tumor, it is often possible to create proton therapy treatment plans that spare organs at risk better than more conventional radiotherapy with photons. Treatment planning comparison studies and clinical series have shown advantages of proton therapy for both Hodgkin lymphoma [69–85] and thymic cancer [86–90].
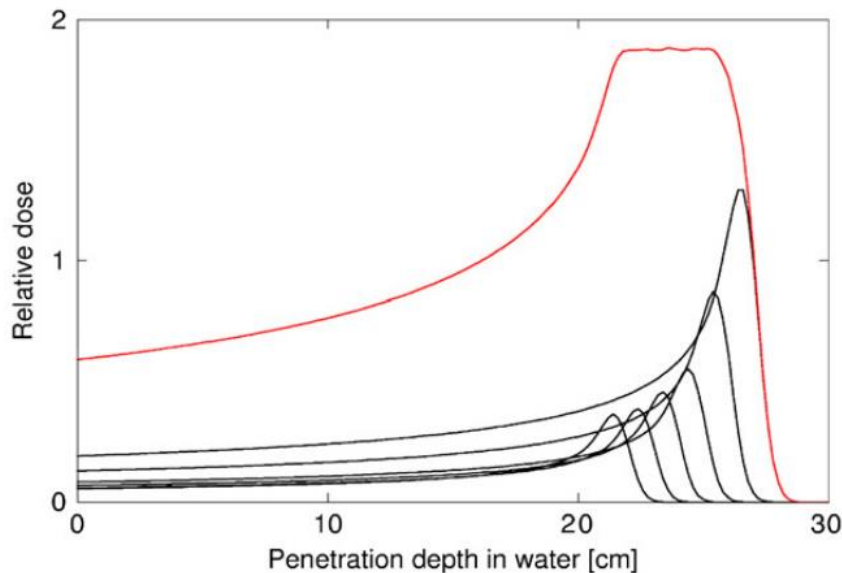
Figure 5. Multiple proton Bragg peaks (black) added together to provide uniform dose coverage from approximately 21-26 cm in depth (red) [65] (Figure 2 from Alfred R Smith 2006 Phys. Med. Biol. 51, reprinted with permission).

While proton therapy has theoretical dosimetric advantages, it also has a few uncertainties associated with biological effects and delivery, which are highly relevant when considering mediastinal irradiation [91,92]. One source of uncertainty in proton therapy is range uncertainty, which causes uncertainty in how deep in the body the protons deposit dose. The conversion of the CT number to proton stopping power has uncertainty [93], which causes some range uncertainty in the patient (Figure 6). In addition, patient positioning uncertainties not only impact the dose deposition in the direction of the patient shift (perpendicular to the proton beam), but also in depth in the patient due to differences in density along the proton's path (Figure 7). Furthermore, when protons traverse a path parallel to an interface of high and low density tissue, scattering causes some of the protons to have a shorter or longer path than expected, causing range straggling [66]. Range uncertainties from the conversion of the CT number to stopping power and from patient

positioning errors can be estimated and/or mitigated in modern commercial proton treatment planning systems.
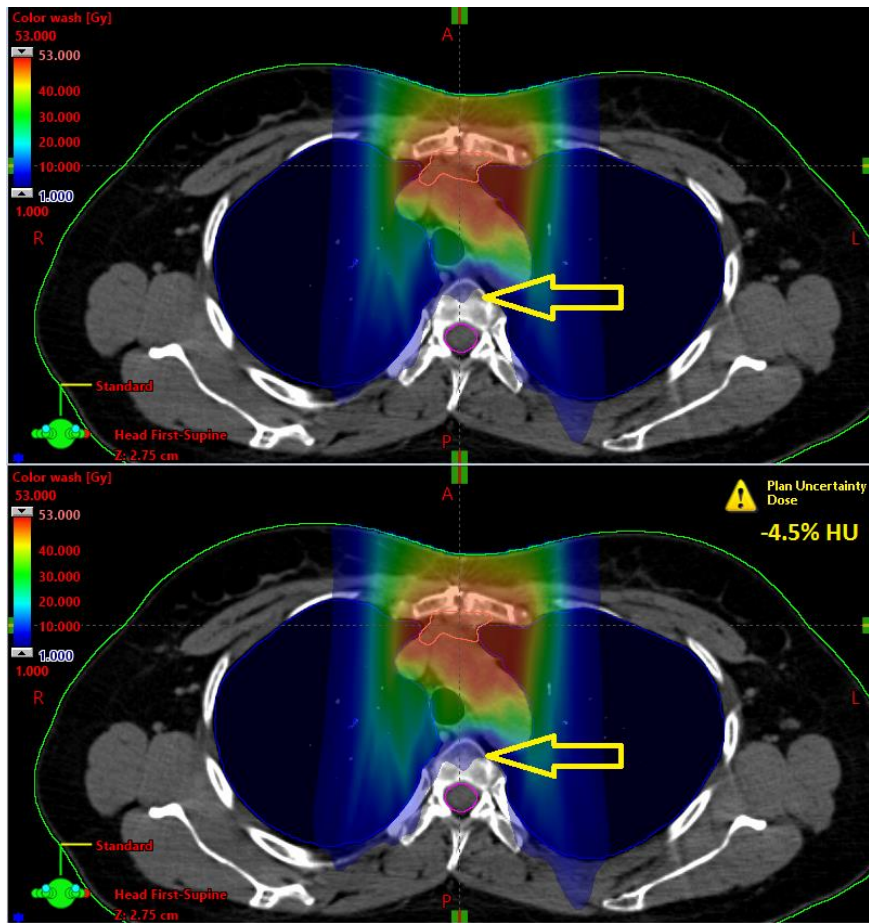
Figure 6. Example of the effect of -4.5% uncertainty in the Hounsfield unit (CT number) to proton stopping power calibration curve (bottom) for a patient with thymoma compared to the nominal plan (top). The increase in proton range can be seen in the vertebra (yellow arrow), where the 1 Gy dose level is 4 mm deeper than in the nominal plan.
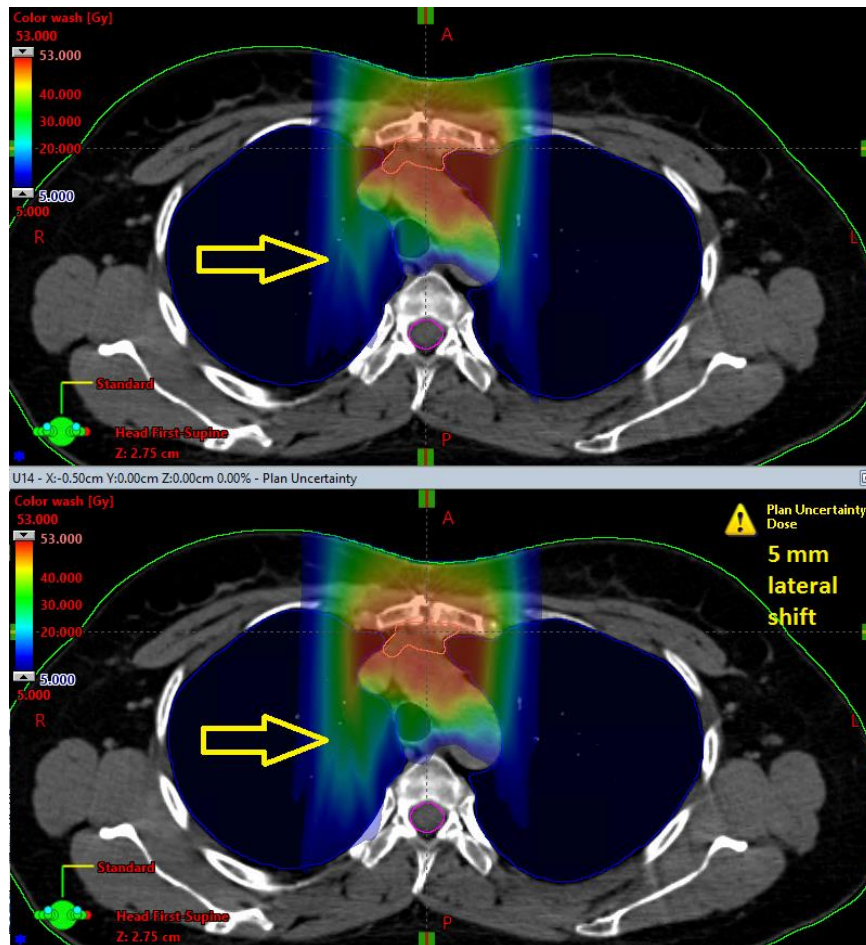
Figure 7. Example of the effect of a 5 mm lateral shift for a patient with thymoma compared to the nominal plan (top). A lateral shift of the patient relative to the proton beams causes the range of protons to change and exposes the patient's right lung to a higher dose of radiation (yellow arrow).

In addition to uncertainties in proton range, there are also uncertainties associated with the biological effect of proton therapy [94], which is a topic of concern for the use of proton therapy for disease sites such as lymphoma [91]. Proton therapy has a slightly larger biological effect than photon therapy for the same measured physical unit of dose [95]. Historically, a uniform correction over the entire proton dose distribution of 1.1 has been used [96]. However, the relative biological effectiveness (RBE) is known to vary with energy of the proton, increasing towards the end of the proton range where the proton energy is low [97]. This is because the RBE is dependent on the linear energy transfer (LET) of the proton (among other factors). LET can be calculated from the proton's energy and is largest for low energy protons (Figure 8) [97,98]. A few studies have shown tissue changes on CT or MRI after radiotherapy that suggest that there might be biological changes that are consistent with a variable RBE [99,100]. There are radiobiological models to calculate variable RBE that use physical dose, LET, and properties of the tissue (alpha/beta ratio [101]) to estimate the RBE [102]. Some commercial treatment planning systems are beginning to allow the calculation and visualization of LET, but variable RBE models are uncertain and are not yet implemented in clinical routine.
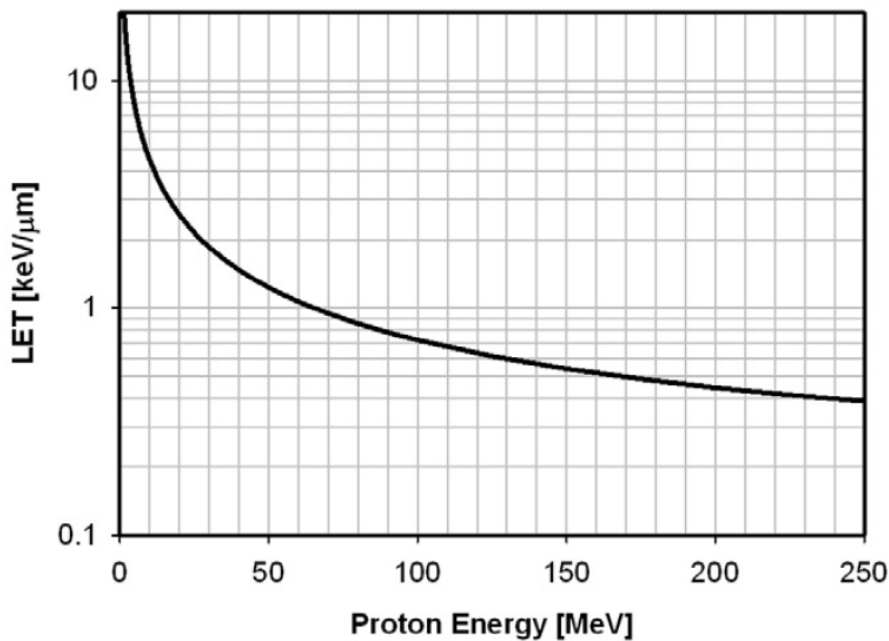
Figure 8. Proton LET as a function of proton energy, showing increased LET with decreasing proton energy [97,98] (Figure 2 from Harald Paganetti 2014 Phys. Med. Biol. 59, reprinted with permission).

2.3.3 Deep Inspiration Breath Hold

Tumors in the thorax, including the mediastinum, and the abdomen move when the patient breathes [103]. Various motion management techniques are available to mitigate the impact of breathing motion in radiotherapy [103] such as motion suppression [104,105], tracking [106,107], rescanning (for pencil beam scanning proton therapy) [108–110], gating with free breathing [111], and gating with breath hold [112,113]. One widely used motion management technique is deep inspiration breath hold (DIBH) [113–115]. There are multiple commercial solutions for monitoring breathing and breath hold, including systems that use surface scanning of the patient's body (e.g. Catalyst, C-RAD; AlignRT, VisionRT), an external marker (e.g. Real-time Position Management (RPM), Varian Medical Systems), or the volume of air inhaled (e.g. Active Breathing Coordinator (ABC), Elekta; SpiroDynr'X (SDX), Oncology Imaging Systems). At Rigshospitalet, the external marker method (Varian RPM) is clinically implemented for DIBH monitoring, which gives visual feedback to the patient to assist with repeating breath holds at the same level. Patients receive coaching before being scanned or treated in breath hold, and are instructed to take a comfortably deep breath and hold it for at least 20 seconds [116]. DIBH increases lung volume and moves the heart inferiorly and has been shown to reduce the dose to critical organs for mediastinal tumors relative to treatment in free breathing [40,113,117–120]. DIBH may also improve the quality of the CBCT used for daily setup [121,122].

2.3.4 Biological Optimization

Inverse optimization based on radiation dose is the current standard method for how radiotherapy treatment plans are created. In this type of optimization, basic properties of the treatment plan (e.g. number of arcs or beams, and their corresponding angles) are set manually, then constraints or objectives for doses to contoured regions of the body are given to the optimizer with some

weighting or importance. For example, typical objectives for a PTV would be to provide a minimum and maximum dose of just below and above the prescription dose. Typical objectives for organs at risk would be a maximum dose (e.g. no more than 45 Gy to the spinal cord [123]), or a dose-volume constraint such as no more than 20 Gy to 20% of the lungs [10]. With these objectives and the manually chosen properties of the plan, the optimizer chooses the details of how the radiation will be delivered.

Radiation dose objectives and constraints are used for treatment plan optimization because dose correlates with biological effect (such as tumor control or normal tissue toxicity). It has been proposed that optimization could be performed directly on the estimated biological effect instead of on the dose [124–128]. While dose-effect relationships do contain uncertainty (and can depend on other patient-specific modifiers such as comorbidities or chemotherapy), this type of optimization could be a more direct way to achieve optimal treatment plans for the desired biological endpoints. In biological optimization, dose is first converted to the probability of given biological effects, and objectives for the effects are given to the optimizer.

For Hodgkin lymphoma, dose-effect relationships can be found in the literature for both tumor control [34,129,130] and toxicity [5,15,16,20,21]. It is often difficult to prioritize between protecting different organs at risk for patients with Hodgkin lymphoma, and in some patients, the risk of treatment might outweigh the benefits. Furthermore, for some patients, dose constraints are easily achieved, and a plan might be accepted for treatment that could have been further improved. Biological optimization could take these factors into account and find the best compromise for each patient. A tool to evaluate biological endpoints has been developed [131], but direct incorporation of such models into the optimization process has not yet been explored for patients with Hodgkin lymphoma.

3. Aims

The purpose of this dissertation was to investigate the impact of the application of these modern techniques, with the objective of learning how to best utilize them to reduce the risk of side effects for patients treated for cancer in the mediastinum. The aims of this thesis range from very applied to more exploratory.

Aim 1: Determine the treatment margins needed for patients with mediastinal lymphoma treated at our institution with DIBH and daily CBCT (Paper I).

Aim 2: Investigate the impact of DIBH and proton therapy, alone and in combination, for patients with Hodgkin lymphoma and thymic cancer (Papers II and III).

Aim 3: Investigate biological uncertainties due to proton LET for pediatric patients with Hodgkin lymphoma for different proton beam arrangements (Paper IV).

Aim 4: Minimize the risk of both tumor recurrence and mortality from late effects by using an optimizer to create biologically optimized plans for patients with Hodgkin lymphoma (Paper V).

4. Summary of Methods and Results

4.1 Aim 1 Methods and Results

4.1.1 Aim 1 Methods: Margin Analysis (Paper I)

Aim 1 was to determine the treatment margins needed for patients with mediastinal lymphoma treated with photon therapy at our institution with DIBH and daily CBCT (Paper I). To accomplish this aim, we sought to quantify the uncertainties in the radiotherapy process for this patient group at our hospital. DIBH was implemented clinically at Rigshospitalet for patients with mediastinal lymphoma in 2012. At that time, the standard IGRT approach was to do CBCT in DIBH weekly and kV images on other days. Recently, the standard IGRT approach at our hospital has transitioned to daily CBCT in DIBH for mediastinal lymphoma patients, but an updated margin analysis had not been performed. 20 consecutive previously treated patients with mediastinal lymphoma treated with photon therapy in DIBH between 2016-2017 were selected for this study. Through a retrospective offline review of IGRT CBCT scans and consulting the literature, we calculated the CTV-to-PTV margin for this patient group. The uncertainties we included in the calculation were inter-fraction positioning uncertainty, intra-fraction motion, and contouring uncertainty.

Positioning Uncertainty

Positioning uncertainty was assessed through comparison of online and offline registration of CBCTs (Clinac, Aria 13.6, Varian Medical Systems). Offline registration was performed for 4 to 5 CBCTs for each patient spaced throughout their treatment course and compared to the online registration. The difference between online and offline registrations was taken as the residual error. Overall positioning uncertainties for all patients were calculated as the root mean square (random) and the standard deviation of the means for each patient (systematic) for each anatomical direction [62].

Estimation of Contouring and Intra-fractional Uncertainties

Contouring uncertainty remains one of the largest sources of uncertainty in radiotherapy [132]. Despite this general agreement, including contouring uncertainty into margin formulas is controversial. Many institutions do not include contouring uncertainty in margin calculations, even though margin formulas are designed to incorporate it [62]. In previous work, we have estimated the contouring uncertainty to be 3 mm in this patient group [133]. To investigate the impact of different assumptions of contouring uncertainties on margins, we also considered contouring uncertainties of 0, 1, 2, and 4 mm.

Intra-fractional motion uncertainty was also estimated from the literature. Due to a lack of published data for mediastinal lymphoma, intra-fractional uncertainty was estimated from breast cancer patients treated in DIBH [134]. We assumed 1.6 mm and 3.0 mm for random, and 0.8 mm and 1.1 mm for systematic uncertainties in the lateral/anterior-posterior and superior-inferior directions, respectively.

Margin Formula

The complex margin formula from van Herk et al [62] was used to calculate the PTV margin required to provide 95% dose coverage of 90% of the patients.

$$m_{ptv} = 2.5\Sigma + 1.64\sqrt{\sigma^2 + \sigma_p^2} - 1.64\sigma_p$$

where m_{ptv} represents the PTV margin from the CTV, Σ represents the systematic uncertainty, σ represents the random uncertainty, and σ_p represents the penumbra (we assumed 3.2 mm for soft tissue and 6.4 mm for lung tissue for 6 MV photons). The systematic uncertainty Σ included uncertainties from positioning (assessed with offline registration), intra-fractional motion, and contouring, which were added in quadrature. The random uncertainty σ included uncertainties from positioning (assessed with offline registration) and intra-fractional motion and were added in quadrature.

4.1.2 Aim 1 Results: Margin Analysis (Paper I)

In paper I, our main finding was that approximately 9-11 mm CTV-to-PTV margins are needed for mediastinal lymphoma patients treated at our institution using DIBH and daily CBCT using photon radiotherapy, assuming 3 mm contouring uncertainty. When other values of contouring uncertainties were assumed (ranging from 0 to 4 mm), the resulting margins varied greatly (Table 1).

Table 1. CTV-to-PTV margins for patients with mediastinal lymphoma treated with DIBH and daily IGRT for different assumed contouring uncertainties for a target abutting soft tissue (or lung tissue in parentheses).

Assumed Contouring Uncertainty (mm)	CTV-to-PTV margin (mm)		
	LAT	AP	SI
0	4.2 (3.7)	4.0 (3.4)	6.0 (5.1)
1	5.1 (4.6)	4.9 (4.4)	6.7 (5.8)
2	7.0 (6.5)	6.9 (6.4)	8.4 (7.5)
3	9.2 (8.7)	9.1 (8.6)	10.6 (9.6)
4	11.6 (11.1)	11.5 (11.0)	12.8 (11.9)

4.2 Methods and Results Aim 2

4.2.1 Aim 2 Methods: DIBH and Proton Therapy for Hodgkin Lymphoma and Thymoma (Papers II and III)

Aim 2 was to investigate the impact of DIBH and proton therapy, alone and in combination, for patients with Hodgkin lymphoma and thymoma. Denmark has recently gained access to proton therapy at the Danish Centre for Particle Therapy in Aarhus and there is a need to identify the patient groups who could benefit the most from proton therapy. It is known that the use of DIBH offer dosimetric benefits for patients with mediastinal tumors like Hodgkin lymphoma and thymoma [118,119,135], but it is unknown how the potential benefit of proton therapy would compare to DIBH (a much less expensive technology), or how proton therapy could benefit these patient groups in combination with DIBH. Therefore, we performed retrospective treatment planning studies for both patient groups to compare these techniques, alone and in combination. Differences in treatment planning techniques reflect not only the different disease sites, but also the collaborating institution's practices and the years in which the studies were conducted. All treatment planning was completed in Eclipse (Varian Medical Systems).

Paper II: DIBH and Proton Therapy for Hodgkin Lymphoma

22 patients with early-stage mediastinal Hodgkin lymphoma from a previous prospective trial (Danish ethics approval H-D-2007-0069)[119] who had both free breathing and DIBH scans were selected for this study. 4 plans were created for each patient: intensity modulated (photon) radiotherapy (IMRT) in free breathing, IMRT in DIBH, proton therapy in free breathing, and proton therapy in DIBH. The prescription dose was 30.6 Gy (Gy (RBE) for protons, assuming an RBE of 1.1) in 17 fractions to the initially involved volume [44]. Clinical priorities for treatment planning in order of highest to lowest were 1) PTV coverage, 2) reduction of the mean dose to the heart and lungs, and 3) reduction of the mean dose to the breasts (for females). Additional objectives were used during optimization as needed for each patient to reduce the dose to normal tissues as much as possible.

IMRT plans were created following the clinical procedure at Rigshospitalet and recommendations of the International Lymphoma Radiation Oncology Group (ILROG) [44]. CTV-to-PTV margins were 1.5 cm in the superior-inferior direction in the mediastinum and 1 cm in other directions for free breathing and 1 cm in all directions for DIBH. The number of fields was usually 5 (range 4-7), most often with 6 MV, but occasionally supplementing with 18 MV (10 MV is not available at our institution). Beam angles were chosen to reduce dose to organs at risk (OARs) as much as possible.

Proton plans were created with guidance from Ron Zhu, Bouthaina Dabaja, and their team at MD Anderson Cancer Center, Texas, USA. PTVs were used for proton planning as well; however, since uncertainties in positioning and CT-calibration cause uncertainties in proton range and dose distribution differently than for photons, special considerations were made for the proton PTVs. For each beam angle for each patient, the beam-specific range uncertainties were calculated following the formula from MD Anderson Cancer Center: 3.5% of the range to the distal edge of the CTV plus 3 mm. If the PTV margin was larger than the calculated beam-specific range uncertainty in that direction, the PTV margin was unchanged. If the PTV margin was smaller than the calculated beam-specific range uncertainty in that direction, the PTV was expanded to incorporate the uncertainty. In most cases, the PTV was unchanged, but was expanded by 1-2 mm in a few cases. The method of using the photon PTV or larger (but never smaller) was chosen to

be conservative for the comparison between proton therapy and photon therapy. An anterior-posterior, posterior-anterior (AP PA) beam arrangement was used and spot scanning, single field optimization (SFO) (which aims to make the dose from each beam uniformly cover the target) was used for most patients. For patients with involved nodes surrounding the heart, beam-specific PTVs and multifield optimization (MFO) (which allows inhomogeneous contributions from different beams and for different beams to cover different parts of the overall target) was used to avoid entrance dose through the heart. Stray neutron doses were estimated and added to proton therapy doses manually after treatment planning [81,136].

We selected the most recent and most relevant studies available in the literature for risk models, using data for Hodgkin lymphoma patients where available. From these studies, hazard ratios (HRs) per Gy were estimated from the literature for heart failure [5], myocardial infarction [5], valvular heart disease [15], lung cancer [20], breast cancer [21] (for females) (Table S1 in Paper II).

To convert doses to an estimation of the impact of the side effects on life expectancy after treatment, the life years lost (LYL) was calculated for each plan [137]. The LYL is the estimated reduction in life expectancy due to late effects from radiotherapy, and includes the age at radiation exposure, the patient's sex, and the prognosis of the late effects. Heart failure, myocardial infarction, valvular heart disease, lung cancer, and breast cancer were included in the LYL calculation, following the methodology of Brodin et al [137] (calculations were performed in Matlab version 2016b, The MathWorks, Inc, Natick, MA).

Paper III: DIBH and Proton Therapy for Thymic cancer

21 consecutive thymic cancer patients treated with curative intent between 2012-2017 who had both free breathing and DIBH scans were selected for this study. 4 plans were generated for each patient: volumetric modulated (photon) radiotherapy (VMAT) in free breathing, VMAT in DIBH, proton therapy in free breathing, and proton therapy in DIBH. The prescription dose was 50 Gy (Gy (RBE) for protons, assuming an RBE of 1.1) in 25 fractions for all patients for the base analysis (a subgroup of patients with residual or unresectable disease was also planned to a higher dose of 60 Gy in 30 fractions). For both VMAT and proton therapy, clinical priorities and dosimetric constraints during treatment planning were guided by the PROthym thymoma trial in Sweden [138]. Priorities during planning were ranked as:

- Spinal cord maximum dose < 48 Gy (RBE)
- Lung (total) $V_{20Gy(RBE)}$ < 35%
- Esophagus mean dose < 45 Gy (RBE)
- CTV $D_{98\%}$ >95%
- PTV (if PTV used) $D_{2\%}$<105%, $D_{98\%}$>95%
- Heart as low as possible

Approximately 2/3 of the patients had metal wires or clips near the target, but the Hounsfield units (HUs) in the CT scans did not extend to the metal range. While this was not considered a problem clinically for photon therapy planning, proton planning is more sensitive to metal objects and large density changes. To address this issue, an extended range CT calibration curve was created [139,140], and all patient scans were duplicated and reassigned the high density calibration curve. The stainless steel wires in the sternum and titanium surgical clips were contoured and overridden. 5300 HU was chosen for stainless steel, which corresponded to half the stopping power relative to

water [139,140]. This choice was made due to the very small diameter of the 0.8 mm wires, where the true thickness of the wire was not possible to contour, but twice the thickness was feasible using thresholding. 8066 HU was used for titanium clips [139,140], which were contoured manually. Intravenous contrast was also overridden and assigned a density of 50 HU.

VMAT plans were created using a 1 cm CTV-to-PTV margin for all patients and 2 full or partial 6 MV arcs. Acuros was used for dose calculation. VMAT plans were considered to have adequate coverage if $D_{98\%}$ to the PTV was greater than 95% of the prescription dose.

Proton plans were created with guidance from collaborators Anna Bäck and Jan Nyman from Sahlgrenska University Hospital, Gothenburg and Skandionkliniken, Uppsala, Sweden. Instead of planning to a PTV, robust optimization to the CTV was used assuming 5 mm positioning uncertainty and 4.5% CT calibration uncertainty. For most patients without metal, two AP oblique beams were used (e.g. 10 and 350 degrees), but beam angles depended on patient anatomy. For patients with metal wires, 3-4 beams were usually used, mostly in an anterior-oblique arrangement, but occasionally from lateral or posterior angles depending on anatomy or difficulty of achieving dose coverage of the CTV. Spot scanning using MFO with robust optimization was used and robust analysis was performed. Proton plans were considered adequately robust if the CTV passed the dosimetric criteria of $D_{98\%}$ to the CTV receiving greater than 95% of the prescription dose for 10 of 12 robustness test cases at the 4.5%, 5 mm uncertainty level.

4.2.2 Aim 2 Results: DIBH and Proton Therapy for Hodgkin Lymphoma and Thymoma (Papers II and III)

Paper II: Hodgkin Lymphoma

In Paper II, our main finding was that proton therapy in DIBH generally yielded the lowest doses to OARs and lowest LYL, and that IMRT in free breathing yielded the plans with the highest doses to OARs and highest LYL. However, when proton therapy in free breathing was compared to IMRT in DIBH, the differences were not statistically significant. Therefore, when deciding between those two combinations of techniques, a patient-specific plan comparison could determine the best option for each individual patient. Average dose-volume histograms for the heart and lungs are shown in Figure 9, and the LYL for two example patients are shown by complication type in Figure 10.
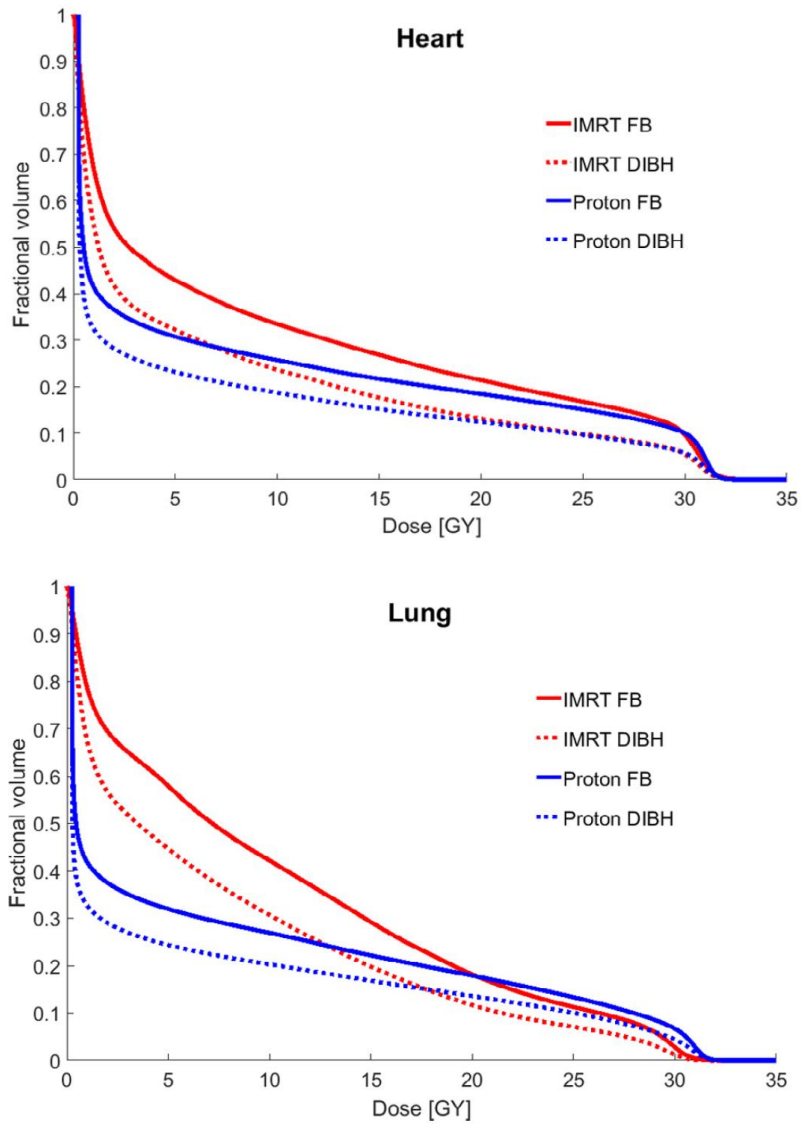
Figure 9. Mean DVHs for all patients for each technique. In general, DIBH slightly reduced the volume of heart and lung for all dose levels relative to free breathing (FB) and proton therapy reduced the volume of heart and lung exposed to a lower dose relative to IMRT [141].
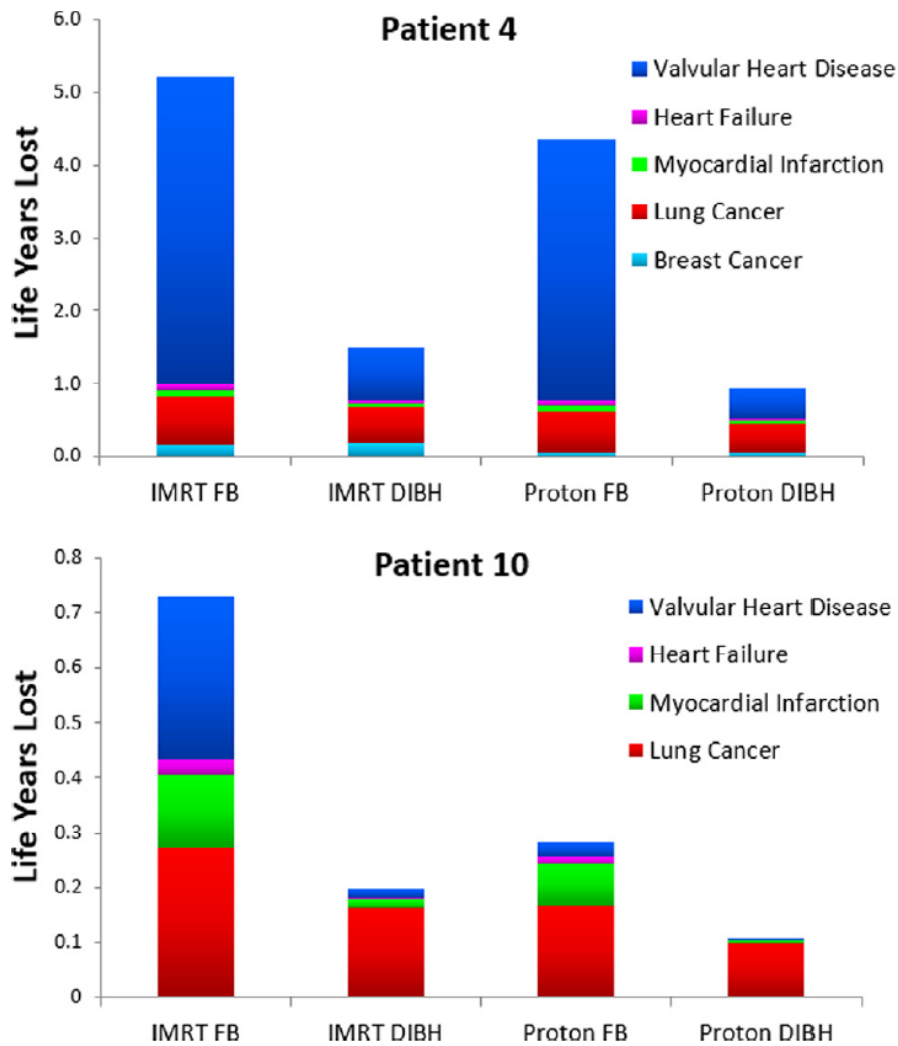
Figure 10. Life years lost (LYL) by complication type for two example patients [141].

Paper III: Thymic cancer

We compared 4 different techniques for patients with thymic cancer (VMAT in free breathing, VMAT in DIBH, IMPT in free breathing, and IMPT in DIBH) and found that the use of IMPT generally had the largest impact on reducing the doses to OARs, with both free breathing and DIBH (Table 2).

Table 2. Dose/volume metrics for the organs at risk (OARs) investigated in this study for all patients in this study for each technique. Breast doses are only shown for female patients. (See paper III for statistical analysis.)

Organ at Risk	Dose Metric	Technique			
		VMAT FB (mean (range))	VMAT DIBH (mean (range))	IMPT FB (mean (range))	IMPT DIBH (mean (range))
Lungs	Mean Dose (Gy (RBE))	14.3 (8.2-26.6)	11.8 (6.6-20.9)	6.8 (2.3-17.6)	5.7 (2.4-13.3)
	$V_{20Gy(RBE)}$ (Fractional Volume)	0.2 (0.10-0.6)	0.2 (0.07-0.5)	0.13 (0.04-0.4)	0.11 (0.03-0.3)
	$V_{5Gy(RBE)}$ (Fractional Volume)	0.7 (0.5-0.99)	0.6 (0.4-0.9)	0.3 (0.09-0.7)	0.2 (0.12-0.5)
Heart	Mean Dose (Gy (RBE))	15.7 (1.8-32.5)	13.9 (0.6-33.5)	10.5 (0.7-31.2)	9.7 (0.0-29.9)
	$V_{20Gy(RBE)}$ (Fractional Volume)	0.3 (0.01-0.6)	0.3 (0.0-0.7)	0.2 (0.01-0.7)	0.2 (0.0-0.6)
Esophagus	Mean Dose (Gy (RBE))	17.2 (8.0-40.1)	15.5 (5.5-42.9)	9.5 (0.2-40.6)	10.4 (0.2-35.7)
	D_{2cc} (Gy (RBE))	32.6 (14.5-52.0)	30.4 (12.3-50.1)	23.7 (0.7-50.0)	25.7 (0.7-50.3)
Spinal Cord	D_{max} (Gy (RBE))	21.1 (9.1-36.6)	18.8 (7.1-43.8)	5.6 (0.02-25.8)	8.6 (0.03-39.7)
Breasts	Mean Dose (Gy (RBE))	9.1 (2.6-16.2)	10.5 (3.3-18.6)	3.3 (0.2-10.6)	3.6 (0.3-11.8)
Body	Integral Dose (Gy (RBE)*L)	150.8 (64.2-423.3)	160.4 (63.0-430.5)	69.3 (24.1-246.0)	76.0 (28.5-267.4)

Abbreviations: Volumetric modulated arc therapy (VMAT), intensity modulated proton therapy (IMPT), free breathing (FB), deep inspiration breath hold (DIBH), fractional volume receiving dose level x (V_x), dose to 2 cc of a structure D_{2cc}, maximum dose to a structure (D_{max}), liter (L).

4.3 Methods and Results for Aim 3

4.3.1 Aim 3 Methods: Proton LET and RBE for Hodgkin Lymphoma (Paper IV)

Aim 3 was to investigate biological uncertainties due to proton LET for pediatric patients with Hodgkin lymphoma for different proton beam arrangements (Paper IV). While the LET and therefore the RBE of proton therapy is known to vary, especially at the end of range [95,142–144], the impact of these uncertainties, to our knowledge, has not yet been investigated for lymphoma

patients. We aimed to quantify the impact of this uncertainty and explore the impact of different beam arrangements on the result. 3 pediatric patients with mediastinal lymphoma who were part of the TEDDI protocol [145] (Danish protocol number H-16035870, clinicaltrials.gov identifier NCT03315546) were selected for this study.

Treatment Planning

3 to 4 proton plans were created for each patient to investigate how the distribution of LET or RBE weighted dose changed with different beam angles (Figure 11):

- 1 beam: AP (0 degrees)
- 2 beams: AP-oblique (+/- 10 degrees from 0)
- 2 beams: wide AP-oblique (+/- 30 degrees from 0) (only for 1 male patient)
- 3 beams: AP-oblique (+/- 10 degrees from 0) and PA
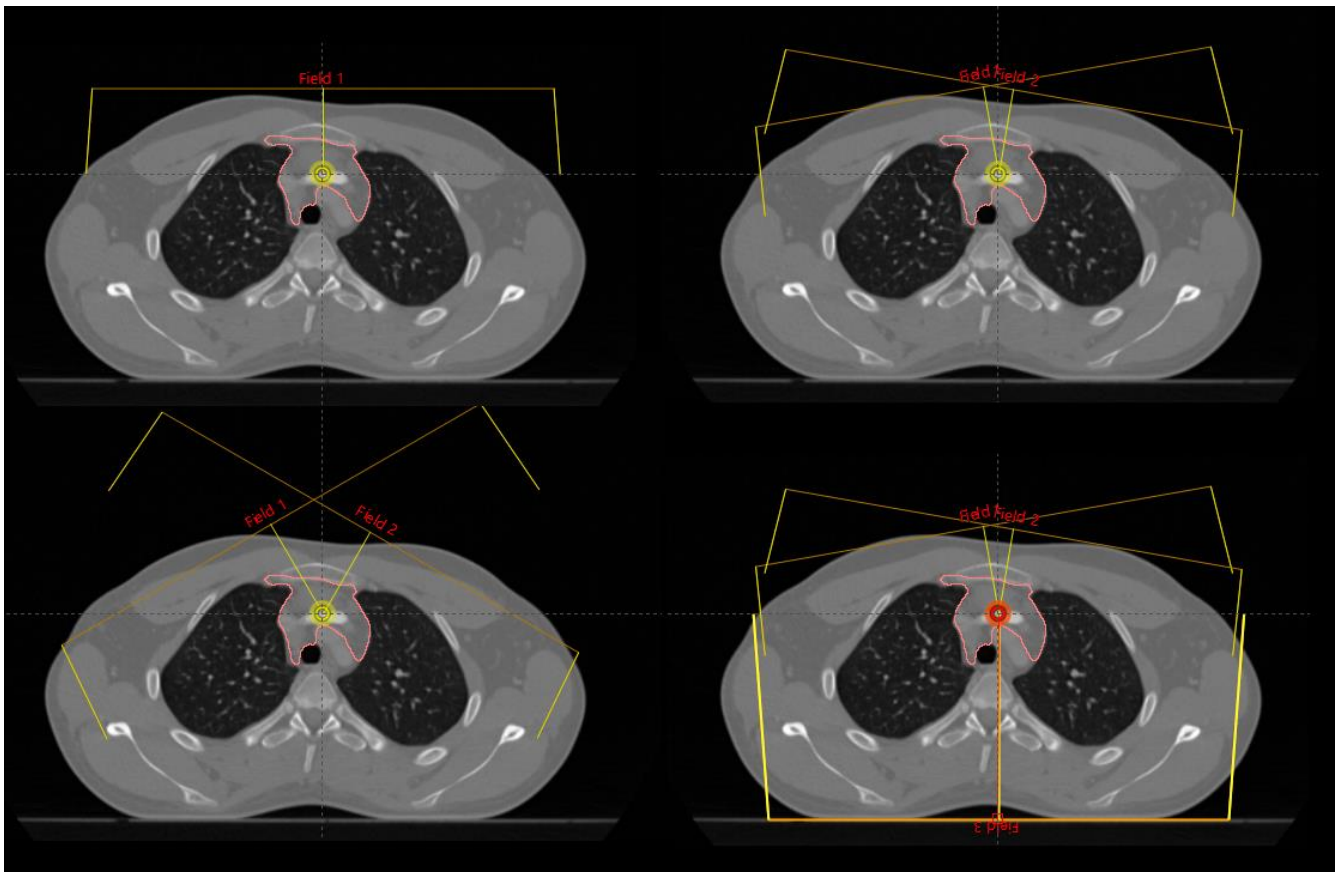
Figure 11. Beam arrangements used for treatment planning to investigate the distribution of LET for pediatric Hodgkin lymphoma patients. The wide AP-oblique beam arrangement (bottom left) was only used for the male patient. The CTV is shown in pink.

Planning was performed using spot scanning proton therapy with robust optimization to the CTV. SFO was used in most cases, but MFO was used for the 3-field plan for one patient who had target surrounding the heart. Robustness was optimized and evaluated with the assumption of 3.5% HU uncertainty and 5 mm positioning uncertainty. Priorities during planning were first CTV coverage,

then to reduce the dose to the heart and lungs as much as possible. Cardiac chambers, cardiac arteries, and female breasts were also contoured for analysis but were not used during optimization.

LET and RBE Calculation

The proton treatment plans created at Rigshospitalet were anonymized, exported, and imported to the system at Manchester in collaboration with Edward Smith and Adam Aitkenhead from the PRECISE research group, University of Manchester, Manchester, UK. Plans were pre-processed for file compatibility and exported to the AUTOMC Monte Carlo system, based in the Monte Carlo system Geant4 (Geometry And Tracking) [146] and the GATE (Geant4 Application for Emission Tomography)[147] toolkit. Monte Carlo simulations were run with an uncertainty of 1% in the high dose region and physical dose and dose-averaged LET were tracked. In order to convert LET into dose, the McNamara formula for variable RBE (vRBE) [143], with an assumed alpha/beta ratio of 2 Gy [101], was applied in post-processing step. Then matrices of LET, physical dose, vRBE, and vRBE-weighted dose were converted into DICOM format and imported back into the treatment planning system at Rigshospitalet for visualization and comparison.

4.3.2 Aim 3 Results: Proton LET and RBE for Hodgkin Lymphoma (Paper IV)

We found that, for the 3 pediatric patients with mediastinal Hodgkin lymphoma in our study, LET generally decreased as the number of beams increased (Figure 12).
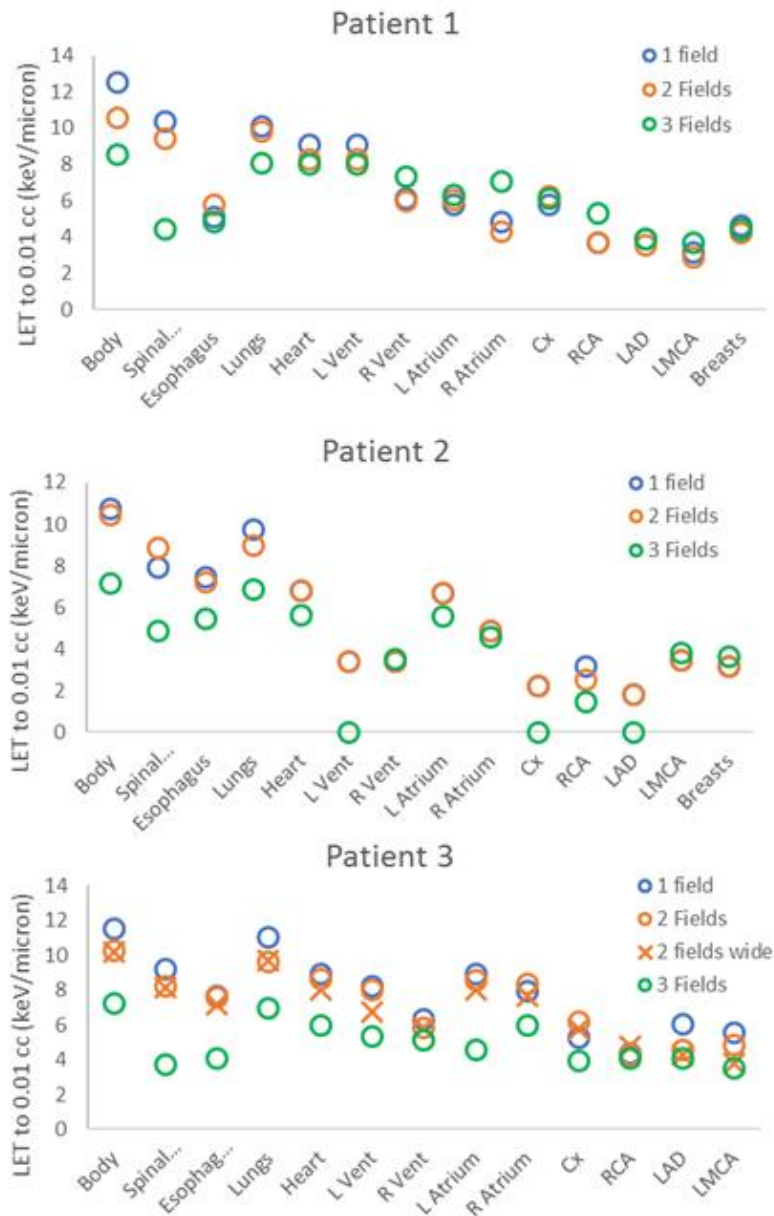
Figure 12. Near-maximum dose-averaged LET for OARs for different beam arrangements for the 3 patients in this study. OARs are listed in the order: body, spinal cord (Spinal…), esophagus, lungs, heart, left ventricle (L Vent), right ventricle (R Vent), left atrium (L Atrium), right atrium (R Atrium), circumflex artery (Cx), right coronary artery (RCA), left anterior descending artery (LAD), left main coronary artery (LMCA), breasts (for females).

When we converted physical dose and LET into vRBE weighted dose [143], we did not find clinically concerning differences for any beam arrangement. Most of the difference between the vRBE weighted dose and the TPS dose was from the use of Monte Carlo (Figures 13 and 14).
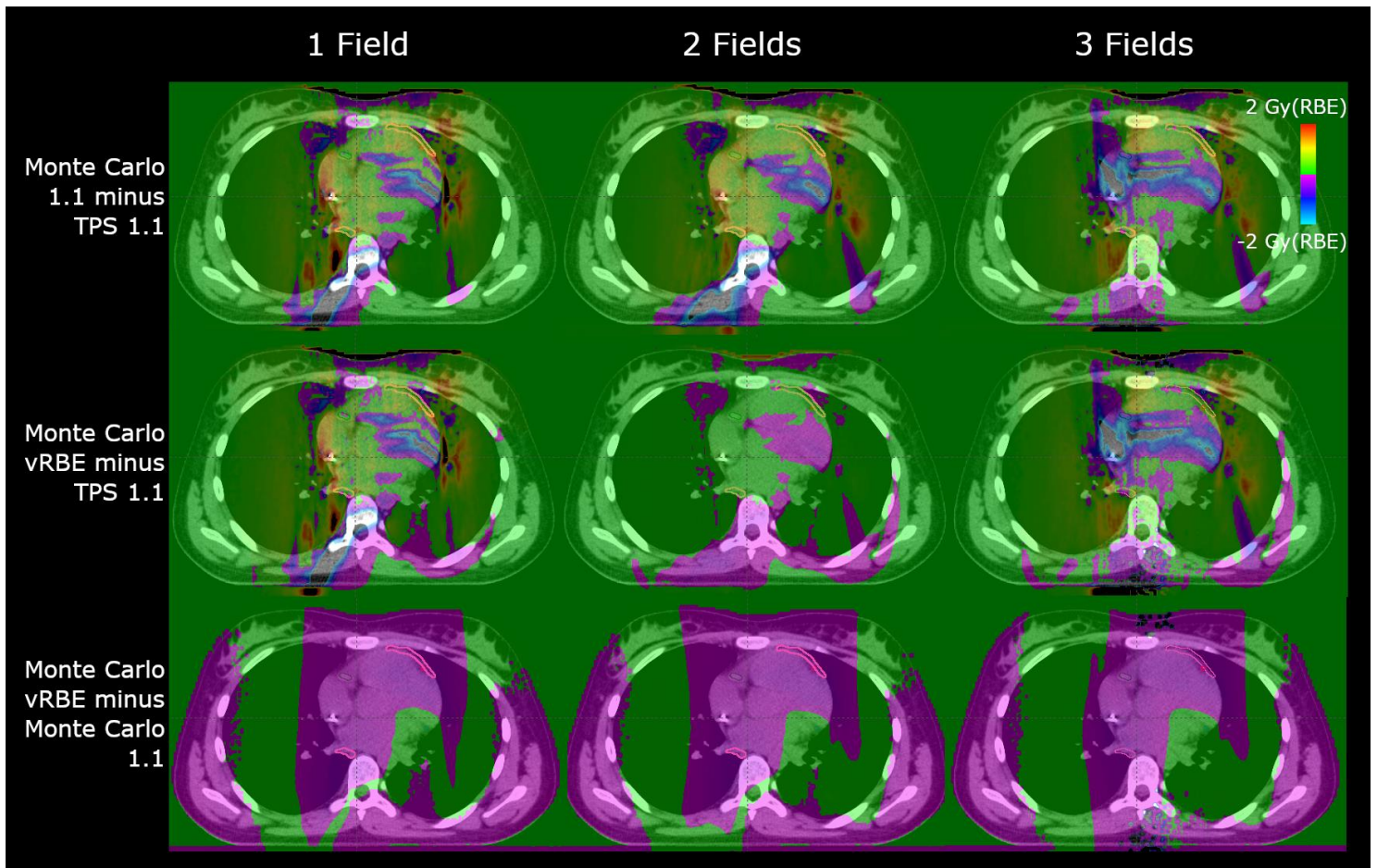
Figure 13. Dose difference distributions for patient 1 for plans with 1, 2, and 3 fields. The dose difference scale is from -2 to 2 Gy (RBE) (regions of black or clear are beyond the scale) and the CTV is shown in pink.
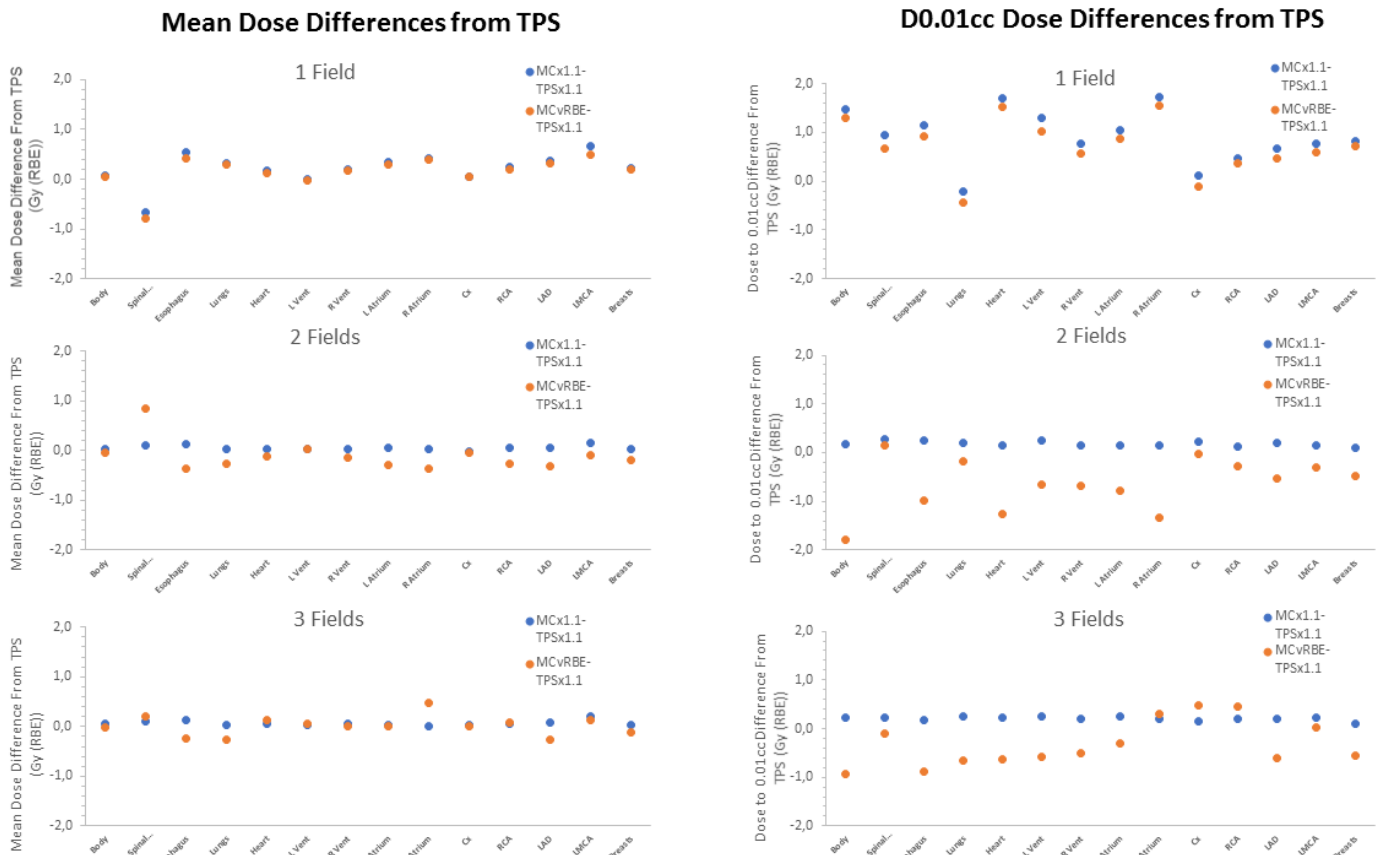
Figure 14. Mean and near-maximum (0.01cc) dose differences between MC dose with either fixed RBE of 1.1 or vRBE and the TPS dose with fixed RBE of 1.1 for patient 1. OARs are listed in the order: body, spinal cord (Spinal…), esophagus, lungs, heart, left ventricle (L Vent), right ventricle (R Vent), left atrium (L Atrium), right atrium (R Atrium), circumflex artery (Cx), right coronary artery (RCA), left anterior descending artery (LAD), left main coronary artery (LMCA), breasts (for females).

4.4 Methods and Results for Aim 4

4.4.1 Aim 4 Methods: Biological Optimization for Hodgkin Lymphoma (Paper V)

Aim 4 was to investigate a novel planning strategy for lymphoma, aiming to directly minimize the risk of both tumor recurrence and mortality from late effects by using an optimizer to create biologically optimized plans (Paper V). We collaborated with Arezoo Modiri and Amit Sawant from The University of Maryland, Baltimore, Maryland, USA who developed an in-house optimization algorithm [148] that could be adjusted and further developed for this study. We selected 34 patients with early-stage mediastinal Hodgkin lymphoma, who were older than 15 years, treated between 2005-2010, and were part of a previous retrospective study [149,150]

Pre-planning

Pre-planning before biological optimization was completed in a commercial treatment planning system (TPS) to provide beam options to the optimizer. 16 photon beam angles were used per patient with 4 fields per beam angle: 1 open, 3 subfields (Figure 15)**.** 6 MV was mostly used, but 18 MV was used for two patients. Preliminary doses were calculated in the TPS with equal beam

weighting. Pre-plans and doses were exported to an in-house code for further optimization as described below.
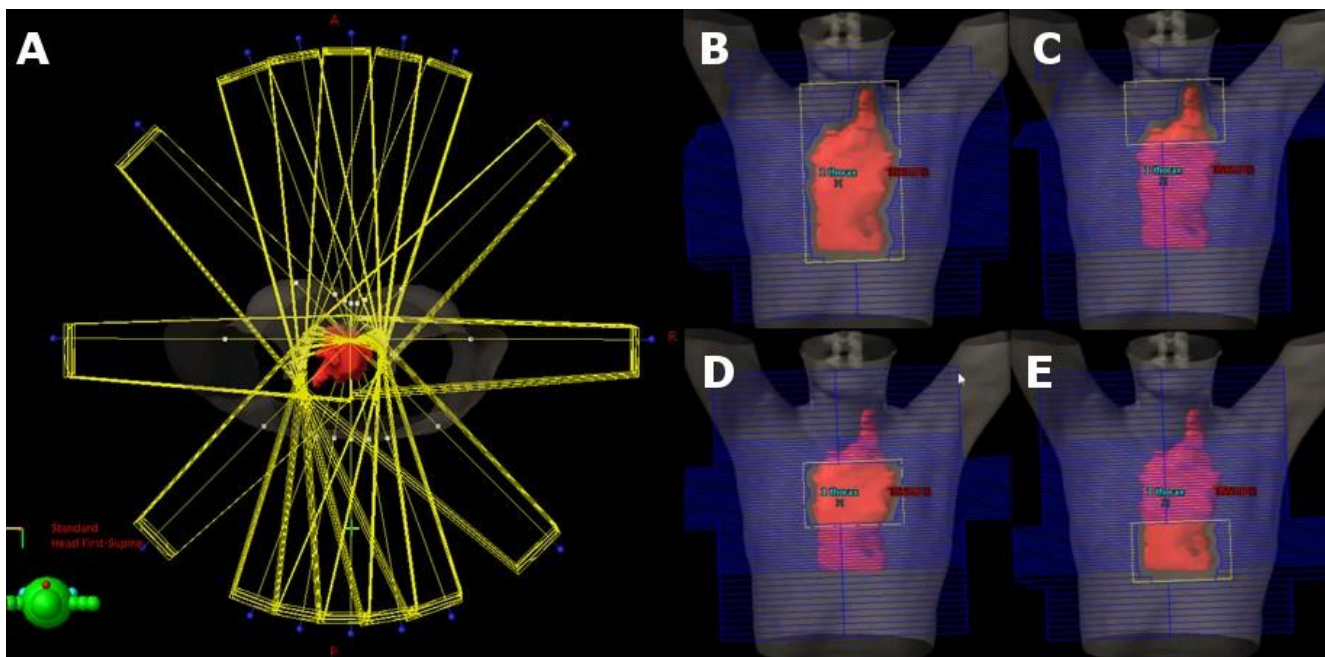
Figure 15. Beam options available to the optimizer created during pre-planning. A. Beam angles. B-E. Open and sub-fields for each beam angle.

Previously created (3-dimensional conformal radiotherapy) 3DCRT (clinical, most often AP-PA beam arrangement) and 2-arc VMAT [150] plans were also used for comparison. The prescription dose was 30.6 Gy in 17 fractions, and all plans were normalized to 30.6 Gy to the mean of the CTV to provide a consistent dose level for comparison in this study.

Outcome Modeling and Biological Optimization

To model the outcome of various endpoints, we selected the most recent follow-up studies available for patients who were treated for Hodgkin lymphoma. Hazard ratios (HRs) per Gy were estimated for secondary lung cancer, breast cancer (for females), coronary heart disease, and the risk of recurrence.

To model recurrence, progression free survival (PFS) at 5 years was obtained from randomized trials for different dose levels [34,129,130]. The hazard ratios (HRs) for 0 Gy (no radiotherapy) and 20 Gy were determined relative to 30.6 Gy, and the 'ideal' PFS at 5 years (for 30.6 Gy) was estimated to be 0.872. To avoid rewarding doses higher than 30.6 Gy, the dose to the CTV was calculated as a 'capped' mean dose, where any voxels above 30.6 Gy were set equal to 30.6 Gy. In addition, the generalized equivalent uniform dose (gEUD) concept was used for the dose to the CTV [151]. For the base analysis the gEUD parameter a was set to 1, but the parameter was also varied for sensitivity analysis.

To model normal tissue complications, HRs were estimated for secondary lung cancer [20], breast cancer [21] (for females), and coronary heart disease [16] (Table S1 in Paper V)), following a similar methodology to the LYL method [137] in Paper II.

To directly optimize on these concepts and create outcome-optimized (O-OPT) plans, penalty functions based on the risk models were created. The penalty function for the risk of disease recurrence was the difference of the plan-specific PFS from the 'ideal' PFS. The penalty function for normal tissue complications was the risk of the complication modulated by a mortality factor. The penalty functions for disease recurrence and mortality from normal tissue late effects were combined into a total objective function that was a proxy for "overall outcome." For details on models and penalty functions, see Paper V.

Optimization was performed with the Maryland in-house particle swarm optimization engine, implemented in MATLAB (R2016a, MathWorks, Matick, MA) [148]. The output of the optimizer was a list of monitor unit (MU) settings for each beam which defined the O-OPT plan for that patient. If the optimizer created a plan that was equal in risk or higher than the clinical 3DCRT plan, the clinical 3DCRT plan was chosen as the O-OPT plan.

To visualize the sensitivity of our results to model parameterization and optimization settings, we performed a sensitivity analysis for a few scenarios. First, an extreme value of -22 for the gEUD parameter was used for optimization for 9 patients to investigate the impact of setting a high importance on the minimum dose to the CTV. Then, for one patient, O-OPT plans were optimized for a range of values of the gEUD parameter and, conversely, the risk of recurrence for a range of values of the parameter was recalculated for when the value of 1 was assumed during optimization but was 'incorrect.' Finally, while the base analysis in this study focused on O-OPT plans that were optimized purely to minimize the total objective function, we also created (i) an O-OPT plan with a requirement that ≥90% of CTV receive the prescription dose and (ii) an O-OPT plan with a requirement of maximum dose of ≥40 Gy to avoid hot spots.

4.4.2 Aim 4 Results: Biological Optimization for Hodgkin Lymphoma (Paper V)

In Paper V, we found that biological optimization for lymphoma patients could benefit some, but not all, patients in our study relative to VMAT or clinical 3DCRT plans (Figure 16). In addition, we found that, for patients who had a large benefit from biological optimization, outcome-optimized (O-OPT) plans were substantially different than the clinical routine, and made large sacrifices to tumor coverage to lower dose to the heart and lungs (Figure 17). Furthermore, sensitivity analysis of our methods revealed large differences in both plan outcome (Figure 18) and estimated risk of recurrence, depending on which parameters were chosen during optimization or calculation.
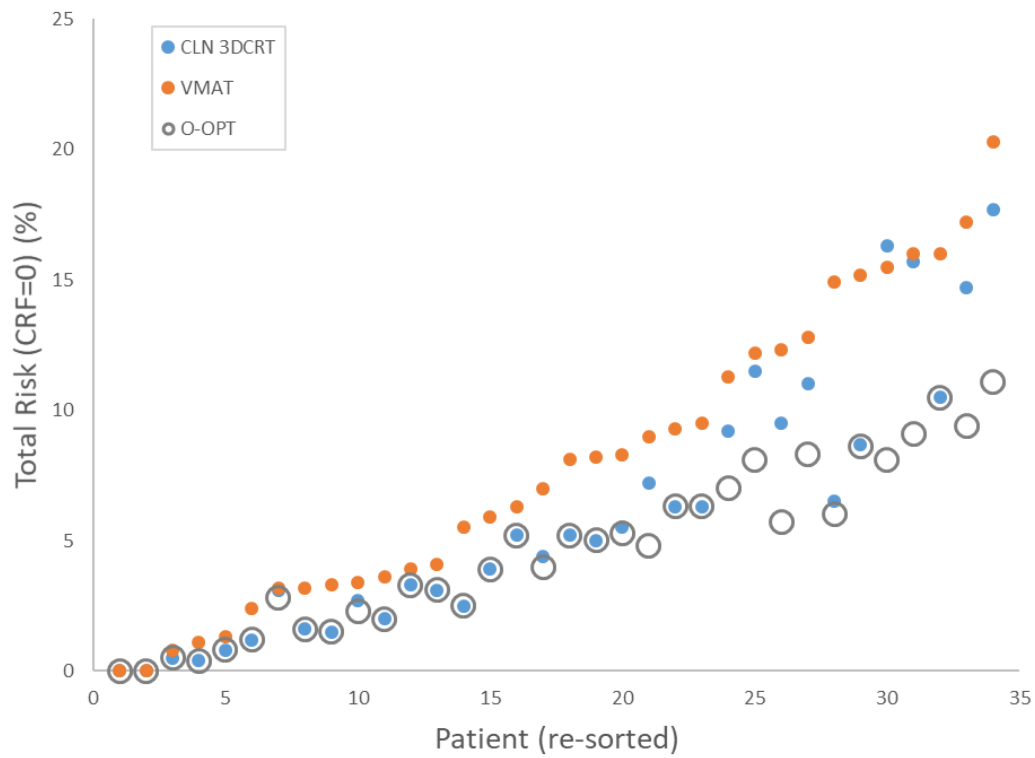
Figure 16. Total risk (recurrence and mortality from late effects) for each patient for each type of plan: clinical (CLN) 3DCRT, VMAT, and O-OPT (assuming no cardiac risk factors (CRF)). Patients are sorted by VMAT risk. Total risk includes risks of recurrence and mortality from lung cancer, breast cancer (females), and coronary heart disease.

Clinical Plan **Outcome-Optimized Plan**
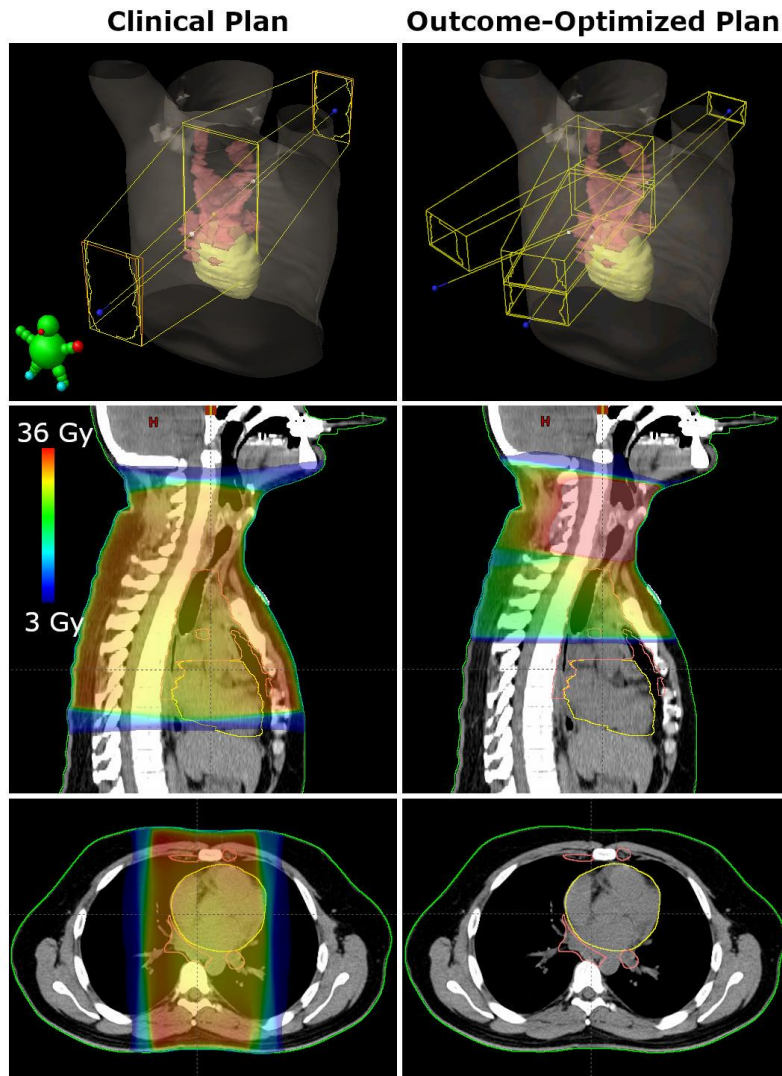
Figure 17. Example of a patient with a large benefit from outcome-optimized (O-OPT) planning compared to the clinical 3DCRT plan, where the inferior target coverage was sacrificed to reduce the dose to the heart and lungs. The CTV is shown in pink and the heart is shown in yellow.
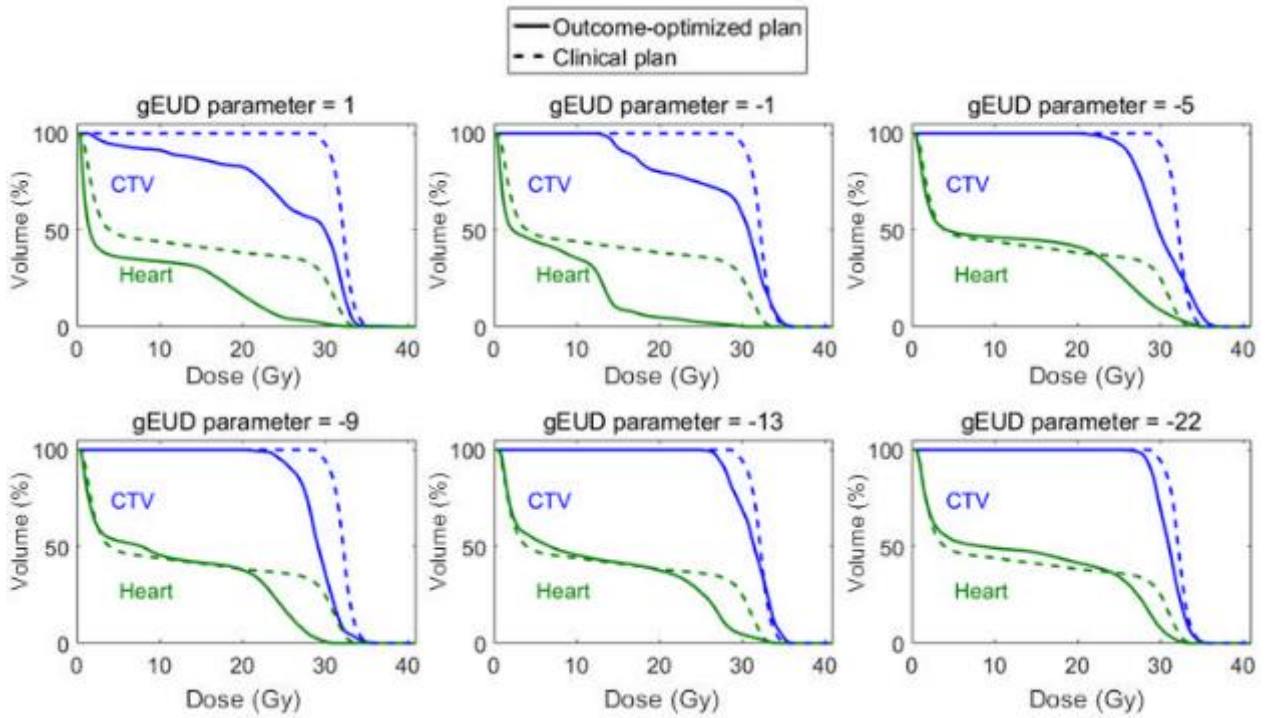
Figure 18. Dose-volume histograms (DVHs) showing the difference in O-OPT plans (CRF=0 with hot-spot avoidance requirement) with respect to gEUD parameter choice in target model for O-OPT planning for one patient (patient 25). The DVHs from the clinical 3CDRT plan are shown in dotted lines.

5. Discussion

This thesis was designed to investigate how we can use existing and future technologies to provide the best possible radiotherapy with the lowest possible doses to normal tissues for patients with mediastinal disease.

In aim 1, we calculated the CTV-to-PTV margin for patients with mediastinal lymphoma treated at our institution with photon therapy, DIBH, and daily CBCT. A limitation of this work was the estimation of contouring and intra-fractional uncertainties from the literature. Contouring uncertainty was estimated from lymphoma patients, but in free breathing [133]. Intra-fractional motion uncertainty was estimated from breast cancer patients treated in DIBH [134], not lymphoma patients. It would have been more ideal to have used data that matched our patient group in both tumor type and treatment techniques, but that data was not available. The inclusion of contouring uncertainty into margin calculations remains controversial, and we evaluated the margins with a range of assumed values for contouring uncertainty (including 0 mm). We also recognize that margin recipes are only one approach to the issue of geometric uncertainties in radiotherapy, and they are designed to prioritize target coverage. An alternative approach to balancing target coverage and dose to normal tissue could be probabilistic planning [152,153], which we did not investigate here.

In aim 2, we investigated the potential of DIBH and proton therapy to reduce the dose to normal tissue for patients with Hodgkin lymphoma and thymic cancer. One limitation of our methods for these studies was that we did not have access to 4-dimensional CT (4DCT) scans, only free breathing or DIBH scans. Therefore, the extent of breathing motion in free breathing was not able to be accounted for and internal target volumes (ITVs) could not be created. In the study with Hodgkin lymphoma patients, breathing motion was accounted for by using an additional 5 mm for the margin in the superior-inferior direction for the free breathing scans [44]. However, while a larger margin for free breathing is used clinically at Rigshospitalet, we felt that it might slightly bias the treatment planning study towards DIBH. Therefore, in our study for thymic cancer we opted to use a uniform 1 cm margin for both free breathing and DIBH. Both approaches have advantages and disadvantages, and it is unclear which approach is best. Furthermore, there are special considerations for moving targets and proton therapy [66,154–156]. For example, anatomical changes during breathing contribute to range uncertainty of the protons, which can further increase the dose to normal tissue. Due to lack of 4DCT scans, we were not able to model patient-specific breathing motion or the interplay effect for our studies, which could be a factor for delivering proton therapy in free breathing [110,157]. Similarly, for proton therapy in DIBH, we did not investigate the impact of breaking up a proton treatment field between multiple breath holds or the impact of intra-fractional motion, which potentially creates a type of interplay effect, but appears to be manageable [158].

In aim 3, we investigated biological uncertainties in the dose from proton therapy for pediatric patients with Hodgkin lymphoma for different beam angles. This study was very small, with only 3 patients, so can only be considered exploratory. One major limitation of this type of study is that the uncertainties of the models and parameters (e.g. the alpha/beta ratio) to calculate vRBE are very large, and little consensus exists on what models or parameters to use. Furthermore, multiple vRBE models are available in the literature [102,159,160], and more will be developed in the future. This type of study should be revisited if new evidence points towards a different vRBE model or tissue parameter. Nevertheless, while uncertainties remain, we decided that it would be prudent to look for any obvious issues with vRBE weighted dose or LET distribution for this patient group, which, at this point, we did not observe.

Finally, in aim 4, we designed an optimizer to create biologically optimized (photon) plans for patients with Hodgkin lymphoma to minimize the risk of both tumor recurrence and mortality from late effects. This study was the most exploratory of the thesis and produced results that were unusual when compared to clinical routine. While this was interesting scientifically, the tumor control model in our study was not built from data that included partial target coverage, which would be very difficult data to produce. Until a tumor control model that has been validated for partial target coverage becomes available, an alternative could be to require adequate target coverage and optimize only on normal tissue complications. In addition, large maximum doses in optimized plans revealed the need for more optimization objectives or constraints to protect the patient from acute toxicities or overdoses in regions that were not contoured as an OAR.

One recent publication has cast a bit of doubt on a central assumption of this thesis: that reducing dose to normal tissue reduces the risk of late effect like secondary cancer. That study from Schaapveld et al. [27] found that the risk of secondary solid cancer was not lower for patients treated for Hodgkin lymphoma in the more recent era (1989-2000) than the earlier eras (1965–1976 and 1977–1988). Radiation treatments have decreased in both intensity and volume of tissue in the more recent eras, so this was a surprising finding. However, their study did not differentiate between type of treatment (chemotherapy, radiation, or both) in the analysis of different eras, and they used death as a competing risk, even though death rates could differ between eras. The authors also point out that it is possible that the less intense radiotherapy regimes may not have been wide-spread enough in the 1990s to have produced a difference in risk. A similar analysis of treatments from the 2000s might yield a different result, but the follow-up data from that era is not yet mature enough to analyze. A few subgroups did have a reduced risk: men treated in the most recent era were at a reduced risk of secondary lung cancer, and women who had less extensive supradiaphragmatic fields were at a reduced risk of breast cancer. The authors concluded that patients treated for Hodgkin lymphoma in the 1990s were still at a significant risk of secondary cancer, and that *further* reduction of radiation dose and avoidance of high-dose procarbazine chemotherapy is the best way to achieve a reduced risk of secondary cancers. Therefore, while this study was surprising and emphasizes the need for further detailed research to better understand how changes and developments in cancer therapy effect patients, we will continue to strive to reduce radiation dose to normal tissue in the hopes of improving long-term outcomes for cancer survivors.

There are multiple ways this thesis could impact the clinical practice at Rigshospitalet. For example, our clinical CTV-to-PTV margin for patients with mediastinal lymphoma treated with DIBH and daily IGRT was already 1 cm, so while our study from aim 1 did not revise our practice, it provided validation and justification for its continuation. In addition, aim 2 provided insight into benefits of DIBH and proton therapy (alone and combined) for patients with mediastinal cancer. For patients with Hodgkin lymphoma, our study has inspired an interest in our clinic in proton therapy, but specifically in combination with DIBH. For patients with thymoma, our study has inspired an interest in our clinic in proton therapy with or without DIBH. We hope that our results will be informative when a formal procedure for referring patients with Hodgkin lymphoma or thymic epithelial tumors to proton therapy in Denmark is created.

6. Conclusions and Future Perspectives

Through this body of work, we elucidated how to best apply current and future technologies in radiotherapy to reduce the doses to OARs for patients with cancer in the mediastinum.

First, we found that the CTV-to-PTV margin needed for patients with Hodgkin lymphoma treated at our institution with the state-of-the-art technologies of IGRT and DIBH is approximately 1 cm. Using an appropriate margin for the combination of technologies and clinical practices for a specific patient group ensures both target coverage and that normal tissues are protected as much as reasonably achievable (by using no larger margin than necessary).

Margin evaluation is a constantly evolving effort and this conclusion would need to be updated with changes in technology, clinical procedures, or available evidence in the literature. For example, if newer on-board imaging systems have improved image quality or image matching software, or if improvements to patient immobilization are implemented, setup uncertainty would need to be reanalyzed. Furthermore, the assumed values for contouring uncertainty or intra-fractional uncertainty should be updated if data becomes available that better matches this patient group and the technologies applied. To address the gap in knowledge of the lack of intra-fractional and intra breath-hold uncertainties for this patient group, we have planned and received funding for a prospective protocol for patients with mediastinal lymphoma to be treated on the MR-linac. Cine MRI images will be acquired to evaluate the position of anatomical features like the sternum, heart, and diaphragm throughout the entire treatment. Finally, the concept of a PTV could be challenged by other concepts like risk-based or probabilistic planning to consider the probabilities of target coverage in balance with probabilities of normal tissue complications. These concepts are not dissimilar from what we investigated in aim 4, but as we discussed in that study, detailed and validated models must be available for that type of planning to be safe to use clinically.

Second, we investigated the techniques of DIBH and proton therapy, compared to free breathing and photon therapy, for patients with mediastinal Hodgkin lymphoma and thymic cancer. While both DIBH and proton therapy appeared to be beneficial to some degree, our conclusions were different for the two patient groups. For patients with Hodgkin lymphoma, proton therapy in DIBH resulted in the lowest doses to OARs. When proton therapy in free breathing was compared to IMRT in DIBH, no statistically significant differences were observed, and there was a large variation between patients. For patients with thymic cancer, the use of proton therapy had the largest impact on the doses to OARs, and the use of DIBH compared to free breathing did not show statistically significant differences. Therefore, if proton therapy was available with free breathing (but *not* with DIBH), and photon therapy was available *with* DIBH, it is conceivable that the best choice between those two options could be different for the two disease sites: photon therapy in DIBH could be the best choice for a patient with Hodgkin lymphoma, and proton therapy in free breathing could be the best choice for a patient with thymic cancer.

In my opinion, the results for proton therapy for patients with Hodgkin lymphoma and thymic cancers were promising enough to warrant consideration of referral to proton therapy. Therefore, one future direction of this work could focus on designing methods for patient selection for these two disease sites. To select individual patients, a model-based approach [161,162] could be used, and the risk of late effects could be incorporated, especially for young patients. An alternative is that patients with Hodgkin lymphoma and thymic cancers could be part of randomized clinical trials comparing proton therapy and photon therapy, but there are challenges with the ethics of equipoise, the accrual of enough patients for adequately powered studies (especially for thymic cancers), and the time before the longer-term results of the trials would be available.

Third, we examined one of the uncertainties associated with proton therapy: biological uncertainty from LET and vRBE. We investigated the distribution of LET for three patients for different beam arrangements and calculated vRBE-weighted dose. While there were differences between the dose from the TPS (assuming an RBE of 1.1) and the dose calculated with Monte Carlo with vRBE, the differences were not very large, and were mostly from the use of Monte Carlo, not vRBE. However, this issue should be revisited in the future if new data regarding vRBE model or tissue-specific parameters become available. The incorporation of LET and vRBE calculations into commercial TPSs is only at the very beginning, and how to apply these models is still under discussion. The calculation of LET and vRBE might become routine in the near future, but based on our small study, it does not seem to be especially critical to implement for patients with mediastinal Hodgkin lymphoma. More critical would be to implement Monte Carlo dose calculation into commercial TPSs, which is now becoming available.

Finally, we investigated biological optimization for patients with Hodgkin lymphoma to minimize both tumor recurrence and the risk of mortality from late effects. We found that we could reduce the risk for some patients, but there were large uncertainties and sensitivities to models and parameterization. Therefore, while this study did not produce a technique that is ready for clinical use, it provided a step towards understanding how to apply this type of technique for this patient group and the associated uncertainties, limitations, and areas of caution needed in future research. To include risk of recurrence in a clinically-viable optimization algorithm that allows partial coverage of the CTV, we would need build a model from data in that context. One way to collect data on recurrence after partial CTV coverage would be to register rare cases in which a clinician made the choice to leave out part if the initially involved volume due to the patient's history, response to treatment, or anatomy. If these rare clinical compromises were logged and registered with an international organization like ILROG, it could be possible to eventually complete an analysis of how partial radiotherapy coverage of initially involved sites correlates with the risk of recurrence.

Today, efforts to estimate the impact of reductions of dose to OARs on the risk of side effects are limited by crude risk models. Many models are built on estimates of mean doses to organs and cannot distinguish between a small dose to a large volume or a large dose to a small volume. With increasing storage and computing power, the utilization of big data could revolutionize radiotherapy risk models and provide levels of detail that could vastly improve our ability to make predictions about outcomes. Furthermore, the field of radiomics [163] could identify early imaging markers of treatment response and toxicity, and enable us to make personalized decisions about a patient's ongoing treatment or follow-up care.

References

[1] Bentzen SM, Constine LS, Deasy JO, Eisbruch A, Jackson A, Marks LB, et al. Quantitative Analyses of Normal Tissue Effects in the Clinic (QUANTEC): An Introduction to the Scientific Issues. Int J Radiat Oncol Biol Phys 2010;76:3–9. doi:10.1016/j.ijrobp.2009.09.040.

[2] Emami B. Tolerance of Normal Tissue to Therapeutic Radiation. Reports Radiother Oncol 2013;1:35–48.

[3] Committee to Assess Health Risks from Exposure to Low Levels of Ionizing Radiation. Health Risks from Exposure to Low Levels of Ionizing Radiation - BEIR VII Phase 2. 2006. doi:10.1093/rpd/ncr278.

[4] Sachs RK, Brenner DJ. Solid tumor risks after high doses of ionizing radiation. Proc Natl Acad Sci U S A 2005;102:13040–5. doi:10.1073/pnas.0506648102.

[5] Mulrooney DA, Yeazel MW, Kawashima T, Mertens AC, Mitby P, Stovall M, et al. Cardiac outcomes in a cohort of adult survivors of childhood and adolescent cancer: retrospective analysis of the Childhood Cancer Survivor Study cohort. BMJ 2009;339:b4606. doi:10.1136/bmj.b4606.

[6] Friedman DL, Whitton J, Leisenring W, Mertens AC, Hammond S, Stovall M, et al. Subsequent neoplasms in 5-year survivors of childhood cancer: The childhood cancer survivor study. J Natl Cancer Inst 2010;102:1083–95.

[7] Castellino SM, Geiger AM, Mertens AC, Leisenring WM, Tooze JA, Goodman P, et al. Morbidity and mortality in long-term survivors of Hodgkin lymphoma : a report from the Childhood Cancer Survivor Study. Blood 2010;117:1806–17. doi:10.1182/blood-2010-04-278796.An.

[8] Mertens AC, Liu Q, Neglia JP, Wasilewski K, Leisenring W, Armstrong GT, et al. Cause-Specific Late Mortality Among 5-Year Survivors of Childhood Cancer : The Childhood Cancer Survivor Study 2015;100. doi:10.1093/jnci/djn310.

[9] Grantzau T, Overgaard J. Risk of second non-breast cancer after radiotherapy for breast cancer: A systematic review and meta-analysis of 762,468 patients. Radiother Oncol 2015;114:56–65. doi:10.1016/j.radonc.2014.10.004.

[10] Marks LB, Bentzen SM, Deasy JO, Kong F-MS, Bradley JD, Vogelius IS, et al. Radiation dose-volume effects in the lung. Int J Radiat Oncol Biol Phys 2010;76:S70-6. doi:10.1016/j.ijrobp.2009.06.091.

[11] Rubin P, Constine LS, Marks Lawrence B L. ALERT-- Adverse Late Effects of Cancer Treatment, Volume 2, Normal Tissue Specific Sites and Systems. Heidelberg: Springer; 2014.

[12] Pinnix CC, Smith GL, Milgrom S, Osborne EM, Reddy JP, Akhtari M, et al. Predictors of radiation pneumonitis in patients receiving intensity modulated radiation therapy for Hodgkin and non-hodgkin lymphoma. Int J Radiat Oncol Biol Phys 2015;92. doi:10.1016/j.ijrobp.2015.02.010.

[13] Werner-Wasik M, Yorke E, Deasy J, Nam J, Marks LB. Radiation Dose-Volume Effects in the Esophagus. Int J Radiat Oncol Biol Phys 2010;76:86–93. doi:10.1016/j.ijrobp.2009.05.070.

[14] Werner-Wasik M. Treatment-related esophagitis. Semin Oncol 2005;32:60–6. doi:10.1053/j.seminoncol.2005.03.011.

[15] Cutter DJ, Schaapveld M, Darby SC, Hauptmann M, van Nimwegen F a, Krol ADG, et al. Risk of valvular heart disease after treatment for hodgkin lymphoma. J Natl Cancer Inst 2015;107:1–9. doi:10.1093/jnci/djv008.

[16] Van Nimwegen FA, Schaapveld M, Cutter DJ, Janus CPM, Krol ADG, Hauptmann M, et al. Radiation dose-response relationship for risk of coronary heart disease in survivors of Hodgkin lymphoma. J Clin Oncol 2016;34:235–43. doi:10.1200/JCO.2015.63.4444.

[17] Aleman BMP, van den Belt-Dusebout AW, De Bruin ML, van 't Veer MB, Baaijens MH a, de Boer JP, et al. Late cardiotoxicity after treatment for Hodgkin lymphoma. Blood 2007;109:1878–86. doi:10.1182/blood-2006-07-034405.

[18] Miltényi Z, Keresztes K, Garai I, Edes I, Galajda Z, Tóth L, et al. Radiation-induced coronary artery disease in Hodgkin's disease. Cardiovasc Radiat Med 2004;5:38–43. doi:10.1016/j.carrad.2004.04.004.

[19] Ng AK, Bernardo MVP, Weller E, Backstrand K, Silver B, Marcus KC, et al. Second malignancy after Hodgkin disease treated with radiation therapy with or without chemotherapy : long-term risks and risk factors. Blood 2002;100:1989–96. doi:10.1182/blood-2002-02-0634.Supported.

[20] Travis LB, Gospodarowicz M, Curtis RE, Clarke EA, Andersson M, Glimelius B, et al. Lung Cancer Following Chemotherapy and Radiotherapy for Hodgkin's Disease. J Natl Cancer Inst 2002;94.

[21] Travis LB, Hill DA, Dores GM. Breast Cancer Following Radiotherapy and Chemotherapy Among Young Women With Hodgkin Disease. JAMA 2003;290:465–75.

[22] Franklin J, Pluetschow a, Paus M, Specht L, Anselmo a-P, Aviles a, et al. Second malignancy risk associated with treatment of Hodgkin's lymphoma: meta-analysis of the randomised trials. Ann Oncol 2006;17:1749–60. doi:10.1093/annonc/mdl302.

[23] Bright CJ, Reulen RC, Winter DL, Stark DP, Mccabe MG, Edgar AB, et al. Risk of subsequent primary neoplasms in survivors of adolescent and young adult cancer (Teenage and Young Adult Cancer Survivor Study): a population-based , cohort study. Lancet Oncol 2019;20:531–45. doi:10.1016/S1470-2045(18)30903-3.

[24] Rubin P, Constine LS, Marks Lawrence B L. ALERT-- adverse late effects of cancer treatment, Volume 1, General concepts and specific precepts. Berlin: Springer; 2014.

[25] Swerdlow AJ, Barber JA, Hudson GV, Cunningham D, Gupta RK, Hancock BW, et al. Risk of Second Malignancy After Hodgkin's Disease in a Collaborative British Cohort: The Relation to Age at Treatment. J Clin Oncol 2000;18:498. doi:10.1200/JCO.2000.18.3.498.

[26] Hodgson DC, Gilbert ES, Dores M, Schonfeld SJ, Lynch CF, Storm H, et al. Long-Term Solid Cancer Risk Among 5-Year Survivors of Hodgkin's Lymphoma. J Clin Oncol 2007;25:1489–97. doi:10.1200/JCO.2006.09.0936.

[27] Schaapveld M, Aleman BMP, van Eggermond AM, Janus CP, Krol ADG et al. Second Cancer Risk Up to 40 Years after Treatment for Hodgkin's Lymphoma. N Engl J Med 2015;373:2499–511. doi:10.1056/NEJMoa1505949.

[28] Eichenauer DA, Aleman BMP, André M, Federico M, Hutchings M, Illidge T, et al. Hodgkin lymphoma: ESMO Clinical Practice Guidelines for diagnosis, treatment and follow-up. Ann Oncol 2018;29:iv19–29. doi:10.1093/annonc/mdy080.

[29] Jaglowski SM, Linden E, Termuhlen AM, Flynn JM. Lymphoma in Adolescents and Young Adults. Semin Oncol 2009;36:381–418. doi:10.1053/j.seminoncol.2009.07.009.

[30] NORDCAN - Cancer statistics for the Nordic countries. Assoc Nord Cancer Regist 2009. http://www-dep.iarc.fr/NORDCAN/english/frame.asp (accessed October 10, 2019).

[31] Bleyer A. Cancer in 15- to 29-Year-Olds by Primary Site. Oncologist 2006;11:590–601. doi:10.1634/theoncologist.11-6-590.

[32] Specht L, Gray R, Clarke M, Peto R. The influence of more extensive radiotherapy and adjuvant chemotherapy on long-term outcome of early stage Hodgkin's disease: A meta-analysis of 23 randomized trials involving 3888 patients. J Clin Oncol 1998;16:830–43.

[33] Picardi M, De Renzo A, Pane F, Nicolai E, Pacelli R, Salvatore M, et al. Randomized comparison of consolidation radiation versus observation in bulky Hodgkin's lymphoma with post-

chemotherapy negative positron emission tomography scans. Leuk Lymphoma 2007;48:1721–7. doi:10.1080/10428190701559140.

[34] Herbst C, Rehan FA, Brillant C, Bohlius J, Skoetz N, Schulz H, et al. Combined modality treatment improves tumor control and overall survival in patients with early stage Hodgkin's lymphoma: a systematic review. Haematologica 2010;95:494 LP – 500.

[35] Radford J, Illidge T, Counsell N, Hancock B, Pettengell R, Johnson P, et al. Results of a Trial of PET-Directed Therapy for Early-Stage Hodgkin's Lymphoma. N Engl J Med 2015;372:1598–607. doi:10.1056/NEJMoa1408648.

[36] Olszewski AJ, Shrestha R, Castillo JJ. Treatment Selection and Outcomes in Early-Stage Classical Hodgkin Lymphoma : Analysis of the National Cancer Data Base. J Clin Oncol 2016;33:625–33.

[37] André M, Girinsky T, Federico M, Reman O, Fortpied C, Gotti M, Casasnovas O, Brice P, van der Maazen R, Re A, Edeline V, Fermé C, van Imhoff G, Merli F, Bouabdallah R, Sebban C, Specht L, Stamatoullas A, Delarue R, Bellei M, Raveloarivahy T, Versari A, Hu RJ. Early PET response adapted treatment in stage I-II Hodgkin lymphoma: Final results of the the randomized EORTC/LYSA/FIL H10 trial. J Clin Oncol 2017;in press.

[38] Koh ES, Tran TH, Heydarian M, Sachs RK, Tsang RW, Brenner DJ, et al. A comparison of mantle versus involved-field radiotherapy for Hodgkin's lymphoma: Reduction in normal tissue dose and second cancer risk. Radiat Oncol 2007;2:1–11. doi:10.1186/1748-717X-2-13.

[39] Engert A, Schiller P, Josting A, Herrmann R, Koch P, Sieber M, et al. Involved-field radiotherapy is equally effective and less toxic compared with extended-field radiotherapy after four cycles of chemotherapy in patients with early-stage unfavorable Hodgkin's lymphoma: Results of the HD8 trial of the German Hodgkin's lymph. J Clin Oncol 2003;21:3601–8. doi:10.1200/JCO.2003.03.023.

[40] Kriz J, Spickermann M, Lehrich P, Schmidberger H, Reinartz G, Eich H, et al. Breath-hold technique in conventional APPA or intensity-modulated radiotherapy for Hodgkin's lymphomaAtemanhaltetechnik in tiefer Inspiration bei konventioneller APPA oder intensitätsmodulierter Radiotherapie beim Hodgkin-Lymphom. Strahlentherapie Und Onkol 2015;191:717–25. doi:10.1007/s00066-015-0839-x.

[41] Glanzmann C, Kaufmann P, Jenni R, Hess OM, Huguenin P. Cardiac risk after mediastinal irradiation for Hodgkin's disease. Radiother Oncol 1998;46:51–62. doi:10.1016/S0167-8140(97)00125-4.

[42] Ibrahim EM, Kazkaz GA, Abouelkhair KM, Bayer AM, Elmasri OA. Increased Risk of Second Lung Cancer in Hodgkin ' s Lymphoma Survivors : A Meta-analysis. Lung 2013;191:117–34. doi:10.1007/s00408-012-9418-4.

[43] Yeoh K-W, Mikhaeel NG. Role of Radiotherapy in Modern Treatment of Hodgkin's Lymphoma. Adv Hematol 2011;2011. doi:10.1155/2011/258797.

[44] Specht L, Yahalom J, Illidge T, Berthelsen AK, Constine LS, Eich T, et al. Modern radiation therapy for Hodgkin lymphoma: Field and dose guidelines from the international lymphoma radiation oncology group (ILROG). Int J Radiat Oncol Biol Phys 2014;89:854–62. doi:10.1016/j.ijrobp.2013.05.005.

[45] Maraldo M V, Jørgensen M, Brodin NP, Aznar MC, Vogelius IR, Petersen PM, et al. The Impact of Involved Node, Involved Field and Mantle Field Radiotherapy on Estimated Radiation Doses and Risk of Late Effects for Pediatric Patients with Hodgkin Lymphoma. Pediatr Blood Cancer 2014;61:717–22. doi:10.1002/pbc.

[46] Maraldo M V, Specht L. A Decade of Comparative Dose Planning Studies for Early-Stage Hodgkin Lymphoma : What Can We Learn ? Int J Radiat Oncol 2014;90:1126–35.

[47] Specht L, Yahalom J. The concept and evolution of involved site radiation therapy for lymphoma.

Int J Clin Oncol 2015;20:849–54. doi:10.1007/s10147-015-0863-y.

[48]   Maraldo M V, Dabaja BS, Filippi AR, Illidge T, Tsang R, Ricardi U, et al. Radiation Therapy Planning for Early-Stage Hodgkin Lymphoma : Experience of the International Lymphoma Radiation Oncology Group n.d.;92:144–52.

[49]   Witkowska M, Majchrzak A, Smolewski P. The Role of Radiotherapy in Hodgkin's Lymphoma: What Has Been Achieved during the Last 50 Years? Biomed Res Int 2015;2015:1–8. doi:10.1155/2015/485071.

[50]   Specht L. Radiotherapy for Hodgkin Lymphoma: Reducing Toxicity while Maintaining Efficacy. Cancer J (United States) 2018;24:237–43. doi:10.1097/PPO.0000000000000332.

[51]   SEER. SEER 9, 13, and 18. Natl Cancer Institute's Surveillance, Epidemiol End Results Progr 2006. www.seer.cancer.gov.

[52]   Engels EA. Epidemiology of thymoma and associated malignancies Eric. J Thorac Oncol 2010;5:S260–S265. doi:10.1097/JTO.0b013e3181f1f62d. Epidemiology.

[53]   Wilkins KB, Sheikh E, Green R, Patel M, George S, Takano M, et al. Clinical and pathologic predictors of survival in patients with thymoma. Ann Surg 1999;230:562.

[54]   Girard N, Ruffini E, Marx A, Faivre-Finn C, Peters S. Thymic epithelial tumours: ESMO Clinical Practice Guidelines for diagnosis, treatment and follow-up. Ann Oncol 2015;26:v40–55. doi:10.1093/annonc/mdv277.

[55]   Patel S, MacDonald OK, Nagda S, Bittner N, Suntharalingam M. Evaluation of the role of radiation therapy in the management of malignant thymoma. Int J Radiat Oncol Biol Phys 2012;82:1797–801. doi:10.1016/j.ijrobp.2011.03.010.

[56]   Parker RP, Hobday PA, Cassell KJ. The direct use of CT numbers in radiotherapy dosage calculations for inhomogeneous media. Phys Med Biol 1979;24:802–9. doi:10.1088/0031-9155/24/4/011.

[57]   Galkin BM, Wu RK, Suntharalingam N. Improved Technique for Obtaining Teletherapy Portal Radiographs with High-Energy Photons. Radiology 1978;127:828–30. doi:10.1148/127.3.828.

[58]   Pisani L, Lockman D, Jaffray D, Yan D, Martinez A, Wong J. Setup error in radiotherapy: On-line correction using electronic kilovoltage and megavoltage radiographs. Int J Radiat Oncol Biol Phys 2000;47:825–39. doi:10.1016/S0360-3016(00)00476-4.

[59]   Verellen D, Ridder M De, Storme G. A (short) history of image-guided radiotherapy. Radiother Oncol 2008;86:4–13. doi:10.1016/j.radonc.2007.11.023.

[60]   Bujold A, Craig T, Jaffray D, Dawson LA. Image-Guided Radiotherapy: Has It Influenced Patient Outcomes? Semin Radiat Oncol 2012;22:50–61. doi:10.1016/j.semradonc.2011.09.001.

[61]   International Commission on Radiation Units & Measurements (ICRU). Prescribing, Recording and Reporting Photon Beam Therapy (Report 62). 1999. doi:https://doi.org/10.1093/jicru/os32.1.Report62.

[62]   Van Herk M, Remeijer P, Rasch C, Lebesque J V. The probability of correct target dosage: dose-population histograms for deriving treatment margins in radiotherapy. Int J Radiat Oncol Biol Phys 2000;47:1121–35. doi:10.1016/S0360-3016(00)00518-6.

[63]   Rechner LA, Howell RM, Zhang R, Newhauser WD. Impact of margin size on the predicted risk of radiogenic second cancers following proton arc therapy and volumetric modulated arc therapy for prostate cancer. Phys Med Biol 2012;57. doi:10.1088/0031-9155/57/23/N469.

[64]   Tobias CA, Lawrence JH, Born JL, McCombs RK, Robers JE, Anger HO, et al. Pituitary Irradiation with High-Energy Proton Beams A Preliminary Report. Cancer Res 1958;18:121–34.

[65]   Smith AR. Proton therapy. Phys Med Biol 2006;51:R491–504. doi:10.1088/0031-9155/51/13/R26.

[66]   Newhauser WD, Zhang R. The physics of proton therapy. Phys Med Biol 2015;60:R155. doi:10.1088/0031-9155/60/8/R155.

[67]   Particle Therapy Co-Operative Group 2019.

[68]   Chu WT, Ludewigt BA, Renner TR. Instrumentation for treatment of cancer using proton and light-ion beams. Rev Sci Instruments 1993;64. doi:doi/10.1063/1.1143946.

[69]   Chera BS, Rodriguez C, Morris CG, Louis D, Yeung D, Li Z, et al. Dosimetric Comparison of Three Different Involved Nodal Irradiation Techniques for Stage II Hodgkin's Lymphoma Patients: Conventional Radiotherapy, Intensity-Modulated Radiotherapy, and Three-Dimensional Proton Radiotherapy. Int J Radiat Oncol Biol Phys 2009;75:1173–80. doi:10.1016/j.ijrobp.2008.12.048.

[70]   Andolino DL, Hoene T, Xiao L, Buchsbaum J, Chang AL. Dosimetric comparison of involved-field three-dimensional conformal photon radiotherapy and breast-sparing proton therapy for the treatment of Hodgkin's lymphoma in female pediatric patients. Int J Radiat Oncol Biol Phys 2011;81:667–71. doi:10.1016/j.ijrobp.2011.01.061.

[71]   Homann K, Howell R, Eley J, Mirkovic D, Etzel C, Giebeler A, et al. The need for individualized studies to compare radiogenic second cancer risk in proton versus photon Hodgkin Lymphoma patient treatments. J Prot Ther 2016;1:3–5. doi:10.14319/jpt.11.8.

[72]   Zeng C, Plastaras JP, James P, Tochner ZA, Hill- CE, Hahn SM, et al. Proton pencil beam scanning for mediastinal lymphoma : treatment planning and robustness assessment 2016. doi:10.1080/0284186X.2016.1191665.

[73]   Baues C, Marnitz S, Engert A, Baus W, Jablonska K, Fogliata A, et al. Proton versus photon deep inspiration breath hold technique in patients with hodgkin lymphoma and mediastinal radiation. Radiat Oncol 2018;13:1–11. doi:10.1186/s13014-018-1066-2.

[74]   Edvardsson A, Kügele M, Alkner S, Enmark M, Nilsson J, Kristensen I, et al. Comparative treatment planning study for mediastinal Hodgkin's lymphoma: impact on normal tissue dose using deep inspiration breath hold proton and photon therapy. Acta Oncol (Madr) 2018;0:1–10. doi:10.1080/0284186X.2018.1512153.

[75]   König L, Bougatf N, Hörner-Rieber J, Chaudhri N, Mielke T, Klüter S, et al. Consolidative mediastinal irradiation of malignant lymphoma using active scanning proton beams: clinical outcome and dosimetric comparison. Strahlentherapie Und Onkol 2019;195:677–87. doi:10.1007/s00066-019-01460-7.

[76]   Everett A, Flampouri S, Louis D, McDonald AM, Mendenhall NP, Li Z, et al. Comparison of Radiation Techniques in Lower Mediastinal Lymphoma. Int J Radiat Oncol 2018;102:S190–1. doi:https://doi.org/10.1016/j.ijrobp.2018.07.080.

[77]   Tseng YD, Cutter DJ, Plastaras JP, Parikh RR, Cahlon O, Chuong MD, et al. Evidence-based Review on the Use of Proton Therapy in Lymphoma From the Particle Therapy Cooperative Group (PTCOG) Lymphoma Subcommittee. Int J Radiat Oncol 2017;99:825–42. doi:https://doi.org/10.1016/j.ijrobp.2017.05.004.

[78]   Li J, Dabaja B, Reed V, Allen PK, Cai H, Amin M V., et al. Rationale for and preliminary results of proton beam therapy for mediastinal lymphoma. Int J Radiat Oncol Biol Phys 2011;81:167–74. doi:10.1016/j.ijrobp.2010.05.007.

[79]   Hoppe BS, Flampouri S, Su Z, Morris CG, Latif N, Dang NH, et al. Consolidative involved-node proton therapy for stage IA-IIIB mediastinal hodgkin lymphoma: Preliminary dosimetric outcomes from a phase II study. Int J Radiat Oncol Biol Phys 2012;83:260–7. doi:10.1016/j.ijrobp.2011.06.1959.

[80]   Knausl B et al. Can treatment of pediatric Hodgkin's lymphoma be improved by PET imaging and

proton therapy ? 2013;c:54–61. doi:10.1007/s00066-012-0235-8.

[81]   Cella L, Conson M, Pressello MC, Molinelli S, Schneider U, Donato V, et al. Hodgkin's lymphoma emerging radiation treatment techniques: trade-offs between late radio-induced toxicities and secondary malignant neoplasms. Radiat Oncol 2013;8:22. doi:10.1186/1748-717X-8-22.

[82]   Zhang R, Howell RM, Homann K, Giebeler A, Taddei PJ, Mahajan A, et al. Predicted risks of radiogenic cardiac toxicity in two pediatric patients undergoing photon or proton radiotherapy. Radiat Oncol 2013;8:184. doi:10.1186/1748-717X-8-184.

[83]   Jørgensen AYS, Maraldo M V, Brodin NP, Aznar MC, Vogelius IR, Rosenschöld PM af, et al. The effect on esophagus after different radiotherapy techniques for early stage Hodgkin's lymphoma. Acta Oncol (Madr) 2013;52:1559–65. doi:10.3109/0284186X.2013.813636.

[84]   Sachsman S, Hoppe BS, Mendenhall NP, Holtzman A, Li Z, Slayton W, et al. Proton therapy to the subdiaphragmatic region in the management of patients with Hodgkin lymphoma. Leuk Lymphoma 2015;56:2019–24. doi:10.3109/10428194.2014.975802.

[85]   Horn S, Pernin V, Peurien D, Vaillant M, Dendale R, Fourquet A, et al. Comparison of passive-beam proton therapy , helical tomotherapy and 3D conformal radiation therapy in Hodgkin ' s lymphoma female patients receiving involved-field or involved site radiation therapy Comparaison entre protonthérapie , tomothérapie hélicoïd. Cancer Radiother 2016;20:98–103. doi:10.1016/j.canrad.2015.11.002.

[86]   Figura NS, Hoppe BC, Flampouri SC, Su ZC, Osian OC, Monroe AC, et al. Postoperative Proton Therapy in the Management of Stage III Thymoma. J Thorac Oncol 2013;8:e38–40. doi:10.1097/JTO.0b013e31827a8911.

[87]   Vogel J, Berman AT, Lin L, Pechet TT, Levin WP, Gabriel P, et al. Prospective study of proton beam radiation therapy for adjuvant and definitive treatment of thymoma and thymic carcinoma: Early response and toxicity assessment. Radiother Oncol 2016;118:504–9. doi:10.1016/j.radonc.2016.02.003.

[88]   Parikh RR, Rhome R, Hug E, Tsai H, Cahlon O, Chon B, et al. Adjuvant Proton Beam Therapy in the Management of Thymoma: A Dosimetric Comparison and Acute Toxicities. Clin Lung Cancer 2016;17:362–6. doi:10.1016/j.cllc.2016.05.019.

[89]   Zhu HJ, Hoppe BS, Flampouri S, Louis D, Pirris J, Nichols RC, et al. Rationale and early outcomes for the management of thymoma with proton therapy. Transl Lung Cancer Res 2018;7:106–13. doi:10.21037/tlcr.2018.04.06.

[90]   Mercado CE, Hartsell WF, Simone CB, Tsai HK, Vargas CE, Zhu HJ, et al. Proton therapy for thymic malignancies: multi-institutional patterns-of-care and early clinical outcomes from the proton collaborative group and the university of Florida prospective registries. Acta Oncol (Madr) 2019;58:1036–40. doi:10.1080/0284186X.2019.1575981.

[91]   Dabaja BS, Mikhaeel N. In the Battle Between Protons and Photons for Hematologic Malignancies, the Patient Must Win. Int J Radiat Oncol Biol Phys 2016;95:43–5. doi:10.1016/j.ijrobp.2015.09.043.

[92]   Dabaja BS, Hoppe BS, Plastaras JP, Newhauser W, Rosolova K, Flampouri S, et al. Proton therapy for adults with mediastinal lymphomas : the International Lymphoma Radiation Oncology Group guidelines. Blood 2019;132:1635–47.

[93]   Schaffner B, Pedroni E. The precision of proton range calculations in proton radiotherapy treatment planning: experimental verification of the relation between CT-HU and proton stopping power. Phys Med Biol 1998;43:1579–92.

[94]   Woodward WA, Amos RA. Proton Radiation Biology Considerations for Radiation Oncologists. Radiat Oncol Biol 2016;95:59–61. doi:10.1016/j.ijrobp.2015.10.022.

[95] Paganetti H, Niemierko A, Ancukiewicz M, Gerweck LE, Goitein M, Loeffler JS, et al. Relative biological effectiveness (RBE) values for proton beam therapy. Int J Radiat Oncol Biol Phys 2002;53:407–21. doi:10.1016/S0360-3016(02)02754-2.

[96] International Commission on Radiation Units & Measurements (ICRU). Prescribing, Recording, and Reporting Proton-Beam Therapy. vol. Report 78. 2007.

[97] Paganetti H. Relative biological effectiveness (RBE) values for proton beam therapy. Variations as a function of biological endpoint, dose, and linear energy transfer. Phys Med Biol 2014;59:R419–72. doi:10.1088/0031-9155/59/22/R419.

[98] Janni JF. Energy loss, range, path length, time-of-flight, straggling, multiple scattering, and nuclear interaction probability. In two parts. Part 1. For 63 compounds Part 2. For elements $1 \leq Z \leq 92$. At Data Nucl Data Tables 1982;27:147–339. doi:10.1016/0092-640X(82)90004-3.

[99] Peeler CR, Mirkovic D, Titt U, Blanchard P, Gunther JR, Mahajan A, et al. Clinical evidence of variable proton biological effectiveness in pediatric patients treated for ependymoma. Radiother Oncol 2016;121:395–401. doi:10.1016/j.radonc.2016.11.001.

[100] Underwood TSA, Grassberger C, Bass R, MacDonald SM, Meyersohn NM, Yeap BY, et al. Asymptomatic Late-phase Radiographic Changes Among Chest-Wall Patients Are Associated With a Proton RBE Exceeding 1.1. Int J Radiat Oncol Biol Phys 2018;101:809–19. doi:10.1016/j.ijrobp.2018.03.037.

[101] Williams M, Denekamp J, Fowler J. A review of alpha/beta ratios for experimental tumors: implications for clinical studies of altered fractionation. Int J Radiat Oncol Biol Phys 1985;11:87–96.

[102] Rørvik E, Fjæra LF, Dahle TJ, Dale JE, Engeseth GM, Stokkevåg CH, et al. Exploration and application of phenomenological RBE models for proton therapy Exploration and application of phenomenological RBE models for proton therapy. Phys Med Biol 2018;63.

[103] Korreman SS. Motion in radiotherapy: Photon therapy. Phys Med Biol 2012;57. doi:10.1088/0031-9155/57/23/R161.

[104] Lovelock DM, Zatcky J, Goodman K, Yamada Y. The Effectiveness of a Pneumatic Compression Belt in Reducing Respiratory Motion of Abdominal Tumors in Patients Undergoing Stereotactic Body Radiotherapy. Technol Cancer Res Treat 2013;13:259–67. doi:10.7785/tcrt.2012.500379.

[105] Péguret N, Ozsahin M, Zeverino M, Belmondo B, Durham AD, Lovis A, et al. Apnea-like suppression of respiratory motion: First evaluation in radiotherapy. Radiother Oncol 2016;118:220–6. doi:10.1016/j.radonc.2015.10.011.

[106] Nuyttens J, Bondiau P, van Zijp N, Hoogeman M. Central and Peripheral Lung Metastases Treated With Real-time Tumor Tracking During Stereotactic Radiotherapy: A 5 Years Experience. Int J Radiat Oncol Biol Phys 2011;81:S607–S607. doi:10.1016/j.ijrobp.2011.06.1141.

[107] Harada K, Katoh N, Suzuki R, Ito YM, Shimizu S, Onimaru R, et al. Evaluation of the motion of lung tumors during stereotactic body radiation therapy (SBRT) with four-dimensional computed tomography (4DCT) using real-time tumor-tracking radiotherapy system (RTRT). Phys Med 2016;32:305–11. doi:10.1016/j.ejmp.2015.10.093.

[108] Knopf A-C, Hong TS, Lomax A. Scanned proton radiotherapy for mobile targets-the effectiveness of re-scanning in the context of different treatment planning approaches and for different motion characteristics. Phys Med Biol 2011;56:7257–71. doi:10.1088/0031-9155/56/22/016.

[109] Schatti A, Zakova M, Meer D, Lomax AJ. The effectiveness of combined gating and re-scanning for treating mobile targets with proton spot scanning. An experimental and simulation-based investigation. Phys Med Biol 2014;59:3813–28. doi:Doi 10.1088/0031-9155/59/14/3813.

[110] Zeng C, Plastaras JP, Tochner ZA, White BM, Hill-Kayser CE, Hahn SM, et al. Proton pencil beam

scanning for mediastinal lymphoma: the impact of interplay between target motion and beam scanning. Phys Med Biol 2015;60:3013–29. doi:10.1088/0031-9155/60/7/3013.

[111] Kubo HD, Hill BC. Respiration gated radiotherapy treatment: a technical study. Phys Med Biol 1996;41:83–91.

[112] Tahir BA, Bragg CM, Lawless SE, Hatton MQF, Ireland RH. Dosimetric evaluation of inspiration and expiration breath-hold for intensity-modulated radiotherapy planning of non-small cell lung cancer. Phys Med Biol 2010;55:N191–9. doi:10.1088/0031-9155/55/8/N01.

[113] Boda-Heggemann J, Knopf AC, Simeonova-Chergou A, Wertz H, Stieler F, Jahnke A, et al. Deep Inspiration Breath Hold - Based Radiation Therapy: A Clinical Review. Int J Radiat Oncol Biol Phys 2016;94:478–92. doi:10.1016/j.ijrobp.2015.11.049.

[114] Sixel KE, Aznar MC, Ung YC. Deep inspiration breath hold to reduce irradiated heart volume in breast cancer patients. Int J Radiat Oncol Biol Phys 2001;49:199–204. doi:10.1016/S0360-3016(00)01455-3.

[115] Korreman SS, Pedersen AN, Nøttrup TJ, Specht L, Nyström H. Breathing adapted radiotherapy for breast cancer: comparison of free breathing gating with the breath-hold technique. Radiother Oncol 2005;76:311–8. doi:10.1016/j.radonc.2005.07.009.

[116] Damkjær SMS, Aznar MC, Pedersen AN, Vogelius IR, Bangsgaard JP, Josipovic M. Reduced lung dose and improved inspiration level reproducibility in visually guided DIBH compared to audio coached EIG radiotherapy for breast cancer patients. Acta Oncol (Madr) 2013;52:1458–63. doi:10.3109/0284186X.2013.813073.

[117] Stromberg JS, Sharpe MB, Kim LH, Kini VR, Jaffray DA, Martinez AA, et al. ACTIVE BREATHING CONTROL (ABC) FOR HODGKIN'S DISEASE: REDUCTION IN NORMAL TISSUE IRRADIATION WITH DEEP INSPIRATION AND IMPLICATIONS FOR TREATMENT. Int J Radiat Oncol Biol Phys 2000;48:797–806.

[118] Paumier A, Ghalibafian M, Gilmore J, Beaudre A, Blanchard P, El Nemr M, et al. Dosimetric benefits of intensity-modulated radiotherapy combined with the deep-inspiration breath-hold technique in patients with mediastinal Hodgkin's lymphoma. Int J Radiat Oncol Biol Phys 2012;82:1522–7. doi:10.1016/j.ijrobp.2011.05.015.

[119] Petersen PM, Aznar MC, Berthelsen AK, Loft A, Schut DA, Maraldo M, et al. Prospective phase II trial of image-guided radiotherapy in Hodgkin lymphoma: Benefit of deep inspiration breath-hold. Acta Oncol (Madr) 2015;54:60–6. doi:10.3109/0284186X.2014.932435.

[120] Aznar MC, Maraldo M V, Schut DA, Lundemann M, Brodin NP, Vogelius IR, et al. Minimizing Late Effects for Patients With Mediastinal Hodgkin Lymphoma: Deep Inspiration Breath-Hold, IMRT, or Both? Int J Radiat Oncol 2016;92:1–6.

[121] Boda-Heggemann J, Fleckenstein J, Lohr F, Wertz H, Nachit M, Blessing M, et al. Multiple breath-hold CBCT for online image guided radiotherapy of lung tumors: Simulation with a dynamic phantom and first patient data. Radiother Oncol 2011;98:309–16. doi:10.1016/j.radonc.2011.01.019.

[122] Josipovic M, Persson GF, Bangsgaard JP, Specht L, Aznar MC. Deep inspiration breath-hold radiotherapy for lung cancer: Impact on image quality and registration uncertainty in cone beam CT image guidance. Br J Radiol 2016;89:1–8. doi:10.1259/bjr.20160544.

[123] Schultheiss TE. The Radiation Dose–Response of the Human Spinal Cord. Int J Radiat Oncol 2008;71:1455–9. doi:https://doi.org/10.1016/j.ijrobp.2007.11.075.

[124] Niemierko A, Urie M, Goitein M. Optimization of 3d radiation therapy with both physical and biological end points and constraints. Int J Radiat Oncol 1992;23:99–108. doi:10.1016/0360-3016(92)90548-V.

[125] Brahme A. Optimized radiation therapy based on radiobiological objectives. Semin Radiat Oncol 1999;9:35–47. doi:10.1016/S1053-4296(99)80053-8.

[126] Markov K, Schinkel C, Stavreva N, Stavrev P, Weldon M, Fallone BG. Reverse mapping of normal tissue complication probabilities onto dose volume histogram space: The problem of randomness of the dose volume histogram sampling. Med Phys 2006;33:3435–43. doi:10.1118/1.2198307.

[127] Peñagarícano JA, Papanikolaou N, Wu C, Yan Y. An assessment of biologically-based optimization (BORT) in the IMRT era. Med Dosim 2005;30:12–9. doi:10.1016/j.meddos.2004.10.003.

[128] Qi XS, Semenenko VA, Li XA. Improved critical structure sparing with biologically based IMRT optimization. Med Phys 2009;36:1790–9. doi:10.1118/1.3116775.

[129] Eich HT, Diehl V, Gorgen H, Pabst T, et al. Intensified Chemotherapy and Dose-Reduced Involved-Field Radiotherapy in Patients With Early Unfavorable Hodgkin ' s Lymphoma : Final Analysis of the German Hodgkin Study Group HD11 Trial. J Clin Oncol 2010;28:4199–206. doi:10.1200/JCO.2010.29.8018.

[130] Engert A, Plütschow A, Eich HT, Lohri A, Dörken B, Borchmann P, et al. Reduced Treatment Intensity in Patients with Early-Stage Hodgkin's Lymphoma. N Engl J Med 2010;363:640–52. doi:10.1056/NEJMoa1000067.

[131] Brodin NP, Maraldo M V, Aznar MC, Vogelius IR, Petersen PM, Bentzen SM, et al. Interactive Decision-Support Tool for Risk-Based Radiation Therapy Plan Comparison for Hodgkin Lymphoma. Int J Radiat Oncol 2014;88:433–45.

[132] Njeh CF. Tumor delineation: The weakest link in the search for accuracy in radiotherapy. J Med Phys 2008;33:136–40. doi:10.4103/0971-6203.44472.

[133] Aznar MC, Girinsky T, Berthelsen AK, Aleman B, Beijert M, Hutchings M, et al. Interobserver delineation uncertainty in involved-node radiation therapy (INRT) for early-stage Hodgkin lymphoma: on behalf of the Radiotherapy Committee of the EORTC lymphoma group. Acta Oncol (Madr) 2017;56:608–13. doi:10.1080/0284186X.2017.1279750.

[134] Remouchamps VM, Huyskens DP, Mertens I, Destine M, Van Esch A, Salamon E, et al. The use of magnetic sensors to monitor moderate deep inspiration breath hold during breast irradiation with dynamic MLC compensators. Radiother Oncol 2007;82:341–8. doi:10.1016/j.radonc.2006.11.015.

[135] Rohrberg KS, Daugaard G, Petersen PM. P32: Comparing radiotherapy with free breathing and deep inspiration breath hold for thymic cancers. J. Thorac. Dis., 2015, p. AB101.

[136] Schneider U, Agosteo S, Pedroni E, Besserer J. Secondary Neutron Dose During Proton Therapy Using Spot Scanning. Int J Radiat Oncol Biol Phys 2002;53:244–51.

[137] Brodin NP, Vogelius IR, Maraldo M V., Munck Af Rosenschold P, Aznar MC, Kiil-Berthelsen A, et al. Life years lost-comparing potentially fatal late complications after radiotherapy for pediatric medulloblastoma on a common scale. Cancer 2012;118:5432–40. doi:10.1002/cncr.27536.

[138] Nyman J (PI). Phase II non-randomized study on proton radiotherapy of thymic malignancies (PROthym). n.d.

[139] Jäkel O. Ranges of ions in metals for use in particle treatment planning. Phys Med Biol 2006;51:N173–7. doi:10.1088/0031-9155/51/9/N01.

[140] Glide-Hurst CK, Chen D, Zhong H, Chetty IJ. Changes realized from extended bit-depth and metal artifact reduction in CT. Med Phys 2013;40.

[141] Rechner LA, Maraldo MV, Vogelius IR, Zhu XR, Dabaja BS, Brodin NP, et al. Life years lost attributable to late effects after radiotherapy for early stage Hodgkin lymphoma: The impact of proton therapy and/or deep inspiration breath hold. Radiother Oncol 2017;125:41–7. doi:10.1016/j.radonc.2017.07.033.

[142] Grassberger C, Trofimov A, Lomax A, Paganetti H. Variations in linear energy transfer within clinical proton therapy fields and the potential for biological treatment planning. Int J Radiat Oncol Biol Phys 2011;80:1559–66.

[143] Mcnamara AL, Schuemann J, Paganetti H. A phenomenological relative biological effectiveness (RBE) model for proton therapy based on all published in vitro cell survival data. Phys Med Biol 2015;60:8399–416. doi:10.1088/0031-9155/60/21/8399.A.

[144] Yepes P, Adair A, Frank SJ, Grosshans DR, Liao Z, Liu A. Fixed- versus Variable-RBE Computations for Intensity Modulated Proton Therapy. Adv Radiat Oncol 2019;4:156–67. doi:10.1016/j.adro.2018.08.020.

[145] Lundgaard AY, Hjalgrim LL, Rechner LA, Josipovic M, Joergensen M, Aznar MC, et al. TEDDI: Radiotherapy delivery in deep inspiration for pediatric patients - A NOPHO feasibility study. Radiat Oncol 2018;13. doi:10.1186/s13014-018-1003-4.

[146] Agostinelli S, Allison J, Amako K, Apostolakis J, Araujo H, Arce P, et al. Geant4—a simulation toolkit. Nucl Instruments Methods Phys Res Sect A Accel Spectrometers, Detect Assoc Equip 2003;506:250–303. doi:https://doi.org/10.1016/S0168-9002(03)01368-8.

[147] Sarrut D, Bardiès M, Boussion N, Freud N, Jan S, Létang J, et al. A review of the use and potential of the GATE Monte Carlo simulation code for radiation therapy and dosimetry applications. Med Phys 2014;41:n/a-n/a. doi:10.1118/1.4871617.

[148] Modiri A, Stick LB, Rice SR, Rechner LA, Vogelius IR, Bentzen SM, et al. Individualized estimates of overall survival in radiation therapy plan optimization — A concept study. Med Phys 2018;45:5332–42.

[149] Maraldo M V, Aznar MC, Vogelius IR, Petersen PM, Specht L. Involved Node Radiation Therapy : An Effective Alternative in Early-Stage Hodgkin Lymphoma. Int J Radiat Oncol Biol Phys 2013;85:1057–65.

[150] Maraldo M V, Brodin P, Aznar MC, Vogelius IR, Munck P, Petersen PM, et al. Doses to Carotid Arteries After Modern Radiation Therapy for Hodgkin Lymphoma: Is Stroke Still a Late Effect of Treatment ? Int J Radiat Oncol Biol Phys 2013;87:297–303.

[151] Niemierko A. Reporting and analyzing dose distributions: a concept of equivalent uniform dose. Med Phys 1997;24:103–10.

[152] Bohoslavsky R, Witte MG, Janssen TM, van Herk M. Probabilistic objective functions for margin-less IMRT planning. Phys Med Biol 2013;58:3563–80. doi:10.1088/0031-9155/58/11/3563.

[153] Unkelbach J, Alber M, Bangert M, Bokrantz R, Chan TCY, Deasy JO, et al. Robust radiotherapy planning. Phys Med Biol 2018;63:22TR02. doi:10.1088/1361-6560/aae659.

[154] Pedroni E, Phillips MH, Boehringer T, Blattmann H, Coray A, Scheib S. Effects of respiratory motion on dose uniformity with a charged particle scanning method. Phys Med Biol 2002;37:223–33. doi:10.1088/0031-9155/37/1/016.

[155] Bert C, Durante M. Motion in radiotherapy: particle therapy. Phys Med Biol 2011;56:R113–44. doi:10.1088/0031-9155/56/16/R01.

[156] Lomax a J. Intensity modulated proton therapy and its sensitivity to treatment uncertainties 1: the potential effects of calculational uncertainties. Phys Med Biol 2008;53:1027–42. doi:10.1088/0031-9155/53/4/014.

[157] Bert C, Grözinger SO, Rietzel E. Quantification of interplay effects of scanned particle beams and moving targets. Phys Med Biol 2008;53:2253–65. doi:10.1088/0031-9155/53/9/003.

[158] Enmark M, Olofsson J, Ceberg S, Jonsson J. [P205] The impact on pencil beam scanning (PBS) proton therapy for mediastinal lymphoma from deep inspiration breath-hold (DIBH) variability.

Phys Medica 2018;52:159. doi:https://doi.org/10.1016/j.ejmp.2018.06.499.

[159] McMahon S, McNamara A, Schuemann J, Paganetti H, Prise K. A general mechanistic model enables predictions of the biological effectiveness of different qualities of radiation. Sci Rep 2017;7:10790. doi:10.1038/s41598-017-10820-1.

[160] Guan F, Geng C, Carlson DJ, Ma DH, Bronk L, Gates D, et al. A mechanistic relative biological effectiveness model-based biological dose optimization for charged particle radiobiology studies. Phys Med Biol 2019;64:15008. doi:10.1088/1361-6560/aaf5df.

[161] Langendijk JA, Lambin P, De Ruysscher D, Widder J, Bos M, Verheij M. Selection of patients for radiotherapy with protons aiming at reduction of side effects: The model-based approach. Radiother Oncol 2013;107:267–73. doi:https://doi.org/10.1016/j.radonc.2013.05.007.

[162] Prayongrat A, Umegaki K, van der Schaaf A, Koong AC, Lin SH, Whitaker T, et al. Present developments in reaching an international consensus for a model-based approach to particle beam therapy. J Radiat Res 2018;59:i72–6. doi:10.1093/jrr/rry008.

[163] Gardin I, Grégoire V, Gibon D, Kirisli H, Pasquier D, Thariat J, et al. Radiomics: Principles and radiotherapy applications. Crit Rev Oncol Hematol 2019;138:44–50. doi:https://doi.org/10.1016/j.critrevonc.2019.03.015.

Funding

Appendix: Papers I-V

Residual errors and PTV margins for modern radiotherapy for mediastinal lymphoma

Laura A. Rechner[1,2]*, Lena Specht[1], Mirjana Josipovic[1], Maja. V. Maraldo[1], Peter M. Petersen[1], and Marianne C. Aznar[3,4]

1. Department of Oncology, Section of Radiotherapy, Rigshospitalet, Copenhagen, Denmark

2. Niels Bohr Institute, University of Copenhagen, Denmark

3. Manchester Cancer Research Centre, Division of Cancer Sciences, The University of Manchester, Manchester, United Kingdom

4. Clinical Trial Service Unit, Nuffield Department of Population Health, University of Oxford, United Kingdom

*Corresponding author:
Department of Oncology, section 3994
Rigshospitalet
Blegdamsvej 9
2100 Copenhagen Ø, Denmark
laura.ann.rechner@gmail.com

Residual errors and PTV margins for modern radiotherapy for mediastinal lymphoma

Abstract: Radiotherapy for mediastinal lymphoma has changed drastically throughout the years, with current practice being smaller volumes treated with lower doses, highly conformal distributions and daily imaging commonly used for positioning. In this modern context, an assessment of the appropriate planning target margin (PTV) is required. Therefore, we assessed the positioning uncertainty for 20 mediastinal lymphoma patients treated in deep-inspiration breath hold (DIBH) through offline registration of cone beam computed tomography (CBCT) images to the planning CT images. Contouring uncertainty and intrafraction motion uncertainty were estimated from the literature. The CTV-to-PTV margin providing 95% dose coverage for 90% of the patients was calculated to be approximately 9-11 mm for patients treated at our institution, assuming daily CBCT. The results varied greatly depending on the assumed contouring uncertainty (range: 3.4 to 12.8 mm margins for contouring uncertainties of 0.0 to 4.0 mm, respectively), which highlights the contribution of contouring uncertainty in modern treatment of mediastinal lymphoma. We acknowledge that uncertainties are institution-specific and advise caution when reducing margins to only include uncertainties from positioning and respiratory motion.

Introduction

Radiotherapy (RT) for mediastinal lymphoma has changed drastically throughout the years. Treatments have evolved from very large fields, for example mantle fields, to smaller treatment volumes using the involved-site (or nodes) radiation therapy (ISRT or INRT) technique [1,2]. To deliver the RT, many departments now have the possibility to use intensity modulated radiation therapy

(IMRT) or volumetric modulated radiation therapy (VMAT) and conform the dose to the target while sparing normal tissue [3]. Furthermore, the ability to accurately position the patient before each treatment has improved with the addition of daily image guided radiotherapy (IGRT) [4,5]. And finally, the use of deep inspiration breath hold (DIBH) for lymphoma patients has provided a dosimetric benefit with respect to sparing normal tissue [6] and might improve the image quality of cone beam computed tomography (CBCT) scan used for IGRT [7,8].

In this modern context, an assessment of the appropriate planning target volume (PTV) margin is required. The margin from the clinical target volume (CTV) to the PTV should be large enough to ensure coverage, but as small as possible to reduce the risk of acute and late toxicities from irradiating healthy tissue [1,9–12].

The goal of this study was to estimate the residual geometric uncertainties for patients treated at our hospital with RT for mediastinal lymphoma in DIBH assuming daily IGRT with CBCT, which is our current standard of care, and estimate appropriate population-based CTV-to-PTV margins.

Methods and Materials

A. Patients

20 sequential patients with mediastinal lymphoma treated with RT between 2016 and 2017 at our hospital were selected for retrospective analysis. Inclusion criteria were treatment in DIBH and availability of acquired CBCT scans used for IGRT for analysis. Patients were immobilized on a breast board (ConChest, Candor Aps, DK) and visual guidance was used for respiratory management (RPM, Varian Medical Systems)[6,13]. All patients were positioned in a breast board with no incline with their

arms up, except one patient who had one arm down on the side of their disease (patient 10). All patients had mediastinal targets and no patients had disease extending inferiorly to the apex region of the heart or beyond. In 15 of the patients the disease extended superiorly at least to a small extent into the neck region and in these patients bite blocks were used to immobilize the head and neck region. This study was registered with the local data protection agency, and ethics approval was not required by law.

B. Positioning Uncertainty

Positioning uncertainty was assessed through registration of CBCT images. CBCTs were acquired prior to the daily treatment and used for positioning correction (Clinac, Varian Medical Systems). Before treatment, CBCTs were rigidly registered with the automatically delineated bone structure chosen as the volume of interest (VOI) and the region of interest (ROI) box surrounding the target volume, which most often included bones of the sternum, spine, and a small amount of medial ribs (see Figure 1(a)). After automatic registration, manual adjustments to the registration to better align to the target volume were allowed. Only deviations in translations and rotation around the vertical axis were applied.

For the offline analysis after treatment, 4 or 5 CBCTs for each patient were rigidly registered to the planning CT scans. CBCTs for offline analysis were arbitrarily selected to be spaced approximately equally throughout the treatment course. Offline registrations were performed in the system used clinically at our hospital (Aria 13.6, Varian Medical Systems). Automatic registration algorithm was used with the bone structure (VOI), i.e. the same as on-line, but the region of interest (ROI) box surrounded only the sternum, i.e. it was smaller than for the on-line procedure (see Figure 1(b)). This method was chosen in order to focus most on the target position in a reproducible way, where

the online procedure with a slightly larger ROI box was chosen for robustness with respect to breath hold level. As opposed to the on-line procedure, in the off-line procedure no manual edits to the automatic registration were allowed. For two patients, the ROI box was expanded to include part of the clavicle due to the proximity to the target volume. The registration corrected for lateral (LAT), anterior-posterior (AP), or superior-inferior (SI) direction. After offline automatic registration to bone, the alignment of the target and the soft tissue in the region was verified visually on all slices, but no manual adjustments were made. The values recorded were the differences between the online registration after correction and offline registration (i.e. residual errors). An example of a daily CBCT registered to the planning CT for one patient is shown in Figure 2.
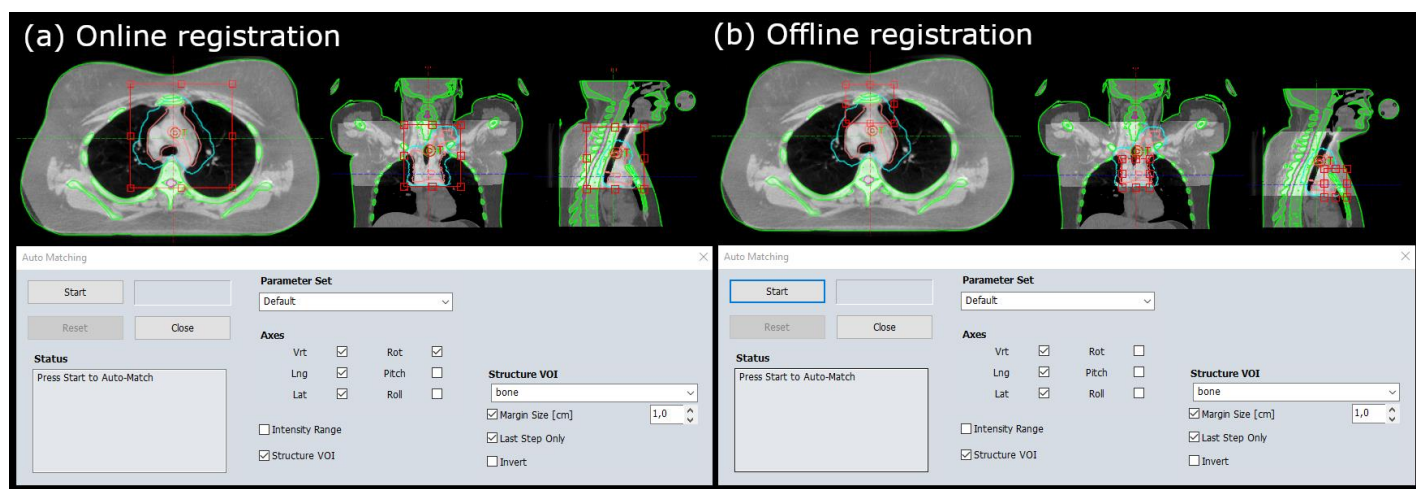
Figure 1. Example of the online (a) versus offline (b) CBCT registration used in this study where the region of interest (ROI) box is shown in red, bones and body in green, CTV in pink, PTV in cyan, and spinal cord in magenta.
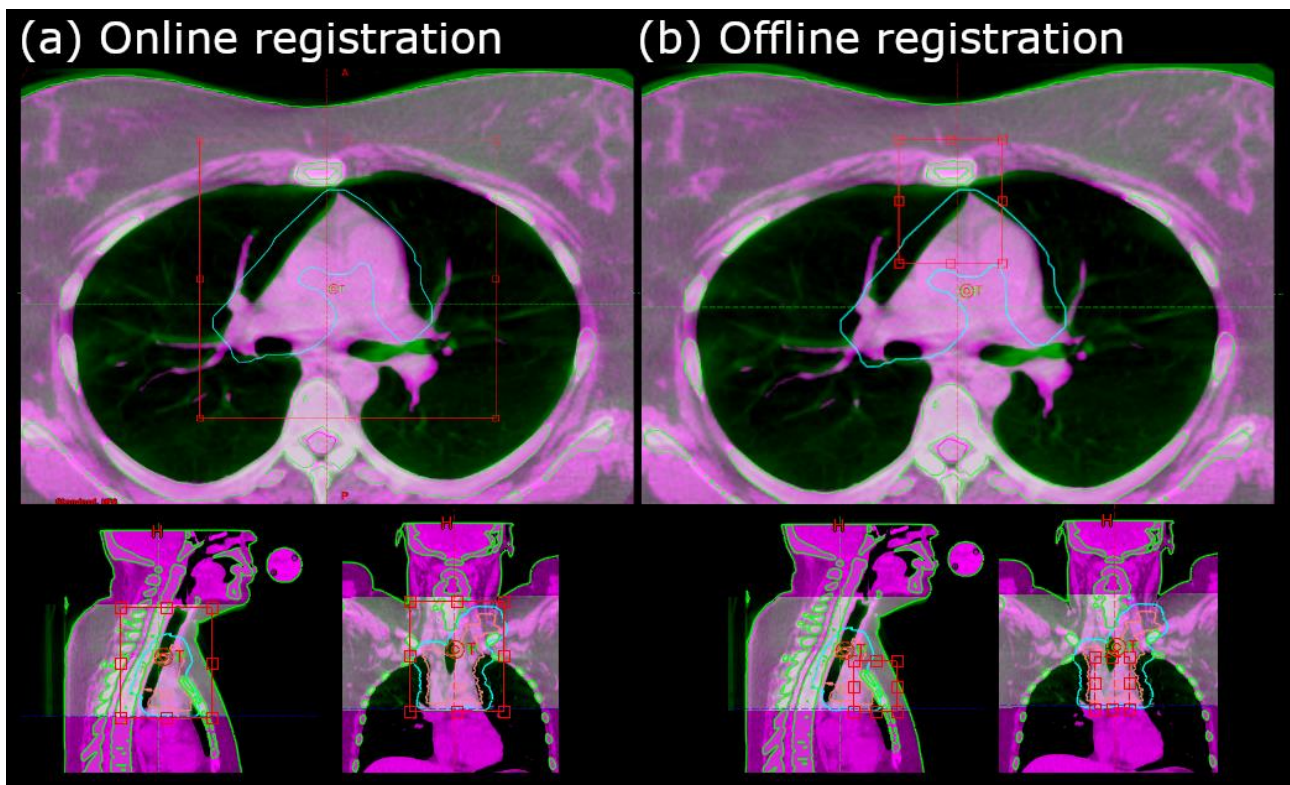
Figure 2. Example of the differences in images comparing the daily CBCT (green) and the planning CT (magenta) after the online (a) registration before treatment and offline (b) registration. The differences between online and offline registrations for this example were 1 mm laterally and -1 mm superior-inferiorly (residual error). The body is shown in green, bones in green, CTV in pink, PTV in cyan, and spinal cord in magenta.

C. Other uncertainties

We considered contouring uncertainty as a systematic uncertainty in our margin calculations. Based on Aznar et al [14], 3.0 mm was expected to be a conservative starting point for contouring uncertainty for this patient group. We also analyzed the required PTV margins with assumptions of 0.0, 1.0, 2.0, 3.0, and 4.0 mm contouring uncertainty.

Another uncertainty for this patient group is the intra-fractional motion uncertainty. Since, to the best of our knowledge, no published data is available for intra-fractional motion for mediastinal lymphoma, this was estimated using data from breast cancer patients treated in DIBH with magnetic sensors on the skin surface to track position [15]. We assumed 1.6, 1.6, and 3.0 mm for random uncertainties, and 0.8, 0.8, and 1.1 mm for systematic uncertainties in the LAT, AP, and SI directions, respectively.

D. Margin calculations

The margin recipe from van Herk et al [16] was used to calculate the PTV margin required for 95% dose coverage of 90% of the patients. The complex formula was used:

$$m_{ptv} = 2.5\Sigma + 1.64\sqrt{\sigma^2 + \sigma_p^2} - 1.64\sigma_p$$

(1)

where m_{ptv} is the margin from CTV-to-PTV, Σ is the systematic uncertainty, σ is the random uncertainty, and σ_p is the penumbra (3.2 mm for soft tissue and 6.4 mm for lung tissue). The systematic uncertainty Σ in this study included uncertainties from positioning, intra-fractional motion, and contouring, added in quadrature. The systematic positioning uncertainty was calculated as the standard deviation of the means of positioning errors from each patient. The random uncertainty σ in this study included uncertainties from positioning and intra-fractional motion, added in quadrature. The random positioning uncertainty was determined by taking the standard deviation over each patient, then calculating the root mean squared over all patients for each anatomical direction.

E. Treatment planning

To illustrate the impact of the different margins found in this study on doses to normal tissue, treatment plans were created for the range of margins found in this study for one example patient (Eclipse, AcurosXB 13.6, Varian Medical Systems). The clinical VMAT plan (with 1 cm PTV margins) was copied and reoptimized for each PTV size, using a corresponding ring for optimization of dose fall-off. The mean dose to the lungs and heart were compared.

Results

Of the 20 patients with mediastinal lymphoma included in the study, 16 were diagnosed with Hodgkin lymphoma, 3 with B-cell lymphoma, and 1 with T-lymphoblastic lymphoma (Table 1). For 17 patients, 5 CBCTs were analyzed. For 3 patients, only 4 CBCTs were available for analysis.

Table 1. Patient characteristics and residual positioning error after offline image registration. The second to last row shows the mean of means and the standard deviation of the means. Abbreviations: HL: Hodgkin lymphoma, Frx: fractions, T-LBL T-lymphoblastic lymphoma, CTV: clinical target volume, CBCT: Cone-beam computed tomography, LAT: lateral, AP: anterior-posterior, SI: superior-inferior, std dev: standard deviation, rms: root mean squared.

Patient	Diagnosis	Frx	CTV volume (cc)	CBCTs analyzed	Bite Block	Residual Error (mm) mean (std dev)		
						LAT	AP	SI
1	HL	17	130.2	5	Yes	0.4 (0.09)	0.0 (1.4)	-1.4 (0.5)
2	HL	17	459.0	5	Yes	2.8 (1.3)	0.2 (1.6)	-0.8 (1.6)
3	HL	17	202.7	5	Yes	1.0 (0.7)	0.0 (0.7)	-0.6 (0.9)
4	HL	17	407.3	5	Yes	-1.2 (0.04)	-0.6 (1.5)	1.8 (0.8)
5	HL	17	174.5	5	Yes	0.0 (0.0)	-1.8 (1.3)	0.0 (1.2)
6	HL	17	136.3	5	Yes	-1.6 (1.1)	-1.0 (0.7)	-0.8 (1.1)
7	HL	17	198.3	4	Yes	-0.8 (0.5)	0.5 (1.0)	-0.3 (0.5)
8	HL	17	285.6	5	Yes	0.4 (0.5)	0.8 (0.4)	-1.2 (1.1)
9	T-LBL	14	147.8	5	No	0.6 (1.5)	0.2 (0.4)	-0.4 (0.5)
10	HL	17	487.2	5	Yes	-0.2 (0.4)	0.0 (0.7)	-0.6 (0.5)
11	HL	10	113.3	5	Yes	0.8 (0.4)	-0.2 (1.3)	2.0 (1.6)
12	HL	17	68.6	5	Yes	0.6 (0.5)	0.0 (0.0)	-1.0 (0.7)
13	HL	17	294.1	5	Yes	-1.0 (0.7)	-0.8 (1.1)	-0.8 (0.8)
14	B-cell	20	216.3	5	No	-0.6 (1.1)	0.2 (0.4)	-0.6 (0.5)
15	B-cell	20	508.4	4	No	0.0 (0.8)	-0.5 (0.6)	-0.5 (0.6)
16	HL	17	1208.4	5	Yes	0.4 (0.9)	0.0 (1.2)	-2.2 (1.9)
17	B-cell	20	484.4	5	No	-0.2 (1.9)	0.4 (0.5)	-2.0 (1.2)
18	HL	10	56.8	5	No	0.4 (1.1)	-2.6 (0.9)	-2.0 (0.7)
19	HL	17	107.3	4	Yes	0.0 (0.0)	0.0 (0.0)	0.3 (0.5)
20	HL	17	95.9	5	Yes	0.6 (0.05)	-0.4 (0.5)	0.2 (0.4)
					mean	0.1 (0.9)	-0.3 (0.8)	-0.5 (1.1)
					rms	0.9	0.9	1.0

Table 2 shows the systematic and random uncertainties that we used in the margin calculations. The calculated CTV-to-PTV margins are shown in Table 3 for a range of assumed contouring uncertainties. When the contouring uncertainty was assumed to be 3 mm, the required CTV-to-PTV margin was approximately 9-11 mm, depending on the anatomical direction and the type of tissue adjacent to the target. Figure 3 shows how the PTV changes with different assumptions of contouring uncertainty for one patient (patient 8: CTV volume approximately equal to the mean of all patients).

Treatment plans were also created for the same patient for each PTV size with different assumptions of contouring uncertainty. All plans were normalized to the prescription dose of 30.6 Gy to the mean of the PTV. The changes in PTV volume and dose metrics for the PTV, lungs, and heart are shown in

Table 4. Mean doses to the lungs and heart were relatively low for all plans but increased slightly

with increasing margin.

Table 2. Systematic and random uncertainties calculated (c) or estimated (e) from literature for patients with mediastinal lymphoma treated in DIBH.

	Source of Uncertainty	Lateral (mm)	Anterior-posterior (mm)	Superior-Inferior (mm)
Systematic	Positioning[c]	0.9	0.8	1.1
	Intrafraction Motion[e]	0.8	0.8	1.1
	Contouring[e]	3.0 (0.0-4.0)	3.0 (0.0-4.0)	3.0 (0.0-4.0)
Random	Positioning[c]	0.9	0.9	1.0
	Intrafraction Motion[e]	1.6	1.6	3.0

Table 3. CTV-to-PTV margins in this study for mediastinal lymphoma patients with DIBH and daily IGRT for a range of contouring uncertainties for a target abutting soft tissue (or lung tissue in parentheses).

Contouring uncertainty (mm)	CTV-to-PTV margin (mm)		
	LAT	AP	SI
0.0	4.2 (3.7)	4.0 (3.4)	6.0 (5.1)
1.0	5.1 (4.6)	4.9 (4.4)	6.7 (5.8)
2.0	7.0 (6.5)	6.9 (6.4)	8.4 (7.5)
3.0	9.2 (8.7)	9.1 (8.6)	10.6 (9.6)
4.0	11.6 (11.1)	11.5 (11.0)	12.8 (11.9)
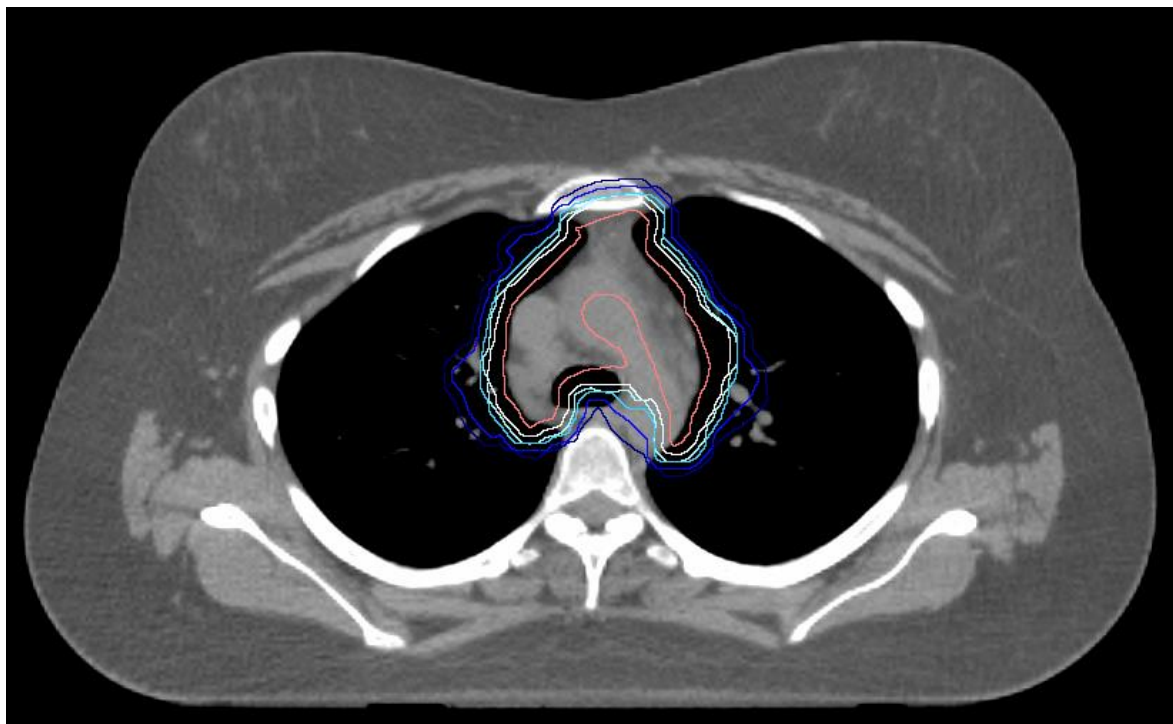
Figure 3. CTV-to-PTV margins for various assumed values for contouring uncertainty for one example patient. The CTV is shown in pink and the PTVs are shown in white to dark blue. CTV-to-PTV margins shown are 4, 5, 7, 9, and 11 mm, corresponding to contouring uncertainty values of 0, 1, 2, 3, and 4 mm, respectively.

Table 4. Change in PTV volume and dose metrics for various CTV-to-PTV margins in this study for one example mediastinal lymphoma patient treated with DIBH and daily CBCT (patient 8).

CTV-to-PTV margin (mm)	PTV Volume (cc)	$D_{95\%}$ to PTV (Gy)	Mean Lung Dose (Gy)	Mean Heart Dose (Gy)
4	481	28.9	6.5	1.9
5	544	28.9	6.8	2.0
7	625	29.1	7.2	2.3
9	743	28.8	7.6	2.6
11	870	28.5	8.1	3.1

Discussion

In this study, we found that the residual positioning uncertainties for patients treated for mediastinal lymphoma in DIBH were small after daily CBCT. The clinical PTV margin currently used at our institution is 1 cm, which, in addition to our calculated positioning uncertainties and estimated intrafraction uncertainties, allows for approximately 3 mm contouring uncertainty. This agrees well with the contouring uncertainty found by Aznar et al [14].

1 cm is either the same as [17] or slightly larger than values used at other institutions (5-7 mm [3], 6-10 mm [18], and 8 mm [19]). Incorporating the contouring uncertainty (which is a systematic uncertainty) in the PTV margin, has a relatively large impact on the size of the resulting necessary margins. Many institutions do not include contouring uncertainty in their margin calculations. One rationale for omitting it is either that contouring uncertainties should be included in the CTV itself, at the discretion of the clinician. However, this method also introduces individual variability and does not follow the CTV definition from the ICRU [20–22]. The second rationale is that ensuring CTV coverage by

incorporating contouring uncertainties is not worth the cost in terms of increased dose to the organs at risk, especially in clinical situations where radiotherapy is used as an adjuvant treatment. Though each institution is best positioned to consider the inclusion of this uncertainty in their specific practice, it is worth noticing that contouring uncertainty is present and is one of the largest contributions to uncertainty in a modern radiotherapy context. As a result, we recommend at least the consideration of including the contouring uncertainty in margin calculations and weighing benefits and risks according to the relevance for each institution's specific practice.

PTV margins for this patient group were evaluated by a group at MD Anderson Cancer Center [23], who use in-room CT on rails for image-guidance, an in-house software for image registration, and a breast board with an incline for patient immobilization. An advantage of the CT on rails system is the ability to image the entire length of large target volumes. Their study focused on positioning uncertainty and did not include intrafraction or contouring uncertainties. Instead of comparing online and offline image registrations to evaluate positioning uncertainty, as we did in this study, they compared offline reference registrations and offline registrations on sub-sections of the target. To simulate the use of CBCT, they used the registration on the mediastinal section of the target as the reference registration. They found that the largest uncertainty was in the neck and the inferior region of heart (margins ranged from 3.6 to 11.6 mm, depending on the region and generally increasing with distance from the center of the mediastinum). In comparison, our results (with 0 mm contouring uncertainty) were approximately 4-6 mm. While their image registration with focus on the mediastinal region was meant to simulate an on-line registration using CBCT with limited field of view, the superior-inferior length of the mediastinal section of the target varied in their study and appeared smaller than the length of a CBCT in their Figure 1a. However, details of the length of the mediastinal PTV sections were not reported, so it is unclear how well this method approximates

a true CBCT. In our study, 13/20 patients had targets that extended superiorly outside the field of view of the CBCT, but, unlike their study, patients with neck involvement had bite blocks to immobilize the head and neck. Only one of the patients in our study had a CTV that extended more than 1 cm inferiorly outside the field of view of the CBCT. Recently available equipment upgrades, with possibility of extended length CBCT, will enable imagining of the entire target, also in patients with large targets, hence solving the issue of limited field of view. One major difference of our methods compared to theirs is that we did not perform different registrations with focus on different parts of the target in our study. In addition, different techniques and routines for patient immobilization (e.g. presence or absence of bite blocks and incline boards), image acquisition and registration could have influenced the difference between our results.

Our study should be understood in the context of a few assumptions. First, rotations and deformations were ignored, and only rigid registrations were performed. Second, positioning uncertainties were calculated from the difference between online and offline registrations, where ROI definition differed slightly, and for which intra-observer uncertainties are implicitly included. Furthermore, contouring uncertainties and intra-fractional motion uncertainties were estimated from the literature [14,15], but more data could be helpful in determining those uncertainties more accurately for this patient group. In the study from which we based our estimation of contouring uncertainty [14], the patients were imaged with positron emission tomography (PET) and CT and treated in free breathing, whereas the patient group in our current study was imaged (with both PET and CT) in DIBH and treated in DIBH. Without available data in DIBH, we have chosen to use 3 mm from the free breathing study with the understanding that it is only an estimate. In addition, the positioning uncertainty values calculated in this study apply to the patients at our institution with our immobilization and positioning procedures for mediastinal lymphoma. Other institutions

might find different uncertainties for the same patient group due to site-specific factors such as immobilization practices, the on-board imaging system, or the software used for image registration. Another limitation is that the intra-fraction uncertainty referred to the surface of the patient. Intra-fraction variations of deeper mediastinal structures, such as the heart or inferior part of the CTV are not well documented and would warrant further investigation.

Another consideration when interpreting our results is that margin recipes such as the formula used in this study are designed to prioritize dose to the CTV above all else. In patient groups with a long life expectancy and where radiotherapy plays a consolidative role, it's possible that compromising on CTV/PTV coverage to avoid a large dose to the heart, lungs, and breasts might have a larger benefit than risk. Alternatives to margin recipes such as probabilistic planning [24–26] might be ideally placed to deal with the risk versus benefit balance in this patient group.

Conclusion

In this study, we calculated between 9-11 mm as the appropriate margin from CTV-to-PTV for patients with mediastinal lymphoma treated at our institution in DIBH, assuming daily IGRT with CBCT and including contouring uncertainty. When contouring uncertainty was excluded from the calculation, margins of approximately 4-6 mm were required. We combined measurements in positioning deviation based on CBCTs acquired for image guidance and estimates from the literature to calculate our clinic-specific uncertainties for this patient group. We also showed a large dependence of margins for different estimates of contouring uncertainty. We acknowledge that

uncertainties are institution-specific and advise caution when reducing margins to only include

uncertainties from positioning and motion.

Acknowledgements

Conflict of Interest

Lena Specht: Research agreement: Varian. Advisory Board and Honoraria: Takeda, MDS, Kyowa

Kirin. Travel expenses: Merck Darmstadt, Takeda. Mirjana Josipovic: Grant from Varian Medical

Systems (research agreement with Rigshospitalet), speaker honoraria from Siemens Healthcare

References

1. Specht L, Yahalom J, Illidge T, et al. Modern Radiation Therapy for Hodgkin Lymphoma : Field and Dose Guidelines From the International Lymphoma Radiation Oncology Group (ILROG). *Int J Radiat Oncol Biol Phys*. 2014;89(4):854-862.

2. Maraldo M V, Jørgensen M, Brodin NP, et al. The Impact of Involved Node, Involved Field and Mantle Field Radiotherapy on Estimated Radiation Doses and Risk of Late Effects for Pediatric Patients with Hodgkin Lymphoma. *Pediatr Blood Cancer*. 2014;61(October 2013):717-722. doi:10.1002/pbc

3. Voong KR, Mcspadden K, Pinnix CC, et al. Dosimetric advantages of a "butterfly" technique for intensity-modulated radiation therapy for young female patients with mediastinal Hodgkin's lymphoma. *Radiat Oncol*. 2014;9:94. doi:10.1186/1748-717X-9-94

4. Bujold A, Craig T, Jaffray D, Dawson LA. Image-Guided Radiotherapy: Has It Influenced Patient Outcomes? *Semin Radiat Oncol*. 2012;22(1):50-61. doi:10.1016/j.semradonc.2011.09.001

5. Eng T, Ha CS. Image-guided radiation therapy in lymphoma management. *Radiat Oncol J*. 2015;33(3):161-171. doi:10.3857/roj.2015.33.3.161

6. Petersen PM, Aznar MC, Berthelsen AK, et al. Prospective phase II trial of image-guided radiotherapy in Hodgkin lymphoma: Benefit of deep inspiration breath-hold. *Acta Oncol (Madr)*. 2015;54:60-66. doi:10.3109/0284186X.2014.932435

7. Boda-Heggemann J, Fleckenstein J, Lohr F, et al. Multiple breath-hold CBCT for online image guided radiotherapy of lung tumors: Simulation with a dynamic phantom and first patient data. *Radiother*

Oncol. 2011;98(3):309-316. doi:10.1016/j.radonc.2011.01.019

8. Josipovic M, Persson GF, Bangsgaard JP, Specht L, Aznar MC. Deep inspiration breath-hold radiotherapy for lung cancer: Impact on image quality and registration uncertainty in cone beam CT image guidance. *Br J Radiol*. 2016;89(1068):1-8. doi:10.1259/bjr.20160544

9. Marks LB, Bentzen SM, Deasy JO, et al. Radiation dose-volume effects in the lung. *Int J Radiat Oncol Biol Phys*. 2010;76(3 Suppl):S70-6. doi:10.1016/j.ijrobp.2009.06.091

10. Gagliardi G, Constine LS, Moiseenko V, et al. Radiation dose-volume effects in the heart. *Int J Radiat Oncol Biol Phys*. 2010;76(3 Suppl):S77-85. doi:10.1016/j.ijrobp.2009.04.093

11. Castellino SM, Geiger AM, Mertens AC, et al. Morbidity and mortality in long-term survivors of Hodgkin lymphoma : a report from the Childhood Cancer Survivor Study. *Blood*. 2010;117(6):1806-1817. doi:10.1182/blood-2010-04-278796.An

12. Landberg T, Chavaudra J, Dobbs J, et al. Report 62. *J Int Comm Radiat Units Meas*. 2016;os32(1):NP-NP. doi:10.1093/jicru/os32.1.Report62

13. Damkjær SMS, Aznar MC, Pedersen AN, Vogelius IR, Bangsgaard JP, Josipovic M. Reduced lung dose and improved inspiration level reproducibility in visually guided DIBH compared to audio coached EIG radiotherapy for breast cancer patients. *Acta Oncol (Madr)*. 2013;52(7):1458-1463. doi:10.3109/0284186X.2013.813073

14. Aznar MC, Girinsky T, Berthelsen AK, et al. Interobserver delineation uncertainty in involved-node radiation therapy (INRT) for early-stage Hodgkin lymphoma: on behalf of the Radiotherapy Committee of the EORTC lymphoma group. *Acta Oncol (Madr)*. 2017;56(4):608-613. doi:10.1080/0284186X.2017.1279750

15. Remouchamps VM, Huyskens DP, Mertens I, et al. The use of magnetic sensors to monitor moderate deep inspiration breath hold during breast irradiation with dynamic MLC compensators. *Radiother Oncol*. 2007;82(3):341-348. doi:10.1016/j.radonc.2006.11.015

16. Van Herk M, Remeijer P, Rasch C, Lebesque J V. The probability of correct target dosage: dose-population histograms for deriving treatment margins in radiotherapy. *Int J Radiat Oncol Biol Phys*. 2000;47(4):1121-1135. doi:10.1016/S0360-3016(00)00518-6

17. Paumier A, Ghalibafian M, Gilmore J, et al. Dosimetric benefits of intensity-modulated radiotherapy combined with the deep-inspiration breath-hold technique in patients with mediastinal Hodgkin's lymphoma. *Int J Radiat Oncol Biol Phys*. 2012;82(4):1522-1527. doi:10.1016/j.ijrobp.2011.05.015

18. Baues C, Marnitz S, Engert A, et al. Proton versus photon deep inspiration breath hold technique in patients with hodgkin lymphoma and mediastinal radiation. *Radiat Oncol*. 2018;13(1):1-11. doi:10.1186/s13014-018-1066-2

19. Edvardsson A, Kügele M, Alkner S, et al. Comparative treatment planning study for mediastinal Hodgkin's lymphoma: impact on normal tissue dose using deep inspiration breath hold proton and photon therapy. *Acta Oncol (Madr)*. 2018;0(0):1-10. doi:10.1080/0284186X.2018.1512153

20. International Commission on Radiation Units & Measurements (ICRU). *Prescribing, Recording and Reporting Photon Beam Therapy (ICRU Report 50)*.; 1993. doi:10.2307/3578862

21. International Commission on Radiation Units & Measurements (ICRU). *Prescribing, Recording and Reporting Photon Beam Therapy (Report 62)*.; 1999. doi:https://doi.org/10.1093/jicru/os32.1.Report62

22. International Commission on Radiation Units & Measurements (ICRU). *Precribing, Recording, and Reporting Photon-Beam Intensity-Modulated Radiation Therapy (IMRT) (Report 83)*.; 2010. doi:https://doi.org/10.1093/jicru/10.1.Report83

23. Aristophanous M, Chi PM, Kao J, et al. Deep-Inspiration Breath-Hold Intensity Modulated Radiation Therapy to the Mediastinum for Lymphoma Patients : Setup Uncertainties and Margins. *Int J Radiat Oncol Biol Phys*. 2018;100(1):254-262. doi:10.1016/j.ijrobp.2017.09.036

24. Bohoslavsky R, Witte MG, Janssen TM, van Herk M. Probabilistic objective functions for margin-less IMRT planning. *Phys Med Biol*. 2013;58(11):3563-3580. doi:10.1088/0031-9155/58/11/3563

25. Xu H, Gordon JJ, Siebers J V. Coverage-based treatment planning to accommodate delineation uncertainties in prostate cancer treatment. *Med Phys*. 2015;42(9):5435-5443. doi:10.1118/1.4928490

26. Unkelbach J, Alber M, Bangert M, et al. Robust radiotherapy planning. *Phys Med Biol*. 2018;63(22):22TR02. doi:10.1088/1361-6560/aae659

Paper II
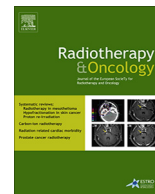
Proton therapy in Hodgkin lymphoma

Life years lost attributable to late effects after radiotherapy for early stage Hodgkin lymphoma: The impact of proton therapy and/or deep inspiration breath hold

Laura Ann Rechner [a,b,*], Maja Vestmø Maraldo [a], Ivan Richter Vogelius [a], Xiaorong Ronald Zhu [c], Bouthaina Shbib Dabaja [d], Nils Patrik Brodin [e], Peter Meidahl Petersen [a], Lena Specht [a], Marianne Camille Aznar [b,f]

[a] Department of Oncology, Rigshospitalet, University of Copenhagen; [b] Niels Bohr Insitute, University of Copenhagen; [c] Department of Radiation Physics, The University of Texas MD Anderson Cancer Center; [d] Department of Radiation Oncology, The University of Texas MD Anderson Cancer Center; [e] Institute for Onco-Physics, Albert Einstein College of Medicine and Montefiore Medical Center, Bronx, USA; [f] Nuffield Department of Population Health, University of Oxford, Oxford, United Kingdom

ARTICLE INFO

ABSTRACT

Background and purpose: Due to the long life expectancy after treatment, the risk of late effects after radiotherapy (RT) is of particular importance for patients with Hodgkin lymphoma (HL). Both deep inspiration breath hold (DIBH) and proton therapy have been shown to reduce the dose to normal tissues for mediastinal HL, but the impact of these techniques in combination is unknown. The purpose of this study was to compare the life years lost (LYL) attributable to late effects after RT for mediastinal HL using intensity modulated radiation therapy (IMRT) in free breathing (FB) and DIBH, and proton therapy in FB and DIBH.
Materials and methods: Plans for each technique were created for 22 patients with HL. Doses were extracted and the risk of late effects and LYL were estimated.
Results: We found that the use of DIBH, proton therapy, and the combination significantly reduced the LYL compared to IMRT in FB. The lowest LYL was found for proton therapy in DIBH. However, when IMRT in DIBH was compared to proton therapy in FB, no significant difference was found.
Conclusions: Patient-specific plan comparisons should be used to select the optimal technique when comparing IMRT in DIBH and proton therapy in FB.
© 2018 The Authors. Published by Elsevier Ireland Ltd. Radiotherapy and Oncology 125 (2017) 41–47 This is an open access article under the CC BY license (http://creativecommons.org/licenses/by/4.0/).

The majority of patients diagnosed with Hodgkin lymphoma (HL) have a long life expectancy following treatment. HL accounts for 12% of cancers in the 15–29-year age group [1], and treatment is highly effective with a 5-year relative survival rate of 93.1% for regional disease [2]. Consequently, HL survivors have a long time span in which they are at risk of developing late effects of treatment such as second cancers and cardiovascular disease [3], and it has been shown that RT contributes to that risk [4–6]. Therefore, it is important to minimize these risks for HL patients whenever possible.

Both deep inspiration breath hold (DIBH) and proton therapy have been shown to reduce the dose to normal tissues for HL patients with mediastinal disease [7–12]; however, to the authors'

knowledge, the impact of these techniques relative to each other or in combination has not been studied. An understanding of which of these has the largest impact on the risk of late effects would enable clinicians to prioritize between techniques, especially if the combination is not available.

Dose-effect models based on epidemiological data can be employed to estimate the risk of late effects from modern treatments. While such models have large uncertainty, they can be used as a tool in the context of comparative analysis of different treatment options. Our group has developed a method of risk modeling that converts organ at risk (OAR) dose into an estimated life years lost (LYL) from various possible late effects [13]. In this way, the severity of different late effects can be placed on a common scale for direct comparison.

In this study, we propose to investigate and compare the LYL from late effects of RT for HL with mediastinal involvement using intensity modulated radiation therapy (IMRT) in free breathing (FB) and in DIBH, and proton therapy in FB and in DIBH.

* Corresponding author at: Blegdamsvej 9, Section 3994, 2100 Copenhagen, Denmark.
  E-mail address: laura.ann.rechner@regionh.dk (L.A. Rechner).

Material and methods

Patients

22 patients with early-stage HL were enrolled in a previous prospective protocol to investigate the benefits of DIBH, described elsewhere [12,14]. In summary, the study included pre-chemotherapy positron emission tomography/computed tomography (PET/CT) scans and planning CT scans both in FB and in DIBH. Contouring was completed on both the FB and DIBH scans to define the CTV by the involved node technique [15]. Treatment plans were created on both scans, and the patients were treated with photons in either FB or DIBH, whichever was more clinically appropriate for the patient. This protocol was approved by the regional ethics committee for Copenhagen H-D-2007-0069.

Treatment planning

For the present retrospective study, four treatment plans were generated for each patient: IMRT in FB, IMRT in DIBH, proton therapy in FB, and proton therapy in DIBH. The prescription dose was 30.6 Gy in 17 fractions to the initially involved volume following the International Lymphoma Radiation Oncology Group (ILROG) guidelines [15]. Proton therapy doses were in Gy (RBE) (relative biological equivalent) assuming an RBE of 1.1 for protons [16], and 1 for photons. All plans were created using the Eclipse treatment planning system (photons: AAA version 10, protons: PCS version 13, Varian Medical Systems, Palo Alto, USA; proton beam data from Skandionkliniken, Uppsala, Sweden).

IMRT plans were created in accordance with the clinical procedure at Rigshospitalet, Copenhagen, Denmark [15]. For plans in FB, the CTV-to-PTV margins were 1.5 cm in the superior-inferior direction in the mediastinum, and 1 cm in other directions. For plans in DIBH, the CTV-to-PTV margins were 1 cm in all directions. The number of fields varied between 4 and 7, with 5 fields being the most common configuration. Whenever possible, fields were positioned to minimize entrance dose through the OARs (heart, lungs, and breasts). In general, 6 MV energy was used, with occasional use of 18 MV for supplementary fields.

Proton plans were created at Rigshospitalet with guidance from the experienced investigators at MD Anderson Cancer Center. Pencil beam scanning with an anterior-posterior and posterior-anterior beam arrangement was used for all patients. Beam-specific range uncertainties were calculated as 3.5% of the range to the distal edge of the CTV plus 3 mm. In cases where the beam-specific range uncertainties were less than the CTV-to-PTV margins used for IMRT planning, the same PTV was used as was used for IMRT planning (1.5 cm superior/inferior and 1 cm otherwise for FB and 1 cm for DIBH). For five patients, the range uncertainties for the posterior beam calculated with the formula above were 1–2 mm greater than the CTV-to-PTV margins that were used for IMRT planning in the anterior direction. For these patients, the PTV was expanded an additional 1–2 mm in the anterior direction to encompass the range uncertainty. For most patients, single-field optimization was used. For five patients with involved nodes surrounding the heart, multi-field optimization (intensity modulated proton therapy (IMPT)) was used to reduce dose to the heart.

During treatment planning for both IMRT and proton plans, the clinical priorities in order of highest to lowest were 1) target coverage, 2) reduction of the mean dose to the heart and lungs, and 3) reduction of the mean dose to the breasts (females). Additional objectives were used during optimization as needed for each patient to reduce the dose to normal tissues as much as possible.

Dosimetric analysis

Dosimetric data for the target and OARs were extracted for all plans. Specifically, the conformity index (CI; volume of body receiving 95% of prescription dose divided by volume of the PTV) and homogeneity index (HI; maximum dose in the PTV divided by the prescription dose) for the PTV were extracted as a measure of coverage of the target. The mean dose was extracted for the heart, heart valves, left anterior descending coronary artery (LADCA), lungs, and breasts (females). For proton plans, neutron doses were added to the therapeutic doses using measured data by Schneider et al. 2002 following the methods of Cella et al. 2013. 6×10^{-14} Sv/proton and 10^{11} protons per Gy (RBE) of therapeutic dose were assumed [17,18]. This corresponds to the neutron dose equivalent in the region of the target, but it was applied to the OARs since all OARs considered in this study were adjacent to or overlapping with the target. Cumulative dose-volume histograms (DVHs) were exported for the heart and lung, neutron dose added to the proton plans, and mean DVHs for all patients for each treatment technique were calculated.

To estimate the effect of uncertainties in positioning and CT calibration on the dose, robustness analysis was performed by calculating the plan uncertainty doses using the built-in tool in the treatment planning system. A positioning uncertainty of 5 mm for both IMRT and proton therapy and Hounsfield Unit (HU) uncertainty of 3.5% for proton therapy were assumed. These uncertainty doses represent 'worst case' scenarios, not an estimation of the actual delivered dose.

Hazard ratios

Hazard ratios (HRs) per Gy relative to the unirradiated population were estimated from the literature for various late effects. The hazard ratios of heart failure [19], myocardial infarction [19], valvular heart disease [20], lung cancer [21], and breast cancer [22] (females) were estimated. Most risk models displayed a linear dose–response relationship and as such, the mean dose to the respective organ was used. An exception was valvular heart disease, where the equivalent dose in 2 Gy fractions (calculated from the differential DVH) to either the mitral valve or the aortic valve, whichever received the higher dose, was used in the risk calculation [20] (personal communication with Dr. Cutter). The risk models used are listed in Table S1.

Life years lost calculation

To convert doses to an estimation of the impact of the late effects on life expectancy after treatment, the LYL was calculated for each plan [13]. The LYL is the estimated reduction in life expectancy attributable to late effects from RT, and takes into account the age at exposure, the patient's sex, and the prognosis of the possible late effects [23–25]. The endpoints included in the LYL were heart failure, myocardial infarction, valvular heart disease, lung cancer, and breast cancer (females). Calculations were performed in Matlab (version 2016b, The MathWorks, Inc, Natick, MA) using the risk models in Table S1 and the methodology and formulae in Brodin et al. [13] to integrate over attained age and account for mortality after an acquired late effect.

Statistical analysis

The Friedman test was used for the dosimetric and risk metrics, with post-hoc two-sided pairwise analysis using Bonferroni correction and *p*-values <0.05 were considered significant. All statistical analyses were performed in Matlab.

Results

Four plans were created for each patient, resulting in a total of 88 plans. Example treatment plans for each technique for a representative patient are shown in Fig. 1. Mean DVHs for the heart and lung are plotted in Figs. 2 and 3, the individual DVHs for each patient can be found in the supplementary material (Figs. S1 and S2). The HI and CI values were considered clinically equivalent for all plans (Table S2). All plans were considered to be robust with respect to positioning and range uncertainties (Table S3).

DIBH reduced the dose to cardiovascular structures compared to FB, regardless of whether proton therapy or IMRT was used (Table 1). This benefit was especially observed for the heart valves, where DIBH led to a median dose reduction of 4.7 Gy for IMRT and 2.3 Gy for proton therapy.

DIBH also reduced the mean dose to the lungs by 2.3 Gy for IMRT and 1.2 Gy for proton therapy, although the difference for proton therapy was not statistically significant. Nevertheless, the lowest mean dose to the lungs was found with proton therapy in DIBH, with a reduction of 4.6 Gy relative to IMRT in FB. Proton

Fig. 2. Mean cumulative dose-volume histograms (DVHs) for the heart for intensity modulated radiation therapy (IMRT) in free breathing (FB), IMRT in deep inspiration breath hold (DIBH), proton therapy in FB, and proton therapy in DIBH for the 22 patients studied.
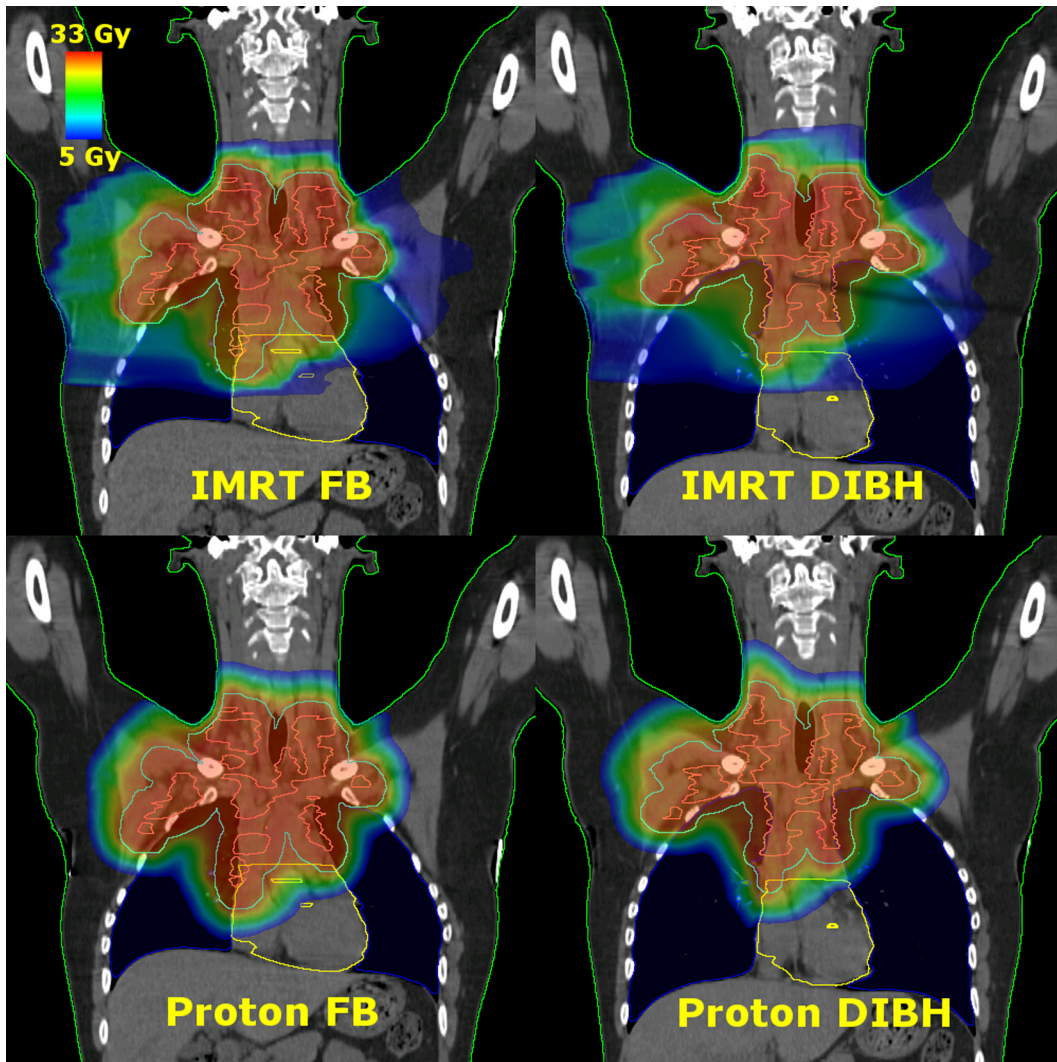
Fig. 1. Coronal images of treatment plans for each treatment technique for a representative patient: intensity modulated radiation therapy (IMRT) in free breathing (FB) (top left), IMRT in deep inspiration breath hold (DIBH) (top right), proton therapy in FB (bottom left), proton therapy in DIBH (bottom right). The contours shown are the body (green), CTV (pink), PTV (cyan), lungs (blue), heart (yellow), and heart valves (yellow).
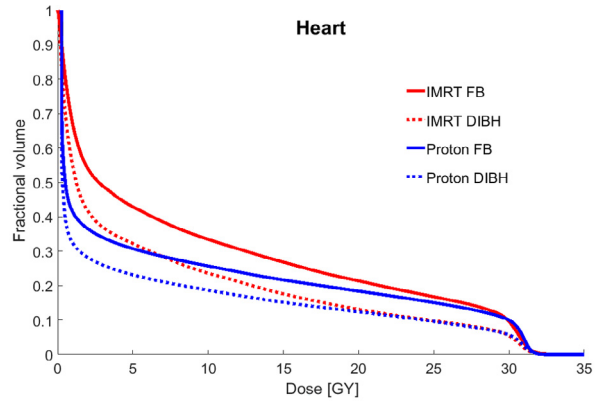
Fig. 3. Mean cumulative dose-volume histograms (DVHs) for the lungs for intensity modulated radiation therapy (IMRT) in free breathing (FB), IMRT in deep inspiration breath hold (DIBH), proton therapy in FB, and proton therapy in DIBH for the 22 patients studied.
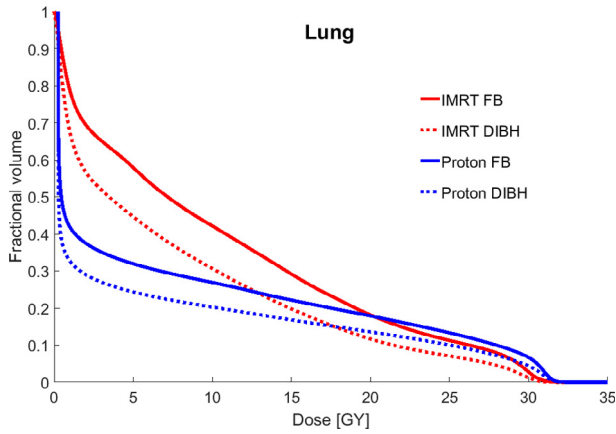
therapy reduced the mean lung dose, but no statistically significant difference was observed between proton therapy in FB and IMRT in DIBH.

In contrast, a significant reduction in mean breast dose of about 3 Gy was found when proton therapy was used compared to IMRT, with or without DIBH.

As most of the risk models used in this study displayed linear dose–response relationships, HR followed the same trend as the mean dose measures (Table 2). The risk of breast cancer was significantly reduced using proton therapy in FB compared to IMRT in DIBH. However, for lung cancer and heart-related risks, no statistically significant difference in HR was seen when proton therapy in FB or DIBH was compared to IMRT in DIBH.

When compared with IMRT in FB, the addition of DIBH and proton therapy, alone or in combination, significantly reduced the LYL, and the lowest LYL from treatment was found for proton therapy in DIBH. However, when proton therapy in FB was compared with IMRT in DIBH, and when proton therapy in DIBH was compared to proton therapy in FB, no significant differences in LYL were found.

The total LYL was either dominated by lung cancer or valvular heart disease for all patients, with the LYL from valvular heart disease being highly variable between patients and techniques. The median LYL (range) for all plans was 0.33 (0.03–1.07) years from lung cancer and 0.46 (0.002–5.35) years from valvular heart disease. The median dose (range) to the aortic or mitral valve was 26.8 (16.3–31.3) Gy for plans where valvular heart disease caused greater than 1 year of LYL. The details of the LYL by cause are shown in Fig. 4 for two representative patients (both had approximately median-sized PTVs of about 1000 cc (range: 123–1943 cc for all patients)). The LYL per technique per patient with 95% confidence intervals are shown in Figs. S9–S13.

Discussion

In this study, we investigated the impact of DIBH and proton therapy, individually and in combination, in a cohort of patients with mediastinal HL. Our study suggests that if only IMRT is available, IMRT in DIBH is superior to IMRT in FB with respect to the risk of late effects. If both IMRT and proton therapy are available in DIBH, our study suggests that proton therapy in DIBH is superior to IMRT in DIBH and FB. If DIBH is available to the patient in combination with IMRT but not with proton therapy, our study did not find any statistically significant difference in the LYL over the

Table 1
Mean doses and their pairwise differences for 22 patients with early-stage mediastinal Hodgkin lymphoma in free breathing (FB) or deep inspiration breath hold (DIBH) delivered with intensity modulated radiation therapy (IMRT) or proton therapy. The Friedman test and post-hoc analysis with Bonferroni correction were used for pairwise comparisons. *P*-values <0.05 and <0.01 are marked with * and **, respectively. Doses are in Gy (RBE) for proton therapy. Breast dose is given for 14 female patients. †Valve doses given as the mean dose to all heart valves: mitral, aortic, pulmonary, and tricuspid. §EQD2 valve doses are given as either the mitral or aortic valves, whichever was higher, to match what is used in the risk model. Plots of mean dose for heart, valves, LADCA, breast, and lung can be found in the supplementary material (Figs. S3–S7). Abbreviations: LADCA: left anterior descending coronary artery, EQD2: equivalent dose in 2 Gy fractions.

Metric	IMRT FB (1) Median (Range)	IMRT DIBH (2) Median (Range)	Proton FB (3) Median (Range)	Proton DIBH (4) Median (Range)	Median of Pairwise Differences (Range)					
					1–2	1–3	1–4	2–3	2–4	3–4
Heart Dose (Gy)	8.0 (0.1–23.2)	3.6 (0.1–17.3)	6.1 (0.3–17.3)	3.7 (0.3–13.6)	2.1** (−0.8–8.7)	1.1* (−1.0–7.8)	2.6** (−0.1–13.3)	−0.2 (−8.0–4.0)	0.5 (−0.7–7.4)	1.3** (−0.5–8.4)
Valve Dose† (Gy)	21.0 (0.3–30.0)	13.4 (0.2–28.8)	16.7 (0.3–30.2)	9.5 (0.3–29.1)	4.7** (−3.5–14.8)	1.3* (−3.0–8.5)	5.7** (−3.0–24.3)	−2.4 (−14.7–7.6)	0.5 (−3.6–10.8)	2.3* (−5.8–19.4)
Valve Dose EQD2§ (Gy)	15.8 (0.2–29.6)	7.8 (0.1–29.6)	11.3 (0.1–30.0)	6.5 (0.1–30.0)	4.1* (−4.0–15.5)	1.2* (−0.4–13.6)	4.1** (−3.3–28.2)	−0.3 (−13.7–10.9)	0.3 (−6.7–13.1)	0.8 (−7.3–19.9)
LADCA Dose (Gy)	7.7 (0.1–29.5)	4.7 (0.1–24.5)	5.2 (0.3–29.9)	2.9 (0.3–24.9)	1.4* (−0.3–13.6)	0.6 (−1.6–10.0)	3.8** (−3.0–14.9)	0.0 (−13.1–6.4)	0.6 (−3.3–10.4)	1.4* (−2.1–14.0)
Lung Dose (Gy)	9.8 (1.8–17.2)	8.0 (1.4–12.6)	7.0 (0.8–12.8)	5.7 (0.9–10.3)	2.3** (0.1–5.9)	2.8** (0.8–5.9)	4.6** (0.8–8.6)	0.6 (−2.9–3.4)	1.9** (0.4–3.6)	1.2 (−0.6–4.5)
Breast Dose (Gy)	4.3 (0.1–14.4)	4.6 (0.2–12.5)	1.4 (0.3–6.3)	1.6 (0.3–4.1)	0.3 (−3.4–3.0)	3.1** (−0.1–11.1)	3.1** (−0.1–11.8)	2.8** (−0.1–10.1)	3.4** (−0.1–9.9)	0.1 (−0.8–3.8)

Table 2
Hazard ratios (HR), life years lost (LYL) estimates, and their pairwise differences for 22 patients with early-stage mediastinal Hodgkin lymphoma in free breathing (FB) or deep inspiration breath hold (DIBH) delivered with intensity modulated radiation therapy (IMRT) or proton therapy. The Friedman test and post-hoc analysis with Bonferroni correction were used for pairwise comparisons. P-values <0.05 and <0.01 are marked with * and **, respectively. Doses are in Gy (RBE) for proton therapy. Breast cancer HR given for 14 female patients. A plot of total LYL can be found in the supplementary material (Fig. S8).

Metric	IMRT FB (1) Median (Range)	IMRT DIBH (2) Median (Range)	Proton FB (3) Median (Range)	Proton DIBH (4) Median (Range)	Median of Pairwise Differences (Range)					
					1–2	1–3	1–4	2–3	2–4	3–4
Heart Failure HR	1.4 (1.01–2.6)	1.2 (1.01–2.2)	1.3 (1.01–2.2)	1.2 (1.01–2.0)	0.1** (−0.04–0.6)	0.1* (−0.1–0.5)	0.2** (−0.01–0.9)	−0.01 (−0.3–0.3)	0.03 (−0.03–0.5)	0.1** (−0.02–0.4)
Myocardial Infarction HR	1.4 (1.005–2.0)	1.2 (1.004–1.8)	1.2 (1.01–1.7)	1.1 (1.01–1.7)	0.1** (−0.05–0.3)	0.1* (−0.04–0.3)	0.1* (0.0–0.5)	−0.01 (−0.2–0.1)	0.02 (−0.04–0.3)	0.04** (−0.03–0.2)
Valvular Heart Disease HR	1.4 (1.001–2.8)	1.1 (1.001–2.8)	1.2 (1.001–2.9)	1.1 (1.001–2.9)	0.1* (−0.3–1.5)	0.1** (−0.1–1.2)	0.2* (−0.3–1.8)	0.0 (−1.2–0.8)	0.0 (−0.4–0.8)	0.01
Lung Cancer HR	2.3 (1.2–3.9)	2.1 (1.2–3.2)	1.9 (1.1–3.2)	1.7 (2.0–2.8)	0.3 (0.01–1.0)	0.4** (0.1–1.4)	0.6** (0.1–1.5)	0.1 (−0.4–0.5)	0.3** (0.1–0.6)	0.2 (−0.5–0.9)
Breast Cancer HR	1.7 (1.02–3.2)	1.7 (1.03–2.9)	1.2 (1.04–2.0)	1.2 (1.04–1.6)	0.05 (−0.5–0.5)	0.5** (0.1–1.5)	0.5** (−0.02–1.5)	0.4** (−0.01–1.5)	0.5** (−0.01–1.5)	0.0 (−0.3–0.8)
Total LYL (years)	2.1 (0.08–6.7)	0.9 (0.07–5.7)	1.3 (0.03–5.6)	0.7 (0.04–5.3)	0.7* (−0.8–4.1)	0.6** (0.05–3.6)	0.9* (−0.4–5.9)	0.02 (−2.9–2.3)	0.1* (−0.9–2.7)	0.3 (−1.5–3.4)
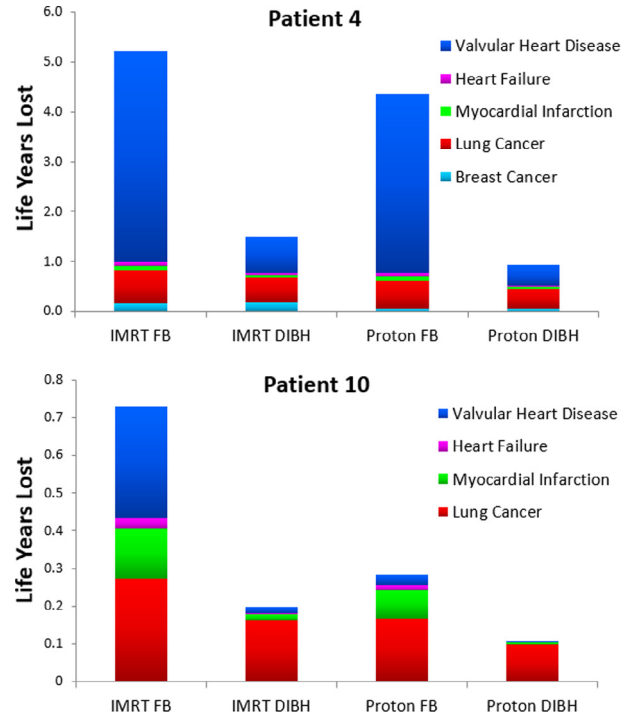
Fig. 4. Life years lost (LYL) by cause for two representative patients: patient 4 (female) and patient 10 (male) for each approach. Mean doses to organs at risk for these two patients are given in supplementary Table S4. Abbreviations: IMRT: intensity modulated radiation therapy; FB (free breathing); DIBH (deep inspiration breath hold).

whole cohort between the two techniques and patient-specific comparative planning would be required to determine the optimal technique. Our study did not find a statistically significant difference when proton therapy in FB was compared with proton therapy in DIBH; however, proton therapy in DIBH did result in the lowest estimated LYL, and, unlike proton therapy in FB, a significant difference was seen when proton therapy in DIBH was compared to IMRT in DIBH.

An earlier study was reported by Cella et al. [18] comparing photon and proton techniques for a patient with HL, without considering DIBH. In their study, the relative risk (RR) of second cancers was estimated after mediastinal RT for conventional RT compared to various intensity modulated photon radiotherapies and proton therapy. They also found a reduction in both breast and lung cancer risk when proton therapy was compared to IMRT, similar to our results.

Toltz et al. [26] also found a reduced risk of breast and lung cancer for proton therapy in FB relative to IMRT in FB in the form of helical tomotherapy for mediastinal HL for 20 patients. However, unlike our study, they did not find a reduction in cardiac mortality between the two techniques. This could in part be due to differences in the choice risk model, which predicted very small excess absolute risks of cardiac toxicity (median of 0.05% for both tomotherapy and proton therapy) in their study.

One strength of the present study is that we have included the most advanced techniques available for this patient group. Plans were created using the involved node technique, contoured using pre-chemotherapy PET/CT acquired in the treatment position in both FB and DIBH, with and planned with pencil beam scanning for the proton plans. Furthermore, we compared different combinations of advanced treatment techniques, so the optimal solution can be selected depending on which techniques are available for the patient. Though DIBH is gaining acceptance in this patient

group [10,27], it is rarely available in combination with proton therapy. Hence, when referring a patient with HL for advanced RT, the most likely treatment alternatives will be IMRT in DIBH or proton therapy in FB.

Photon RT is constantly evolving. Alternative photon techniques, such as the butterfly technique, which could reduce the low dose bath at the expense of a slight decrease in conformity [28], have gained interest [29,30]. One advantage of reducing the low-dose bath is that recently published data have found that low doses to the lung, such as the volume of lung receiving 5 Gy or more (V_5) or mean lung dose of >13.5 Gy, can be important for the risk of radiation pneumonitis [31]. However, the treatment planning in the present study was completed without specific attention to the volume of tissue receiving a low dose of radiation. Therefore, we think that future work could be done investigating this type of photon planning and as compared to proton planning.

Margins from the CTV-to-PTV have been shown to affect both the dose to normal tissue and the risk of late effects [32]. The margins used in this study were based on the recommendations from ILROG [15]. However, with the availability of daily online image guidance, these might be reduced [33]. More research into optimal margins for photons and protons, possibility in combination with proton plans optimized for robustness, is warranted.

A limitation of the present study is that FB plans were generated on FB CT datasets without four-dimensional CT information. It should be noted that the interplay of motion and plan delivery could affect the proton plans more than the photon plans. This has been investigated by Zeng et al. [34] for 7 patients with mediastinal lymphoma, who found that when averaged over 17 fractions, the proton dose to 98% of the internal target volume was degraded less than 2%.

Additionally, the assumptions made in this work could affect the conclusion. While the risk models were selected to be as appropriate as possible, very large uncertainty remains (Figs. S9–S13). In addition, the majority of risk models used in this study were adjusted for smoking status, and therefore estimate the risk associated with increasing dose of radiation independent of the effect of smoking (except for the risk model for breast cancer, where smoking status was not taken into account [22]). While these issues would limit the ability to accurately and precisely estimate the risk for an individual patient, the focus of this study was on relative comparisons of techniques and not absolute risk calculations for individual patients. Another assumption of this work was that the RBE for proton therapy is a constant value of 1.1, without any adjustment for the possibility of a higher RBE at the distal end [35]. A higher RBE for proton therapy would effectively increase the dose in that region, but detailed modeling of proton RBE is still very uncertain and was beyond the scope of this work. In summary, as with all modeling studies, the results and conclusions of this work should be interpreted within the context of the assumptions and limitations made in this study.

Furthermore, the LYL calculations in the present study only consider mortality, but morbidity is also a major concern for patients' quality of life. However, weighting of morbidities to a common scale is challenging, and beyond the scope of the current work. Correspondingly, another future application of this method could be to extend model-based selection schemes for proton therapy such as the models proposed by Langendijk et al. [36,37].

Finally, it should be noted that the results from this study are simulated from risk models and the plans were created in the context of a retrospective plan comparison study. Randomized trials are the golden standard of medical evidence, but for assessment of late effects, the challenge is that such a trial would require 10–15 years follow-up. Hence, modeling studies are needed to guide current treatments.

Conflicts of interest statement

Acknowledgements

Appendix A. Supplementary data

Supplementary data associated with this article can be found, in the online version, at http://dx.doi.org/10.1016/j.radonc.2017.07.033.

References

[1] Jaglowski SM, Linden E, Termuhlen AM, Flynn JM. Lymphoma in adolescents and young adults. Semin Oncol 2009;36:381–418.

[2] National Cancer Institute. Cancer Stat Facts: Hodgkin Lymphoma. Surveillance, Epidemiology, and End Results Program (SEER) 2017. https://seer.cancer.gov/.

[3] Ng AK. Current survivorship recommendations for patients with Hodgkin lymphoma: focus on late effects. Blood 2016;124:3373–80.

[4] Aleman BMP, van den Belt-Dusebout AW, De Bruin ML, et al. Late cardiotoxicity after treatment for Hodgkin lymphoma. Blood 2007;109:1878–86.

[5] Castellino SM, Geiger AM, Mertens AC, et al. Morbidity and mortality in long-term survivors of Hodgkin lymphoma : a report from the Childhood Cancer Survivor Study. Blood 2010;117:1806–17.

[6] Ibrahim EM, Kazkaz GA, Abouelkhair KM, Bayer AM, Elmasri OA. Increased risk of second lung cancer in Hodgkin' s Lymphoma Survivors: a meta-analysis. Lung 2013;191:117–34.

[7] Chera BS, Rodriguez C, Morris CG, et al. Dosimetric comparison of three different involved nodal irradiation techniques for stage II Hodgkin's lymphoma patients: conventional radiotherapy, intensity-modulated radiotherapy, and three-dimensional Proton radiotherapy. Int J Radiat Oncol Biol Phys 2009;75:1173–80.

[8] Li J, Dabaja B, Reed V, et al. Rationale for and preliminary results of proton beam therapy for mediastinal lymphoma. Int J Radiat Oncol Biol Phys 2011;81:167–74.

[9] Andolino DL, Hoene T, Xiao L, Buchsbaum J, Chang AL. Dosimetric comparison of involved-field three-dimensional conformal photon radiotherapy and breast-sparing proton therapy for the treatment of Hodgkin's lymphoma in female pediatric patients. Int J Radiat Oncol Biol Phys 2011;81:667–71.

[10] Paumier A, Ghalibafian M, Gilmore J, et al. Dosimetric benefits of intensity-modulated radiotherapy combined with the deep-inspiration breath-hold technique in patients with mediastinal Hodgkin's lymphoma. Int J Radiat Oncol Biol Phys 2012;82:1522–7.

[11] Hoppe BS, Flampouri S, Su Z, et al. Consolidative involved-node proton therapy for stage IA-IIIB mediastinal hodgkin lymphoma: preliminary dosimetric outcomes from a phase II study. Int J Radiat Oncol Biol Phys 2012;83:260–7.

[12] Petersen PM, Aznar MC, Berthelsen AK, et al. Prospective phase II trial of image-guided radiotherapy in Hodgkin lymphoma: benefit of deep inspiration breath-hold. Acta Oncol (Madr) 2015;54:60–6.

[13] Brodin NP, Vogelius IR, Maraldo MV, et al. Life years lost-comparing potentially fatal late complications after radiotherapy for pediatric medulloblastoma on a common scale. Cancer 2012;118:5432–40.

[14] Aznar MC, Maraldo MV, Schut DA, et al. Minimizing late effects for patients with mediastinal Hodgkin lymphoma: deep inspiration breath-hold, IMRT, or Both? Int J Radiat Oncol 2016;92:1–6.

[15] Specht L, Yahalom J, Illidge T, et al. Modern radiation therapy for Hodgkin lymphoma: field and dose guidelines from the International Lymphoma Radiation Oncology Group (ILROG). Int J Radiat Oncol Biol Phys 2014;89:854–62.

[16] Paganetti H, Niemierko A, Ancukiewicz M, et al. Relative biological effectiveness (RBE) values for proton beam therapy. Int J Radiat Oncol Biol Phys 2002;53:407–21.

[17] Schneider U, Agosteo S, Pedroni E, Besserer J. Secondary neutron dose during proton therapy using spot scanning. Int J Radiat Oncol Biol Phys 2002;53:244–51.

[18] Cella L, Conson M, Pressello MC, et al. Hodgkin's lymphoma emerging radiation treatment techniques: trade-offs between late radio-induced toxicities and secondary malignant neoplasms. Radiat Oncol 2013;8:22.

[19] Mulrooney DA, Yeazel MW, Kawashima T, et al. Cardiac outcomes in a cohort of adult survivors of childhood and adolescent cancer: retrospective analysis of the Childhood Cancer Survivor Study cohort. BMJ 2009;339:b4606.

[20] Cutter DJ, Schaapveld M, Darby SC, et al. Risk of valvular heart disease after treatment for hodgkin lymphoma. J Natl Cancer Inst 2015;107:1–9.

[21] Travis LB, Gospodarowicz M, Curtis RE, et al. Lung cancer following chemotherapy and radiotherapy for Hodgkin's disease. J Natl Cancer Inst 2002;94.

[22] Travis LB, Hill DA, Dores GM. Breast cancer following radiotherapy and chemotherapy among young women with hodgkin disease. JAMA 2003;290:465–75.

[23] Howlader N, Noone A, M K, Al. E. SEER Cancer Statistics Review. Natl Cancer Inst n.d. http://seer.cancer.gov/csr/1975_2008. (accessed June 14, 2011).

[24] Centers for Disease Control and Prevention. National Center for Health Statistics. Health Data Interactive. n.d. www.cdc.gov/nch/hdi.htm (accessed January 11, 2011).

[25] Nkomo VT, Gardin JM, Skelton TN, et al. Burden of valvular heart diseases: a population-based study. Lancet 2006;368:1005–11.

[26] Toltz A, Shin N, Mitrou E, et al. Late radiation toxicity in Hodgkin lymphoma patients: Proton therapy's potential. J Appl Clin Med Phys 2015;16:167–78.

[27] Charpentier A, Conrad T, Sykes J, et al. Active breathing control for patients receiving mediastinal radiation therapy for lymphoma: impact on normal tissue dose. Pract Radiat Oncol 2014;4:174–80.

[28] Voong KR, Mcspadden K, Pinnix CC, et al. Dosimetric advantages of a "butterfly" technique for intensity-modulated radiation therapy for young female patients with mediastinal Hodgkin's lymphoma. Radiat Oncol 2014;9:94.

[29] Fiandra C, Filippi AR, Catuzzo P, et al. Different IMRT solutions vs. 3D-conformal radiotherapy in early stage Hodgkin's lymphoma: dosimetric comparison and clinical considerations. Radiat Oncol 2012;7:186.

[30] Filippi AR, Ragona R, Piva C, et al. Optimized volumetric modulated arc therapy versus 3d-crt for early stage mediastinal Hodgkin lymphoma without axillary involvement: a comparison of second cancers and heart disease risk. Int J Radiat Oncol Biol Phys 2015;92:161–8.

[31] Pinnix CC, Smith GL, Milgrom S, et al. Predictors of radiation pneumonitis in patients receiving intensity modulated radiation therapy for Hodgkin and non-hodgkin lymphoma. Int J Radiat Oncol Biol Phys 2015;92.

[32] Rechner LA, Howell RM, Zhang R, Newhauser WD. Impact of margin size on the predicted risk of radiogenic second cancers following proton arc therapy and volumetric modulated arc therapy for prostate cancer. Phys Med Biol 2012;57: N469–79.

[33] Filippi AR, Ciammella P, Piva C, et al. Involved-site image-guided intensity modulated versus 3d conformal radiation therapy in early stage supradiaphragmatic Hodgkin lymphoma. Int J Radiat Oncol Biol Phys 2014;89:370–5.

[34] Zeng C, Plastaras JP, Tochner ZA, et al. Proton pencil beam scanning for mediastinal lymphoma: the impact of interplay between target motion and beam scanning. Phys Med Biol 2015;60:3013–29.

[35] Paganetti H. Relative biological effectiveness (RBE) values for proton beam therapy. Variations as a function of biological endpoint, dose, and linear energy transfer. Phys Med Biol 2014;59:R419–R1172.

[36] Langendijk JA, Lambin P, De Ruysscher D, et al. Selection of patients for radiotherapy with protons aiming at reduction of side effects: The model-based approach. Radiother Oncol 2013;107:267–73.

[37] Van Der Schaaf A, Langendijk JA, Fiorino C, Rancati T. Embracing phenomenological approaches to normal tissue complication probability modeling: a question of method. Int J Radiat Oncol Biol Phys 2015;91:468–71.

Paper III

Proton therapy and deep inspiration breath hold for patients with thymic cancer

Laura Ann Rechner[1,2], Per Munck af Rosenschöld[3], Anna Bäck[4], Tanja Stagaard Johansen[1], Deborah Anne Schut[1], Marianne Camille Aznar[5], Jan Nyman[6], and Peter Meidahl Petersen[1]

1. Department of Oncology, Center for Cancer and Organ Diseases, Rigshospitalet, Copenhagen, Denmark
2. Niels Bohr Institute, University of Copenhagen, Copenhagen, Denmark
3. Radiation Physics, Skåne University Hospital, Lund, Sweden
4. Department of Therapeutic Radiation Physics, Sahlgrenska University Hospital, Gothenburg, Sweden
5. Manchester Cancer Research Centre, Division of Cancer Sciences, The University of Manchester, Manchester, United Kingdom
6. Department of Oncology, Sahlgrenska University Hospital, Gothenburg, Sweden

Abstract

Thymic epithelial tumors are a rare type of cancer in the mediastinum, which are treated with a combination of chemotherapy, surgery, and radiotherapy. Both deep inspiration breath hold (DIBH) and proton therapy have shown promise in reducing the radiation dose to organs at risk for patients with mediastinal disease, but the data for patients with thymic cancers is limited. In this study, we retrospectively investigated the impact of both DIBH and proton therapy on doses to organs at risk, alone and in combination, relative to treatment in free breathing with photon therapy for 21 patients with thymic cancer. We created four treatment plans per patient: volumetric modulated (photon) arc therapy (VMAT) in free breathing, VMAT in DIBH, proton therapy in free breathing, and proton therapy in DIBH, to a prescription dose of 50 Gy (RBE). We found that the use of proton therapy relative to VMAT statistically significantly reduced many of the dose metrics analyzed; however, the use of DIBH relative to free breathing did not produce statistically significant differences. In conclusion, we found that the use of proton therapy was beneficial for reducing the doses to organs at risk for the patients in this study with thymic cancers.

Introduction

Thymoma and thymic carcinoma are rare types of cancer of the thymus gland in the anterior mediastinum, occurring in approximately 0.15 per 100,000 persons per year [1–3]. Treatment often includes a combination of chemotherapy, surgery, and radiotherapy, and radiotherapy prescription doses usually range from approximately 45 Gy to 60 Gy depending on the stage and degree of resection [4]. Radiation doses in this range in the mediastinum introduce a risk of normal tissue complications such as pneumonitis, esophagitis, secondary cancers, and cardiac toxicity [5–12].

Photon radiotherapy has so far been the standard type of radiotherapy for mediastinal thymic epithelial tumors; however, proton radiotherapy has been used for various thoracic/mediastinal treatment sites to reduce the dose to organs at risk (OARs) relative to treatment with photon radiotherapy [13–19]. Thymic epithelial tumors are rare and therefore difficult to study, there are only a few, but promising, reports showing low doses to OARs and low rates of normal tissue complications after proton therapy [20–24].

Another technique that has been shown to be beneficial for reducing doses to organs at risk (OARs) for patients with thoracic/mediastinal disease is deep inspiration breath hold (DIBH) [15,25–31]. In theory, DIBH should also benefit thymic cancer patients, but data is very limited [32].

1

The purpose of this study was to investigate the impact of proton therapy and DIBH when compared with volumetric modulated (photon) arc therapy (VMAT) and free breathing on doses to OARs for patients with thymic cancer, considering all four combinations of techniques.

Methods

21 consecutive patients with thymoma or thymic carcinoma treated with photon radiotherapy at our institution between 2012 and 2017 were selected for this retrospective study. Inclusion criteria were to have had radiotherapy planning CT-scans in both free breathing and DIBH and curatively intended treatment.

Radiotherapy treatment planning was completed in a commercial treatment planning system (Eclipse, v15.5, Varian Medical Systems, Palo Alto, CA, USA). The prescription dose for this study was 50 Gy (Gy (RBE) for proton therapy assuming an RBE of 1.1 [33,34]). Planning goals were guided by the Swedish PROthym protocol and were ranked as:

- Spinal cord: maximum dose less than 48 Gy (RBE),
- Lung (total): $V_{20Gy(RBE)}$ less than 35%,
- Esophagus: mean dose less than 45 Gy (RBE),
- CTV: $D_{98\%}$ less than 95%,
- PTV: (if PTV used) $D_{2\%}$ less than 105% and $D_{98\%}$ less than 95%, and
- Heart: mean dose as low as possible.

Metal was contoured in the CT-images and assigned a corresponding Hounsfield Unit (HU) value and proton stopping power relative to that of water [35,36]. The true thickness of 0.8 mm was not possible to contour for the stainless steel wire in the sternum, so twice the thickness and half the stopping power was used. Titanium clips were manually contoured and overridden to an HU value that corresponded to titanium. When present, intravenous contrast in the heart and vessels was also contoured and overridden to a value of 50 HU.

VMAT plans were created using 1 cm CTV-to-PTV margins. Two full or partial arcs were used, depending on patient anatomy. Three arcs were used for one patient with a very large target. Dose was calculated using the Acuros XB algorithm.

Proton plans were created using proton beam spot scanning and multifield optimization, also known as the intensity modulated proton therapy (IMPT) technique. Instead of optimizing to a PTV, field-specific PTVs were used for spot placement and robust optimization to the CTV was used with uncertainty parameters of 4.5% uncertainty in CT calibration and 0.5 cm positioning uncertainty. Beam directions depended on patient anatomy, but anterior-oblique fields were most commonly used. For patients without metal wires, a two-field arrangement was the most common (e.g. 10 and 350 degrees). For patients with metal wires, three to four fields were most commonly used, with the occasional use of a posterior field, depending on the difficulty of achieving dose coverage of the CTV. Contours of 'cold spots' (created by converting isodose lines to a contour) behind the metal wires were often used during optimization iterations to achieve better dose coverage.

Dose/volume metrics for the heart, lungs, esophagus, breasts (for females), spinal cord, and body were exported and analyzed. To test for statistically significant differences, the Friedman test with post-hoc analysis using the Bonferroni correction was performed in MATLAB® (R2018b, The MathWorks, Inc., Natick, MA), with two-tailed analysis assuming a significance level for p-values of 0.05.

Results

Characteristics of the patients in this study are summarized in Table 1.

Table 1. Patient characteristics of the 21 patients with thymic cancer in this study.

Patient Characteristics	
Total patients (n)	21
Male	9
Female	12
Surgery (of which have metal wires in sternum)	18 (14)
Residual or unresected disease	8
Thymoma	15
Thymic carcinoma	6
CTV volume FB [median (range)] (cc)	70 (24-1432)
CTV volume DIBH [median (range)] (cc)	77 (20-1491)
Age [median (range)] (years)	55 (24-78)

Abbreviations: number (n), clinical target volume (CTV), free breathing (FB), deep inspiration breath hold (DIBH), cubic centimeters (cc).

VMAT and IMPT plans were created for each patient on both their free breathing and DIBH CT-scans, yielding a total of 84 plans. All plans achieved acceptable target coverage and robustness according to the planning goals. Dose distributions in a transversal CT-slice and dose volume histograms for an example patient (with metal wires in the sternum) who was representative with respect to CTV size and doses to the heart and lungs are shown in Figure 1.
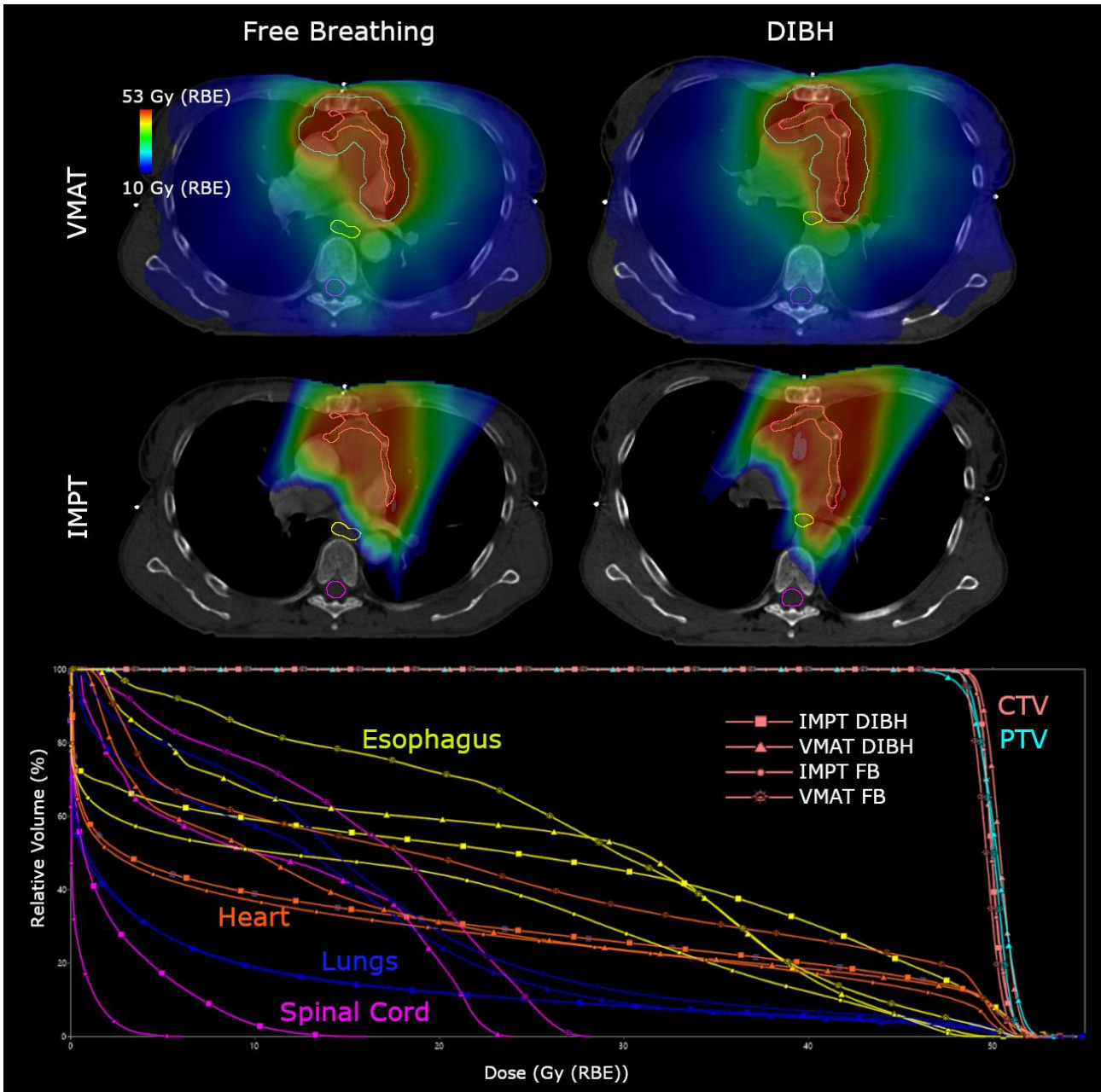
Figure 1. Dose distributions in a transversal CT-slice for a representative patient (patient 6) for each technique: VMAT in free breathing (FB), VMAT in deep inspiration breath hold (DIBH), IMPT in FB, and IMPT in DIBH. The CTV is shown in pink, PTV (for VMAT) in cyan, esophagus in yellow, and spinal cord in magenta. Cumulative dose volume histograms for each technique are shown in the bottom pane for the CTV, PTV (for VMAT), esophagus, heart, lungs, and spinal cord.

Dose/volume metrics were generally more favorable for IMPT when compared to VMAT, regardless of the use of free breathing or DIBH (Table 2) with many statistically significant differences (Table 3). Graphs showing mean doses to the heart, lungs, breast, and esophagus, $V_{20Gy(RBE)}$ to the lungs, $V_{5Gy(RBE)}$ to the lungs, and D_{2cc} to the esophagus for all patients for all plans can be found in the appendix. No statistically significant differences were seen for any of the dose/volume metrics when VMAT in free breathing was compared to VMAT in DIBH, nor when IMPT in free breathing was compared with IMPT in DIBH. However, there was a large variability between patients and some individual patients benefited greatly from DIBH (appendix). For

the dose to 2cc (D_{2cc}) of the esophagus, only VMAT in free breathing compared to IMPT in free breathing was significantly different. Dose metrics for the heart were not statistically different when VMAT in DIBH was compared to IMPT in FB.

Table 2. Dose metrics for the organs at risk (OARs) investigated in this study for all patients and each technique.

Organ at Risk	Dose/Volume Metric	Technique			
		VMAT FB (mean (range))	VMAT DIBH (mean (range))	IMPT FB (mean (range))	IMPT DIBH (mean (range))
Lungs	Mean Dose (Gy (RBE))	14.3 (8.2-26.6)	11.8 (6.6-20.9)	6.8 (2.3-17.6)	5.7 (2.4-13.3)
	$V_{20Gy(RBE)}$ (Fractional Volume)	0.2 (0.10-0.6)	0.2 (0.07-0.5)	0.13 (0.04-0.4)	0.11 (0.03-0.3)
	$V_{5Gy(RBE)}$ (Fractional Volume)	0.7 (0.5-0.99)	0.6 (0.4-0.9)	0.3 (0.09-0.7)	0.2 (0.12-0.5)
Heart	Mean Dose (Gy (RBE))	15.7 (1.8-32.5)	13.9 (0.6-33.5)	10.5 (0.7-31.2)	9.7 (0.0-29.9)
	$V_{20Gy(RBE)}$ (Fractional Volume)	0.3 (0.01-0.6)	0.3 (0.0-0.7)	0.2 (0.01-0.7)	0.2 (0.0-0.6)
Esophagus	Mean Dose (Gy (RBE))	17.2 (8.0-40.1)	15.5 (5.5-42.9)	9.5 (0.2-40.6)	10.4 (0.2-35.7)
	D_{2cc} (Gy (RBE))	32.6 (14.5-52.0)	30.4 (12.3-50.1)	23.7 (0.7-50.0)	25.7 (0.7-50.3)
Spinal Cord	D_{max} (Gy (RBE))	21.1 (9.1-36.6)	18.8 (7.1-43.8)	5.6 (0.02-25.8)	8.6 (0.03-39.7)
Breasts	Mean Dose (Gy (RBE))	9.1 (2.6-16.2)	10.5 (3.3-18.6)	3.3 (0.2-10.6)	3.6 (0.3-11.8)
Body	Integral Dose (Gy (RBE)*L)	150.8 (64.2-423.3)	160.4 (63.0-430.5)	69.3 (24.1-246.0)	76.0 (28.5-267.4)

Abbreviations: Volumetric modulated arc therapy (VMAT), intensity modulated proton therapy (IMPT), free breathing (FB), deep inspiration breath hold (DIBH), fractional volume receiving dose level x (V_x), dose to 2 cc of a structure D_{2cc}, maximum dose to a structure (D_{max}), liter (L).

Table 3. Statistical analysis showing the p-values from the Friedman test with post-hoc two-tailed analysis using the Bonferroni correction. Comparisons that were found to be significant (p≤0.05) are marked in bold.

	Lungs Mean Dose (Gy (RBE))	Lungs V20 (Fractional Volume)	Lungs V5 (Fractional Volume	Heart Mean Dose (Gy (RBE))	Heart V20 (Fractional Volume	Esophagus Mean Dose (Gy (RBE))	Esophagus D2cc (Gy (RBE))	Spinal Cord Max Dose (Gy (RBE))	Breasts Mean Dose (Gy (RBE))	Integral Dose (Gy (RBE)*L)
VMAT FB vs VMAT DIBH	0.3	0.5	0.4	0.3	0.3	1	1	0.6	1	1
VMAT FB vs IMPT FB	**<0.001**	**<0.001**	**<0.001**	**<0.001**	**<0.001**	**<0.001**	**<0.01**	**<0.001**	**<0.01**	**<0.001**
VMAT FB vs IMPT DIBH	**<0.001**	**<0.001**	**<0.001**	**<0.001**	**<0.001**	**<0.001**	0.9	**<0.01**	**0.04**	**<0.01**
VMAT DIBH vs IMPT FB	**<0.01**	**0.013**	**<0.01**	0.2	0.2	**<0.001**	0.1	**<0.001**	**<0.001**	**<0.001**
VMAT DIBH vs IMPT DIBH	**<0.001**	**<0.001**	**<0.001**	**<0.001**	**<0.001**	**<0.001**	1	0.3	**<0.001**	**<0.001**
IMPT FB vs IMPT DIBH	1	0.5	1	0.4	0.4	1	0.14	0.2	1	1

Abbreviations: Volumetric modulated arc therapy (VMAT), intensity modulated proton therapy (IMPT), free breathing (FB), deep inspiration breath hold (DIBH), fractional volume receiving dose level x (V_x), dose to 2 cc of a structure D_{2cc}, maximum dose to a structure (D_{max}).

Discussion

In this treatment planning study, we investigated the dosimetric impact of both DIBH and proton therapy for patients with thymic cancer. Reduction of doses to the lungs and heart dose is especially important in patients with thymic epithelial tumors because many of the patients have poorer lung function due to chemotherapy and surgery and impaired cardiac function due to anthracyclines.

We found that proton therapy generally reduced the doses to OARs in comparison to VMAT. To our surprise, while some individual patients benefited from DIBH, we did not find a statistically significant impact of DIBH for either proton therapy or VMAT. This conflicts with the evidence from mediastinal Hodgkin lymphoma [25,26] and could be due to the slight differences in anatomical location of the different diseases. DIBH might still be advantageous for individual patients or as a motion management tool when considering treatment margins or robustness and interplay effects, an especially important consideration for proton therapy [37].

We found that proton therapy reduced the doses to OARs relative to VMAT, which is consistent with other studies. One case report [20] described reductions in mean dose to the heart, lungs, and esophagus of 8 Gy, 6 Gy, and 20 Gy, respectively, from proton therapy when compared to intensity modulated radiotherapy (IMRT) for a young woman with thymoma. In a study of 10 patients comparing passively-scatter proton therapy with IMRT, Vogel et al. [38] reported reductions of 12 Gy, 4.5 Gy, and 17.7 Gy on average for the mean dose to the heart, lungs, and esophagus. Similarly, Zhu et al. [23] reported average reductions in mean dose to the heart, lungs, and esophagus of 36.5%, 33.5%, and 60%, respectively from passively-scattered proton therapy relative to IMRT. Finally, Haefner et al. [39] compared a few different modalities for 10 patients with thymoma and found that spot scanning proton therapy reduced doses to OARs when compared to photon therapies. In our study comparing spot scanning proton therapy to VMAT, we found corresponding reductions of 5 Gy (RBE), 7.5 Gy (RBE), and 7.7 Gy (RBE) for proton therapy (free breathing, average of paired differences). While these differences are not quite as large as some of the other studies, they are still quite substantial.

In conclusion, we found that for the patients in this study with thymic cancer, IMPT generally reduced the dose to OARs relative to VMAT, with or without the use of DIBH.

References

[1]   SEER. SEER 9, 13, and 18. Natl Cancer Institute's Surveillance, Epidemiol End Results Progr 2006. www.seer.cancer.gov.

[2]   Engels EA. Epidemiology of thymoma and associated malignancies Eric. J Thorac Oncol 2010;5:S260–S265. doi:10.1097/JTO.0b013e3181f1f62d. Epidemiology.

[3]   Bushan K, Sharma S, Verma H. A review of thymic tumors. Indian J Surg Oncol 2013;4:112–6. doi:10.1007/s13193-013-0214-2.

[4]   Girard N, Ruffini E, Marx A, Faivre-Finn C, Peters S. Thymic epithelial tumours: ESMO Clinical Practice Guidelines for diagnosis, treatment and follow-up. Ann Oncol 2015;26:v40–55. doi:10.1093/annonc/mdv277.

[5]   Moiseenko V, Craig T, Bezjak A, Dyk J Van. Dose–volume analysis of lung complications in the radiation treatment of malignant thymoma: a retrospective review. Radiother Oncol 2003;67:265–74. doi:10.1016/S0167-8140(03)00003-3.

[6]   Aleman BMP, van den Belt-Dusebout AW, De Bruin ML, van 't Veer MB, Baaijens MH a, de Boer JP, et al. Late cardiotoxicity after treatment for Hodgkin lymphoma. Blood 2007;109:1878–86. doi:10.1182/blood-2006-07-034405.

[7]   Werner-Wasik M, Yorke E, Deasy J, Nam J, Marks LB. Radiation Dose-Volume Effects in the Esophagus. Int J Radiat Oncol Biol Phys 2010;76:86–93. doi:10.1016/j.ijrobp.2009.05.070.

[8]   Marks LB, Bentzen SM, Deasy JO, Kong F-MS, Bradley JD, Vogelius IS, et al. Radiation dose-volume effects in the lung. Int J Radiat Oncol Biol Phys 2010;76:S70-6. doi:10.1016/j.ijrobp.2009.06.091.

[9]   Ibrahim EM, Kazkaz GA, Abouelkhair KM, Bayer AM, Elmasri OA. Increased Risk of Second Lung Cancer in Hodgkin ' s Lymphoma Survivors : A Meta-analysis. Lung 2013;191:117–34. doi:10.1007/s00408-012-9418-4.

[10]   Cutter DJ, Schaapveld M, Darby SC, Hauptmann M, van Nimwegen F a, Krol ADG, et al. Risk of valvular heart disease after treatment for hodgkin lymphoma. J Natl Cancer Inst 2015;107:1–9. doi:10.1093/jnci/djv008.

[11]   Van Nimwegen FA, Schaapveld M, Cutter DJ, Janus CPM, Krol ADG, Hauptmann M, et al. Radiation dose-response relationship for risk of coronary heart disease in survivors of Hodgkin lymphoma. J Clin Oncol 2016;34:235–43. doi:10.1200/JCO.2015.63.4444.

[12]   Darby SC, Ewertz M, McGale P, Bennet AM, Blom-Goldman U, Brønnum D, et al. Risk of ischemic heart disease in women after radiotherapy for breast cancer. N Engl J Med 2013;368:987–98. doi:10.1056/NEJMoa1209825.

[13]   Li J, Dabaja B, Reed V, Allen PK, Cai H, Amin M V., et al. Rationale for and preliminary results of proton beam therapy for mediastinal lymphoma. Int J Radiat Oncol Biol Phys 2011;81:167–74. doi:10.1016/j.ijrobp.2010.05.007.

[14]   Rechner LA, Maraldo MV, Vogelius IR, Zhu XR, Dabaja BS, Brodin NP, et al. Life years lost attributable to late effects after radiotherapy for early stage Hodgkin lymphoma: The impact of proton therapy and/or deep inspiration breath hold. Radiother Oncol 2017;125:41–7. doi:10.1016/j.radonc.2017.07.033.

[15]   Edvardsson A, Kügele M, Alkner S, Enmark M, Nilsson J, Kristensen I, et al. Comparative treatment planning study for mediastinal Hodgkin's lymphoma: impact on normal tissue dose using deep inspiration breath hold proton and photon therapy. Acta Oncol (Madr) 2018;0:1–10. doi:10.1080/0284186X.2018.1512153.

[16]   Plastaras JP, Berman AT, Freedman GM. Special cases for proton beam radiotherapy: Re-irradiation, lymphoma, and breast cancer. Semin Oncol 2014;41:807–19. doi:10.1053/j.seminoncol.2014.10.001.

[17]   Stick LB, Yu J, Maraldo M V, Aznar MC, Pedersen AN, Bentzen SM, et al. Joint Estimation of Cardiac Toxicity and Recurrence Risks After Comprehensive Nodal Photon Versus Proton Therapy for Breast

Cancer. Int J Radiat Oncol 2017;97:754–61. doi:https://doi.org/10.1016/j.ijrobp.2016.12.008.

[18] Weber DC, Ares C, Lomax AJ, Kurtz JM. Radiation therapy planning with photons and protons for early and advanced breast cancer: an overview. Radiat Oncol 2006;1:22. doi:10.1186/1748-717X-1-22.

[19] Wu C-T, Motegi A, Motegi K, Hotta K, Kohno R, Tachibana H, et al. Dosimetric comparison between proton beam therapy and photon radiation therapy for locally advanced non-small cell lung cancer. Jpn J Clin Oncol 2016;46:1008–14. doi:10.1093/jjco/hyw108.

[20] Figura NS, Hoppe BC, Flampouri SC, Su ZC, Osian OC, Monroe AC, et al. Postoperative Proton Therapy in the Management of Stage III Thymoma. J Thorac Oncol 2013;8:e38–40. doi:10.1097/JTO.0b013e31827a8911.

[21] Vogel J, Berman AT, Lin L, Pechet TT, Levin WP, Gabriel P, et al. Prospective study of proton beam radiation therapy for adjuvant and definitive treatment of thymoma and thymic carcinoma: Early response and toxicity assessment. Radiother Oncol 2016;118:504–9. doi:10.1016/j.radonc.2016.02.003.

[22] Parikh RR, Rhome R, Hug E, Tsai H, Cahlon O, Chon B, et al. Adjuvant Proton Beam Therapy in the Management of Thymoma: A Dosimetric Comparison and Acute Toxicities. Clin Lung Cancer 2016;17:362–6. doi:10.1016/j.cllc.2016.05.019.

[23] Zhu HJ, Hoppe BS, Flampouri S, Louis D, Pirris J, Nichols RC, et al. Rationale and early outcomes for the management of thymoma with proton therapy. Transl Lung Cancer Res 2018;7:106–13. doi:10.21037/tlcr.2018.04.06.

[24] Mercado CE, Hartsell WF, Simone CB, Tsai HK, Vargas CE, Zhu HJ, et al. Proton therapy for thymic malignancies: multi-institutional patterns-of-care and early clinical outcomes from the proton collaborative group and the university of Florida prospective registries. Acta Oncol (Madr) 2019;58:1036–40. doi:10.1080/0284186X.2019.1575981.

[25] Paumier A, Ghalibafian M, Gilmore J, Beaudre A, Blanchard P, El Nemr M, et al. Dosimetric benefits of intensity-modulated radiotherapy combined with the deep-inspiration breath-hold technique in patients with mediastinal Hodgkin's lymphoma. Int J Radiat Oncol Biol Phys 2012;82:1522–7. doi:10.1016/j.ijrobp.2011.05.015.

[26] Petersen PM, Aznar MC, Berthelsen AK, Loft A, Schut DA, Maraldo M, et al. Prospective phase II trial of image-guided radiotherapy in Hodgkin lymphoma: Benefit of deep inspiration breath-hold. Acta Oncol (Madr) 2015;54:60–6. doi:10.3109/0284186X.2014.932435.

[27] Rechner LA, Maraldo MV, Vogelius IR, Zhu XR, Dabaja BS, Brodin NP, et al. Life years lost attributable to late effects after radiotherapy for early stage Hodgkin lymphoma: The impact of proton therapy and/or deep inspiration breath hold. Radiother Oncol 2017. doi:10.1016/j.radonc.2017.07.033.

[28] Damkjær SMS, Aznar MC, Pedersen AN, Vogelius IR, Bangsgaard JP, Josipovic M. Reduced lung dose and improved inspiration level reproducibility in visually guided DIBH compared to audio coached EIG radiotherapy for breast cancer patients. Acta Oncol (Madr) 2013;52:1458–63. doi:10.3109/0284186X.2013.813073.

[29] Pedersen AN, Korreman S, Nyström H, Specht L. Breathing adapted radiotherapy of breast cancer: reduction of cardiac and pulmonary doses using voluntary inspiration breath-hold. Radiother Oncol 2004;72:53–60.

[30] Korreman SS, Pedersen AN, Nøttrup TJ, Specht L, Nyström H. Breathing adapted radiotherapy for breast cancer: comparison of free breathing gating with the breath-hold technique. Radiother Oncol 2005;76:311–8. doi:10.1016/j.radonc.2005.07.009.

[31] Josipovic M, Persson G, Hakansson K, Damkjaer S, Westman G, Bangsgaard J, et al. Deep Inspiration Breath-Hold Radiation Therapy for Advanced Stage Lung Cancer Is Feasible and Facilitates Lung Toxicity Reduction. Int J Radiat Oncol Biol Phys 2013;87:S542–3.

[32] Rohrberg KS, Daugaard G, Petersen PM. P32: Comparing radiotherapy with free breathing and deep

inspiration breath hold for thymic cancers. J. Thorac. Dis., 2015, p. AB101.

[33]   Paganetti H. Relative biological effectiveness (RBE) values for proton beam therapy. Variations as a function of biological endpoint, dose, and linear energy transfer. Phys Med Biol 2014;59:R419–72. doi:10.1088/0031-9155/59/22/R419.

[34]   Paganetti H, Blakely E, Carabe-fernandez A, Carlson DJ, Held KD. Report of the AAPM TG-256 on the relative biological effectiveness of proton beams in radiation therapy. Med Phys 2019;46. doi:10.1002/mp.13390.

[35]   Jäkel O. Ranges of ions in metals for use in particle treatment planning. Phys Med Biol 2006;51:N173–7. doi:10.1088/0031-9155/51/9/N01.

[36]   Glide-Hurst CK, Chen D, Zhong H, Chetty IJ. Changes realized from extended bit-depth and metal artifact reduction in CT. Med Phys 2013;40.

[37]   Zeng C, Plastaras JP, Tochner ZA, White BM, Hill-Kayser CE, Hahn SM, et al. Proton pencil beam scanning for mediastinal lymphoma: the impact of interplay between target motion and beam scanning. Phys Med Biol 2015;60:3013–29. doi:10.1088/0031-9155/60/7/3013.

[38]   Vogel J, Lin L, Litzky LA, Berman AT, Simone CB. Predicted Rate of Secondary Malignancies Following Adjuvant Proton Versus Photon Radiation Therapy for Thymoma. Int J Radiat Oncol Biol Phys 2017;99:427–33. doi:10.1016/j.ijrobp.2017.04.022.

[39]   Haefner MF, Verma V, Bougatf N, Mielke T, König L, Rwigema JM, et al. Dosimetric comparison of advanced radiotherapy approaches using photon techniques and particle therapy in the postoperative management of thymoma. Acta Oncol (Madr) 2018;57:1713–20. doi:10.1080/0284186X.2018.1502467.

Heart Mean Dose

Lung Mean Dose

Lung V20Gy

Lung V5Gy

Esophagus Mean Dose

Esophagus D2cc
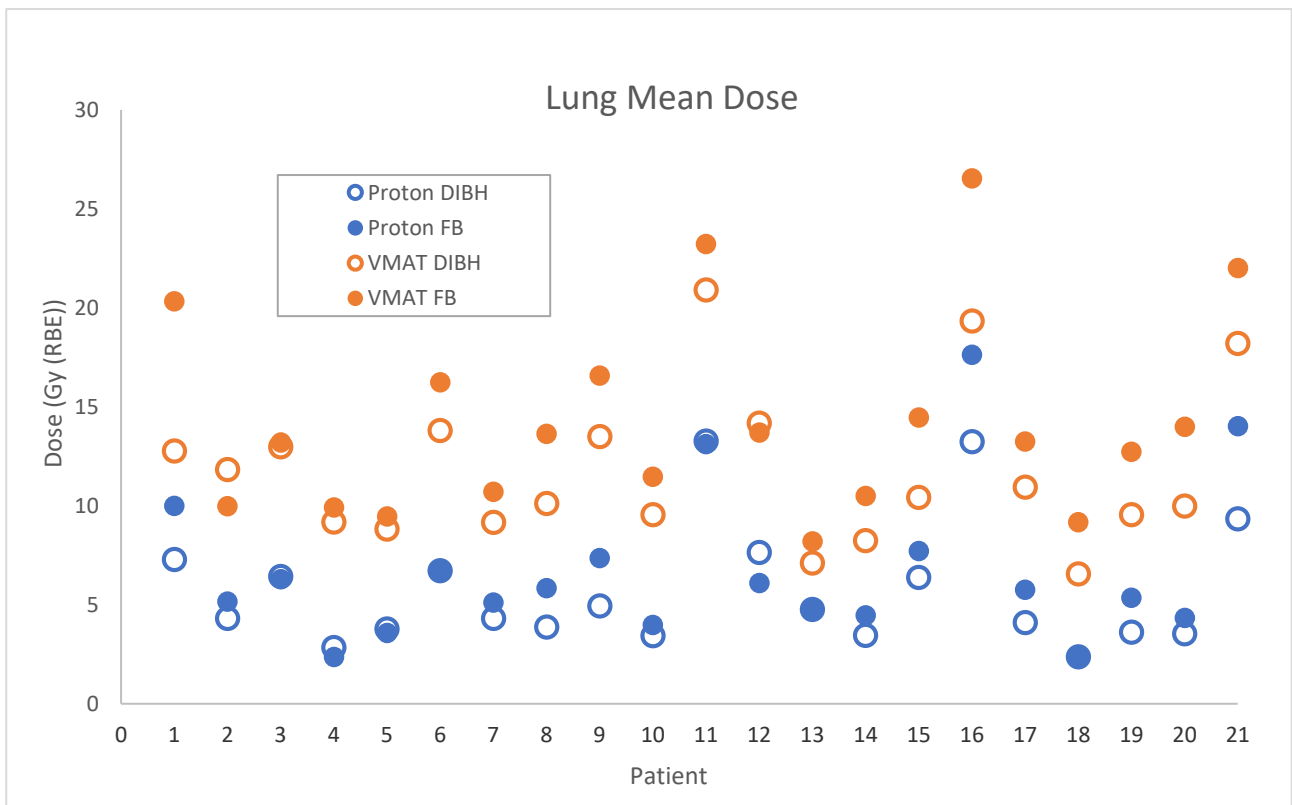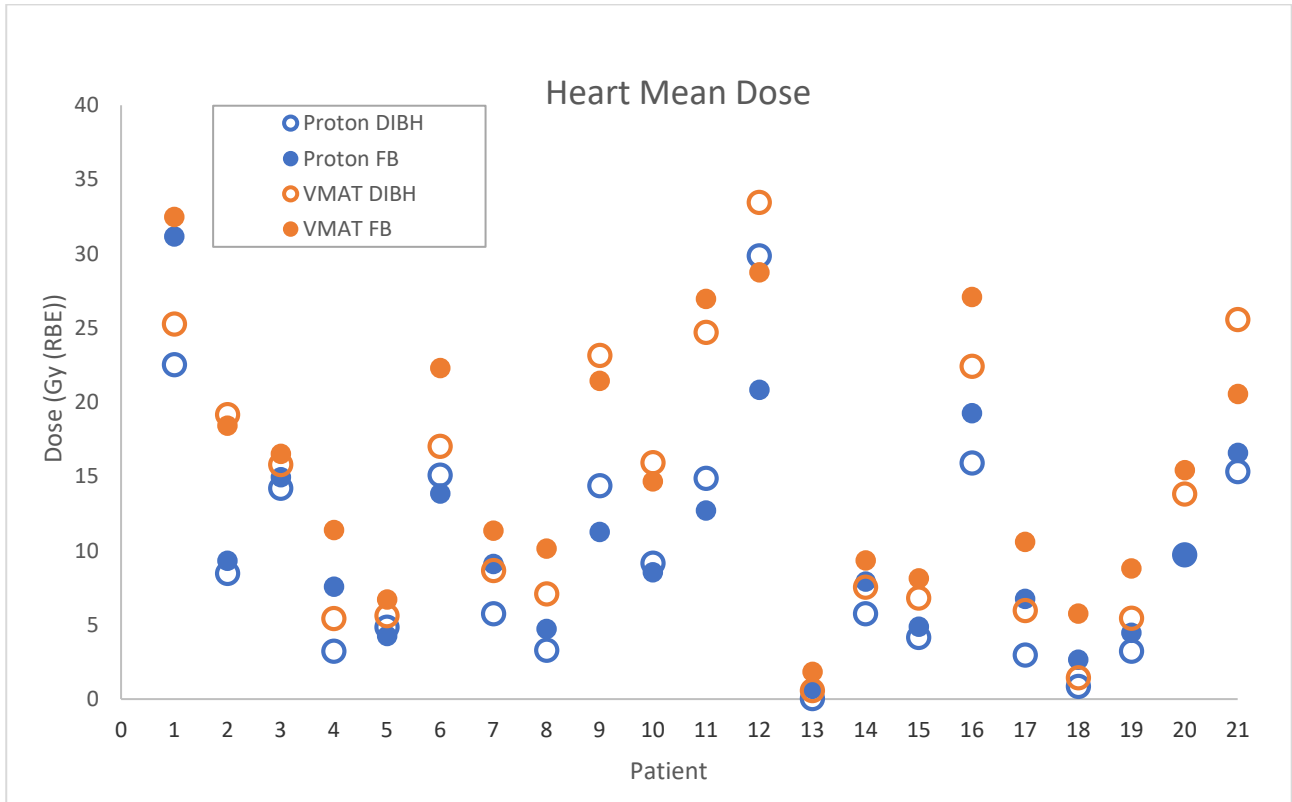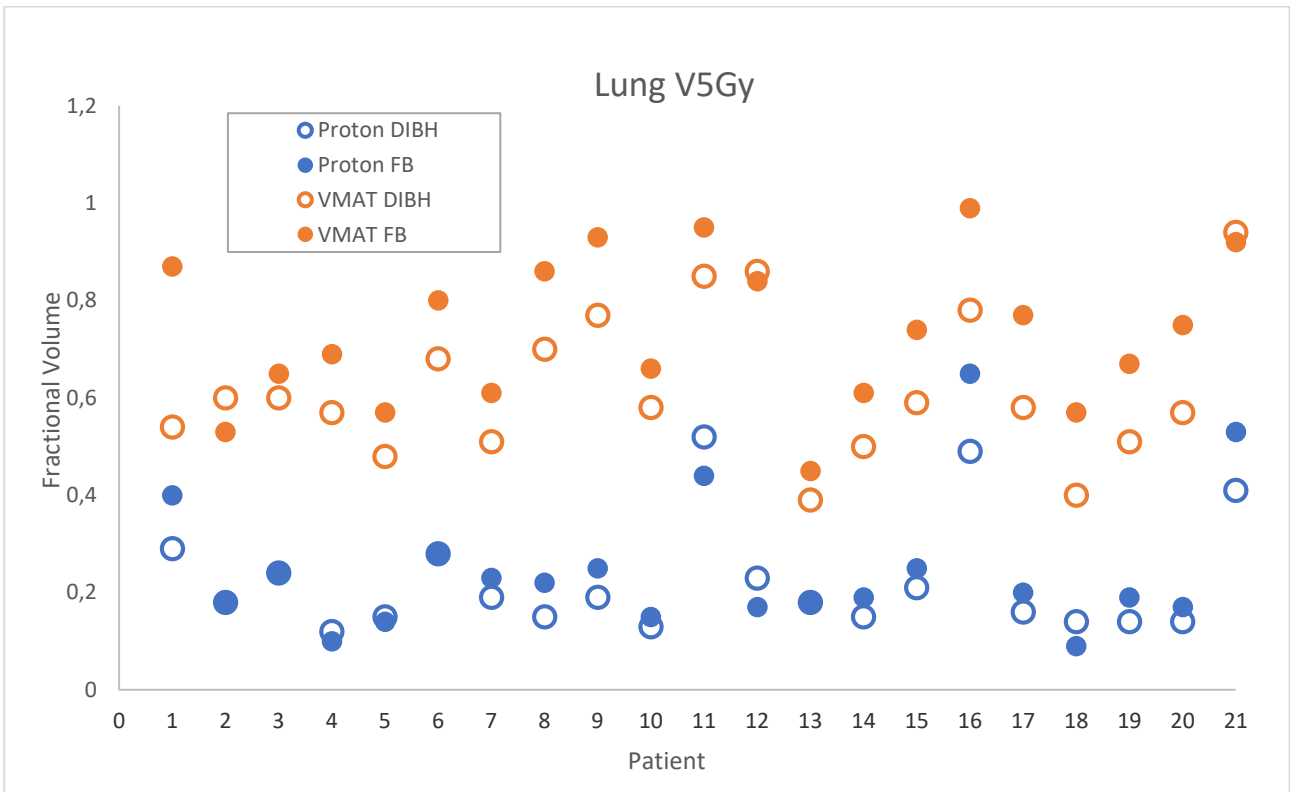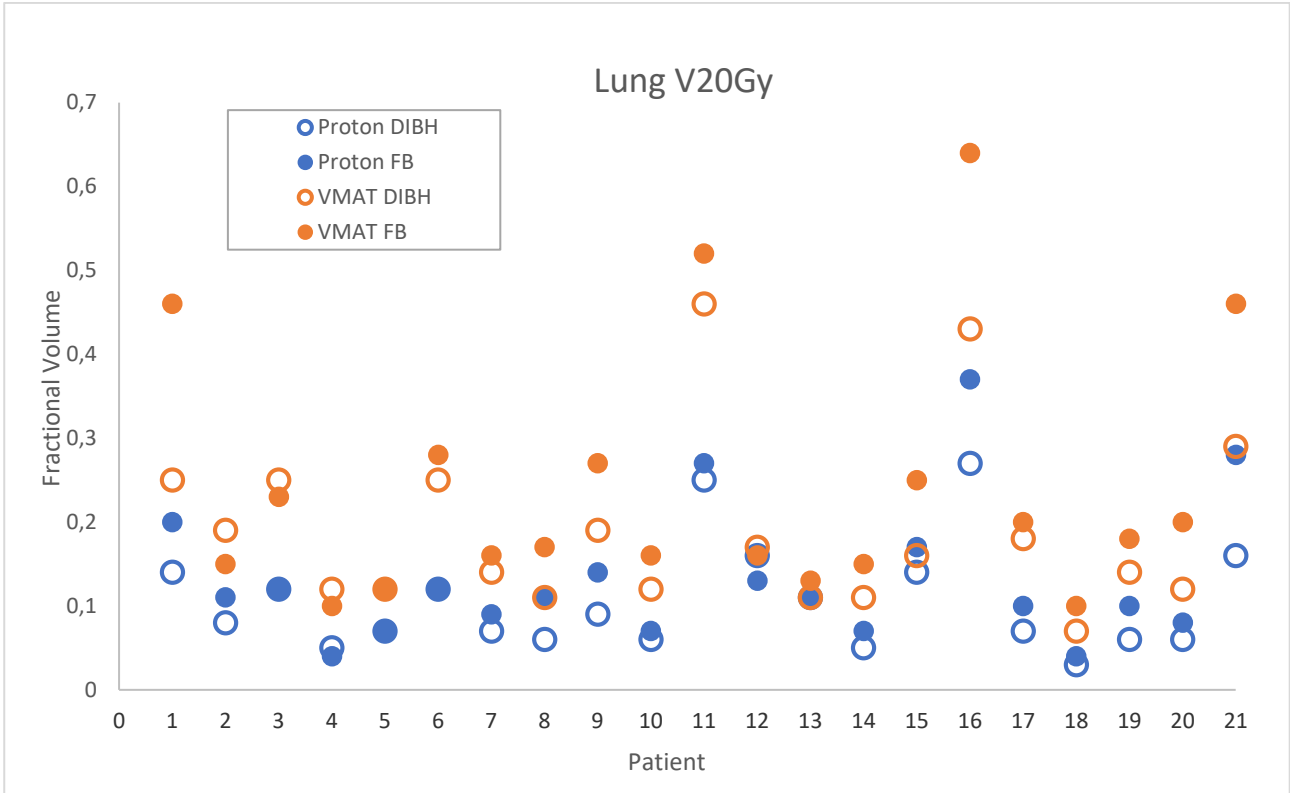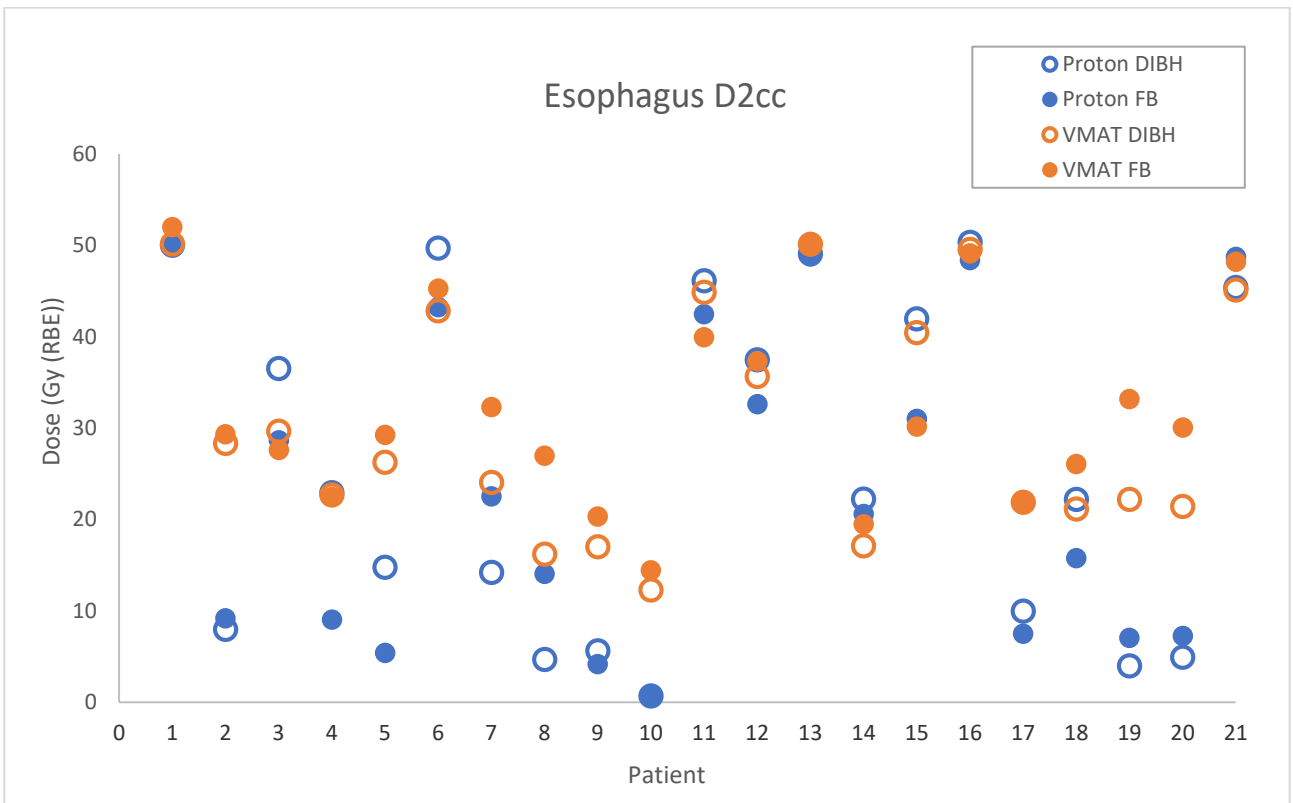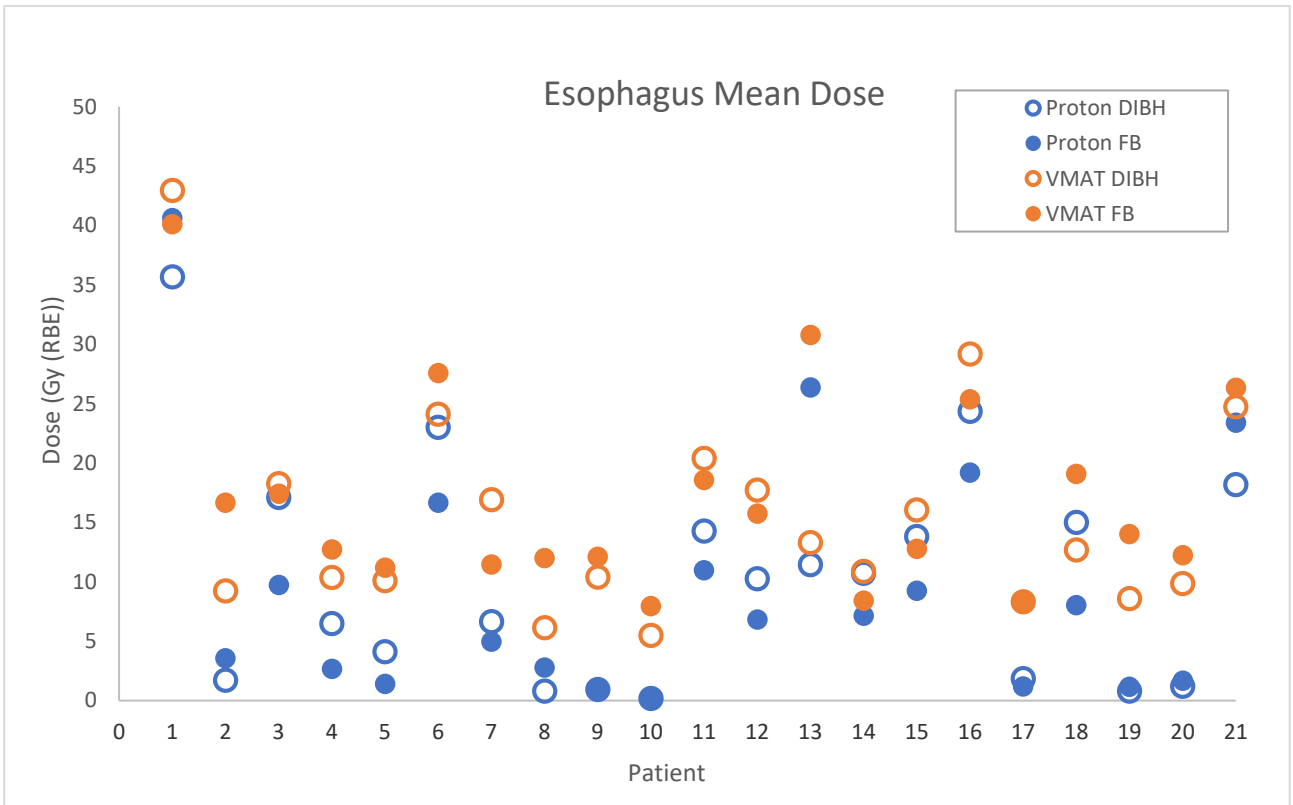
Paper IV

Proton LET and variable RBE for pediatric patients with Hodgkin lymphoma

Laura A. Rechner[1,2]* & Maja Maraldo[1,2]*, Edward A. K. Smith[3,4], Anni Y. Lundgaard[1], Lisa L. Hjalgrim[1], Akmal Safwat[6], Ranald I. MacKay[3,4], Adam H. Aitkenhead[3,4†] & Marianne C. Aznar[3,5 †]

1 Department of Oncology, Rigshospitalet, Copenhagen, DK
2 Niels Bohr Institute, University of Copenhagen, Copenhagen, DK
3 Division of Cancer Sciences, School of Medical Sciences, Faculty of Biology, Medicine and Health, The University of Manchester, UK
4 Christie Medical Physics and Engineering, The Christie NHS Foundation Trust, Manchester, UK
5 Clinical Trial Service Unit, Nuffield Department of Population Health, University of Oxford, United Kingdom
6 Department of Oncology and Danish Center for Particle Therapy, Aarhus University Hospital, Aarhus, DK
* co first authors
† co senior authors

Abstract

Proton therapy has a theoretical dosimetric advantage due to the Bragg peak, but the linear energy transfer (LET), and therefore the relative biological effectiveness (RBE), increase at the end of range. It is unknown if this effect is relevant for doses to organs at risk for pediatric patients with Hodgkin lymphoma. The purpose of this project was to investigate these biological uncertainties for protons for pediatric patients with Hodgkin lymphoma and the impact of different beam arrangements on these uncertainties. We selected three previously treated pediatric patients with mediastinal Hodgkin lymphoma and retrospectively created 3 to 4 proton plans per patient with 1, 2, and 3 beams. All plans were recalculated with Monte Carlo (MC) (AutoMC, Manchester), and dose-averaged LET was scored. Doses with variable RBE were calculated using the McNamara model and an assumed alpha/beta ratio of 2. We found that the LET decreased as the number of beams increased, but that the differences between the MC dose with fixed RBE (1.1) and the MC dose with vRBE was small for all plans. Furthermore, the MC dose with vRBE was often lower than the MC dose with fixed RBE. In conclusion, while uncertainties remain in variable RBE models, we did not find that increased LET and therefore RBE at the end of range is likely to be clinically significant for doses to organs at risk for pediatric patients with mediastinal Hodgkin lymphoma.

Introduction

Proton therapy is an attractive modality for pediatric patients due to the dosimetric advantages of the Bragg peak [1,2], which often enables a reduction in the dose to normal tissue and therefore the risk of side effects [3,4]. Current practice in proton therapy is to use a constant relative biological effectiveness (RBE) factor of 1.1 [5,6], which was chosen based on radiobiological experiments [5,7]. However, it is known that a single value of 1.1 is a simplification, and that RBE is dependent on factors such as dose, tissue (α/β), endpoint, and linear energy transfer (LET) [8–11]. There are a few studies suggesting clinical evidence of a variable RBE (vRBE) effect for proton therapy [12,13], and there is a growing effort to model vRBE for proton therapy [14–19] and investigate its potential impact [20–27]. However, it is unknown how much vRBE impacts the dose for pediatric patients with mediastinal Hodgkin lymphoma.

While the biological models for vRBE are quite uncertain, LET is a calculable physical parameter of the protons and can be scored during Monte Carlo simulations. An increase in LET corresponds to an increase in RBE [6], so some have proposed reviewing LET distributions and avoiding high LET in organs at risk (OARs) to reduce the risk of unintentional overdosage [28]. Currently, this can be achieved by manually replanning with different beam angles or with beam specific planning volumes to avoid protons stopping in the region of concern [29–31]. Moreover, incorporation of LET as an optimization parameter has been investigated [32–35].

In this study, we investigated the LET and vRBE-weighted dose distributions for 3 pediatric patients with mediastinal Hodgkin lymphoma for different beam arrangements with a focus on dose to organs at risk (OARs).

Method and Materials

Patient data

For this retrospective analysis, we selected three previously treated pediatric patients with mediastinal Hodgkin lymphoma. Patients were treated as part of the TEDDI protocol (radio**th**erapy **d**elivery in **d**eep **i**nspiration for pediatric patients − a NOPHO feasibility study, Danish Ethical Committee H-16035870, clinicaltrials.gov NCT03315546) [36]. The patients were the first three consecutive patients treated with radiotherapy under the protocol and were adolescent at the time of treatment (ages 15, 14, and 17 years). Contours from the clinical dataset

were used for treatment planning and analysis and additional contours of heart substructures were completed by an oncologist [37]. CTVs varied in size and were 241, 30, and 194 cc, respectively.

Treatment planning

We created 3 or 4 proton plans for each patient to investigate how the beam arrangement affected the LET and vRBE distributions (Eclipse v13.7, Varian Medical Systems, Palo Alto, CA). For all patients, plans with 1, 2, and 3 fields (0 degrees, 10 and 350 degrees, and 10, 180 and 350 degrees, respectively) were created, and for the one male patient (due to lack of breast tissue), a 'wide' 2-field plan was also created (30 and 330 degrees) (Figure 1).
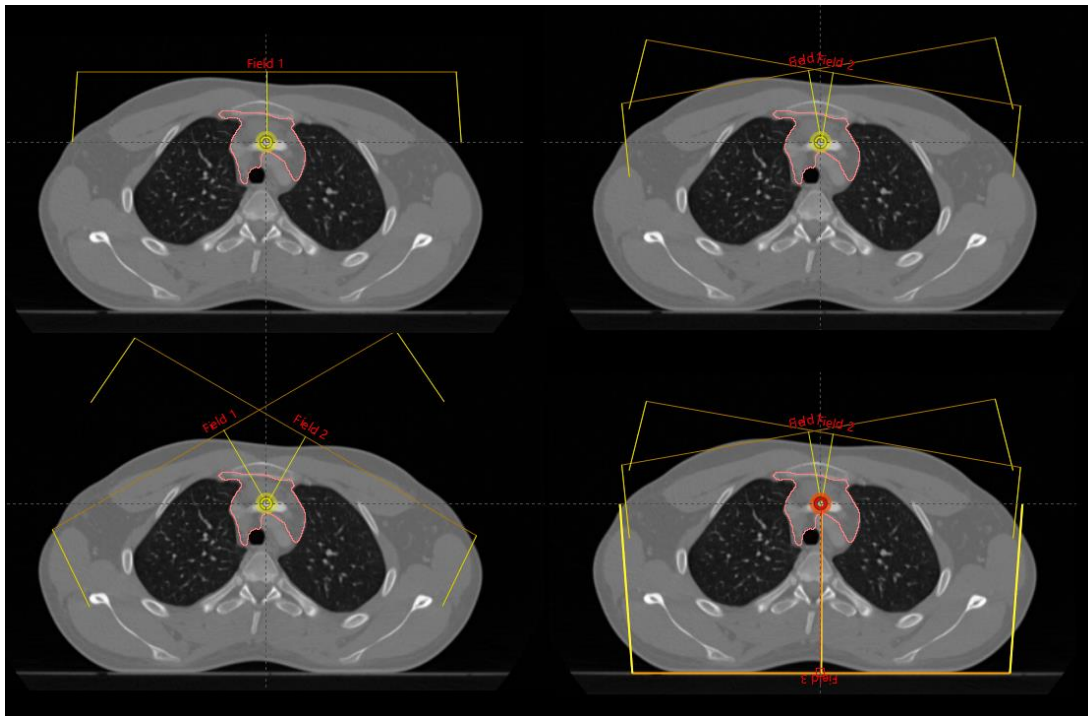
Figure 1. Beam arrangements for the patients in this study: 0 degrees (top left), 10 and 350 degrees (top right), 30 and 330 degrees (bottom left, patient 3 (male) only), 10, 180 and 350 degrees (bottom right). The CTV is shown in pink.

Treatment planning was performed to a prescription dose of 19.8 Gy in 11 fractions using robust optimization to the CTV, assuming an uncertainty of 3.5% in CT calibration and 5 mm in positioning. For most plans, single field optimization (SFO) was used; however, for patient 1, the target surrounded the heart and multifield optimization (MFO) was used for the 3-field plan to avoid entrance dose through the heart. Priorities during optimization were first CTV coverage, and second to reduce the dose to the lungs and the heart as much as possible. Female breasts, cardiac chambers, and cardiac arteries were contoured for analysis but were not used during optimization. Robust evaluation was performed with the same uncertainty assumptions and plans were considered acceptably robust if 98% of the CTV received at least 95% of the prescription dose for 10/12 uncertainty scenarios. The dose grid for calculation in the treatment planning system (TPS) was 2.5 mm.

LET and variable RBE calculation

Plans were exported, pre-processed for file compatibility, and imported to the in-house Monte Carlo (MC) system AUTOMC (v190621ES). AUTOMC is based in Geant4 (v10.3.2) [38] and Gate (Geant4 Application for Emission Tomography, v8.1) (RTIon v1.0) [39] and commissioned for the ProBeam delivery system (Varian Medical Systems). The physics list was set to QGSP_BIC, voxels were 2 mm, and cuts were 0.1 mm for gammas, electrons,

and positrons, and 1 mm for protons. The QGSP_BIC physics list has been previously shown to match other well-established physics lists used for proton therapy applications [40]. Physical dose to material was scored and converted to physical dose to water [41], and dose-averaged LET to water was scored using the 'GetElectronicStoppingPowerDEDX' method [42]. The number of histories was scaled to achieve an approximate uncertainty level of 1% in dose in the high dose region.

Post-processing of output files was completed in MATLAB (R2018b, MathWorks, Inc., Natick, MA). For plans with multiple beams, LET matrices from each beam were combined to one matrix using weighting factors of the relative dose to the voxel from each beam. LET matrices were thresholded to regions of at least 0.5% of the maximum dose to remove voxels containing very few particles. Then, matrices of physical dose and LET were used to obtain vRBE using the McNamara model [18] with an assumed α/β of 2 Gy [43]. Finally, matrices of LET, physical dose, vRBE, and vRBE-weighted dose were converted to DICOM format and imported back into the treatment planning system for visualization and analysis.

Comparison metrics

To compare how these distributions changed for different beam arrangements with respect to the OARs, metrics were extracted for the body, lungs, spinal cord, esophagus, breasts (for females), heart, heart chambers (left and right atria and left and right ventricle), and coronary arteries (right coronary artery (RCA), left main coronary artery (LMCA), left circumflex (Cx), and left anterior descending (LAD)).

Specifically, for LET comparisons, near-maximum ($D_{0.01cc}$) LET values were extracted. For dose comparisons, mean and near-maximum dose values were analyzed for the TPS dose with a fixed RBE of 1.1, MC dose with a fixed RBE of 1.1, and MC dose with vRBE. Near-maximum metrics were first extracted and then compared, so could be from different locations. In addition, voxel-by-voxel dose difference maps and the overlap of regions of 80% physical dose from MC and regions of LET greater than or equal to 6 keV/μm were visually examined.

Results

All treatment plans had acceptable coverage and robustness (for the TPS dose) with the criterion of 98% of the CTV receiving at least 95% of the prescription dose for all uncertainty scenarios for all plans, except for the 'wide' 2-field plan for patient 3, which fulfilled the criteria for 10/12 uncertainty scenarios.

We found that LET varied slightly with beam arrangement (Figure 2). In general, more beams decreased the near-maximum LET in OARs, but not always. Overlap of regions of 80% dose and high LET ($\geq$6 keV/μm) were evaluated visually. For most plans there was no overlap. For two plans, a few voxels overlapped, but the regions were very small. Patient 1 had a region of overlap for the 1-field plan of 0.004 cc in muscle, and patient 3 had a region of overlap for the 1-field plan of 0.11 cc located in the vertebra, carina, and descending aorta. Details of mean and near-maximum LET for all patients can be found in the appendix (Table S1).
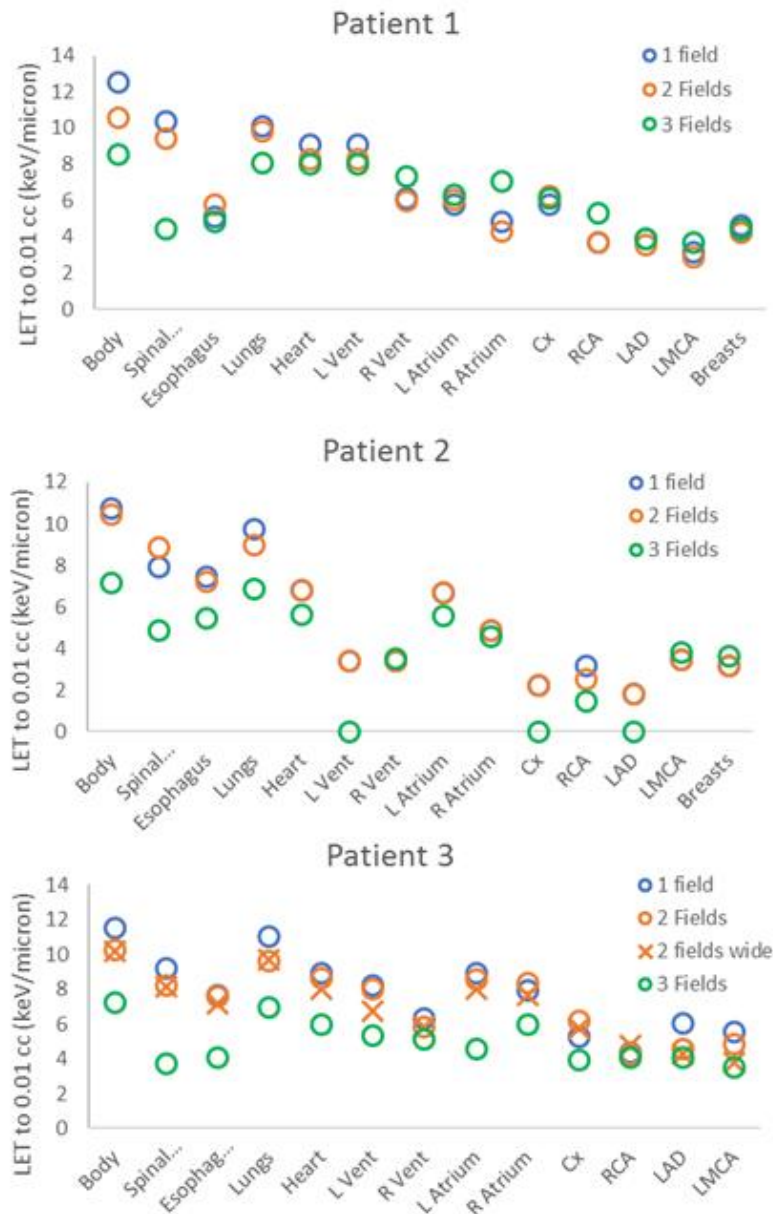
Figure 2. Near-maximum dose-averaged LET for OARs for different beam arrangements for the 3 patients in this study. OARs are listed in the order: body, spinal cord (Spinal…), esophagus, lungs, heart, left ventricle (L Vent), right ventricle (R Vent), left atrium (L Atrium), right atrium (R Atrium), circumflex artery (Cx), right coronary artery (RCA), left anterior descending artery (LAD), left main coronary artery (LMCA), breasts (for females).

Figure 3 shows an example of the TPS dose with a fixed RBE of 1.1, MC dose with a fixed RBE of 1.1, LET, vRBE, and MC dose with vRBE. LET and vRBE distributions increased at the end of range. It can also be seen that some of the regions of high LET and vRBE in the 1- and 2-field plans near the end of range were mitigated in the 3-field plan that contains a posterior beam. Despite these differences, the vRBE-weighted dose distribution was very similar to the fixed RBE distributions for all plans due to the regions of high vRBE corresponding to regions of low dose.
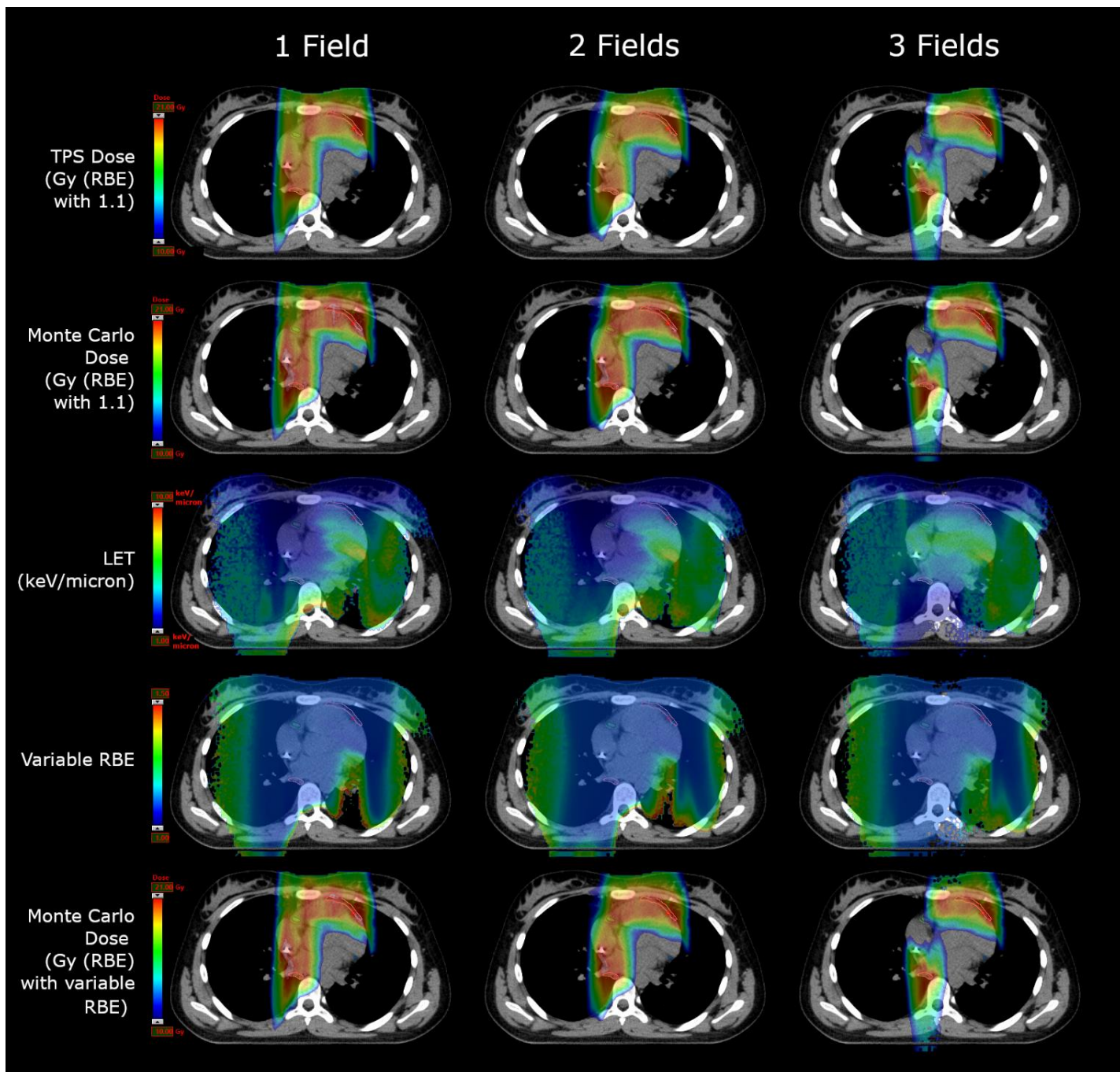
Figure 3. Distributions of TPS dose (1.1 RBE), MC dose (1.1 RBE), LET, variable RBE, and MC dose with vRBE for patient 1 for 3 plans with 1, 2, and 3 fields, respectively. Abbreviations: Treatment planning system (TPS), relative biological effectiveness (RBE), linear energy transfer (LET), Monte Carlo (MC).

A comparison of the MC physical dose distribution (no RBE factor applied) and the vRBE distribution and corresponding profiles for patient 1 for the 1-field plan is shown in Figure 4. The increase in vRBE to approximately 1.5 occurs where the dose is very low (much less than 1 Gy).
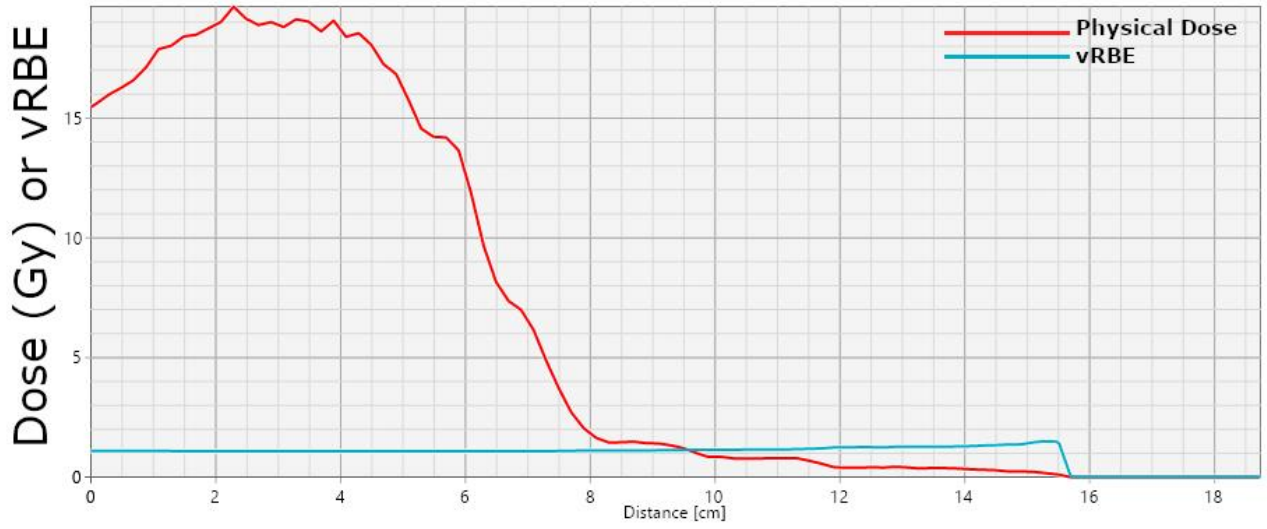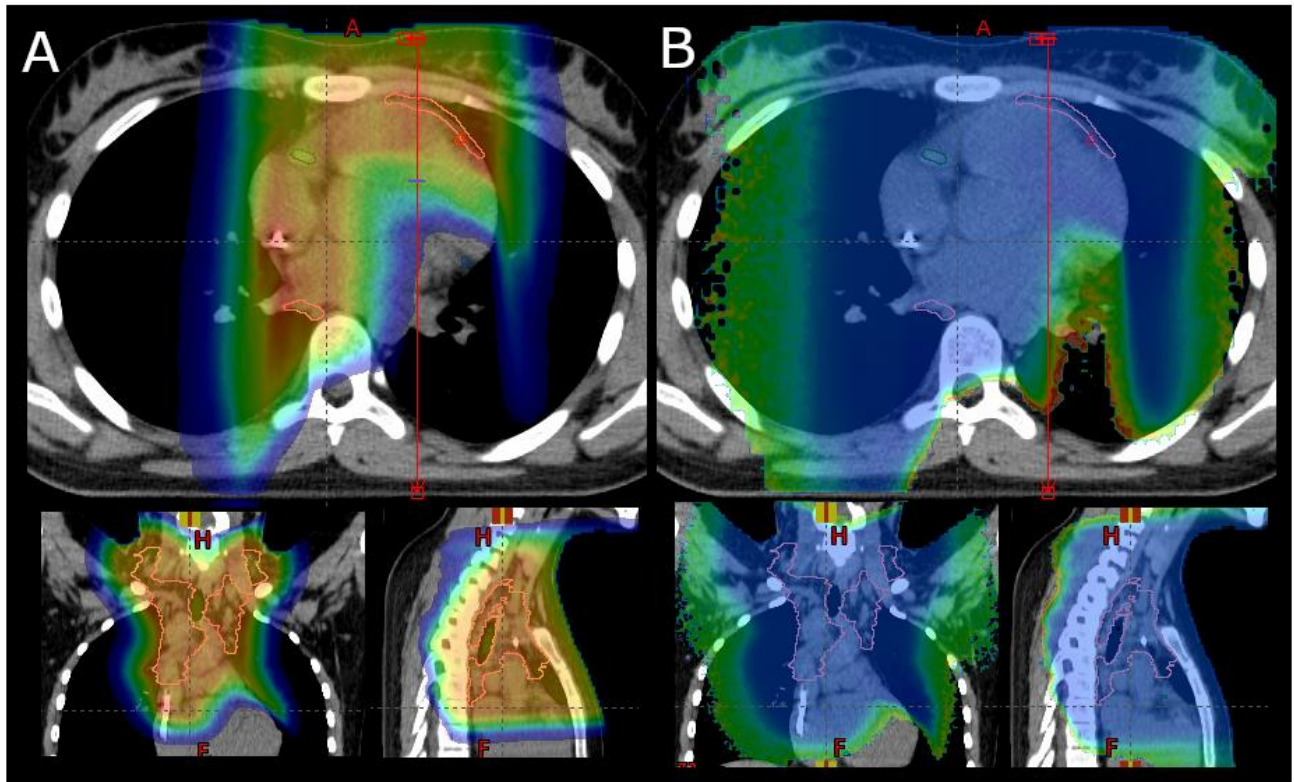
Figure 4. Physical dose from Monte Carlo (MC) (A, scale 1 to 21 Gy) and vRBE (B, scale 1 to 1.5) distributions and corresponding profiles at the location of the red anterior-posterior line for patient 1, 1-field plan. The CTV is shown in pink.

Dose-difference distributions are shown in Figure 5 for patient 1. The differences in dose (when compared to TPS dose) from the use of MC (first row) are on the same order as the use of MC and variable RBE weighting (second row), and differences between the two MC doses are very small (third row).
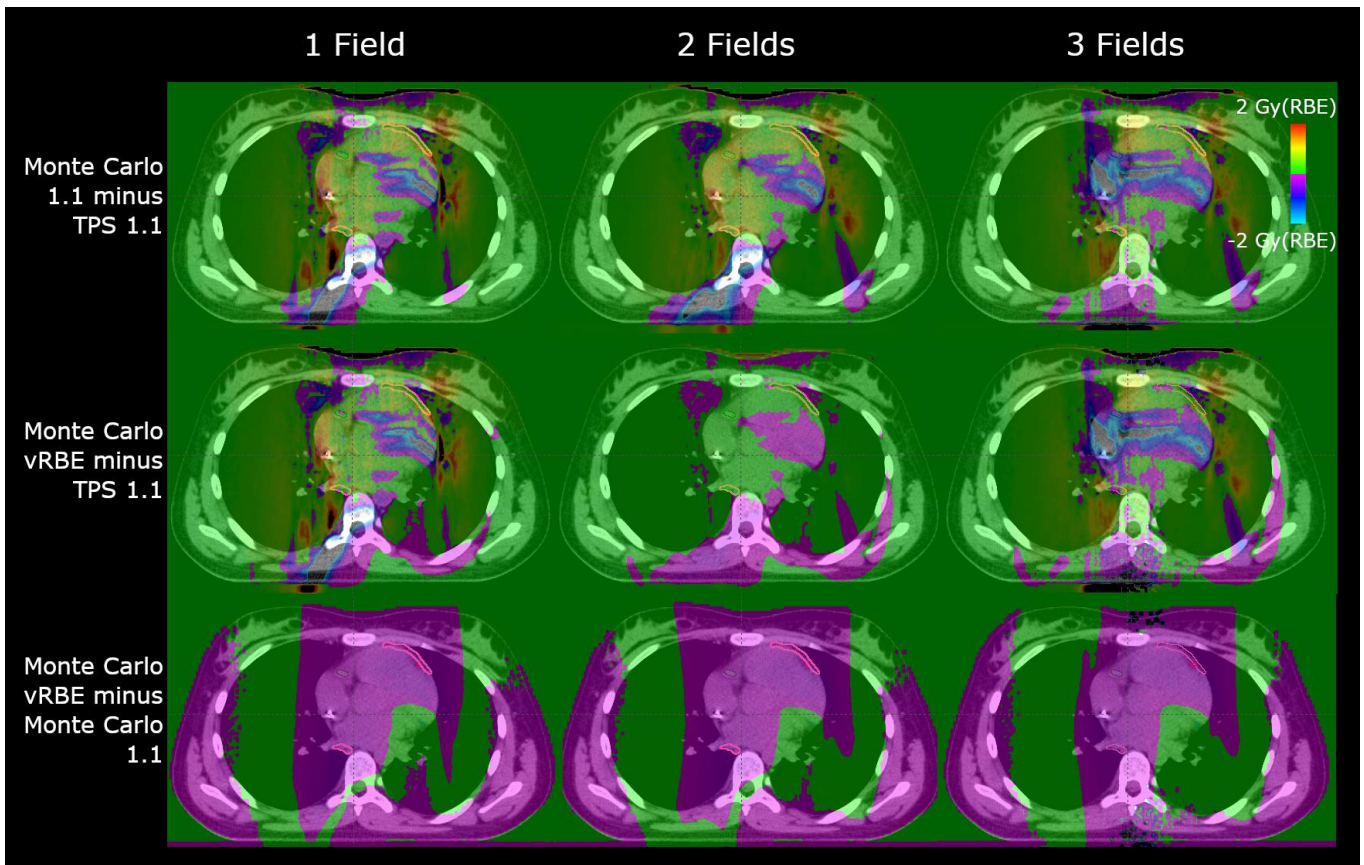
Figure 5. Dose-difference distributions for patient 1 for plans with 1, 2, and 3 fields. The dose-difference scale is from -2 to 2 Gy (RBE) (regions of black or clear are beyond the scale) and the CTV is shown in pink.

Differences in both mean and near-maximum doses to OARs relative to the TPS dose with 1.1 were small (Figure 6), and the MC doses with vRBE were generally less than MC doses with 1.1. Results were similar for the other two patients, and detailed results of the dose metrics can be found in the appendix (Tables S2-S4).
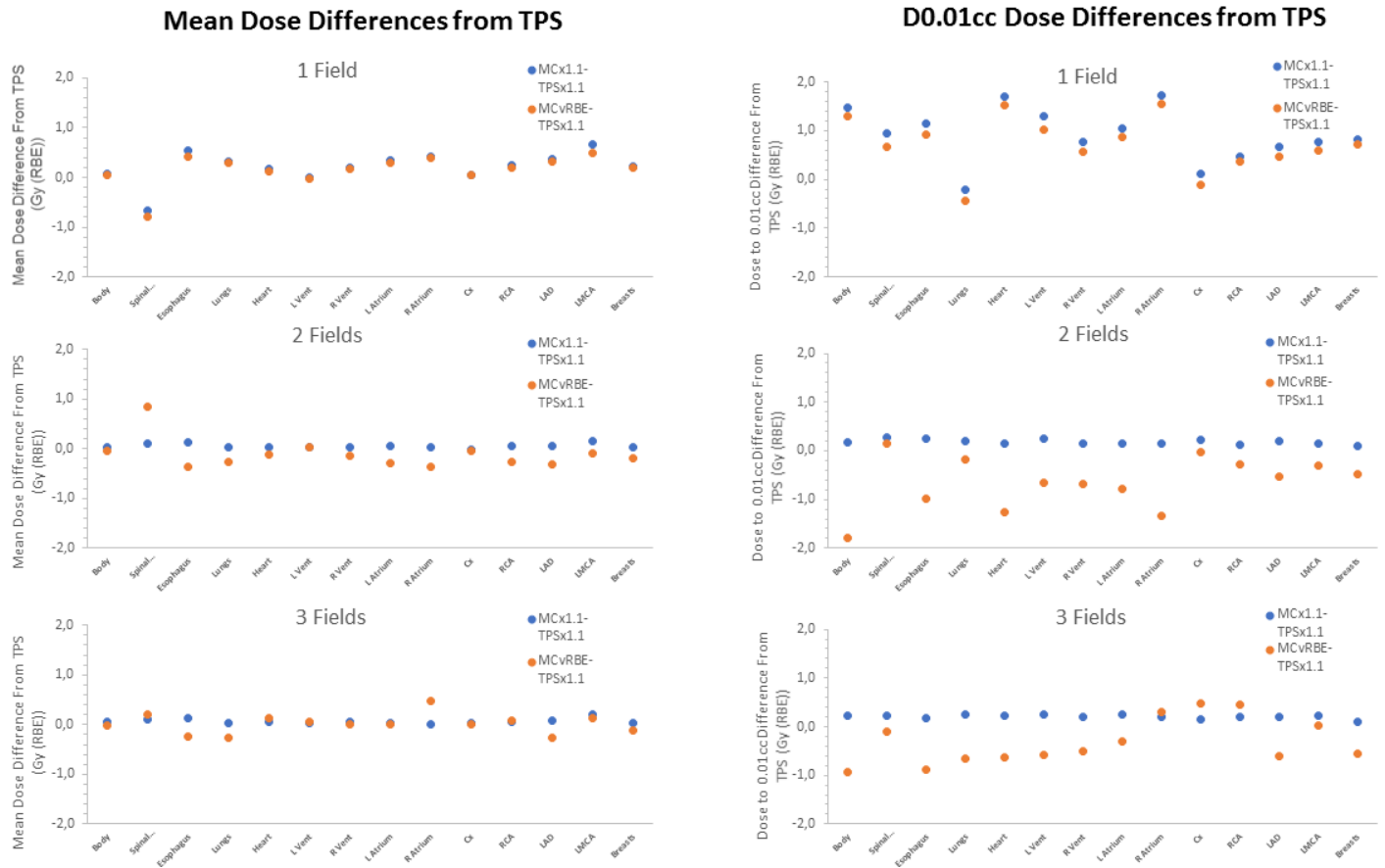
Figure 6. Mean and near-maximum (0.01cc) dose differences between MC dose with either fixed RBE of 1.1 or vRBE and the TPS dose with fixed RBE of 1.1 for patient 1. OARs are listed in the order: body, spinal cord (Spinal…), esophagus, lungs, heart, left ventricle (L Vent), right ventricle (R Vent), left atrium (L Atrium), right atrium (R Atrium), circumflex artery (Cx), right coronary artery (RCA), left anterior descending artery (LAD), left main coronary artery (LMCA), breasts (for females).

Discussion and Conclusion

In this study, we found that increasing number of beams decreased the near-maximum LET in OARs for adolescent pediatric patients with mediastinal Hodgkin lymphoma; however, we did not find that the distribution of LET or the vRBE-weighted dose was clinically concerning. The use of MC accounted for the largest differences in this study, not the use of fixed or variable RBE. The implementation of MC models in commercial treatment planning systems and clinical routine will improve accuracy for this patient group.

Tseng et al. [44] presented results in 2018 showing similar results to ours for patients with mediastinal lymphoma. In their study, the doses to OARs with vRBE were slightly lower with MC and vRBE when compared to MC and fixed RBE. Other studies have investigated LET and vRBE in proton therapy for other treatment sites. The magnitude of LET values in our study agree with one of the largest studies [27], which investigated different

9

treatment sites, including thoracic patients. They found near-maximum values of LET in the OARs in the thorax of approximately 8-11 keV/μm on average, which agree well with our results of approximately 6-9 keV/μm. However, unlike our study, Ödén *et al.* [25] found relatively large difference in mean OAR doses (compared to using 1.1) for prostate cancer patients on the order of 2-3 Gy (RBE) (Table 4 in [25]) and an increased probability of rectal toxicity (Table 6 in [25]). Another study from Carabe *et al.* [21] investigated the impact of vRBE for prostate, brain, and liver patients, and found a large range of differences in the dose to 10% of the volume ($D_{10\%}$), ranging from differences of approximately 10 Gy (RBE) in OARs in the brain to differences as small as approximately 1 Gy (RBE) in the lung and healthy liver. The differences between the results in these studies and in ours could be explained by the anatomical location of the target and the low prescription dose for Hodgkin lymphoma (which is also low for adult regimens, around 30 Gy).

One limitation of this study is the uncertainty of the variable RBE model. There is a lack of data regarding validation of RBE models and therefore little clinical consensus about choice of model. However, we chose a model that was built with experimental data from the relevant range [19], and other studies have shown that the McNamara model [18] is a reasonably conservative choice with respect to OARs [25,27]. Furthermore, this was a small study with only 3 adolescent patients, and should not be considered exhaustive, but rather exploratory.

In conclusion, we did not find clinically significant differences in doses to OARs due to vRBE or regions of high LET overlapping with high dose for the pediatric patients with Hodgkin lymphoma in this study. Due to this negative finding, we cannot recommend any specific beam arrangement for the purpose of modulating the LET distribution; however, using multiple beams maybe be advantageous for other reasons such as plan robustness and quality.

References
[1]   Smith AR. Proton therapy. Phys Med Biol 2006;51:R491–504. doi:10.1088/0031-9155/51/13/R26.

[2]   Newhauser WD, Zhang R. The physics of proton therapy. Phys Med Biol 2015;60:R155. doi:10.1088/0031-9155/60/8/R155.

[3]   Miralbell R, Lomax A, Cella L, Schneider U. Potential reduction of the incidence of radiation-induced second cancers by using proton beams in the treatment of pediatric tumors. vol. 54. 2002.

[4]   Merchant TE. Proton Beam Therapy in Pediatric Oncology. Cancer J 2009;15.

[5]   Paganetti H, Niemierko A, Ancukiewicz M, Gerweck LE, Goitein M, Loeffler JS, et al. Relative biological effectiveness (RBE) values for proton beam therapy. Int J Radiat Oncol Biol Phys 2002;53:407–21. doi:10.1016/S0360-3016(02)02754-2.

[6]   Paganetti H, Blakely E, Carabe-fernandez A, Carlson DJ, Held KD. Report of the AAPM TG-256 on the relative biological effectiveness of proton beams in radiation therapy. Med Phys 2019;46. doi:10.1002/mp.13390.

[7]   International Commission on Radiation Units & Measurements (ICRU). Prescribing, Recording, and

Reporting Proton-Beam Therapy. vol. Report 78. 2007.

[8]   Gerweck LE, Kozin S V. Relative biological effectiveness of proton beams in clinical therapy. Radiother Oncol 1999;50:135. doi:10.1016/S0167-8140(98)00092-9.

[9]   Dasu A, Toma-Dasu I. Impact of variable RBE on proton fractionation. Med Phys 2013;40:11705. doi:10.1118/1.4769417.

[10]   Wouters BG, Skarsgard LD, Gerweck LE, Carabe-Fernandez A, Wong M, Durand RE, et al. Radiobiological intercomparison of the 160 MeV and 230 MeV proton therapy beams at the Harvard Cyclotron Laboratory and at Massachusetts General Hospital. Radiat Res 2015;183:174. doi:10.1667/RR13795.1.

[11]   Paganetti H. Relative biological effectiveness (RBE) values for proton beam therapy. Variations as a function of biological endpoint, dose, and linear energy transfer. Phys Med Biol 2014;59:R419–72. doi:10.1088/0031-9155/59/22/R419.

[12]   Peeler CR, Mirkovic D, Titt U, Blanchard P, Gunther JR, Mahajan A, et al. Clinical evidence of variable proton biological effectiveness in pediatric patients treated for ependymoma. Radiother Oncol 2016;121:395–401. doi:10.1016/j.radonc.2016.11.001.

[13]   Underwood TSA, Grassberger C, Bass R, MacDonald SM, Meyersohn NM, Yeap BY, et al. Asymptomatic Late-phase Radiographic Changes Among Chest-Wall Patients Are Associated With a Proton RBE Exceeding 1.1. Int J Radiat Oncol Biol Phys 2018;101:809–19. doi:10.1016/j.ijrobp.2018.03.037.

[14]   Wilkens JJ, Oelfke U. A phenomenological model for the relative biological effectiveness in therapeutic proton beams. Phys Med Biol 2004;49:2811–25. doi:10.1088/0031-9155/49/13/004.

[15]   Carabe-Fernandez A, Dale RG, Jones B. The incorporation of the concept of minimum RBE (RBEmin) into the linear-quadratic model and the potential for improved radiobiological analysis of high-LET treatments. Int J Radiat Biol 2007;83:27–39. doi:10.1080/09553000601087176.

[16]   Chen Y, Ahmad S. Empirical model estimation of relative biological effectiveness for proton beam therapy†. Radiat Prot Dosimetry 2011;149:116–23. doi:10.1093/rpd/ncr218.

[17]   Wedenberg M, Lind BK, Hårdemark B. A model for the relative biological effectiveness of protons: The tissue specific parameter α/β of photons is a predictor for the sensitivity to LET changes. Acta Oncol (Madr) 2013;52:580–8. doi:10.3109/0284186X.2012.705892.

[18]   Mcnamara AL, Schuemann J, Paganetti H. A phenomenological relative biological effectiveness (RBE) model for proton therapy based on all published in vitro cell survival data. Phys Med Biol 2015;60:8399–416. doi:10.1088/0031-9155/60/21/8399.A.

[19]   Rørvik E, Fjæra LF, Dahle TJ, Dale JE, Engeseth GM, Stokkevåg CH, et al. Exploration and application of phenomenological RBE models for proton therapy Exploration and application of phenomenological RBE models for proton therapy. Phys Med Biol 2018;63.

[20]   Tilly N, Johansson J, Isacsson U, Medin J, Blomquist E, Grusell E, et al. The influence of RBE variations in a clinical proton treatment plan for a hypopharynx cancer. Phys Med Biol 2005;50:2765–77. doi:10.1088/0031-9155/50/12/003.

[21]   Carabe A, España S, Grassberger C, Paganetti H. Clinical consequences of relative biological effectiveness variations in proton radiotherapy of the prostate, brain and liver. Phys Med Biol

2013;58:2103–17. doi:10.1088/0031-9155/58/7/2103.

[22]   Underwood T, Giantsoudi D, Moteabbed M, Zietman A, Efstathiou J, Paganetti H, et al. Can We Advance Proton Therapy for Prostate? Considering Alternative Beam Angles and Relative Biological Effectiveness Variations When Comparing Against Intensity Modulated Radiation Therapy. Int J Radiat Oncol 2016;95:454–64. doi:https://doi.org/10.1016/j.ijrobp.2016.01.018.

[23]   Giovannini G, Böhlen T, Cabal G, Bauer J, Tessonnier T, Frey K, et al. Variable RBE in proton therapy: comparison of different model predictions and their influence on clinical-like scenarios. Radiat Oncol 2016;11:1–17. doi:10.1186/s13014-016-0642-6.

[24]   Giantsoudi D, Sethi R V, Yeap BY, Eaton BR, Ebb DH, Caruso PA, et al. Incidence of CNS Injury for a Cohort of 111 Patients Treated With Proton Therapy for Medulloblastoma: LET and RBE Associations for Areas of Injury. Int J Radiat Oncol 2016;95:287–96. doi:https://doi.org/10.1016/j.ijrobp.2015.09.015.

[25]   Ödén J, Eriksson K, Toma-Dasu I. Inclusion of a variable RBE into proton and photon plan comparison for various fractionation schedules in prostate radiation therapy. Med Phys 2017;44:810–22. doi:10.1002/mp.12117.

[26]   Ödén J, Eriksson K, Toma-Dasu I. Incorporation of relative biological effectiveness uncertainties into proton plan robustness evaluation. Acta Oncol (Madr) 2017;56:769–78. doi:10.1080/0284186X.2017.1290825.

[27]   Yepes P, Adair A, Frank SJ, Grosshans DR, Liao Z, Liu A. Fixed- versus Variable-RBE Computations for Intensity Modulated Proton Therapy. Adv Radiat Oncol 2019;4:156–67. doi:10.1016/j.adro.2018.08.020.

[28]   Grassberger C, Trofimov A, Lomax A, Paganetti H. Variations in linear energy transfer within clinical proton therapy fields and the potential for biological treatment planning. Int J Radiat Oncol Biol Phys 2011;80:1559–66.

[29]   Fager M, Toma-Dasu I, Kirk M, Dolney D, Diffenderfer ES, Vapiwala N, et al. Linear Energy Transfer Painting With Proton Therapy: A Means of Reducing Radiation Doses With Equivalent Clinical Effectiveness. Int J Radiat Oncol 2015;91:1057–64. doi:https://doi.org/10.1016/j.ijrobp.2014.12.049.

[30]   Giantsoudi D, Adams J, Macdonald SM, Paganetti H. Proton Treatment Techniques for Posterior Fossa Tumors: Consequences for Linear Energy Transfer and Dose-Volume Parameters for the Brainstem and Organs at Risk. Int J Radiat Oncol Biol Phys 2017;97:401. doi:10.1016/j.ijrobp.2016.09.042.

[31]   Fjæra LF, Li Z, Ytre-Hauge KS, Muren LP, Indelicato DJ, Lassen-Ramshad Y, et al. Linear energy transfer distributions in the brainstem depending on tumour location in intensity-modulated proton therapy of paediatric cancer. Acta Oncol (Madr) 2017;56:763–8. doi:10.1080/0284186X.2017.1314007.

[32]   Giantsoudi D, Grassberger C, Craft D, Niemierko A, Trofimov A, Paganetti H. Linear Energy Transfer-Guided Optimization in Intensity Modulated Proton Therapy: Feasibility Study and Clinical Potential. Int J Radiat Oncol 2013;87:216–22. doi:https://doi.org/10.1016/j.ijrobp.2013.05.013.

[33]   Unkelbach J, Botas P, Giantsoudi D, Gorissen BL, Paganetti H. Reoptimization of Intensity Modulated Proton Therapy Plans Based on Linear Energy Transfer. Int J Radiat Oncol 2016;96:1097–106. doi:https://doi.org/10.1016/j.ijrobp.2016.08.038.

[34]   Cao W, Khabazian A, Yepes PP, Lim G, Poenisch F, Grosshans DR, et al. Linear energy transfer incorporated intensity modulated proton therapy optimization. Phys Med Biol 2018;63:15013.

doi:10.1088/1361-6560/aa9a2e.

[35]   Traneus E, Ödén J. Introducing Proton Track-End Objectives in Intensity Modulated Proton Therapy Optimization to Reduce Linear Energy Transfer and Relative Biological Effectiveness in Critical Structures. Int J Radiat Oncol 2019;103:747–57. doi:https://doi.org/10.1016/j.ijrobp.2018.10.031.

[36]   Lundgaard AY, Hjalgrim LL, Rechner LA, Josipovic M, Joergensen M, Aznar MC, et al. TEDDI: Radiotherapy delivery in deep inspiration for pediatric patients - A NOPHO feasibility study. Radiat Oncol 2018;13. doi:10.1186/s13014-018-1003-4.

[37]   Duane F, Aznar MC, Bartlett F, Cutter DJ, Darby SC, Jagsi R, et al. A cardiac contouring atlas for radiotherapy. Radiother Oncol 2017;122:416. doi:10.1016/j.radonc.2017.01.008.

[38]   Agostinelli S, Allison J, Amako K, Apostolakis J, Araujo H, Arce P, et al. Geant4—a simulation toolkit. Nucl Instruments Methods Phys Res Sect A Accel Spectrometers, Detect Assoc Equip 2003;506:250–303. doi:https://doi.org/10.1016/S0168-9002(03)01368-8.

[39]   Sarrut D, Bardiès M, Boussion N, Freud N, Jan S, Létang J, et al. A review of the use and potential of the GATE Monte Carlo simulation code for radiation therapy and dosimetry applications. Med Phys 2014;41:n/a-n/a. doi:10.1118/1.4871617.

[40]   Winterhalter C, Aitkenhead A, Safai S, Weber DC, Mackay RI, Lomax AJ. Abstract ID: 34 Comparison of two Monte Carlo calculation engines for proton pencil beam scanning. Phys Medica 2017;42:5–6. doi:10.1016/j.ejmp.2017.09.014.

[41]   Paganetti H. SU-FF-T-405: Dose to Water Versus Dose to Medium in Proton Beam Therapy. Med Phys 2009;36:2615. doi:10.1118/1.3181887.

[42]   Granville DA, Sawakuchi GO. Comparison of linear energy transfer scoring techniques in Monte Carlo simulations of proton beams. Phys Med Biol 2015;283:N283. doi:10.1088/0031-9155/60/14/N283.

[43]   Williams M, Denekamp J, Fowler J. A review of alpha/beta ratios for experimental tumors: implications for clinical studies of altered fractionation. Int J Radiat Oncol Biol Phys 1985;11:87–96.

[44]   Tseng YD, Maes SM, Kicska G, Traneus E, Wong TP, Stewart RD, et al. Comparative Photon and Proton Dosimetry for Patients with Mediastinal Lymphoma in the Era of Monte Carlo Treatment Planning and Variable RBE. Int J Radiat Oncol 2018;102:S86–7. doi:10.1016/j.ijrobp.2018.06.227.

Appendix

Table S1. Mean and near-maximum (0.01cc) dose-averaged linear energy transfer (LET) values (keV/μm) for the 3 patients in this study. Abbreviations: left ventricle (L Vent), right ventricle (R Vent), left atrium (L Atrium), right atrium (R Atrium), circumflex artery (Cx), right coronary artery (RCA), left anterior descending artery (LAD), left main coronary artery (LMCA).

Patient 1	1 Field		2 Fields		3 Fields	
	Mean	0.01cc	Mean	0.01cc	Mean	0.01cc
Body	1.27	12.52	1.33	10.57	1.13	8.57
Spinal Cord	4.23	10.4	4.56	9.39	2.8	4.4
Esophagus	2.49	5.07	2.59	5.76	2.25	4.86
Lungs	2.91	10.09	2.89	9.81	2.74	8.04
Heart	2.68	9.06	2.73	8.24	3.1	7.98
L Vent	2.75	9.06	2.85	8.24	2.72	7.98
R Vent	2.91	6.1	2.99	5.98	3.14	7.32
L Atrium	2.98	5.75	2.86	6.06	3.69	6.3
R Atrium	2.27	4.82	2.28	4.3	4.21	7.04
Cx	3.34	5.75	3.8	6.27	1.94	6.1
RCA	1.48	3.71	1.55	3.67	2.91	5.31
LAD	2.82	3.88	2.77	3.56	2.72	3.87
LMCA	2.86	3.11	2.69	2.9	3.51	3.65
Breasts	1.67	4.65	1.66	4.19	1.63	4.41

Patient 2	1 Field		2 Fields		3 Fields	
	Mean	0.01cc	Mean	0.01cc	Mean	0.01cc
Body	0.38	10.74	0.4	10.42	0.35	7.13
Spinal Cord	4.59	7.93	4.78	8.84	2.74	4.84
Esophagus	2.1	7.43	2.07	7.21	1.89	5.48
Lungs	1.4	9.71	1.53	8.96	1.34	6.87
Heart	0.78	6.78	0.78	6.78	0.68	5.65
L Vent	0.01	3.38	0.01	3.38	0	0.02
R Vent	0.15	3.41	0.15	3.41	0.04	3.53
L Atrium	1.97	6.7	1.97	6.7	1.75	5.56
R Atrium	1.6	4.88	1.6	4.88	1.41	4.55
Cx	0.08	2.21	0.08	2.21	0	0.02
RCA	0.47	3.14	0.43	2.55	0.06	1.48
LAD	0.06	1.8	0.06	1.8	0	0.02
LMCA	3.26	3.46	3.26	3.46	3.58	3.83
Breasts	0.17	3.18	0.17	3.18	0.19	3.66

Patient 3	1 Field		2 Fields		2 Fields Wide		3 Fields	
	Mean	0.01cc	Mean	0.01cc	Mean	0.01cc	Mean	0.01cc
Body	0.71	11.53	0.78	10.28	0.9	10.19	0.71	7.21
Spinal Cord	3.99	9.22	4.29	8.25	4.18	8.17	1.84	3.72
Esophagus	2.05	7.67	2.03	7.58	2.02	7.19	1.69	4.06
Lungs	1.63	11.05	1.77	9.65	2.18	9.72	1.55	6.99
Heart	1.38	8.96	1.44	8.62	1.59	7.98	1.3	5.98
L Vent	0.32	8.22	0.38	8.01	0.44	6.73	0.41	5.31
R Vent	1.16	6.35	1.25	5.84	1.54	5.83	1.18	5.16
L Atrium	2.06	8.95	2.26	8.59	2.75	7.98	1.63	4.54
R Atrium	2.72	7.95	2.73	8.35	3.02	7.65	2.62	5.98
Cx	1.88	5.25	2.26	6.21	2.59	5.76	1.95	3.9
RCA	2.39	4.37	2.47	4.27	2.93	4.75	2.47	4.1
LAD	1.73	6.05	1.62	4.6	1.88	4.3	1.56	4.08
LMCA	4.85	5.54	4.54	4.84	3.48	3.78	3.28	3.5

Table S2. Mean doses and near-maximum ($D_{0.01cc}$) doses for patient 1 for plans with 1, 2, and 3 beams. Doses are in Gy (RBE), where the RBE is a fixed 1.1 for the first two columns (treatment planning system (TPSx1.1), and Monte Carlo (MCx1.1), and variable for the third column (MC vRBE). Abbreviations: left ventricle (L Vent), right ventricle (R Vent), left atrium (L Atrium), right atrium (R Atrium), circumflex artery (Cx), right coronary artery (RCA), left anterior descending artery (LAD), left main coronary artery (LMCA).

	1 Field					
	TPSx1.1		MCx1.1		MC vRBE	
	Mean	0.01cc	Mean	0.01cc	Mean	0.01cc
Body	2.37	21.73	2.44	23.20	2.41	23.02
Spinal Cord	8.47	19.75	7.80	20.69	7.69	20.43
Esophagus	12.92	20.43	13.47	21.59	13.33	21.36
Lungs	3.86	21.69	4.18	21.48	4.15	21.26
Heart	5.25	21.31	5.42	23.01	5.37	22.83
L Vent	1.84	20.52	1.84	21.81	1.81	21.54
R Vent	4.38	20.47	4.57	21.24	4.54	21.04
L Atrium	8.80	20.23	9.15	21.28	9.09	21.11
R Atrium	7.15	21.17	7.57	22.90	7.54	22.73
Cx	0.87	13.14	0.92	13.25	0.91	13.03
RCA	8.22	19.76	8.46	20.24	8.41	20.14

	TPSx1.1		MCx1.1		MC vRBE	
LAD	6.48	20.34	6.85	21.02	6.80	20.80
LMCA	17.56	18.24	18.23	19.00	18.05	18.83
Breasts	1.82	19.16	2.03	19.99	2.01	19.87

2 Fields						
	TPSx1.1		**MCx1.1**		**MC vRBE**	
	Mean	**0.01cc**	**Mean**	**0.01cc**	**Mean**	**0.01cc**
Body	2.39	20.8	2.47	22.76	2.44	22.58
Spinal Cord	8.07	19.17	7.32	19.29	7.22	19.01
Esophagus	12.88	20.1	13.37	21.33	13.24	21.09
Lungs	3.89	20.73	4.19	21.11	4.16	20.92
Heart	5.21	20.68	5.37	22.11	5.33	21.95
L Vent	2.02	20.2	2.02	21.1	1.99	20.86
R Vent	4.52	20.17	4.7	20.98	4.67	20.84
L Atrium	8.31	20.31	8.65	21.26	8.6	21.1
R Atrium	6.44	20.31	6.83	21.8	6.81	21.65
Cx	0.99	13.88	1.02	14.12	1.03	13.9
RCA	8.13	20.34	8.46	20.73	8.4	20.61
LAD	6.83	20.01	7.2	20.73	7.15	20.53
LMCA	16.79	17.43	17.04	17.88	16.89	17.73
Breasts	1.95	19	2.15	19.6	2.13	19.49

3 Fields						
	TPSx1.1		**MCx1.1**		**MC vRBE**	
	Mean	**0.01cc**	**Mean**	**0.01cc**	**Mean**	**0.01cc**
Body	2.46	21.58	2.53	22.73	2.48	22.5
Spinal Cord	9.68	19.18	9.57	19.5	9.47	19.28
Esophagus	12.32	20.19	12.69	21.26	12.57	21.08
Lungs	3.6	21.36	3.89	22.25	3.86	22.01
Heart	4.37	20.49	4.31	21.35	4.25	21.12
L Vent	1.9	20.18	1.87	20.99	1.84	20.75
R Vent	4.05	20.13	4.11	20.83	4.05	20.63
L Atrium	6.17	20.07	6.21	20.61	6.17	20.37
R Atrium	3.79	18.83	3.33	18.71	3.32	18.52
Cx	0.78	11.17	0.8	10.83	0.76	10.68
RCA	5.26	18.01	5.25	17.75	5.19	17.56
LAD	6.87	20.06	7.2	20.88	7.13	20.67
LMCA	16.65	17.66	16.71	17.85	16.51	17.63
Breasts	1.67	19.07	1.82	19.73	1.79	19.63

Table S3. Mean doses and near-maximum ($D_{0.01cc}$) doses for patient 2 for plans with 1, 2, and 3 beams. Doses are in Gy (RBE), where the RBE is a fixed 1.1 for the first two columns (treatment planning system (TPSx1.1), and Monte Carlo (MCx1.1), and variable for the third column (MC vRBE). Abbreviations: left ventricle (L Vent), right ventricle (R Vent), left atrium (L Atrium), right atrium (R Atrium), circumflex artery (Cx), right coronary artery (RCA), left anterior descending artery (LAD), left main coronary artery (LMCA).

	1 Field					
	TPSx1.1		MCx1.1		MC vRBE	
	Mean	0.01cc	Mean	0.01cc	Mean	0.01cc
Body	0,55	21,67	0,56	22,24	0,55	21,97
Spinal Cord	7,17	17,72	6,15	18,12	6,06	17,82
Esophagus	5,99	20,17	5,84	20,78	5,78	20,57
Lungs	1,33	21,65	1,52	22,01	1,49	21,75
Heart	0,41	15,69	0,47	16,65	0,45	16,52
L Vent	0	0,02	0,03	0,14	0	0,16
R Vent	0	0,17	0,05	0,3	0,01	0,32
L Atrium	0,38	6,03	0,45	6,14	0,43	6,1
R Atrium	0,39	9,28	0,54	10,02	0,52	9,97
Cx	0	0,02	0,04	0,12	0	0,07
RCA	0	0,04	0,07	0,2	0,03	0,22
LAD	0	0,02	0,05	0,12	0	0,07
LMCA	0,06	0,11	0,2	0,24	0,23	0,27
Breasts	0,02	5,83	0,08	7,04	0,04	7,02

	2 Fields					
	TPSx1.1		MCx1.1		MC vRBE	
	Mean	0.01cc	Mean	0.01cc	Mean	0.01cc
Body	0,55	21,02	0,56	22,15	0,55	21,91
Spinal Cord	5,73	15,82	4,82	15,88	4,76	15,62
Esophagus	5,78	19,97	5,62	20,31	5,56	20,12
Lungs	1,37	20,73	1,55	21,56	1,52	21,31
Heart	0,4	14,57	0,47	15,55	0,44	15,42
L Vent	0	0,02	0,03	0,14	0	0,16
R Vent	0	0,25	0,05	0,37	0,01	0,39

	Mean	0.01cc	Mean	0.01cc	Mean	0.01cc
L Atrium	0,39	5,5	0,45	5,62	0,43	5,59
R Atrium	0,35	8,24	0,5	8,91	0,48	8,87
Cx	0	0,03	0,04	0,12	0	0,08
RCA	0	0,05	0,07	0,2	0,03	0,21
LAD	0	0,02	0,05	0,12	0	0,09
LMCA	0,11	0,19	0,23	0,3	0,26	0,33
Breasts	0,06	6,61	0,12	7,13	0,09	7,11

	3 Fields					
	TPSx1.1		MCx1.1		MC vRBE	
	Mean	0.01cc	Mean	0.01cc	Mean	0.01cc
Body	0,58	20,89	0,59	21,64	0,58	21,43
Spinal Cord	7,98	16,76	7,27	16,7	7,21	16,51
Esophagus	5,77	20	5,6	20,3	5,54	20,11
Lungs	1,29	20,55	1,47	21,11	1,44	20,88
Heart	0,33	14,41	0,38	15,49	0,35	15,34
L Vent	0	0,02	0,03	0,11	0	0,02
R Vent	0	0,11	0,04	0,21	0	0,23
L Atrium	0,29	4,85	0,36	4,92	0,34	4,9
R Atrium	0,27	7,19	0,39	7,89	0,37	7,84
Cx	0	0,02	0,05	0,11	0	0,02
RCA	0	0,03	0,05	0,13	0	0,09
LAD	0	0,02	0,04	0,11	0	0,02
LMCA	0,06	0,11	0,18	0,22	0,21	0,25
Breasts	0,04	5,67	0,09	6,26	0,06	6,23

Table S4. Mean doses and near-maximum ($D_{0.01cc}$) doses for patient 3 for plans with 1, 2, 2 'wide', and 3 beams. Doses are in Gy (RBE), where the RBE is a fixed 1.1 for the first two columns (treatment planning system (TPSx1.1), and Monte Carlo (MCx1.1), and variable for the third column (MC vRBE). Abbreviations: left ventricle (L Vent), right ventricle (R Vent), left atrium (L Atrium), right atrium (R Atrium), circumflex artery (Cx), right coronary artery (RCA), left anterior descending artery (LAD), left main coronary artery (LMCA). Large differences in near-maximum doses for the body for this patient were located in the air in the bronchi, not in tissue.

	1 Field					
	TPSx1.1		MCx1.1		MC vRBE	
	Mean	0.01cc	Mean	0.01cc	Mean	0.01cc
Body	1,35	21,23	1,37	26,29	1,35	26

Spinal Cord	3,03	13,64	2,89	14,1	2,87	13,86
Esophagus	9,26	20,11	9,36	20,98	9,26	20,74
Lungs	2,11	21,16	2,2	21,27	2,16	21,04
Heart	2,28	20,37	2,39	21,22	2,34	21,02
L Vent	0,05	10,34	0,08	10,58	0,05	10,41
R Vent	0,35	12,85	0,51	13,93	0,47	13,81
L Atrium	0,54	13,04	0,49	12,48	0,46	12,23
R Atrium	6,24	20,36	6,45	21,21	6,38	21
Cx	0,52	4,92	0,55	4,57	0,54	4,55
RCA	2,88	15,89	3,12	16,75	3,09	16,6
LAD	0,38	5,38	0,51	5,64	0,49	5,59
LMCA	11,92	13,92	10,52	12,45	10,37	12,25

2 Fields						
	TPSx1.1		**MCx1.1**		**MC vRBE**	
	Mean	**0.01cc**	**Mean**	**0.01cc**	**Mean**	**0.01cc**
Body	1,36	20,9	1,39	26,15	1,36	25,86
Spinal Cord	2,04	11,53	1,66	10,24	1,67	10,07
Esophagus	9,21	20,03	9,32	20,79	9,22	20,58
Lungs	2,11	20,48	2,19	20,92	2,15	20,74
Heart	2,35	20,26	2,47	21,12	2,42	20,92
L Vent	0,06	10,71	0,09	11,26	0,07	11,11
R Vent	0,39	13,9	0,55	14,94	0,52	14,81
L Atrium	0,64	15,75	0,57	14,45	0,54	14,15
R Atrium	6,22	20,24	6,47	21,08	6,4	20,88
Cx	0,69	6	0,64	5,28	0,63	5,23
RCA	2,87	16,17	3,11	17	3,07	16,86
LAD	0,39	5,07	0,51	5,27	0,49	5,23
LMCA	11,36	13,07	11,02	12,78	10,87	12,61

2 Fields WIDE						
	TPSx1.1		**MCx1.1**		**MC vRBE**	
	Mean	**0.01cc**	**Mean**	**0.01cc**	**Mean**	**0.01cc**
Body	1,47	21,17	1,5	26,05	1,47	25,75
Spinal Cord	3,18	11,89	2,91	12,18	2,89	12,01
Esophagus	9,16	20,01	9,27	20,89	9,16	20,66
Lungs	2,49	21,01	2,54	21,33	2,5	21,17
Heart	2,41	20,51	2,54	21,29	2,5	21,11

	Mean	0.01cc	Mean	0.01cc	Mean	0.01cc
L Vent	0,05	7,96	0,1	8,19	0,06	8,1
R Vent	0,58	14,5	0,73	15,56	0,69	15,42
L Atrium	0,82	13,84	0,79	13,68	0,77	13,44
R Atrium	6,39	20,49	6,7	21,29	6,63	21,11
Cx	1,01	7,04	1,03	6,94	1,02	6,88
RCA	2,97	15,64	3,22	16,66	3,21	16,51
LAD	0,58	5,52	0,72	5,68	0,69	5,64
LMCA	11,01	12,69	11,26	12,93	11,14	12,79

3 Fields					
TPSx1.1		**MCx1.1**		**MC vRBE**	
Mean	**0.01cc**	**Mean**	**0.01cc**	**Mean**	**0.01cc**
Body	1,63	20,76	1,67	26,24	1,62	25,97
Spinal Cord	6,22	13,42	5,99	12,56	5,87	12,42
Esophagus	9,82	19,96	9,94	20,8	9,84	20,63
Lungs	2,3	20,65	2,39	20,87	2,36	20,65
Heart	2,5	20,45	2,65	21,33	2,6	21,14
L Vent	0,06	10,75	0,11	11,22	0,08	11,1
R Vent	0,39	13,54	0,53	14,47	0,5	14,35
L Atrium	1,95	16,69	2,02	16,05	1,99	15,81
R Atrium	6,28	20,44	6,56	21,32	6,5	21,13
Cx	0,93	8,06	1,03	7,66	1,01	7,6
RCA	2,92	16,13	3,15	17,01	3,11	16,87
LAD	0,34	4,6	0,48	4,91	0,46	4,88
LMCA	12,71	14,75	12,52	14,69	12,39	14,54

Example Monte Carlo Uncertainty Report (patient 1, 1-field plan)
Median uncertainty (%) within various isodose surfaces

Patient	Plan	Field	Files	SplitProgress	PrimariesPerSplit	PrimariesTotal	CPU.hours	0-0.1%	0.1-1%	1-10%	10-20%	20-50%	50-70%	70-90%	90-100%
1	1	1	27	1.000	2.0663e+05	1.3834e+08	460.157	39.90	16.63	6.04	2.05	1.25	0.89	0.86	0.73

Biological optimization for mediastinal lymphoma radiotherapy – a preliminary study

- Laura Ann Rechner*, MSc, Department of Oncology, Section of Radiotherapy, Rigshospitalet, University of Copenhagen, Copenhagen, Denmark and Niels Bohr Institute, Faculty of Science, University of Copenhagen, Copenhagen, Denmark
- Arezoo Modiri*, PhD, Department of Radiation Oncology, University of Maryland, School of Medicine, Baltimore, MD
- Line Bjerregaard Stick, MSc, Department of Oncology, Section of Radiotherapy, Rigshospitalet, University of Copenhagen, Copenhagen, Denmark and Niels Bohr Institute, Faculty of Science, University of Copenhagen, Copenhagen, Denmark
- Maja V. Maraldo, MD PhD, Department of Oncology, Section of Radiotherapy, Rigshospitalet, University of Copenhagen, Copenhagen, Denmark
- Marianne C. Aznar, PhD, Manchester Cancer Research Centre, Division of Cancer Sciences, The University of Manchester, Manchester, United Kingdom and Clinical Trial Service Unit, Nuffield Department of Population Health, University of Oxford, United Kingdom
- Stephanie R. Rice, MD, University of Maryland Medical Center, Baltimore, MD
- Amit Sawant, PhD, Department of Radiation Oncology, University of Maryland, School of Medicine, Baltimore, MD
- Søren M. Bentzen, PhD DMSc, Greenebaum Comprehensive Cancer Center and Department of Epidemiology and Public Health, University of Maryland School of Medicine, Baltimore, MD
- Ivan Richter Vogelius, PhD DMSc, Department of Oncology, Section of Radiotherapy, Rigshospitalet, University of Copenhagen, Copenhagen, Denmark
- Lena Specht, MD DMSc, Department of Oncology, Section of Radiotherapy, Rigshospitalet, University of Copenhagen, Copenhagen, Denmark

*These authors contributed equally to this work and share the first authorship

Corresponding author:
Laura Ann Rechner
Rigshospitalet
Blegdamsvej 9
Finsen Center 3997
2100 Copenhagen, Denmark
Phone number: +45 3545 8960
Email: laura.ann.rechner@gmail.com

Abstract

Purpose/Objective(s):

In current radiotherapy (RT) planning and delivery, population-based dose-volume constraints are used to limit the risk of toxicity from incidental irradiation of organs at risk (OARs). However, weighing trade-offs between target coverage and doses to OARs (or prioritizing different OARs) in a quantitative way for each patient is challenging. We introduce a novel RT planning approach for patients with mediastinal Hodgkin lymphoma that aims to maximize overall outcome for each patient by optimizing on tumor control and mortality from late effects simultaneously.

Methods and Materials:

We retrospectively analyzed 34 Hodgkin lymphoma patients treated with conformal RT (3DCRT). We used published data to develop risk models for recurrence and radiation-induced mortality from coronary heart disease and secondary lung and breast cancers. Patient-specific doses to the heart, lung, breast, and tumor target were incorporated in the models as well as age, sex and cardiac risk factors (CRFs). Pre-plans were created with 16 co-planar gantry angles and 4 beam options per gantry angle. Beam doses were calculated in a commercial treatment planning system and monitor units were optimized in an in-house, particle swarm optimization code to create outcome-optimized (O-OPT) plans. O-OPT plans were compared to VMAT plans and clinical 3DCRT plans.

Results:

In general, O-OPT plans had the lowest risk, followed by the clinical 3DCRT plans, then the VMAT plans with the highest risk with median (maximum) total risk values of 4.9 (11.1), 5.1 (17.7), and 7.6 (20.3)%, respectively (assuming no CRFs). Compared to clinical 3DCRT plans, O-OPT planning reduced the total risk by more than 1% for 9/34 patient cases assuming no CRFs and 11/34 patient cases assuming presence of CRFs.

Conclusions:

We developed an individualized, outcome-optimized planning technique for Hodgkin lymphoma. Some of the resulting plans were substantially different from clinical routine plans. The results varied depending on how risk models were defined or prioritized.

Introduction

Follow-up studies of long-term Hodgkin lymphoma (HL) survivors with mediastinal disease have documented an excess risk of cardiac disease and secondary cancers [1,2] compared with population controls. The goal of radiotherapy (RT) planning is to optimize the therapeutic ratio, and population-based dose-volume constraints are used in current clinical practice to limit the risk of adverse effects. However, this method's capability to take the patient's specific anatomy and extent of the tumor into account is limited. For example, for patients with extensive disease, doses close to or exceeding the usual constraints may be accepted if maximum tumor control is prioritized. Conversely, for patients with limited disease, the conventional dose constraints may lead to acceptance of plans that are suboptimal. Ideally, doses to all normal structures should be kept as low as reasonably achievable, with emphasis on the most critical organs [3]. In the particular case of early-stage HL, it might even be clinically preferable in some cases to accept a small compromise of target coverage in order to reduce the dose to a critical OAR and the associated risk of late effects. However, most treatment planning systems are not suited to this scenario, and those compromises are performed subjectively. To this end we need a flexible dose-planning tool that allows us to optimize the trade-off between the risks of recurrence and various severe late effects to achieve the "best deal" for each patient with HL.

To directly balance these trade-offs during planning, the incorporation of biological or normal tissue complication probability (NTCP) models into treatment plan optimization has been proposed [4-8]. Various biological optimization methods have been explored for disease sites such as prostate cancer [9-12], head and neck cancer

[13,14], brain cancer [15], breast cancer [16], and intrahepatic tumors [17]. For HL, a tool for evaluating biological endpoints for already created treatment plans has been developed [18], but the direct application of biological models in RT plan optimization, to the authors' knowledge, has not yet been investigated. In addition, most reports focus on the probability of a side effect, without considering that the severity/mortality burden is greater from some than others (e.g. second lung cancer vs second breast cancer). The goal of this study was to explore the potential benefit of an individualized outcome-optimized (O-OPT) HL RT planning approach which considers the dose-response effect of radiation on tumor control and mortality from late effects of treatment simultaneously. We also investigated the sensitivity of the O-OPT plan result to model parameters.

Methods and Materials

Patients

CT datasets from 34 patients (17 male, 17 female) with biopsy proven mediastinal HL and median age 33.5 years (range 16-76), were selected for this retrospective study. All patients were treated between 2006 and 2010 (Figure S1 in the supplementary material) [19]. Contours from the clinical RT plans were used for outcome-optimized (O-OPT) planning, and the clinical plans were used as a reference for comparison with O-OPT plans. The clinical plans were 3D conformal radiation therapy (3DCRT), mostly with anterior-posterior posterior-anterior (AP-PA) beam setup with energy of 6 MV. In addition, 2-arc volumetric modulated arc therapy (VMAT) plans were also used for comparison with O-OPT plans [19]. All clinical 3DCRT and VMAT plans were renormalized to a mean dose of 30.6 Gy to the clinical target volume (CTV) (1.8 Gy/fraction) for this study (AAA, Eclipse V13.6 Varian Medial Systems, Palo Alto, CA).

Pre-planning beam setup

4

Pre-planning was performed by creating a set of beams from which the optimization algorithm could choose for the O-OPT plans. Sixteen co-planar gantry angles (0, 10, 20, 45, 90, 135, 160, 170, 180, 190, 200, 225, 270, 315, 340 and 350 degrees) were considered in addition to the clinically used angles if not listed. The higher resolution of angles in the AP-PA regions was chosen to mimic a "butterfly" technique as an option in the solution space [20]. The majority of fields were 6 MV, except two patients who were planned with 18 MV fields, following their 3DCRT clinical plans. To allow basic dose modulation, four fields were created for each angle: one open field and three subfields that together fully covered the target (e.g. superior, middle, and inferior), yielding a total of at least 64 beams (Figure 1). Initial doses from each beam using equal field weighting were calculated using a commercial treatment planning system (TPS) (AAA, Eclipse V13.6) then exported for optimization.
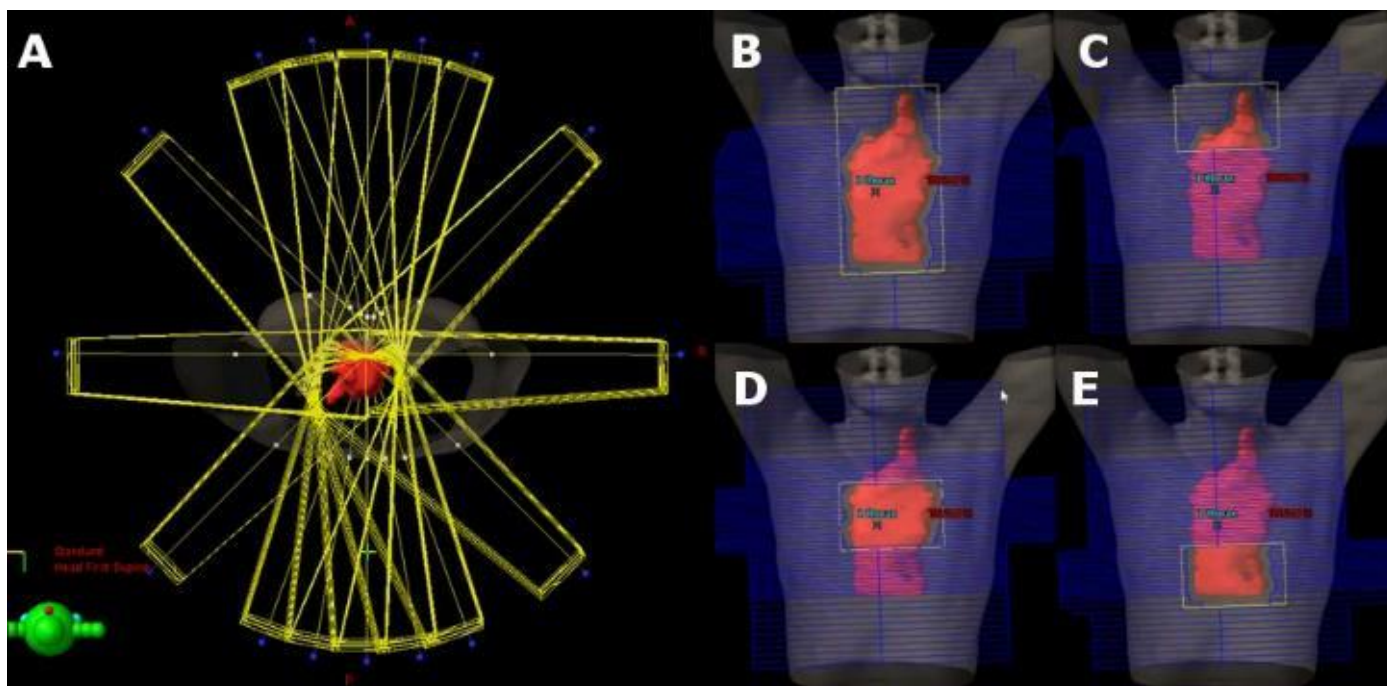
Figure 1. Beam setup for pre-planning before optimization with 16 beam angles surrounding the patient (A) and examples of open and partially closed subfields that were created for each beam angle (B-E). The CTV is shown in red.

Inverse plan optimization

Inverse planning was performed by our in-house particle swarm optimization (PSO) engine, implemented in

MATLAB (R2016a, MathWorks, Matick, MA) [21]. PSO algorithm's highly-parallelizable, metaheuristic and global

nature has been thoroughly introduced in the literature [22,23] and applied to various RT inverse planning

studies [24-26]. In this study, a swarm of 30 particles were used over 30 iterations, and a perturbation was

applied at iteration 20 to avoid local minima. At each perturbation step, the particle with the best solution was

kept, while the others were randomly re-distributed without erasing their personal bests from their memories.

The output of the optimization was a list of monitor unit (MU) values for each beam that described the O-OPT

plan. Beams with <5 MU were eliminated during optimization. If the optimization algorithm created a plan that

was equal in risk with the clinical 3DCRT plan, the clinical 3DCRT plan was chosen. The objective function was a

proxy for "overall outcome" defined as a summation of the probabilities of disease recurrence and the normal

tissue complications given by the equation

$$p_{tot} = p_{DR} + p_{CHD} + p_{LC} + p_{BC} \tag{1}$$

where p_{tot} is the total penalty function, and the penalty functions for disease recurrence, mortality due to

coronary heart disease, mortality due to secondary lung cancer, and mortality due to secondary breast cancer

are given by p_{DR}, p_{CHD}, p_{LC} and p_{BC}, respectively. We equally weighted the objective terms to indicate the

seriousness of both a recurrence and a fatal late normal tissue complication, but, in a prospective scenario, the

priorities of these terms can be adjusted according to the clinician's or patient's preference. The models for each

penalty function are described below.

While the base analysis in this study focused on O-OPT plans that were optimized purely to minimize p_{tot}, for one patient we also created (i) an O-OPT plan with a hard requirement for ≥90% of CTV receiving the prescription dose and (ii) another O-OPT plan with a hard requirement of avoiding hot spot ≥40 Gy as a sensitivity analysis.

Disease recurrence model

Progression free survival (PFS) at 5 years for different dose levels were obtained from randomized trials in literature [27-29] assuming uniform irradiation of the CTV. From these studies, hazard ratios (HRs) were estimated at HR=2.44 for 0 Gy (no RT) relative to 30.6 Gy and HR=1.44 for 20 Gy relative to 30.6 Gy. Therefore, the estimated PFS at 5 years was given by

$$PFS(D) = 0.872^{HR(D)} \qquad (2)$$

where 0.872 is the 'ideal' PFS (for dose D=30.6 Gy) and $HR(D)$ is calculated by linear interpolation between the 0, 20 and 30.6 Gy estimates above.

The penalty function for risk of disease recurrence was given by

$$p_{DR} = 0.872 - PFS(D). \qquad (3)$$

In the more general case of a non-uniform target dose, the mean dose to the CTV in equation 2 was calculated as generalized equivalent uniform dose (gEUD) [30]. For voxels with dose >30.6 Gy, dose was 'capped' and set to 30.6 Gy while for voxels with dose ≤30.6 Gy, dose values were unchanged. This capping of target dose was performed for the calculation of the gEUD so the model did not assume that 'hot spots' in the target were associated with improved local control.

To explore and quantify the common clinical challenge of tradeoffs between target coverage and normal tissue dose, we allowed the O-OPT technique to suggest a target compromise to spare critical risk organs. One approach is to assume that tumor control is a function of mean dose over the target volume. Another common hypothesis is that the minimum dose to the target drives the risk of recurrence. Both situations can be modeled within the formulation of the gEUD model suggested by Niemierko by adjusting the model parameter a (gEUD = $\left(\frac{1}{n}\sum_{i=1}^{n}d_i^a\right)^{1/a}$), where n is the number of voxels in the CTV) [31]. In this formula, setting a =1 corresponds to the mean dose model, and setting a equal to a large negative value corresponds to a high importance of the minimum dose (Figure S2). In this study, we assumed a=1, but also varied the value of a as a sensitivity analysis.

Normal tissue complication models

Following Brodin et al. [32], the penalty functions for normal tissue late effect x were assumed to depend on mean dose to the relevant organ (and other patient-specific factors):

$$p_x = w_x * PFS * hr_{excess,x}(D_x) \int_{e+5yr}^{80\,yr} \dot{h}_{gen.pop.,x}(a, sex) * \left(S_{gen}(a, sex)\right)da \qquad (4)$$

where p_x is the penalty for the optimizer (coronary heart disease [CHD], lung cancer [LC], or breast cancer [BC]). w_x is the weighting factor for the mortality associated with x. PFS is calculated in equation 2. $hr_{excess,x}(D_x)$ is the excess hazard ratio for complication x, which depends on dose (D_x) (Table S1). $\dot{h}_{gen.pop.,x}(a, sex)$ is the population incidence for complication x, which can depend on age (a) and sex. $S_{gen}(a, sex)$ is the sex-specific survival of the general population for each age [33]. The integral is from the age at exposure (e) plus 5 years to 80 years (assuming a latency of late effects of 5 years). The risk of CHD depended on the presence of cardiac risk factors (CRFs) and all patients were optimized twice: assuming CRF=0 and CRF>0. (For details see Tables S1-S4 [34-43].)

Outcome-optimized planning and analysis summary

For each patient, the pre-plan created in the TPS was exported to the in-house PSO engine where the optimal combination of beams and MUs was determined through minimization of the summed risk of adverse outcomes (modeled as p_{tot} in equation 1). The clinical 3DCRT, VMAT, and O-OPT plans were compared based on their p_{tot} values as well as dosimetric results; i.e.; dose volume histograms (DVHs) and mean doses to the CTV and the OARs.

Results

O-OPT plans were created for 34 patients and compared with clinical 3DCRT plans and VMAT plans. In general, O-OPT plans had the lowest risk, followed by the clinical 3DCRT plans, then the VMAT plans with the highest risk with median (maximum) total risk values of 4.9 (11.1), 5.1 (17.7), and 7.6 (20.3)%, respectively (assuming no CRFs) (Tables S5 and S6 and Figure S3). Figure 2 shows a comparison between the clinical 3DCRT, VMAT, and O-OPT plans for a patient that had a large modeled benefit from O-OPT planning. O-OPT plans did not provide a risk benefit beyond the clinical 3DCRT plans for 19 of the 34 patients assuming no cardiac risk factors (CRF=0) (and 13 of 34 assuming CRF>0), so for those patients the clinical 3DCRT plan was determined to be optimal and chosen as the O-OPT plan. The total modeled risk benefit was greater than 1% for 9 patients assuming no CRFs and 11 patients assuming the presence of CRFs when compared to the clinical 3DCRT plans. Tables S5a and S5b in the supplementary material summarize the differences between the O-OPT and clinical 3DCRT plans for all patients with and without CRFs, and Table S6 summarizes the differences between the O-OPT and VMAT plans. Figure 3 shows the total risk from O-OPT plans compared to clinical 3DCRT plans (Figure S4 shows a comparison with VMAT plans).
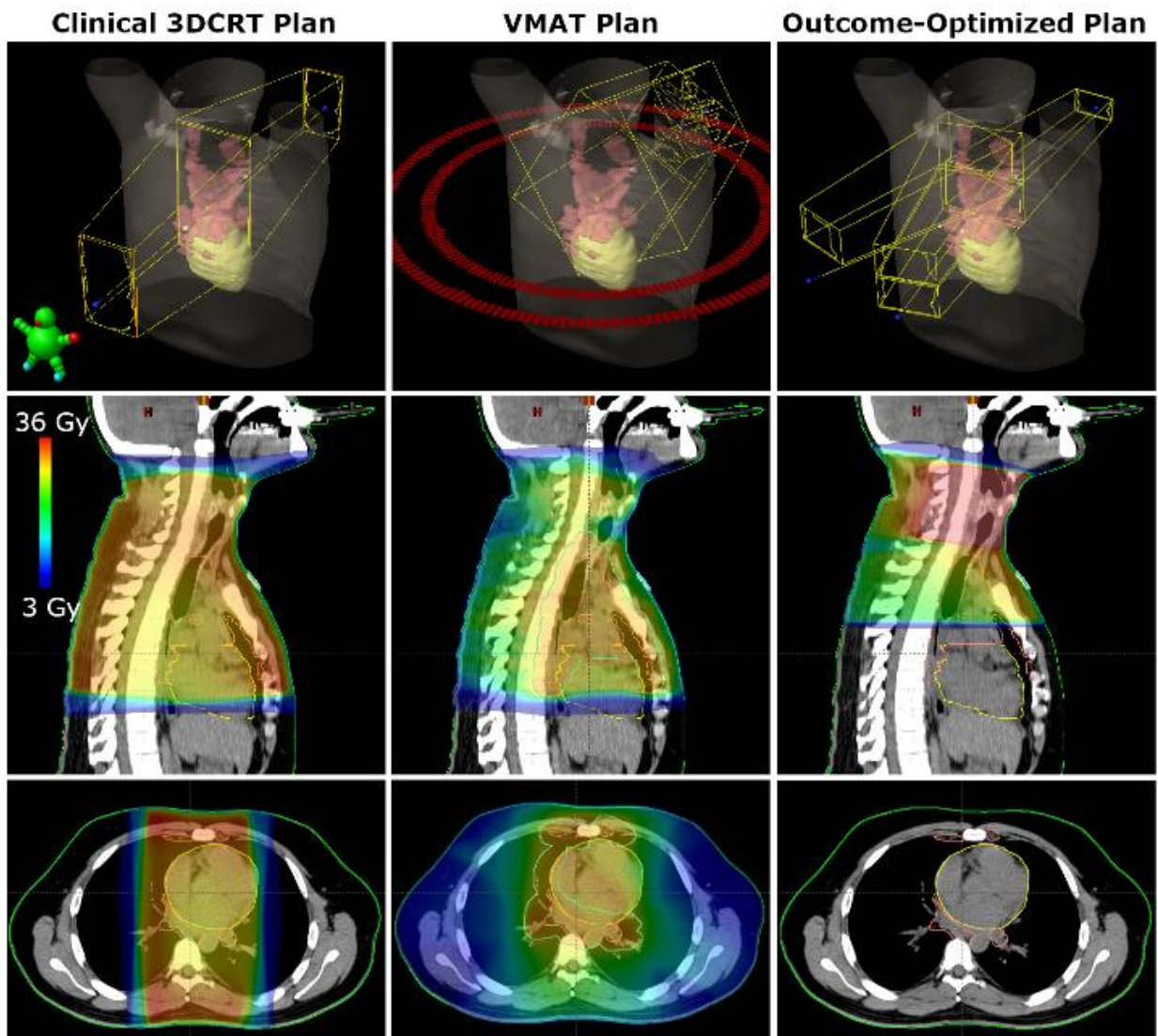
Figure 2. Comparison of beams and dose distributions for clinical 3DCRT, VMAT, and outcome-optimized (O-OPT) plans for an example patient with a large benefit (patient 3 in Table S5). The CTV is shown in pink and the heart is shown in yellow. The PTV is shown in cyan for the VMAT plan.
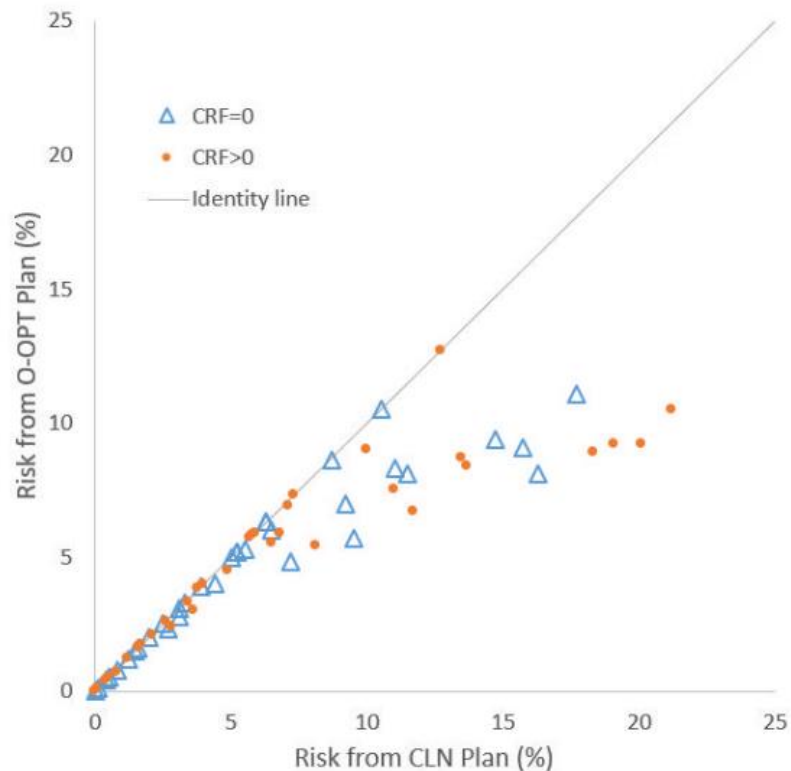
Figure 3. Total risk for outcome-optimized (O-OPT) plans compared to clinical (CLN) 3DCRT plans for all patients in two cardiac risk factor (CRF) scenarios (CRF=0 and CRF>0).

For sensitivity analysis of our method and models, O-OPT planning with different scenarios was completed. We conducted a sensitivity analysis of the effect of the choice of gEUD parameter in our target. In an illustrative patient who had a considerable (but not extreme) benefit from O-OPT planning in the base analysis (patient 25), it was seen that as the gEUD parameter became a larger negative number, the resulting O-OPT plan prioritized target coverage and approached the clinical plan (Figure 4). Then, we created O-OPT plans with an extreme value of the gEUD parameter of -22 (which heavily penalized under-dosing any part of the target) for the 9 patients who had a benefit from O-OPT planning relative to the clinical 3DCRT plans of more than 1% assuming CRF=0. Out of these 9 patients, only 3 had a predicted benefit from the O-OPT planning with the gEUD parameter of -22

(Table S7). Furthermore, to investigate the potential increased risk of recurrence if the gEUD parameter was ("incorrectly") assumed to be 1 during optimization, we recalculated the risk of recurrence for various ("true") values of the gEUD parameter (Table 1) while keeping the plan and dose distribution constant. We found that the increased risk of recurrence due to an incorrect assumption during optimization could be up to 11.7%.
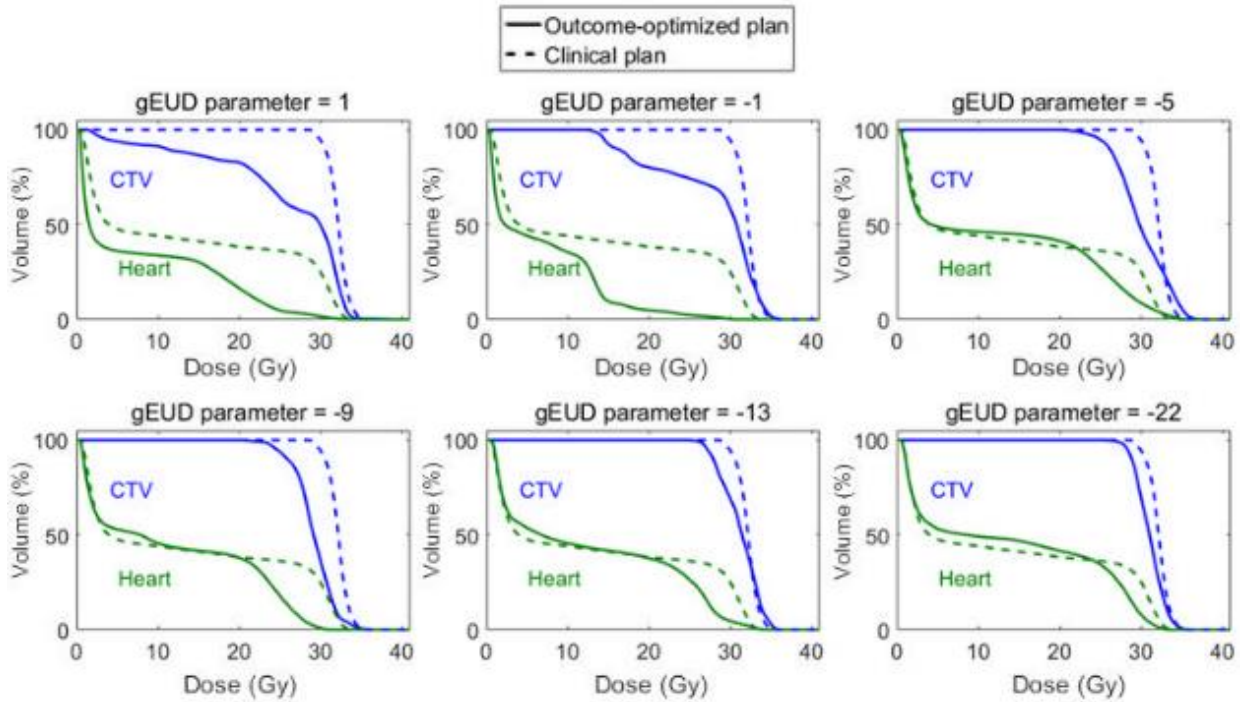
Figure 4. Dose-volume histograms (DVHs) showing the difference in O-OPT plans (CRF=0 with hot-spot avoidance requirement) with respect to gEUD parameter choice in target model for O-OPT planning for one patient (patient 25). The DVHs from the clinical 3CDRT plan are shown in dotted lines.

Table 1. Recalculation of the term p_{DR} (risk of disease recurrence) for various values of the gEUD parameter a for one patient (patient 25). For this recalculation, the O-OPT plan that was analyzed was created with the assumption of a=1. Then, the plan was kept constant and p_{DR} was recalculated to see the impact of a different "true" value of a if 1 was assumed during optimization but was incorrect.

gEUD parameter a (for recalculation, not optimization)	1	-1	-5	-9	-13	-22
Recalculated p_{DR} for clinical 3DCRT plan (%)	0.04	0.05	0.05	0.06	0.06	0.07

Recalculated p_{DR} for O-OPT plan (%)	3.0	8.1	13.9	14.4	14.6	14.8
Increase in p_{DR} for the O-OPT plan relative to clinical 3DCRT plan for each value of a (O-OPT$_a$-3DCRT$_a$) (%)	3.0	8.0	13.9	14.4	14.5	14.7
Increase in p_{DR} for the O-OPT plan for each value of a relative to O-OPT plan with a =1 (O-OPT$_a$-O-OPT$_{a=1}$) (%)	0.0	5.0	10.9	11.4	11.6	11.7

Finally, we performed a sensitivity analysis with additional 'requirements' during optimization (assuming CRF=0) for the same patient as the other sensitivity analyses (patient 25). Three O-OPT plans were created for this patient: (1) O-OPT plan (with no extra optimization requirements), (2) O-OPT plan with a target coverage requirement (≥90% of CTV receiving 100% prescribed dose) and (3) O-OPT plan with hot-spot avoidance requirement (40 Gy maximum). Figure S5 compares the DVHs of the clinical 3DCRT plan and the resulting O-OPT plans with the dosimetric requirements. Adding requirements either for target coverage or hot spot avoidance reduced the benefit achievable by O-OPT planning.

Discussion

In this retrospective study, we investigated the potential of a novel planning approach for patients with mediastinal HL and created individualized plans that aimed to provide the best outcome for the patient by simultaneously optimizing the risk of disease recurrence and mortality due to normal tissue complications. The ultimate aim of this study was not a planning comparison in the traditional sense of the term, but rather to show that including the risk of recurrence and mortality from late toxicity within the optimization function can drastically alter the resulting optimal dose distribution in some patients. While the study contained equal numbers of males and females, 8 of the 9 patients with a benefit >1% from O-OPT planning were male. It is possible that the lack of objectives for breast, or the difference in background rates of complications (Tables S2 and S3) influenced this difference. The O-OPT plan was more likely to reduce the risk when the doses to the heart

and lungs from the clinical 3DCRT plan or VMAT plan were high (Figure S6). For the patients with the largest doses to the heart and lungs from the clinical 3DCRT plan and largest benefit from O-OPT planning (>1%), the optimizer would entirely avoid treating the inferior part of the CTV near the heart. Hot spots were observed in O-OPT plans (Figure S7), which were mostly due to the overlap of subfields with collimator rotation from different beam angles or from heavy field weighting from one direction. The total number of beams was comparable in both clinical 3DCRT and O-OPT plans for most patients, so the O-OPT plans would be feasible with respect to delivery time.

These results should be understood within the context of the assumptions and limitations of this study.

First, all risk models reflect our current best evidence regarding dose-risk relationships. Other risk models exist, and more detailed models could become available in the future. Substantial compromises to target coverage were observed in our results. They are, however, driven by our choice of a mean dose model for tumor control probability after an inhomogeneous dose distribution. While we performed a sensitivity analysis of the gEUD model parameter, PFS data after partial target compromise are not available in the literature and this is a major limitation of our approach. Therefore, while this study is a first step in demonstrating the potential of this type of optimization, clinical use should await improved models that account for partial coverage of the CTV. An alternative to including PFS in O-OPT planning would be to constrain the optimizer to provide adequate CTV coverage and only optimize on normal tissue biological endpoints (Figure S5).

Second, for the base analysis in this study, no purely dosimetric constraints were used, and we observed dose distributions and maximum doses that were different from usual clinical practice. For example, large maximum doses were seen from subfield overlap and heavy weighting of fields from one direction. When the heavily

weighted field was posterior, four plans exceeded the clinical spinal cord constraint of 45 Gy, which may not be acceptable for treatment. Additional optimization objectives might be needed to achieve dose distributions that are also acceptable for the risk of acute toxicity.

Third, the prioritization and weighting were selected to consider disease recurrence to be as equally important as mortality from radiation-induced coronary heart disease, lung cancer, and breast cancer. As the impact of a recurrence on a patient's quality of life and the high associated risk of mortality might occur earlier than the mortality from a late effect, disease recurrence could theoretically have a time-modulated weighting factor during optimization. Furthermore, non-fatal normal tissue complications could have effects on morbidity and quality of life, which were not modeled here.

Finally, the planning technique limited the degrees of freedom available to create the O-OPT plans. While we provided the optimizer with many fields and allowed simple modulation with subfields, the O-OPT plans were still effectively 3DCRT plans. The limited degrees of freedom (combined with a lack of dosimetric constraints) resulted in hot spots in the O-OPT plans (Figure S7). This O-OPT strategy could be directly integrated with the TPS and combined with VMAT or intensity modulated radiation therapy (IMRT), where it might find more complex solutions with even lower risks.

Despite the above caveats, the approach used in this study, allows a critical examination of the empirical knowledgebase used in treatment plan optimization. It demonstrates the complexities of plan optimization, which is at present carried out in the clinic by crude, semi-quantitative or qualitative methods. Specifically, this individualized dose planning approach represents a framework for considering quantitative estimates of multiple

risks, explores the uncertainty in our assumptions, and allows patient-level risk factors to be taken into account. With current capabilities in storing, analyzing, and linking dose plans with treatment outcomes, it is likely that this type of complex, computationally expensive planning will become increasingly reliable in a not too distant future.

In conclusion, we investigated an RT planning strategy where we directly optimized on a metric for patient-specific outcome. Total risk was defined as an equally-weighted summation of risks of disease recurrence and mortality due to radiation-induced coronary heart disease and secondary lung and breast cancers. Our technique reduced the maximum total risk considerably for patients who had large OAR doses in their VMAT plans or clinical 3DCRT plans; however, for patients with relatively low OAR doses in clinical 3DCRT plans, there was no improvement achieved through O-OPT planning. Sensitivity analyses investigating dependence of our results on the TCP model (the gEUD parameter) and dosimetric requirements revealed large variation in both plan result and risk of recurrence, demonstrating a need for caution in future work on biologically optimized planning for HL.

References

1.   Aleman BM, van den Belt-Dusebout AW, De Bruin ML, et al. Late cardiotoxicity after treatment for Hodgkin lymphoma. Blood. 2007 Mar 01;109(5):1878-86.

2.   Schaapveld M, Aleman BMP, van Eggermond AM, et al. Second Cancer Risk Up to 40 Years after Treatment for Hodgkin's Lymphoma. New England Journal of Medicine. 2015 2015/12/24;373(26):2499-2511.

3.   Specht L. Radiotherapy for Hodgkin Lymphoma: Reducing Toxicity While Maintaining Efficacy. Cancer journal (Sudbury, Mass). 2018 Sep/Oct;24(5):237-243.

4.   Niemierko A, Urie M, Goitein M. Optimization of 3d radiation therapy with both physical and biological end points and constraints. International Journal of Radiation Oncology*Biology*Physics. 1992 1992/01/01/;23(1):99-108.

5.   Brahme JNDBA. Biologically Optimized Radiation Therapy. Acta Oncologica. 2001 2001/01/01;40(6):725-734.

6. Markov K, Schinkel C, Stavreva N, et al. Reverse mapping of normal tissue complication probabilities onto dose volume histogram space: the problem of randomness of the dose volume histogram sampling. Med Phys. 2006 Sep;33(9):3435-43.

7. Peñagarícano JA, Papanikolaou N, Wu C, et al. An assessment of Biologically-based Optimization (BORT) in the IMRT era. Medical Dosimetry. 2005 2005/03/01/;30(1):12-19.

8. Qi XS, Semenenko VA, Li XA. Improved critical structure sparing with biologically based IMRT optimization. Medical Physics. 2009 2009/05/01;36(5):1790-1799.

9. Rechner LA, Eley JG, Howell RM, et al. Risk-optimized proton therapy to minimize radiogenic second cancers. Phys Med Biol. 2015 May 21;60(10):3999-4013.

10. Witte MG, van der Geer J, Schneider C, et al. IMRT optimization including random and systematic geometric errors based on the expectation of TCP and NTCP. Med Phys. 2007 Sep;34(9):3544-55.

11. Mihaylov IB, Fatyga M, Bzdusek K, et al. Biological Optimization in Volumetric Modulated Arc Radiotherapy for Prostate Carcinoma. International Journal of Radiation Oncology*Biology*Physics. 2012 2012/03/01/;82(3):1292-1298.

12. Sanchez-Nieto B, Romero-Exposito M, Terron JA, et al. Uncomplicated and Cancer-Free Control Probability (UCFCP): A new integral approach to treatment plan optimization in photon radiation therapy. Phys Med. 2017 Oct;42:277-284.

13. Kierkels RGJ, Korevaar EW, Steenbakkers RJHM, et al. Direct use of multivariable normal tissue complication probability models in treatment plan optimisation for individualised head and neck cancer radiotherapy produces clinically acceptable treatment plans. Radiotherapy and Oncology. 2014 2014/09/01/;112(3):430-436.

14. Kierkels RGJ, Wopken K, Visser R, et al. Multivariable normal tissue complication probability model-based treatment plan optimization for grade 2-4 dysphagia and tube feeding dependence in head and neck radiotherapy. Radiother Oncol. 2016 Dec;121(3):374-380.

15. Corwin D, Holdsworth C, Rockne RC, et al. Toward patient-specific, biologically optimized radiation therapy plans for the treatment of glioblastoma. PloS one. 2013;8(11):e79115-e79115.

16. Ferreira BC, Mavroidis P, Adamus-Górka M, et al. The impact of different dose–response parameters on biologically optimized IMRT in breast cancer. Physics in Medicine and Biology. 2008 2008/05/01;53(10):2733-2752.

17. Thomas EE, Ten Haken RK, Chapet O, et al. The use of biological parameters (EUD and NTCP) in IMRT optimization and its impact on the maximum safe dose deliverable to intrahepatic tumors. International Journal of Radiation Oncology • Biology • Physics. 2004;60(1):S179-S180.

18. Brodin NP, Maraldo MV, Aznar MC, et al. Interactive decision-support tool for risk-based radiation therapy plan comparison for Hodgkin lymphoma. Int J Radiat Oncol Biol Phys. 2014 Feb 1;88(2):433-45.

19. Maraldo MV, Brodin P, Aznar MC, et al. Doses to carotid arteries after modern radiation therapy for Hodgkin lymphoma: is stroke still a late effect of treatment? Int J Radiat Oncol Biol Phys. 2013 Oct 1;87(2):297-303.

20. Voong KR, McSpadden K, Pinnix CC, et al. Dosimetric advantages of a "butterfly" technique for intensity-modulated radiation therapy for young female patients with mediastinal Hodgkin's lymphoma. Radiat Oncol. 2014 Apr 15;9:94.

21. Modiri A, Stick LB, Rice SR, et al. Individualized estimates of overall survival in radiation therapy plan optimization - A concept study. Med Phys. 2018 Nov;45(11):5332-5342.

22. Eberhart R, Kennedy J, editors. A new optimizer using particle swarm theory. Micro Machine and Human Science, 1995. MHS '95., Proceedings of the Sixth International Symposium on; 1995 4-6 Oct 1995.

23. Eberhart R, Shi Y, Kennedy J. Swarm Intelligence. The Morgan Kaufmann Series in Artificial Intelligence; 2001.

24. Li Y, Yao D, Yao J, et al. A particle swarm optimization algorithm for beam angle selection in intensity-modulated radiotherapy planning. Phys Med Biol. 2005 Aug 7;50(15):3491-514.

25. Modiri A, Gu X, Hagan A, et al. Radiotherapy Planning Using an Improved Search Strategy in Particle Swarm Optimization. IEEE Transactions on Biomedical Engineering. 2016;PP(99):1-1.

26. Yang J, Zhang P, Zhang L, et al. Particle swarm optimizer for weighting factor selection in intensity-modulated radiation therapy optimization algorithms. Physica Medica. 2017 1//;33:136-145.

27. Eich HT, Diehl V, Gorgen H, et al. Intensified chemotherapy and dose-reduced involved-field radiotherapy in patients with early unfavorable Hodgkin's lymphoma: final analysis of the German Hodgkin Study Group HD11 trial. J Clin Oncol. 2010 Sep 20;28(27):4199-206.

28. Engert A, Plutschow A, Eich HT, et al. Reduced treatment intensity in patients with early-stage Hodgkin's lymphoma. N Engl J Med. 2010 Aug 12;363(7):640-52.

29. Herbst C, Rehan FA, Brillant C, et al. Combined modality treatment improves tumor control and overall survival in patients with early stage Hodgkin's lymphoma: a systematic review. Haematologica. 2010 Mar;95(3):494-500.

30. Sovik A, Ovrum J, Olsen DR, et al. On the parameter describing the generalised equivalent uniform dose (gEUD) for tumours. Phys Med. 2007 Dec;23(3-4):100-6.

31. Niemierko A. Reporting and analyzing dose distributions: a concept of equivalent uniform dose. Med Phys. 1997 Jan;24(1):103-10.

32. Brodin NP, Vogelius IR, Maraldo MV, et al. Life years lost--comparing potentially fatal late complications after radiotherapy for pediatric medulloblastoma on a common scale. Cancer. 2012 Nov 01;118(21):5432-40.

33. CDC. Centers for Disease Control and Prevention - Relative Cancer Survival. Available from: https://www.cdc.gov/cancer/npcr/uscs/technical_notes/stat_methods/survival.htm

34. Travis LB, Gospodarowicz M, Curtis RE, et al. Lung Cancer Following Chemotherapy and Radiotherapy for Hodgkin's Disease. JNCI: Journal of the National Cancer Institute. 2002;94(3):182-192.

35. Travis LB, Hill DA, Dores GM, et al. Breast cancer following radiotherapy and chemotherapy among young women with Hodgkin disease. Jama. 2003 Jul 23;290(4):465-75.

36. van Nimwegen FA, Schaapveld M, Cutter DJ, et al. Radiation Dose-Response Relationship for Risk of Coronary Heart Disease in Survivors of Hodgkin Lymphoma. J Clin Oncol. 2016 Jan 20;34(3):235-43.

37. CDC. Centers for Disease Control and Prevention - Age-adjusted death rates for selected causes of death, by sex, race, and Hispanic origin. Available from: https://www.cdc.gov/nchs/data/hus/2017/017.pdf

38. CDC. Centers for Disease Control and Prevention - Death rates for diseases of heart, by sex, race, Hispanic origin, and age. Available from: https://www.cdc.gov/nchs/data/hus/2017/022.pdf

39. NIH. SEER Cancer Statistics Review 1975-2013 - Table 15.19 - Cancer of the Lung and Bronchus in males. National Cancer Institute Surveillance, Epidemiology and End Results Program, accessible at https://seercancergov/csr/1975_2013/browse_csrphp?sectionSEL=15&pageSEL=sect_15_table19html.

40. NIH. SEER Cancer Statistics Review 1975-2013 - Table 15.20 - Cancer of the Lung and Bronchus in females. National Cancer Institute Surveillance, Epidemiology and End Results Program, accessible at https://seercancergov/csr/1975_2013/browse_csrphp?sectionSEL=15&pageSEL=sect_15_table20html.

41. NIIH. SEER Cancer Stat Facts: Lung and Bronchus Cancer. National Cancer Institute Surveillance, Epidemiology and End Results Program, accessible at https://seercancergov/statfacts/html/lungbhtml.

42.   NIH. SEER Cancer Statistics Review 1975-2013 , Table 4.17 , Cancer of Female Breast (Invasive). National Cancer Institute Surveillance, Epidemiology and End Results Program, accessible at https://seercancergov/csr/1975_2013/browse_csrphp?sectionSEL=4&pageSEL=sect_04_table17html.

43.   NIH. SEER Cancer Stat Facts: Female Breast Cancer. National Cancer Institute Surveillance, Epidemiology and End Results Program, accessible at https://seercancergov/statfacts/html/breasthtml.

Biological optimization for mediastinal lymphoma radiotherapy – a preliminary study

Supplementary material

118 patients located in database from Jan 2005 to Aug 2010

Not early stage, classical Hodgkin lymphoma (HL)
Exclusion: 30 patients
        17 not HL
        8 Lymphocyte predominant histology
        1 Uncharacteristic disease
        2 Relapsed/refractory HL
        1 Advanced HL
        1 Pediatric

Non-mediastinal disease
Exclusion: 33 patients
        28 infradiaphragmatic
        1 epitrochlear localization
        9 neck, axillary, or clavicular location

Not suitable for the study
Exclusion: 16 patients
        1 initial RT as modified mantle field
        3 received simultaneous integrated boost
        12 planning CT inadequate in length

Included: **34 patients**

Figure S1: Flowchart of patient inclusion in this study [7].
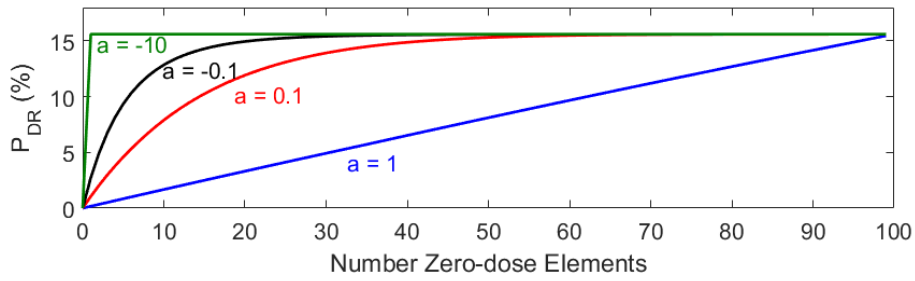
Figure S2. Illustration of the impact of using gEUD [18,19] with various parameter (a) values in recurrence risk calculation (P_{DR} is the penalty for disease risk). A 100-voxel tumor model is considered for this example.
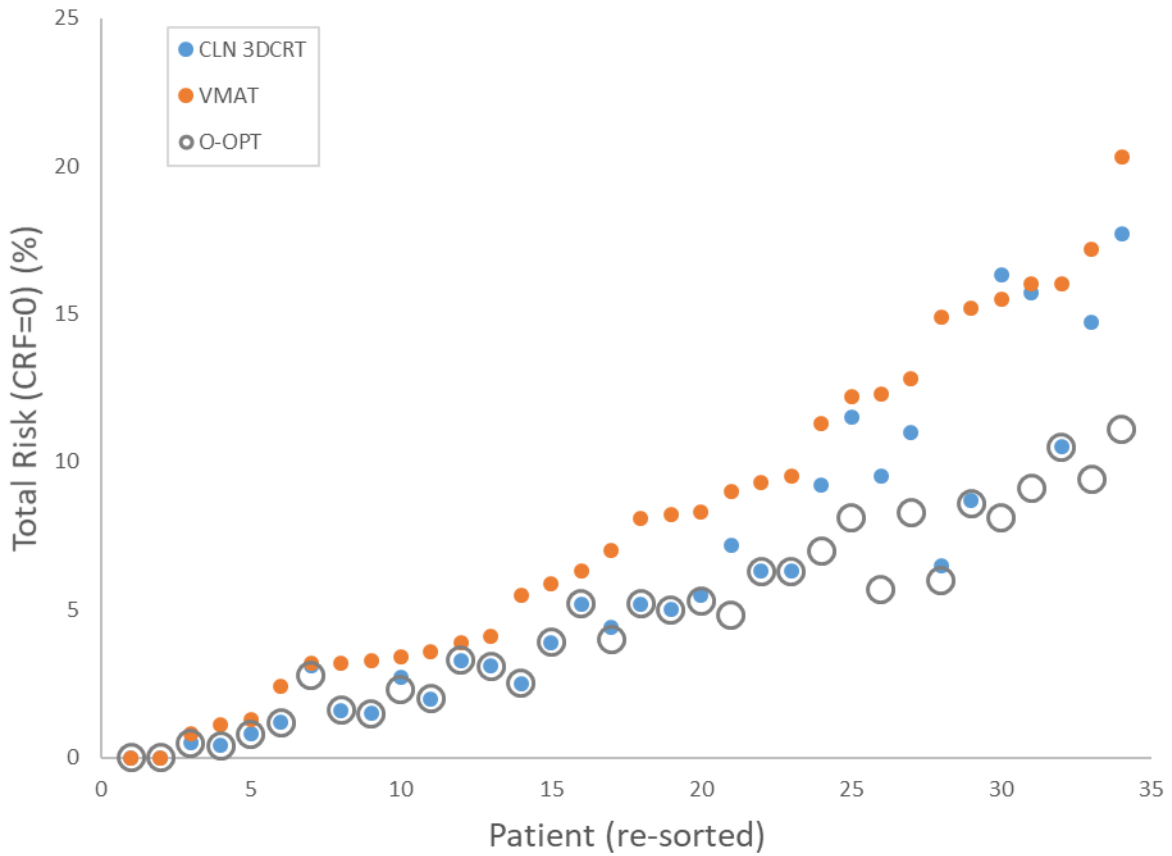
Figure S3. Total risk (recurrence and mortality from late effects) for each patient for each type of plan: clinical (CLN) 3DCRT, VMAT, and O-OPT (assuming CRF=0). Patients are sorted by VMAT risk.
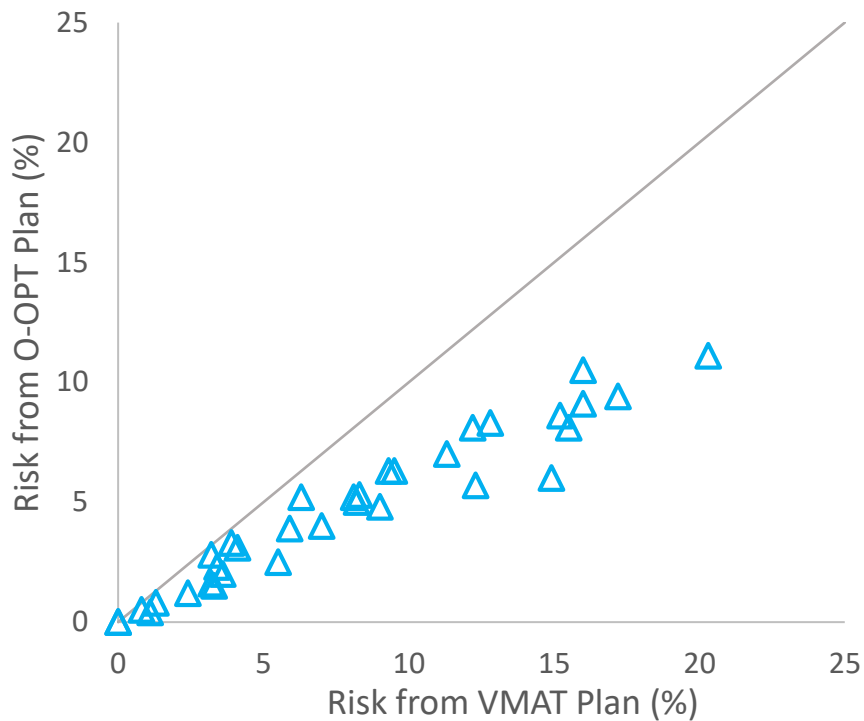
Figure S4. Total risk for outcome-optimized (O-OPT) plans compared to VMAT plans for all patients (CRF=0).
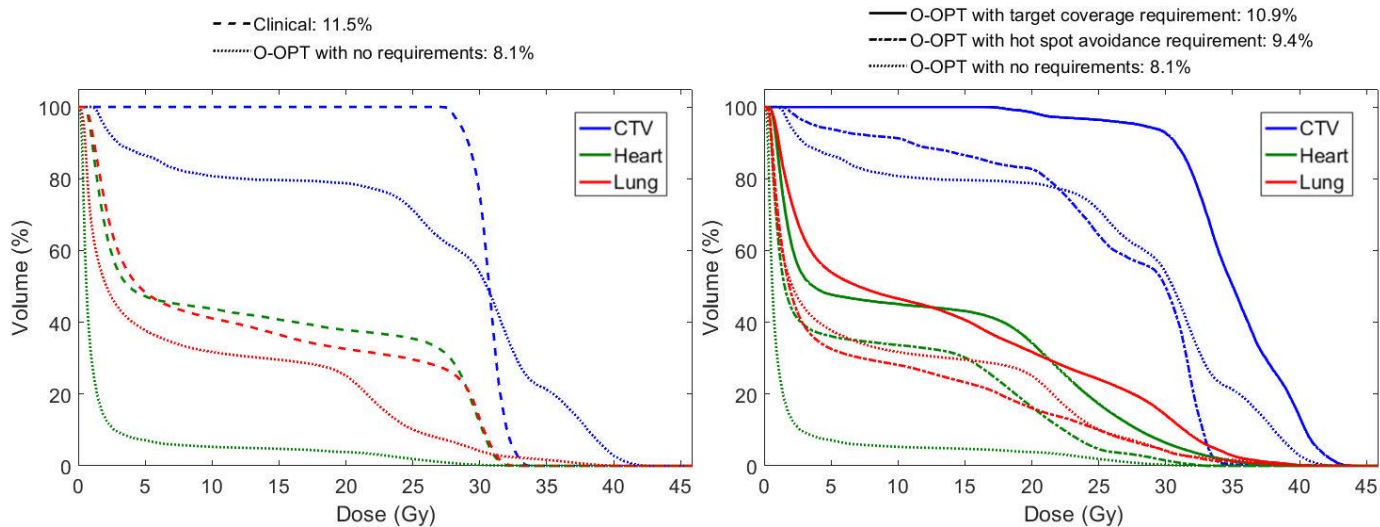
Figure S5. Change of dose-volume histogram (DVH) with respect to target coverage and hot-spot avoidance requirements in outcome-optimized (O-OPT) planning (CFR=0) for one patient. The total risk for each is listed in the legend. Clinical plan for comparison is the 3DCRT plan.
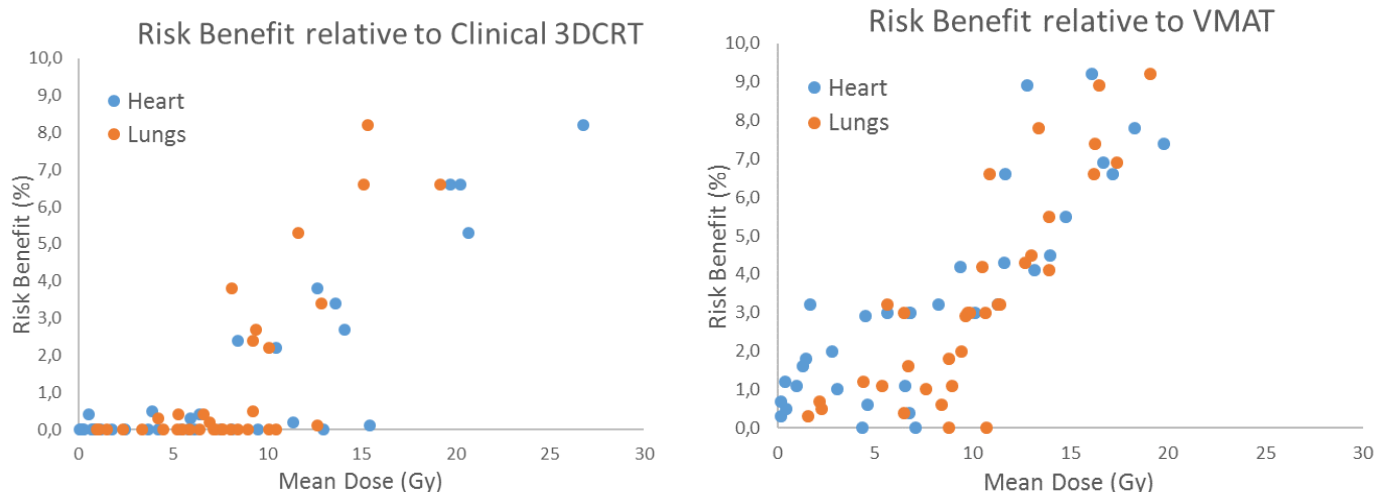
Figure S6. The total risk benefit from O-OPT planning compared to the mean dose to the heart or lungs from the clinical 3DCRT plan (left) or VMAT plan (right), (CRF=0).
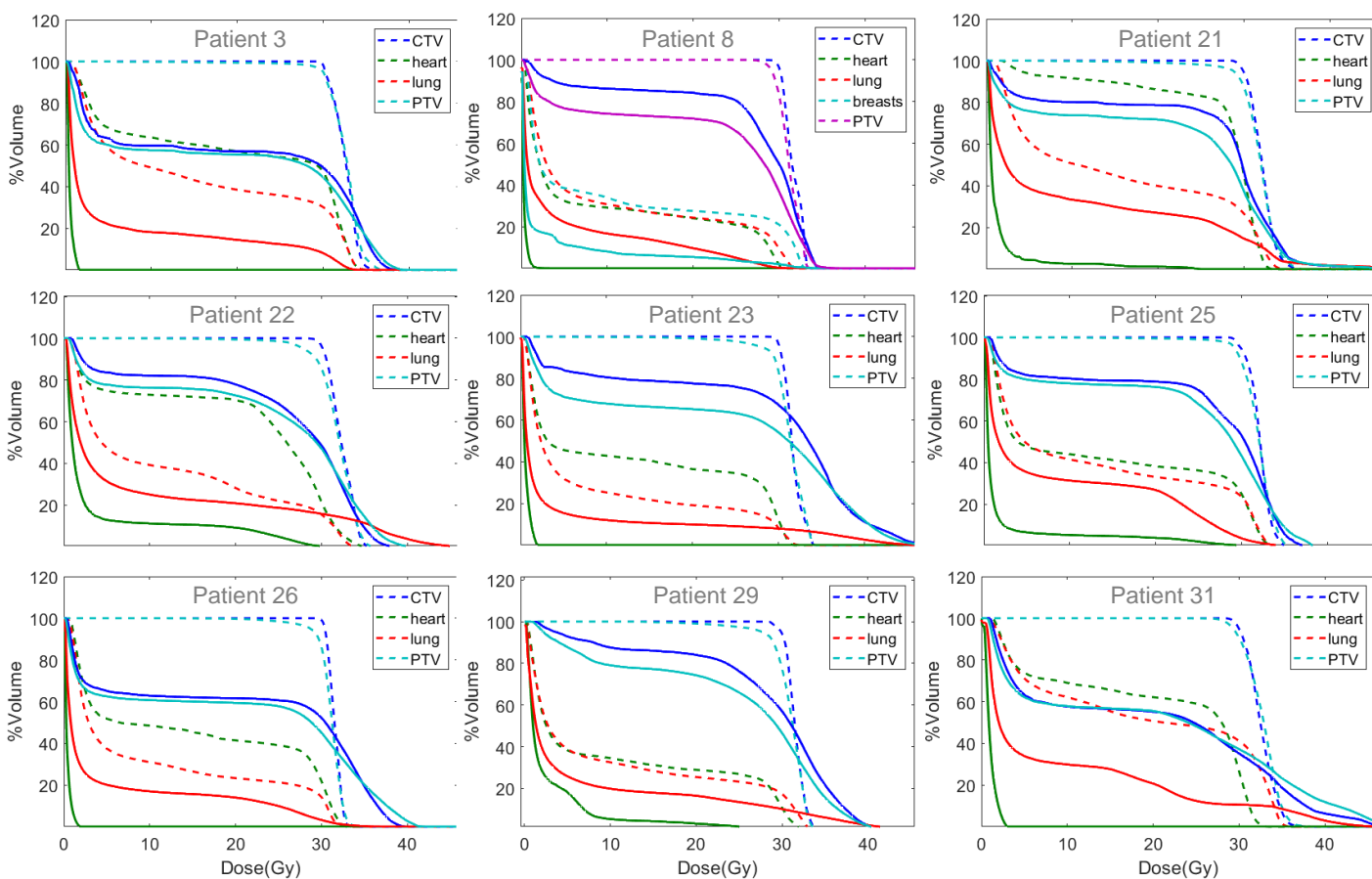
Figure S7. Dose-volume histograms for the clinical 3DCRT plan (dashed) compared to the O-OPT plan (solid) for CRF=0 for the 9 patients with benefit >1%.

Table S1. The risk models used to calculate the excess hazard ratios (hr_{excess}) of the normal tissue complications in this study. Abbreviations: MHD: mean heart dose (Gy), MLD: mean lung dose (Gy), MBD: mean breast dose (Gy) of glandular tissue, CRF. Cardiac risk factor.

Complication (x)	$hr_{excess,x}(male)$	$hr_{excess,x}(female)$	Reference
Coronary Heart Disease (CHD)	0.070*MHD (CRF=0) 0.097*MHD (CRF>0)	0.070*MHD (CRF=0) 0.097*MHD (CRF>0)	van Nimwegen et al 2016 [36]
Lung Cancer (LC)	0.141*MLD	0.141*MLD	Travis et al 2002[34]
Breast Cancer (BC)	N/A	0.149*MBD	Travis et al 2003[35]

Table S2: Background death rates from all heart disease (HD) [37]

Age range (a) (years)	$\dot{h}_{gen.pop.,HD}(a, male)$ (rate per year %)	$\dot{h}_{gen.pop.,HD}(a, female)$ (rate per year %)
15-24	0.0027	0.0016
25-34	0.0103	0.0050
35-44	0.0348	0.0164
45-54	0.1135	0.0475
55-64	0.2681	0.1093
65-74	0.5257	0.2617
75-84	1.3548	0.8548

The ratio between the death rates of coronary heart disease (CHD) and death rates of all heart disease (HD) was calculated by assuming that this ratio is not age dependent [38]:

$$w_{CHD}(male) = \frac{death\ rate\ of\ CHD}{death\ rate\ of\ HD} = \frac{133.5}{210.9} = 0.63$$

$$w_{CHD}(female) = \frac{death\ rate\ of\ CHD}{death\ rate\ of\ HD} = \frac{71.6}{131.8} = 0.54$$

Table S3: Background rates of lung cancer [39,40]

Age range (a) (years)	$\dot{h}_{gen.pop.,LC}(a, male)$ (% per year)	$\dot{h}_{gen.pop.,LC}(a, female)$ (% per year)
20-29	0.000	0.001
30-39	0.002	0.002
40-49	0.014	0.014
50-59	0.067	0.056
60-69	0.190	0.146
70-79	0.344	0.263

The weighting factor for mortality for lung cancer was 1 minus the 5 year survival of lung cancer [41]:

w_{LC} = 1-0.177 = 0.823.

Table S4. Background rates of breast cancer [42]

Age range (a) (years)	$\dot{h}_{gen.pop.,BC}(a, female)$ (% per year)
20-29	0.006
30-39	0.045
40-49	0.147
50-59	0.230
60-69	0.347
70-79	0.395

The weighting factor for mortality for breast cancer was 1 minus the 5-year survival rate of breast cancer [43]:

w_{BC} = 1-0.897 = 0.103.

Table S5(a). Dosimetric and risk comparison between the clinical (CLN) 3DCRT plans and outcome-optimized (O-OPT) plans for no cardiac risk factors (CRF=0).

Patient Info				Heart D$_{mean}$ (Gy)		Lung D$_{mean}$ (Gy)		Breast D$_{mean}$ (Gy)		CTV D$_{mean}$ (Gy)		Total Risk (%)		Risk Benefit (%)	CLN 3DCRT plan chosen as O-OPT
ID	sex	age	CTV (cc)	CLN 3DCRT	O-OPT	CLN 3DCRT	O-OPT	CLN 3DCRT	O-OPT	CLN 3DCRT	O-OPT	CLN 3DCRT	O-OPT	3DCRT – O-OPT	
1	F	24	106.6	6.41	5.80	6.60	5.98	1.74	1.17	30.60	30.24	4.4	4.0	0.4	
2	M	22	298.9	3.66	3.66	7.66	7.66	0.00	0.00	30.60	30.60	5.2	5.2	0	X
3	M	32	561.4	19.73	0.54	15.12	5.79	0.00	0.00	30.60	18.51	15.7	9.1	6.6	
4	F	22	44.2	0.06	0.06	0.93	0.93	0.04	0.04	30.60	30.60	0.4	0.4	0	X
5	M	46	70.5	0.26	0.26	1.51	1.51	0.00	0.00	30.60	30.60	0.8	0.8	0	X
6	M	41	61.3	0.21	0.21	2.34	2.34	0.00	0.00	30.60	30.60	1.2	1.2	0	X
7	M	76	122.8	2.43	2.43	7.18	7.18	0.00	0.00	30.60	30.60	0.0	0.0	0	X
8	F	22	161.2	8.42	0.65	9.27	5.26	10.2	2.39	30.60	28.79	7.2	4.8	2.4	
9	F	36	39.5	5.92	4.16	4.20	3.66	0.58	0.42	30.60	29.58	3.1	2.8	0.3	
10	F	25	130.8	1.16	1.16	5.51	5.51	0.15	0.15	30.60	30.60	2.5	2.5	0	X
11	M	63	174	5.44	5.44	7.24	7.24	0.00	0.00	30.60	30.60	3.3	3.3	0	X
12	F	43	644.7	15.46	3.41	12.67	9.13	3.89	5.90	30.60	23.72	8.7	8.6	0.1	
13	F	27	197	0.85	0.85	4.48	4.48	0.13	0.13	30.60	30.60	2.0	2.0	0	X
14	F	35	123.5	1.77	1.77	6.39	6.39	6.86	6.86	30.60	30.60	3.9	3.9	0	X
15	F	18	1097	3.87	2.68	9.23	8.13	13.20	12.63	30.60	29.83	6.5	6.0	0.5	
16	F	27	160.9	9.50	5.73	8.98	7.71	3.60	3.67	30.60	27.72	6.3	6.3	0	X
17	M	22	85.8	0.50	0.48	5.27	4.19	0.00	0.00	30.60	30.31	2.7	2.3	0.4	
18	M	31	213.6	5.84	5.84	8.08	8.08	0.00	0.00	30.60	30.60	6.3	6.3	0	X
19	F	30	28.6	0.10	0.10	1.08	1.08	0.08	0.08	30.60	30.60	0.5	0.5	0	X
20	F	43	197.5	7.52	7.52	7.61	7.61	3.54	3.54	30.60	30.60	5.0	5.0	0	X
21	M	52	777.6	26.81	1.25	15.37	8.55	0.00	0.00	30.60	20.38	16.3	8.1	8.2	
22	M	16	584.4	20.67	0.94	11.66	8.00	0.00	0.00	30.60	21.42	14.7	9.4	5.3	
23	M	17	277.1	12.65	0.46	8.10	5.67	0.00	0.00	30.60	23.24	9.5	5.7	3.8	
24	M	36	325.2	13.01	13.01	10.46	10.46	0.00	0.00	30.60	30.6	10.5	10.5	0	X
25	M	44	227.1	13.61	1.88	12.87	8.66	0.00	0.00	30.60	23.8	11.5	8.1	3.4	
26	M	22	415.7	14.1	0.42	9.39	5.5	0.00	0.00	30.60	20.93	11.0	8.3	2.7	
27	F	40	117	8.13	8.13	8.45	8.45	0.31	0.31	30.60	30.60	5.2	5.2	0	X
28	F	51	96.1	4.20	4.20	5.89	5.89	1.27	1.27	30.60	30.60	3.1	3.1	0	X
29	M	38	330.4	10.46	2.12	10.12	8.02	0.00	0.00	30.60	25.52	9.2	7.0	2.2	
30	F	17	138.2	11.36	0.26	6.95	3.96	0.75	0.08	30.60	23.30	5.5	5.3	0.2	
31	M	35	1559	20.27	0.41	19.18	7.38	0.00	0.00	30.60	17.00	17.7	11.1	6.6	
32	F	76	136.4	6.16	6.16	10.11	10.11	0.44	0.44	30.60	30.60	0.0	0.0	0	X
33	M	64	219.1	0.69	0.69	5.25	5.25	0.00	0.00	30.60	30.60	1.5	1.5	0	X
34	F	18	113.1	0.73	0.73	3.37	3.37	0.13	0.13	30.60	30.60	1.6	1.6	0	X
median		33.5	167.6	6.04	1.51	7.64	6.19	0.02	0.02	30.6	30.6	5.1	4.9	0	
stdev		16.3	324.6	7.05	2.99	4.13	2.48	3.05	2.65	0.0	4.2	5.0	3.2	2.3	

Table S5(b). Dosimetric and risk comparison between the clinical (CLN) 3DCRT plans and outcome-optimized (O-OPT) plans for cardiac risk factors present (CRF>0).

ID	sex	age	CTV (cc)	Heart D$_{mean}$ (Gy) CLN 3DCRT	O-OPT	Lung D$_{mean}$ (Gy) CLN 3DCRT	O-OPT	Breast D$_{mean}$ (Gy) CLN 3DCRT	O-OPT	CTV D$_{mean}$ (Gy) CLN 3DCRT	O-OPT	Total Risk (%) CLN 3DCRT	O-OPT	Risk Benefit (%) 3DCRT – O-OPT	CLN 3DCRT plan chosen as O-OPT
1	F	24	106.6	6.41	6.05	6.60	5.94	1.74	0.71	30.60	30.32	4.9	4.5	0.4	
2	M	22	298.9	3.66	3.66	7.66	7.66	0.00	0.00	30.60	30.60	5.8	5.8	0	X
3	M	32	561.4	19.73	0.46	15.12	5.89	0.00	0.00	30.60	18.59	19.1	9.2	9.9	
4	F	22	44.2	0.06	0.06	0.93	0.93	0.04	0.04	30.60	30.60	0.4	0.4	0	X
5	M	46	70.5	0.26	0.11	1.51	0.70	0.00	0.00	30.60	11.54	0.8	0.7	0.1	
6	M	41	61.3	0.21	0.21	2.34	2.34	0.00	0.00	30.60	30.60	1.2	1.2	0	X
7	M	76	122.8	2.43	2.43	7.18	7.18	0.00	0.00	30.60	30.60	0	0	0	X
8	F	22	161.2	8.42	0.33	9.27	5.02	10.2	2.13	30.60	25.34	8.1	5.4	2.7	
9	F	36	39.5	5.92	5.71	4.20	3.42	0.58	0.58	30.60	30.52	3.6	3.0	0.6	
10	F	25	130.8	1.16	1.16	5.51	5.51	0.15	0.15	30.60	30.60	2.6	2.6	0	X
11	M	63	174	5.44	5.44	7.24	7.24	0.00	0.00	30.60	30.60	3.8	3.8	0	X
12	F	43	644.7	15.46	8.71	12.67	9.88	3.89	3.43	30.60	25.68	10.0	9.0	1	
13	F	27	197	0.85	0.85	4.48	4.48	0.13	0.13	30.60	30.60	2.1	2.1	0	X
14	F	35	123.5	1.77	1.77	6.39	6.39	6.86	6.86	30.60	30.60	4.0	4.0	0	X
15	F	18	1097	3.87	2.58	9.23	9.07	13.20	9.53	30.60	30.40	6.8	5.9	0.9	
16	F	27	160.9	9.50	9.50	8.98	8.98	3.60	3.60	30.60	30.60	7.1	6.9	0.2	
17	M	22	85.8	0.50	0.49	5.27	4.26	0.00	0.00	30.60	30.38	2.8	2.4	0.4	
18	M	31	213.6	5.84	5.84	8.08	8.08	0.00	0.00	30.60	30.60	7.3	7.3	0	X
19	F	30	28.6	0.10	0.10	1.08	1.08	0.08	0.08	30.60	30.60	0.5	0.5	0	X
20	F	43	197.5	7.52	7.52	7.61	7.61	3.54	3.54	30.60	30.60	5.7	5.7	0	X
21	M	52	777.6	26.81	1.41	15.37	10.48	0.00	0.00	30.60	23.76	20.1	9.2	10.9	
22	M	16	584.4	20.67	3.69	11.66	9.19	0.00	0.00	30.60	23.68	18.3	8.9	9.4	
23	M	17	277.1	12.65	0.55	8.10	4.78	0.00	0.00	30.60	24.38	11.7	6.7	5	
24	M	36	325.2	13.01	13.01	10.46	10.46	0.00	0.00	30.60	30.6	12.7	12.7	0	X
25	M	44	227.1	13.61	1.89	12.87	8.68	0.00	0.00	30.60	23.82	13.7	8.4	5.3	
26	M	22	415.7	14.1	0.37	9.39	5.16	0.00	0.00	30.60	19.40	13.5	8.7	4.8	
27	F	40	117	8.13	8.13	8.45	8.45	0.31	0.31	30.60	30.60	5.9	5.9	0	X
28	F	51	96.1	4.20	4.20	5.89	5.89	1.27	1.27	30.60	30.60	3.4	3.3	0.1	
29	M	38	330.4	10.46	2.86	10.12	7.08	0.00	0.00	30.60	25.69	11.0	7.5	3.5	
30	F	17	138.2	11.36	10.85	6.95	6.41	0.75	0.64	30.60	30.25	6.5	5.5	1	
31	M	35	1559	20.27	0.98	19.18	9.14	0.00	0.00	30.60	17.65	21.2	10.5	10.7	
32	F	76	136.4	6.16	6.16	10.11	10.11	0.44	0.44	30.60	30.60	0.0	0.0	0	X
33	M	64	219.1	0.69	0.69	5.25	5.25	0.00	0.00	30.60	30.60	1.6	1.6	0	X
34	F	18	113.1	0.73	0.73	3.37	3.37	0.13	0.13	30.60	30.60	1.7	1.7	0	X
median		33.5	167.6	6.04	2.51	7.64	6.40	0.02	0.06	30.6	30.6	5.8	5.5	0.1	
stdev		16.3	324.6	7.05	3.51	4.13	2.94	3.05	5.50	0.0	6.6	6.1	3.5	3.5	

Table S6. Dosimetric and risk comparison between the VMAT plans and outcome-optimized (O-OPT) plans for no cardiac risk factors (CRF = 0).

	Patient Info			Heart D$_{mean}$ (Gy)		Lung D$_{mean}$ (Gy)		Breast D$_{mean}$ (Gy)		CTV D$_{mean}$ (Gy)		Total Risk (%)		Risk Benefit (%)	CLN 3DCRT plan chosen as O-OPT
ID	sex	age	CTV (cc)	VMAT	O-OPT	VMAT	O-OPT	VMAT	O-OPT	VMAT	O-OPT	VMAT	O-OPT		
1	F	24	106.6	6.82	5.80	9.84	5.98	4.56	1.17	30.6	30.2	7.0	4.0	3.0	
2	M	22	298.9	4.53	3.66	9.65	7.66	0.00	0.00	30.6	30.6	8.1	5.2	2.9	X
3	M	32	561.4	16.7	0.54	17.4	5.79	0.00	0.00	30.6	18.5	16.0	9.1	6.9	
4	F	22	44.2	0.16	0.06	2.17	0.93	0.20	0.04	30.6	30.6	1.1	0.4	0.7	X
5	M	46	70.5	0.43	0.26	2.28	1.51	0.00	0.00	30.6	30.6	1.3	0.8	0.5	X
6	M	41	61.3	0.38	0.21	4.41	2.34	0.00	0.00	30.6	30.6	2.4	1.2	1.2	X
7	M	76	122.8	4.36	2.43	8.81	7.18	0.00	0.00	30.6	30.6	0.0	0.0	0.0	X
8	F	22	161.2	9.4	0.65	10.5	5.26	8.56	2.39	30.6	28.8	9.0	4.8	4.2	
9	F	36	39.5	6.75	4.16	6.50	3.66	4.04	0.42	30.6	29.6	3.2	2.8	0.4	
10	F	25	130.8	6.74	1.16	6.49	5.51	4.04	0.15	30.6	30.6	5.5	2.5	3.0	X
11	M	63	174	4.60	5.44	8.42	7.24	0.00	0.00	30.6	30.6	3.9	3.3	0.6	X
12	F	43	644.7	17.2	3.41	16.2	9.13	11.0	5.90	30.6	23.7	15.2	8.6	6.6	
13	F	27	197	1.30	0.85	6.72	4.48	0.89	0.13	30.6	30.6	3.6	2.0	1.6	X
14	F	35	123.5	2.79	1.77	9.43	6.39	7.77	6.86	30.6	30.6	5.9	3.9	2.0	X
15	F	18	1097	12.78	2.68	16.50	8.13	13.03	12.63	30.6	29.8	14.9	6.0	8.9	
16	F	27	160.9	11.3	5.73	11.3	7.71	7.59	3.67	30.6	27.7	9.5	6.3	3.2	X
17	M	22	85.8	0.97	0.48	5.38	4.19	0.00	0.00	30.6	30.3	3.4	2.3	1.1	
18	M	31	213.6	5.61	5.84	10.66	8.08	0.00	0.00	30.6	30.6	9.3	6.3	3.0	X
19	F	30	28.6	0.16	0.10	1.58	1.08	0.35	0.08	30.6	30.6	0.8	0.5	0.3	X
20	F	43	197.5	8.24	7.52	11.40	7.61	8.65	3.54	30.6	30.6	8.2	5.0	3.2	X
21	M	52	777.6	19.8	1.25	16.3	8.55	0.00	0.00	30.6	20.4	15.5	8.1	7.4	
22	M	16	584.4	18.3	0.94	13.4	8.00	0.00	0.00	30.6	21.4	17.2	9.4	7.8	
23	M	17	277.1	11.7	0.46	10.9	5.67	0.00	0.00	30.6	23.2	12.3	5.7	6.6	
24	M	36	325.2	14.79	13.01	13.92	10.46	0.00	0.00	30.6	30.6	16.0	10.5	5.5	X
25	M	44	227.1	13.2	1.88	13.9	8.66	0.00	0.00	30.6	23.8	12.2	8.1	4.1	
26	M	22	415.7	14.0	0.42	13.0	5.5	0.00	0.00	30.6	20.9	12.8	8.3	4.5	
27	F	40	117	6.54	8.13	8.96	8.45	0.88	0.31	30.6	30.6	6.3	5.2	1.1	X
28	F	51	96.1	3.09	0.52	7.60	4.57	3.84	0.50	30.6	30.6	4.1	3.1	1.0	X
29	M	38	330.4	11.6	2.12	12.7	8.02	0.00	0.00	30.6	25.5	11.3	7.0	4.3	
30	F	17	138.2	10.15	0.26	9.74	3.96	2.58	0.08	30.6	23.3	8.3	5.3	3.0	
31	M	35	1559	16.1	0.41	19.1	7.38	0.00	0.00	30.6	17.0	20.3	11.1	9.2	
32	F	76	136.4	7.06	6.16	10.71	10.11	1.30	0.44	30.6	30.6	0.0	0.0	0.0	X
33	M	64	219.1	1.44	0.69	8.81	5.25	0.00	0.00	30.6	30.6	3.3	1.5	1.8	X
34	F	18	113.1	1.67	0.73	5.64	3.37	0.50	0.13	30.6	30.6	3.2	1.6	1.6	X
median		**33.5**	**167.6**	**6.79**	**1.51**	**9.79**	**6.19**	**0.10**	**0.02**	**30.6**	**30.6**	**7.6**	**4.9**	**3.0**	
stdev		**16.3**	**324.6**	**5.94**	**2.99**	**4.38**	**2.48**	**3.69**	**2.65**	**0.0**	**4.2**	**5.7**	**3.2**	**2.7**	

Note that 0% risk values in Tables S5 and S6 resulted from two patients who were 76 years old at treatment and were beyond the age at which the risk of late effects would contribute to p_{tot}.

Table S7. Dosimetric and risk comparison between the O-OPT 3DCRT plans for CRF=0 with gEUD parameter of 1 and -22 for the 9 patients who were found to have a benefit >1% when O-OPT 3DCRT plans were compared to clinical 3DCRT plans in this study (Table S1a).

Patient Info				O-OPT Heart D_{mean} (Gy)		O-OPT Lung D_{mean} (Gy)		O-OPT Breast D_{mean} (Gy)		O-OPT CTV D_{mean} (Gy)		O-OPT Total Risk (%)		CLN Total Risk (%)
ID	sex	age	CTV (cc)	gEUDp = -22	gEUDp = 1	gEUDp = -22	gEUDp = 1	gEUDp = -22	gEUDp = 1	gEUDp = -22	gEUDp = 1	gEUDp = -22	gEUDp = 1	
3	M	32	561.4	13.62	0.54	12.71	5.79	0.00	0.00	27.16	18.51	13.2	9.1	15.7
8	F	22	161.2	8.42	0.65	9.27	5.26	10.2	2.39	30.60	28.79	7.2	4.8	7.2
21	M	52	777.6	16.32	1.25	14.41	8.55	0.00	0.00	29.32	20.38	13.1	8.1	16.3
22	M	16	584.4	13.13	0.94	10.42	8.00	0.00	0.00	28.27	21.42	12.9	9.4	14.7
23	M	17	277.1	12.65	0.46	8.10	5.67	0.00	0.00	30.60	23.24	9.5	5.7	9.5
25	M	44	227.1	13.61	1.88	12.87	8.66	0.00	0.00	30.60	23.8	11.5	8.1	11.5
26	M	22	415.7	12.96	0.42	10.31	5.5	0.00	0.00	30.60	20.93	11.0	8.3	11.0
29	M	38	330.4	10.46	2.12	10.12	8.02	0.00	0.00	30.60	25.52	9.2	7.0	9.2
31	M	35	1559	20.27	0.41	19.18	7.38	0.00	0.00	30.60	17.00	17.7	11.1	17.7